

DOCTOR OF PHILOSOPHY

Fast pyrolysis and nitrogenolysis of  
biomass and biogenic residues

*production of a sustainable slow release fertiliser*

Allan Harms

2013

Aston University

# **FAST PYROLYSIS AND NITROGENOLYSIS OF BIOMASS AND BIOGENIC RESIDUES**

Production of a sustainable slow release fertiliser

**Dipl.-Ing. ALLAN BJÖRN HARMS**

Doctor of Philosophy (by research)

ASTON UNIVERSITY

December 2012

© Allan Björn Harms, 2012

Allan Björn Harms asserts his moral right to be identified as the author of this thesis.

This copy of the thesis has been supplied on condition that anyone who consults it is understood to recognise that its copyright rests with its author and that no quotation from the thesis and no information derived from it may be published without proper acknowledgement.

**ASTON UNIVERSITY**  
**FAST PYROLYSIS AND NITROGENOLYSIS OF BIOMASS AND BIOGENIC RESIDUES**

Production of a sustainable slow release fertiliser

**Dipl.-Ing. ALLAN BJÖRN HARMS**

Doctor of Philosophy (by research)

December 2012

## **Summary**

The production of agricultural and horticultural products requires the use of nitrogenous fertiliser that can cause pollution of surface and ground water and has a large carbon footprint as it is mainly produced from fossil fuels. The overall objective of this research project was to investigate fast pyrolysis and in-situ nitrogenolysis of biomass and biogenic residues as an alternative route to produce a sustainable solid slow release fertiliser mitigating the above stated problems.

A variety of biomasses and biogenic residues were characterized by proximate analysis, ultimate analysis, thermogravimetric analysis (TGA) and Pyrolysis – Gas chromatography – Mass Spectroscopy (Py–GC–MS) for their potential use as feedstocks using beech wood as a reference material. Beech wood was virtually nitrogen free and therefore suitable as a reference material as added nitrogen can be identified as such while Dried Distillers Grains with Solubles (DDGS) and rape meal had a nitrogen content between 5.5wt.% and 6.1wt.% qualifying them as high nitrogen feedstocks.

Fast pyrolysis and in-situ nitrogenolysis experiments were carried out in a continuously fed 1kg/h bubbling fluidized bed reactor at around 500°C quenching the pyrolysis vapours with iso-paraffin. In-situ nitrogenolysis experiments were performed by adding ammonia gas to the fast pyrolysis reactor at nominal nitrogen addition rates between 5wt.%C and 20wt.%C based on the dry feedstock's carbon content basis. Mass balances were established for the processing experiments. The fast pyrolysis and in-situ nitrogenolysis products were characterized by proximate analysis, ultimate analysis and GC–MS. High liquid yields and good mass balance closures of over 92% were obtained. The most suitable nitrogen addition rate for the in-situ nitrogenolysis experiments was determined to be 12wt.%C on dry feedstock carbon content basis. However, only a few nitrogen compounds that were formed during in-situ nitrogenolysis could be identified by GC–MS.

A batch reactor process was developed to thermally solidify the fast pyrolysis and in-situ nitrogenolysis liquids of beech wood and Barley DDGS producing a brittle solid product. This was obtained at 150°C with an addition of 2.5wt% char (as catalyst) after a processing time of 1h. The batch reactor was also used for modifying and solidifying fast pyrolysis liquids derived from beech wood by adding urea or ammonium phosphate as post processing nitrogenolysis. The results showed that this type of combined approach was not suitable to produce a slow release fertiliser, because the solid product contained up to 65wt.% of highly water soluble nitrogen compounds that would be released instantly by rain.

To complement the processing experiments a comparative study via Py–GC–MS with inert and reactive gas was performed with cellulose, hemicellulose, lignin and beech wood. This revealed that the presence of ammonia gas during analytical pyrolysis did not appear to have any direct impact on the decomposition products of the tested materials. The chromatograms obtained showed almost no differences between inert and ammonia gas experiments indicating that the reaction between ammonia and pyrolysis vapours does not occur instantly. A comparative study via Fourier Transformed Infrared Spectroscopy of solidified fast pyrolysis and in-situ nitrogenolysis products showed that there were some alterations in the spectra obtained. A shift in frequencies indicating C=O stretches typically related to the presence of carboxylic

acids to C=O stretches related to amides was observed and no double or triple bonded nitrogen was detected. This indicates that organic acids reacted with ammonia and that no potentially harmful or non-biodegradable triple bonded nitrogen compounds were formed.

The impact of solid slow release fertiliser (SRF) derived from pyrolysis and in-situ nitrogenolysis products from beech wood and Barley DDGS on microbial life in soils and plant growth was tested in cooperation with Rothamsted Research. The microbial incubation tests indicated that microbes can thrive on the SRFs produced, although some microbial species seem to have a reduced activity at very high concentrations of beech wood and Barley DDGS derived SRF. The plant tests (pot trials) showed that the application of SRF derived from beech wood and barley DDGS had no negative impact on germination or plant growth of rye grass. The fertilizing effect was proven by the dry matter yields in three harvests after 47 days, 89 days and 131 days.

The findings of this research indicate that in general a slow release fertiliser can be produced from biomass and biogenic residues by in-situ nitrogenolysis. Nevertheless the findings also show that additional research is necessary to identify which compounds are formed during this process.

Keywords: pyrolysis, nitrogenolysis, biomass, residues, slow release fertiliser

Hans Carl von Carlowitz (1713):

„Wird derhalben die größte Kunst/Wissenschaft/Fleiß und Einrichtung hiesiger Lande darinnen beruhen / wie eine sothane Conservation und Anbau des Holtzes anzustellen / daß es eine continuierliche beständige und nachhaltige Nutzung gebe / weiln es eine unentberliche Sache ist / ohne welche das Land in seinem Esse (im Sinne von Wesen, Dasein, d. Verf.) nicht bleiben mag.“ (S. 105-106 in der „Sylvicultura Oeconomica“)[1].

„Hence the biggest skill, science, effort of this county relies on, how such a conservation and cultivation of wood can be implemented, so that a continuous, lasting and sustainable use can be achieved, because this is an essential cause, without that the county cannot persist in its being.“ (Translation of pages 105-106 in “Sylvicultura Oeconomica”)[1].

# Dedication

To Tristan, Maité and Sophie!

## Acknowledgments

I would like to acknowledge my supervisor Professor Anthony V. Bridgwater for his guidance, patience and support throughout the project and his valuable suggestions for my dissertation writing.

I would like to thank Dr. Daniel J. Nowakowski for the scientific discussions, guidance in chemistry questions and steady encouragement to push my limits and finish the project.

I would also like to thank my colleague Charles E. Greenhalf for our successful research collaborations and I would like to thank him as well as my fellow researchers at the Aston University Bioenergy Research Group for the encouraging scientific discussions.

I owe sincere thanks to my colleagues at Rothamsted Research for our useful discussions and their advice for and help with the microbial and plant test.

Thanks also to Dr. Gouzhan Jiang, Surila Darbar and Emma Wylde for their support.

Finally I am truly indebted and thankful for the patience and support of my wife and for my children reminding me every day, why research is essential.

# Table of contents

|  |    |
|--|----|
| List of tables .....   | 12 |
| List of figures.....   | 14 |
| List of abbreviations.....   | 17 |
| 1 Introduction .....   | 18 |
| 1.1 Context and background .....   | 18 |
| 1.2 Objectives .....   | 20 |
| 1.2.1 Subtask 1: Feedstocks and characterization .....                       | 20 |
| 1.2.2 Subtask 2: Fast pyrolysis .....  | 20 |
| 1.2.3 Subtask 3: In-situ nitrogenolysis .....                                | 21 |
| 1.2.4 Subtask 4: Solidification of liquid nitrogenolysis product.....        | 21 |
| 1.2.5 Subtask 5: Nitrogenolysis via fast pyrolysis liquid modification ..... | 21 |
| 1.2.6 Subtask 6: Microbial and plant tests.....                              | 22 |
| 2 Literature review.....   | 23 |
| 2.1 Introduction.....  | 23 |
| 2.2 Biomass and biogenic residues.....                                       | 23 |
| 2.2.1 Introduction .....   | 23 |
| 2.2.2 Cellulose .....  | 24 |
| 2.2.3 Hemicellulose .....  | 24 |
| 2.2.4 Lignin .....   | 24 |
| 2.2.5 Thermal decomposition behaviour of biomass .....                       | 24 |
| 2.3 Fast Pyrolysis .....   | 26 |
| 2.3.1 Introduction and fast pyrolysis.....                                   | 26 |
| 2.3.2 Fast pyrolysis reactor types.....                                      | 28 |
| 2.4 Fast pyrolysis products of biomass.....                                  | 29 |
| 2.4.1 Introduction .....   | 29 |
| 2.4.2 Fast pyrolysis liquid .....  | 30 |
| 2.4.3 Applications of fast pyrolysis liquids .....                           | 32 |
| 2.4.4 Fast pyrolysis gas.....  | 33 |
| 2.4.5 Fast pyrolysis char .....  | 33 |
| 2.4.6 Pyrolysis char as soil amendment .....                                 | 33 |
| 2.5 Plant nutrition.....   | 35 |
| 2.5.1 Introduction .....   | 35 |
| 2.5.2 Plant nutrients.....   | 35 |

|         |   |    |
|---------|---|----|
| 2.5.3   | Nitrogen cycle / bio-degradation .....                                | 36 |
| 2.5.4   | Microbes.....   | 37 |
| 2.6     | Nitrogenolysis and Slow release fertiliser .....                      | 39 |
| 2.6.1   | Introduction .....  | 39 |
| 2.6.2   | Methods of producing organic slow-release nitrogenous fertiliser..... | 39 |
| 2.6.2.1 | Claims of Patent EP0716056 A1 .....                                   | 40 |
| 2.6.2.2 | Results according to Patent EP0716056 A1.....                         | 41 |
| 2.6.3   | European project on slow-release fertiliser from biomass.....         | 42 |
| 2.6.3.1 | In-situ processing route.....   | 43 |
| 2.6.3.2 | Post processing route .....   | 43 |
| 2.6.4   | Slow release fertiliser via ammoxidation .....                        | 45 |
| 2.6.5   | State of the art of slow release fertiliser production.....           | 46 |
| 3       | Methods .....   | 48 |
| 3.1     | Sample preparation .....  | 48 |
| 3.2     | Moisture content of biomass .....                                     | 48 |
| 3.3     | Ash content.....  | 49 |
| 3.4     | Proximate analysis.....   | 49 |
| 3.5     | Elemental analysis .....  | 49 |
| 3.6     | Extraction methods .....  | 50 |
| 3.7     | Higher heating value.....   | 50 |
| 3.8     | Water content of liquids.....   | 51 |
| 3.9     | pH-value.....   | 52 |
| 3.10    | Thermogravimetric Analysis .....                                      | 52 |
| 3.11    | Gas Chromatography-Mass Spectroscopy analysis of liquid samples.....  | 53 |
| 3.12    | Pyrolysis-Gas Chromatography-Mass Spectroscopy .....                  | 54 |
| 3.13    | Online Gas Chromatograph .....  | 55 |
| 3.14    | Fourier Transform Infrared Spectroscopy .....                         | 56 |
| 4       | Feedstock choice and characterization.....                            | 57 |
| 4.1     | Introduction.....   | 57 |
| 4.2     | Results of feedstock characterization and discussions .....           | 59 |
| 4.2.1   | Proximate analysis.....   | 59 |
| 4.2.2   | Ultimate analysis .....   | 60 |
| 4.2.3   | Extraction experiments .....  | 61 |
| 4.2.4   | Thermogravimetric Analysis.....                                       | 62 |
| 4.2.5   | Py-GC-MS.....   | 66 |

|         |  |    |
|---------|--|----|
| 5       | Processing by fast pyrolysis and nitrogenolysis .....                      | 68 |
| 5.1     | General – Bubbling fluidized bed reactors .....                            | 68 |
| 5.1.1   | 1kg/h bubbling fluidized bed reactor .....                                 | 68 |
| 5.1.2   | Modifications to the unit .....  | 70 |
| 5.1.2.1 | Temperature control bed heaters .....                                      | 70 |
| 5.1.2.2 | Temperature control trace heaters .....                                    | 70 |
| 5.1.2.3 | Data-Logging .....   | 71 |
| 5.1.2.4 | Additional water cooled heat exchanger .....                               | 71 |
| 5.1.3   | Mass balancing scheme .....  | 71 |
| 5.2     | Process parameters .....   | 73 |
| 5.2.1   | Minimum fluidization velocity .....  | 74 |
| 5.2.1.1 | Theoretical minimum fluidization velocity .....                            | 74 |
| 5.2.1.2 | Empirical determination of minimum fluidization velocity .....             | 75 |
| 5.2.1.3 | Evaluation of fluidization velocity .....                                  | 76 |
| 5.2.2   | Bed material and particle size .....                                       | 77 |
| 5.2.3   | Pyrolysis reactor temperature .....  | 78 |
| 5.2.4   | Hot vapour residence time .....  | 79 |
| 5.2.5   | Feed rate of biomass .....   | 80 |
| 5.2.6   | Feedstock moisture .....   | 80 |
| 5.2.7   | Quench system and liquid .....   | 81 |
| 5.3     | In-situ Nitrogenolysis .....   | 81 |
| 5.3.1   | Nitrogen compound, injection point and preheating .....                    | 81 |
| 5.3.2   | Nitrogen addition rate .....   | 83 |
| 6       | Pyrolysis and in-situ nitrogenolysis experiments .....                     | 84 |
| 6.1     | Introduction .....   | 84 |
| 6.2     | Pyrolysis of beech wood .....  | 86 |
| 6.2.1   | Results .....  | 86 |
| 6.2.2   | Analysis and discussion .....  | 89 |
| 6.3     | Fast pyrolysis of agricultural residues with a high nitrogen content ..... | 90 |
| 6.3.1   | Results .....  | 90 |
| 6.3.2   | Analysis and discussion .....  | 94 |
| 6.4     | Pyrolysis of agricultural and forestry residue with low N .....            | 95 |
| 6.4.1   | Results .....  | 95 |
| 6.4.2   | Analysis and discussion .....  | 97 |
| 6.5     | In-situ nitrogenolysis of beech wood at different N addition rates .....   | 98 |

|       |   |     |
|-------|---|-----|
| 6.5.1 | Results .....   | 98  |
| 6.5.2 | Analysis and discussion .....   | 103 |
| 6.6   | In-situ nitrogenolysis of beech wood – SRF production experiments.....  | 105 |
| 6.6.1 | Results .....   | 105 |
| 6.6.2 | Analysis and discussion .....   | 108 |
| 6.7   | Nitrogenolysis of DDGS – SRF production experiments.....                | 109 |
| 6.7.1 | Results .....   | 109 |
| 6.7.2 | Analysis and discussion .....   | 112 |
| 6.8   | Trouble shooting.....   | 113 |
| 7     | Solidification and modification of liquid products.....                 | 115 |
| 7.1   | Introduction.....   | 115 |
| 7.2   | Batch reactor .....   | 116 |
| 7.3   | Process parameters .....  | 117 |
| 7.3.1 | Temperature .....   | 117 |
| 7.3.2 | Pressure.....   | 117 |
| 7.3.3 | Processing time .....   | 117 |
| 7.3.4 | Catalyst.....   | 118 |
| 7.3.5 | Mass balances .....   | 118 |
| 7.4   | Solidification experiments – fast pyrolysis liquid .....                | 119 |
| 7.4.1 | Results and discussion.....   | 119 |
| 7.5   | Nitrogenolysis via fast pyrolysis liquid modification .....             | 121 |
| 7.5.1 | Fast pyrolysis liquid modification and solidification experiments ..... | 121 |
| 7.5.2 | Results and discussion.....   | 122 |
| 7.5.3 | Modification and solidification product washing experiments .....       | 124 |
| 7.5.4 | Results and discussion.....   | 125 |
| 7.6   | Solidification experiments of in-situ nitrogenolysis liquid .....       | 128 |
| 7.6.1 | Results and discussion.....   | 128 |
| 7.7   | Summary.....  | 129 |
| 8     | Analysis of fast pyrolysis and in-situ nitrogenolysis liquids .....     | 130 |
| 8.1   | Introduction.....   | 130 |
| 8.2   | Analytical Py-GC-MS in inert and reactive gas.....                      | 130 |
| 8.2.1 | Method.....   | 131 |
| 8.2.2 | Results .....   | 132 |
| 8.2.3 | Analysis and discussion .....   | 139 |
| 8.3   | GC-MS analysis of pyrolysis and in-situ nitrogenolysis liquids .....    | 140 |

|   |  |     |
|---|--|-----|
| 8.3.1   | Method.....  | 141 |
| 8.3.2   | Results .....  | 141 |
| 8.3.3   | Analysis and discussion .....  | 153 |
| 8.4   | Analysis of solidified fast pyrolysis and in-situ nitrogenolysis liquids via FTIR..... | 154 |
| 8.4.1   | Method.....  | 156 |
| 8.4.2   | Results .....  | 156 |
| 8.4.3   | Analysis and discussion .....  | 161 |
| 8.5   | Summary.....   | 162 |
| 9   | Microbial and plant testing .....  | 163 |
| 9.1   | Introduction.....  | 163 |
| 9.2   | Study on the impact of solidified fast pyrolysis products on microbial life in soil .. | 163 |
| 9.2.1   | Methods .....  | 164 |
| 9.2.2   | Results .....  | 164 |
| 9.2.3   | Analysis and discussion .....  | 168 |
| 9.3   | Study on the effect of in-situ nitrogenolysis derived SRF on plant growth.....         | 169 |
| 9.3.1   | Experimental setup and methods .....   | 169 |
| 9.3.2   | Results .....  | 171 |
| 9.3.3   | Analysis and Discussion.....   | 174 |
| 9.4   | Summary.....   | 175 |
| 10  | Conclusions .....  | 177 |
| 11  | Recommendations .....  | 181 |
| 12  | References.....  | 183 |
| Appendix .....  |  | 191 |
| Appendix A: Py-GC-MS analysis of high nitrogen feedstocks.....  |  | 191 |
| Appendix B: Analytical Py-GC-MS in inert and reactive gas ..... |  | 207 |

## List of tables

|   |     |
|---|-----|
| Table 1: Cellulose, hemicellulose and lignin content of biomass .....                           | 24  |
| Table 2: Pyrolysis types and typical product yield in wt.% on dry wood basis [19].....          | 27  |
| Table 3: Most relevant characteristics of fast pyrolysis liquid.....                            | 31  |
| Table 4: Functional groups in organic fraction of liquid product [34] .....                     | 41  |
| Table 5: Concentration of compounds in wt.% of organic fraction of liquid product [34].....     | 41  |
| Table 6: Balance of N in product according to Hanser’s mass balance .....                       | 45  |
| Table 7: Feedstock list.....  | 58  |
| Table 8: Proximate analyses of feedstocks .....   | 59  |
| Table 9: Ultimate analyses of feedstocks .....  | 61  |
| Table 10: Ether and hot water extraction results .....  | 62  |
| Table 11: Decomposition peaks of DTG analysis of selected feedstocks .....                      | 65  |
| Table 12: Suggested peak assignments of barley DDGS chromatogram .....                          | 67  |
| Table 13: Mass balancing scheme for 1kg/h bubbling fluidized bed rig.....                       | 72  |
| Table 14: Minimum fluidization data.....  | 75  |
| Table 15: Calculation of maximum hot vapour residence time.....                                 | 79  |
| Table 16: Product data ISOPAR™ V [85].....  | 81  |
| Table 17: Properties of Ammonia [86].....   | 82  |
| Table 18: Calculation of new nitrogen pre-heater set point .....                                | 82  |
| Table 19: List of pyrolysis and in-situ nitrogenolysis experiments .....                        | 85  |
| Table 20: Process parameters beech wood .....   | 86  |
| Table 21: Mass balance beech wood .....   | 87  |
| Table 22: Fast pyrolysis gas composition beech wood excluding fluidization nitrogen .....       | 88  |
| Table 23: Elemental analysis of beech wood fast pyrolysis products.....                         | 89  |
| Table 24: Process parameters high N feedstocks .....  | 90  |
| Table 25: Mass balance high N feedstocks .....  | 92  |
| Table 26: Elemental analyses and yields for high N feedstocks and fast pyrolysis products ..... | 93  |
| Table 27: Process parameters low N feedstocks .....   | 95  |
| Table 28: Mass balance low N feedstocks .....   | 96  |
| Table 29: Elemental analysis of low N feedstocks and FP chars.....                              | 97  |
| Table 30: Process parameters for beech wood with different N addition rates .....               | 99  |
| Table 31: Mass balance for beech wood with different N addition rates .....                     | 100 |
| Table 32: Elemental analysis of nitrogenolysis products at different N addition rates.....      | 101 |

|   |     |
|---|-----|
| Table 33: Process parameters for beech wood nitrogenolysis production runs.....             | 106 |
| Table 34: Mass balance for beech wood nitrogenolysis production runs.....                   | 107 |
| Table 35: Process parameters for Barley DDGS nitrogenolysis production runs.....            | 110 |
| Table 36: Mass balances of Barley DDGS nitrogenolysis production runs .....                 | 111 |
| Table 37: Mass balancing scheme of batch reactor setup.....                                 | 119 |
| Table 38: Conversion experiments with beech wood FP liquid.....                             | 119 |
| Table 39: Results of solidifying beech wood fast pyrolysis liquid.....                      | 120 |
| Table 40: Post processing experiments with fast pyrolysis liquid .....                      | 122 |
| Table 41: Results of modifying and solidifying beech wood FP liquid.....                    | 123 |
| Table 42: Recovered solids and nitrogen contents [in wt.%] .....                            | 125 |
| Table 43: Conversion experiments with nitrogenolysis liquids .....                          | 128 |
| Table 44: Results of conversion of nitrogenolysis products .....                            | 128 |
| Table 45: Py-GC-MS analysis sequence.....   | 131 |
| Table 46: Assigned Peaks in Py-GC-MS chromatogram for beech wood runs, RT 1-18min .....     | 138 |
| Table 47: Assigned Peaks in Py-GC-MS chromatogram for beech wood runs, RT 18-55min ...      | 139 |
| Table 48: Elemental analysis of investigated liquids .....                                  | 140 |
| Table 49: Assigned peaks for beech wood pyrolysis and nitrogenolysis liquids, RT 4-19min .. | 146 |
| Table 50: Assigned peaks for beech wood pyrolysis and nitrogenolysis liquids, RT 19-36min   | 148 |
| Table 51: Assigned peaks for barley DDGS pyrolysis and nitrogenolysis liquids, RT 19-36min  | 152 |
| Table 52: IR frequencies of specific bond types in functional groups [67, 68].....          | 155 |
| Table 53: Interpretation of IR spectra.....   | 160 |
| Table 54: Samples for microbial biomass study.....  | 164 |
| Table 55: Plant test treatments .....   | 170 |
| Table 56: Elemental analysis of dry matter samples of 1 <sup>st</sup> harvest .....         | 174 |

## List of figures

|  |     |
|--|-----|
| Figure 1: Research themes in the SUPERGEN Bioenergy II Consortium [3].....   | 19  |
| Figure 2: Routes to produce a renewable and sustainable nitrogenous fertiliser [5] .....   | 19  |
| Figure 3: Thermal decomposition of hemi-, cellulose, lignin and wood, redrawn from [12] .....  | 25  |
| Figure 4: Simplified kinetic scheme of the pyrolytic decomposition of biomass [13] .....   | 26  |
| Figure 5: Examples of applications of fast pyrolysis liquid .....  | 32  |
| Figure 6: van Krevelen Diagram (redrawn from [44, 45]) .....   | 34  |
| Figure 7: Essential plant nutrients [46] .....   | 35  |
| Figure 8: Nitrogen cycle (main cycle in bold lines) [46] .....   | 37  |
| Figure 9: Scheme of post-processing laboratory reactor setup, redrawn from [27].....   | 44  |
| Figure 10: Impact of urea addition to nitrogen content in product, redrawn from [27] .....   | 44  |
| Figure 11: Pyroprobe sample .....  | 54  |
| Figure 12: Pyrolysis TGA curve of selected feedstocks I .....  | 63  |
| Figure 13: Pyrolysis DTG of selected feedstocks I.....   | 63  |
| Figure 14: Pyrolysis TGA curve of selected feedstocks II .....   | 64  |
| Figure 15: Pyrolysis DTG of selected feedstocks II.....  | 64  |
| Figure 16: Example of Py-GC-MS Chromatogram of barley DDGS .....   | 66  |
| Figure 17: Flow diagram of fast pyrolysis reactor with condensation train (numbers are explained in the text that follows).....          | 68  |
| Figure 18: Reh diagram [81] with recalculated results indicated .....  | 77  |
| Figure 19: Fast pyrolysis yields of Aspen Poplar at different temperatures [16] .....  | 78  |
| Figure 20: Fast pyrolysis product yields for beech wood pyrolysis experiments (dfb).....   | 88  |
| Figure 21: Fast pyrolysis product yields of high N feedstocks .....  | 91  |
| Figure 22: Feedstock nitrogen distribution in fast pyrolysis products .....  | 94  |
| Figure 23: Fast pyrolysis product yields of low N feedstocks .....   | 97  |
| Figure 24: In-situ nitrogenolysis product yields for beech wood according to N addition rates  | 99  |
| Figure 25: Distribution of feedstock nitrogen in nitrogenolysis products and losses .....  | 102 |
| Figure 26: N content in nitrogenolysis liquids (black lines) and relative amount of N bound in nitrogenolysis products (grey line) ..... | 102 |
| Figure 27: Nitrogen distribution of added nitrogen in nitrogenolysis char and liquids.....   | 103 |
| Figure 28: Product distribution of beech wood nitrogenolysis production runs.....  | 108 |
| Figure 29: Product distribution of barley DDGS nitrogenolysis production runs .....  | 112 |
| Figure 30: Batch reactor setup.....  | 116 |

|   |     |
|---|-----|
| Figure 31: Fate of nitrogen in urea sample, experiment 8 .....  | 126 |
| Figure 32: Fate of nitrogen in ammonium phosphate sample, experiment 9.....                                       | 127 |
| Figure 33: Chromatogram of beech wood analytical pyrolysis in inert atmosphere .....                              | 133 |
| Figure 34: Chromatogram of beech wood analytical pyrolysis in ammonia atmosphere.....                             | 134 |
| Figure 35: Chromatogram of beech wood analytical pyrolysis with ammonium carbonate ...                            | 135 |
| Figure 36: Chromatogram of beech wood analytical pyrolysis in inert and reactive atmosphere,<br>RT 1-18min .....  | 136 |
| Figure 37: Chromatogram of beech wood analytical pyrolysis in inert and reactive atmosphere,<br>RT 18-55min ..... | 137 |
| Figure 38: Chromatogram of beech wood pyrolysis liquid .....  | 142 |
| Figure 39: Chromatogram of beech wood nitrogenolysis liquid top phase .....                                       | 143 |
| Figure 40: Chromatogram of beech wood nitrogenolysis liquid bottom phase.....                                     | 144 |
| Figure 41: Chromatogram of beech wood pyrolysis and nitrogenolysis liquids, RT 4-19min ..                         | 145 |
| Figure 42: Chromatogram of beech wood pyrolysis and nitrogenolysis liquids, RT 19-36min                           | 147 |
| Figure 43: Chromatogram of barley DDGS pyrolysis liquid.....  | 149 |
| Figure 44: Chromatogram of barley DDGS nitrogenolysis liquid .....  | 150 |
| Figure 45: Chromatogram of barley DDGS pyrolysis and nitrogenolysis liquids, RT 4-36min ..                        | 151 |
| Figure 46: IR spectra of beech wood solidified fast pyrolysis and nitrogenolysis liquid .....                     | 158 |
| Figure 47: IR spectra of barley DDGS solidified fast pyrolysis and nitrogenolysis liquid .....                    | 159 |
| Figure 48: CO <sub>2</sub> evolution of microbial study samples [95].....   | 165 |
| Figure 49: Microbial biomass carbon in microbial study samples [95] .....   | 165 |
| Figure 50: Bio-oil carbon degree of mineralization in microbial study samples [95] .....                          | 166 |
| Figure 51: NO <sub>3</sub> evolution of microbial study samples [95] .....  | 166 |
| Figure 52: NH <sub>4</sub> evolution of microbial study samples [95] .....  | 167 |
| Figure 53: Degree of N mineralization of microbial study samples [95] .....                                       | 167 |
| Figure 54: CO <sub>2</sub> evolution in different treatments in microbial study samples [95].....                 | 168 |
| Figure 55: Biomass carbon in different treatments of microbial study samples [95] .....                           | 168 |
| Figure 56: Randomized plant tests before the 1 <sup>st</sup> harvest.....   | 171 |
| Figure 57: Untreated soil sample, light green foliage.....  | 171 |
| Figure 58: SRF sample, darker green foliage.....  | 171 |
| Figure 59: Dry matter harvest yields of plant experiments .....   | 173 |

## List of equations

|   |    |
|---|----|
| Equation 1: Higher Heating Value according to unified correlation of Channiwala ..... | 50 |
| Equation 2: Higher Heating Value of Pyrolysis Gas.....                                | 51 |
| Equation 3: ERGUN equation .....  | 74 |
| Equation 4: Pressure drop of reactor bed .....  | 74 |
| Equation 5: WEN and YU equation .....   | 75 |
| Equation 6: Maximum hot vapour residence time .....                                   | 79 |
| Equation 7: Calculation of ammonia gas addition flow rate.....                        | 83 |

## List of abbreviations

|                  |  |
|------------------|--|
| AD               | Anaerobic digestion                                  |
| ar               | as received  |
| ATP              | ambient temperature and pressure, 20°C and 0.1MPa    |
| bdl.             | below detection level                                |
| daf              | dry ash free   |
| db               | dry basis  |
| dfb              | dry feedstock basis                                  |
| DTG              | Differential Thermo Gravimetry                       |
| Exp.             | Experiment   |
| FP               | fast pyrolysis                                       |
| GC               | Gas Chromatograph                                    |
| GC-MS            | Gas Chromatography-Mass Spectroscopy                 |
| DDGS             | Dried Distillers Grains with Solubles                |
| FTIR             | Fourier Transformed Infrared Spectroscopy            |
| HHV              | Higher Heating Value                                 |
| NCG              | non condensable gases                                |
| nd.              | not determined                                       |
| ni.              | Nitrogenolysis                                       |
| No.              | Number   |
| Py-GC-MS         | Pyrolysis-Gas Chromatography-Mass Spectroscopy       |
| RT               | retention time                                       |
| SRF              | Slow Release Fertiliser                              |
| T <sub>max</sub> | maximum residence time in hot reaction zone          |
| TCD              | Thermal Conductivity Detector                        |
| TGA              | Thermogravimetric Analysis                           |
| O*               | oxygen by difference                                 |
| wt.%             | weight percent                                       |
| wt.%C            | weight percent on dry feedstock carbon content basis |

# 1 Introduction

## ***1.1 Context and background***

The production of agricultural and horticultural products requires the use of nitrogenous fertiliser to provide the necessary growing conditions for the crops. At the same time conventional inorganic nitrogenous fertilisers can lead to large scale pollution of surface and ground water from nitrate leaching and run off leading to eutrophication of water courses. This loss also reduces the effectiveness of these fertilisers and increases costs. Additionally artificial nitrogenous fertilisers are produced from ammonia which causes a large carbon footprint as ammonia is mainly produced using the Haber Bosch process from fossil fuels such as natural gas or oil to provide the hydrogen and using nitrogen by air separation. In 2009 the worldwide production of ammonia was 130 million tonnes [2] causing a carbon dioxide release of 334 million tonnes. Slow release fertilisers can mitigate this problem by their controlled slow way to release nitrogen for plant growth. The use of slow release fertilisers can reduce the risk of run off and nitrogen leaching by their controlled way to release the nutrients, thereby reducing the amount of fertiliser applied and consequently lowering the carbon footprint. In addition a slow release fertiliser derived from biomass can even further lower the carbon footprint as biomass is carbon neutral.

This research project aims at and investigates the production of a slow release fertiliser from biomass and biogenic residues by fast pyrolysis to develop an alternative, sustainable and more effective route to supply the nitrogen needed for plant growth. This concept is very attractive as it reduces or even fossil fuel inputs, recycles biogenic residues and can reduce the risk of nitrogenous fertiliser run off and nitrate leaching. The production of ammonia via gasification of biomass and the production of slow release fertiliser from this biomass derived ammonia would be an alternative approach to the one chosen for this project. Nevertheless this route is far more energy intense and complex, because it requires an air separation unit, a gasifier, gas cleaning, CO-shift conversion and the ammonia synthesis.

The project was embedded in the SUPERGEN Bioenergy II Consortium as part of theme 5. SUPERGEN Bioenergy II follows a holistic approach investigating the different aspects of biomass and bioenergy from cradle to grave. The scope of research in SUPERGEN Bioenergy II is illustrated in Figure 1.



**Figure 1: Research themes in the SUPERGEN Bioenergy II Consortium [3]**

The method employed in this research project for the production of slow release fertiliser is nitrogenolysis. The term nitrogenolysis was coined by Bridgwater [4] combining the words nitrogen and pyrolysis. Nitrogenolysis is a process that aims to utilise the nitrogen in a nitrogen rich feedstock, such as rape meal or DDGS, and/or adds nitrogen during fast pyrolysis or to the fast pyrolysis products of biomass in order to produce a high nitrogen product for use as a fertiliser. An illustration of routes to produce a renewable and sustainable nitrogenous fertiliser is given in Figure 2.



**Figure 2: Routes to produce a renewable and sustainable nitrogenous fertiliser [5]**

## **1.2 Objectives**

The overall objective of this research project is to investigate a renewable route to slow release fertilisers from biomass and biogenic residues. The aim is to develop a product that can be used in present farming machines, is easy to store and handle and slowly releases its nitrogen. Due to the nature of liquid-pyrolysis products it was decided to aim at the production of a solid. In order to achieve this objective the research project investigates fast pyrolysis to determine the conversion behaviour of biomass and establish a data base for evaluation, and nitrogenolysis of biomass and biogenic residues by either utilising the nitrogen contained in the residues or by adding a source of nitrogen during the process. For a systematic approach the overall objective was subdivided into six subtasks that are described in the following sections.

### **1.2.1 Subtask 1: Feedstocks and characterization**

A variety of biomass feedstocks and biogenic residues were acquired and investigated for their potential use as feedstocks in the nitrogenolysis process. As one method for nitrogenolysis aimed to utilise the nitrogen present in the feedstock (see section 1.2.3), materials with high nitrogen were preferred. The feedstocks were characterized using proximate and ultimate analysis, extraction methods for oil and hot water soluble content, Thermogravimetric Analysis (TGA) and analytical Pyrolysis-Gas Chromatography-Mass Spectroscopy (Py-GC-MS). Section 4 is dedicated to this subtask.

### **1.2.2 Subtask 2: Fast pyrolysis**

After characterization, the feedstocks were processed using fast pyrolysis. A 1kg/h bubbling fluidized bed fast pyrolysis reactor was used for the experiments due to its demonstrably reliable feeding system and overall processing capacity over many years of operation. The reactor was critically reviewed to improve process control and minimise the possibility of system break-down and a number of modifications were implemented. These are discussed and described in section 5.1.2. Sections 5 and 6 are dedicated to the processing part of this subtask and section 8 to the analytical part.

### **1.2.3 Subtask 3: In-situ nitrogenolysis**

There are three ways of carrying out nitrogenolysis in order to achieve a product with high nitrogen content. The first way is to use a high nitrogen feedstock in the fast pyrolysis process. The second way is to use a high or low nitrogen feedstock combined with a nitrogen containing reactant and processing both together by fast pyrolysis. Both ways are in-situ processes as the high nitrogen product is formed in the fast pyrolysis step. The third way is to use a high or low nitrogen feedstock, pyrolysing it in a fast pyrolysis process to obtain fast pyrolysis liquid and reacting the fast pyrolysis liquid with a nitrogen containing reactant (post processing).

In this research project in-situ nitrogenolysis experiments on an analytical scale were performed using Py-GC-MS without and with ammonia or ammonium carbonate to investigate their impact on the product spectrum (see section 8.2). A strategy to feed a nitrogen containing compound into the 1kg/h bubbling fluidized bed fast pyrolysis reactor was developed. Feeding gaseous ammonia was decided to be more suitable than the use of ammonia salts. In-situ nitrogenolysis experiments were performed to establish an optimal nitrogen addition rate and produce in-situ nitrogenolysis product for further testing. Sections 5 and 6 are dedicated to the processing part of this subtask and section 8 to the analytical part.

### **1.2.4 Subtask 4: Solidification of liquid nitrogenolysis product**

In order to obtain a solid product a suitable solidification process was developed. A solid product was preferred as fast pyrolysis liquids are known for ageing issues and as industry and farming sector prefers solids for the ability of mixing and use of existing spreading machines. Due to the specific characteristics of fast pyrolysis liquid and its production process a thermal solidification process was chosen. Section 7 is dedicated to this subtask.

### **1.2.5 Subtask 5: Nitrogenolysis via fast pyrolysis liquid modification**

Additionally an alternative approach of post processing nitrogenolysis via fast pyrolysis liquid modification was investigated in a combined nitrogen enrichment and solidification process (see third way of nitrogenolysis, section 1.2.3). This work was carried out as an alternative to the in-situ nitrogenolysis routes. Section 7 is dedicated to this subtask.

### **1.2.6 Subtask 6: Microbial and plant tests**

The products obtained from fast pyrolysis and in-situ nitrogenolysis were tested regarding their impact on microbial life in soils and in plant tests in cooperation with the agricultural research centre Rothamsted Research in Harpenden (UK). These experiments investigated the toxicity, bio degradability and use of the products as slow release fertiliser. Furthermore the in-situ nitrogenolysis products were compared to conventional fertilisers. The experimental setup and parameters for these experiments were developed in close cooperation with the project partners at Rothamsted Research. The material tested was produced in the fast pyrolysis unit by the in-situ nitrogenolysis experiments and solidified in a batch process. The actual microbial and plant tests were executed by Rothamsted Research. The data obtained from the microbial tests was provided by Rothamsted Research including an interpretation and the biological plant test data was provided as raw data. Section 9 is dedicated to this subtask.

## **2 Literature review**

### ***2.1 Introduction***

This research project utilises high and low nitrogen biomass and biogenic residues in the fast pyrolysis and nitrogenolysis processes. It is important to review the basic characteristics of such materials as well as their thermal decomposition behaviour, because the nitrogenolysis process is based on the thermal fast pyrolysis process. Therefore biomass and biogenic residue components are reviewed in section 2.2, the fast pyrolysis process in section 2.3 and the fast pyrolysis products in section 2.4 in order to give a better understanding of the feedstock, the technical process, its parameters and products. The state of the art of the Nitrogenolysis process is presented in a separate section 2.6.

Slow release fertiliser was the desired product in this research project and was investigated in cooperation with Rothamsted Research in microbial and biological plant tests as part of the project. In order to understand the requirements for a fertiliser and the mechanisms of nutrient mineralization and uptake these topics are reviewed in section 2.5. State of the art slow release fertilisers and their production methods are presented in section 2.6.

### ***2.2 Biomass and biogenic residues***

#### **2.2.1 Introduction**

The present research project uses biomass and biogenic residues as feedstocks with the restriction that only solid terrestrial biomass from plants and their residues were used. In this thesis the term biomass just refers to such materials. As nitrogenolysis is based on fast pyrolysis (see section 1.2.3) it is important to understand the thermal decomposition behaviour of biomass. This behaviour is mainly determined by its three main components cellulose, hemicellulose and lignin. Table 1 lists the content of these components in beech wood, DDGS, rape meal and wheat straw. The thermal decomposition products of these components can be found in the fast pyrolysis and nitrogenolysis products. In order to understand the properties of the products and to analyse these, e.g. by Py-GC-MS and GC-MS (see sections 4.2.5, 8.2, 8.3), it is important to review cellulose, hemicellulose and lignin.

**Table 1: Cellulose, hemicellulose and lignin content of biomass**

| Biomass     | Unit     | Cellulose | Hemicellulose | Lignin | Extractives | Literature |
|-------------|----------|-----------|---------------|--------|-------------|------------|
| Beech wood  | wt.%, db | 43.3      | 31.8          | 24.4   | 0.5         | [6]        |
| DDGS        | wt.%, db | 15.1      | 30.3          | 6.1    | 48.5        | [7]        |
| Rape meal   | wt.%, db | 28.6      | 41.0          | 5.0    | 25.4        | [8]        |
| Wheat straw | wt.%, db | 45.4      | 28.3          | 18.7   | 7.6         | [9]        |

### 2.2.2 Cellulose

Cellulose is a structural component of the cell walls in biomass. It is an unbranched polymer (linear homopolysaccharide) of  $\beta$ -D-glucopyranose moieties joined by  $\beta$ -(1-4)-glycosidic bonds [10]. It is intra and inter molecular bonded by hydrogen bonds and water insoluble. Cellulose can be hydrolysed forming glucose using concentrated acids and elevated temperatures.

### 2.2.3 Hemicellulose

Hemicellulose is a heteropolysaccharide. In contrast to cellulose it contains different sugar monomers and consist of hexoses (D-glucose D-mannose, D-galactose) and pentoses (D-xylose, L-arabinose) and other components such as mannuronic acid and galacturonic acid [10]. Hemicellulose is part of any cell wall in lignocellulosic biomass.

### 2.2.4 Lignin

Lignin is the most complex chemical compound within lignocellulosic biomass and is one of the major components in wood (see Table 1). The term lignin is derived from the Latin word *lignum*, meaning wood. In contrast to cellulose and hemicellulose, lignin is a three-dimensional cross-linked polymer with rather random structure and forms an amorphous insoluble thermoplastic. The monomers of lignin can be regarded as aromatic phenyl-propane units and are therefore hydrophobic [10]. Lignin fills spaces in the cell wall between other components and is covalently linked to hemicellulose. The cross linking of different cell wall components increases the mechanical strength.

### 2.2.5 Thermal decomposition behaviour of biomass

The decomposition reactions of biomass show differences due to the different bond energies of the chemical bonds within and in between the monomers of macro molecules [11]. Figure 3 shows the thermogravimetric analysis of cellulose, hemicellulose lignin and wood.

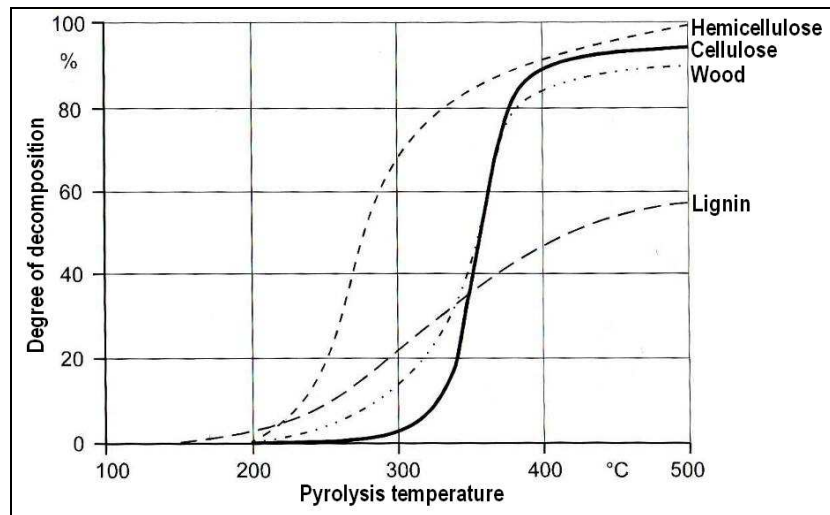


**Figure 3: Thermal decomposition of hemi-, cellulose, lignin and wood, redrawn from [12]**

Hemicellulose is thermally unstable and decomposes quickly. Cellulose is thermally more stable than hemicellulose and decomposes into gaseous products that are mainly condensable. In contrast lignin decomposes relatively slowly over a wide temperature range and produces higher char yields [11].

As illustrated in Figure 3 the decomposition of the cellulose and hemicellulose begins at about 220°C initially creating water, carbon monoxide, carbon dioxide, methanol and acetic acid [11]. At temperatures around 350°C most of the hemicellulose is already decomposed and cellulose reaches its highest decomposition rate. The weight loss curves indicate the end of cellulose and hemicellulose decomposition at about 400°C with typically more than 85wt.% weight loss, as well as the beginning of the end of the lignin decomposition. This characteristic behaviour is important as it indicates that biomass consisting of these components should show similar decomposition behaviour. Thermogravimetric analysis results of feedstocks investigated are presented in section 4.2.4.

A simplified kinetic reaction scheme can be assumed for the pyrolysis of biomass which is presented in Figure 4. It is assumed that three parallel reaction alternatives with different coefficients for the reaction rate ( $k_1$ ,  $k_2$ ,  $k_3$ ) exist. The activation energies  $E_1$  till  $E_3$  are increasing. Additionally secondary reactions of condensable products in the gas phase are considered ( $k_4$ ), which are further decomposing condensable products into permanent gases or form char. [13]

Reaction 1 ( $k_1$ ) is the main reaction path at lower temperatures, typical for conventional slow pyrolysis processes; the main products are char, carbon dioxide and water vapour. At elevated temperatures reaction 2 ( $k_2$ ) is predominant, which leads to higher yields in liquid product. This is the desired reaction for the fast pyrolysis. Due to further secondary reactions in the vapour phase condensable compounds are cracked ( $k_4$ ) and form carbon dioxide, hydrogen and methane. Reaction 3 ( $k_3$ ) mainly takes place at high temperatures and leads to high yields in gases. [13]

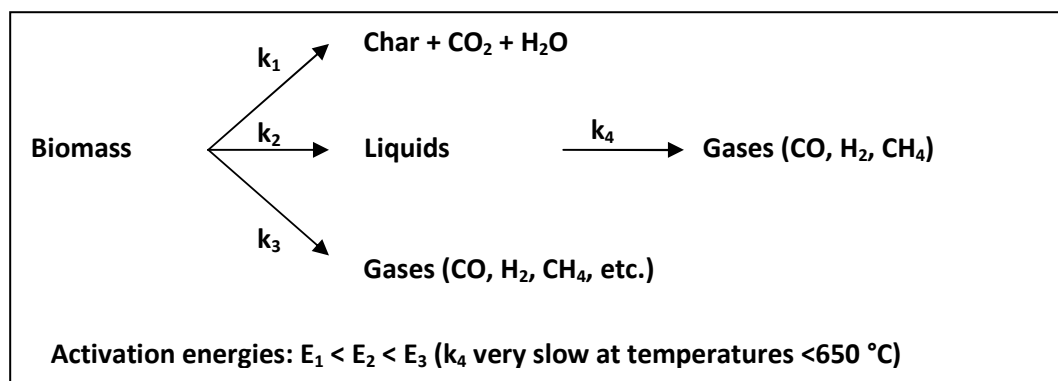


**Figure 4: Simplified kinetic scheme of the pyrolytic decomposition of biomass [13]**

An exact prediction of the different pyrolysis product yields cannot be made according to this simplified model, because of the heterogeneous nature of biomass, the high reactivity of the volatile products, the poor thermal conductivity of biomass and the catalytic effect of char particles [11] and alkaline metals in the ash [14, 15]. The product yields therefore can just be interpreted as a sum of the three reactions displayed in Figure 4 [11].

## 2.3 Fast Pyrolysis

### 2.3.1 Introduction and fast pyrolysis

Pyrolysis is a the thermo-chemical conversion processes in the absence of oxygen [16, 17]. During pyrolysis of biomass, organic materials are heated in an inert atmosphere up to 1000°C. Due to thermal decomposition solid, liquid and gaseous products are formed. The C-C and C-H bonds of the macro molecules are preserved although in a different structural composition during pyrolysis [18]. There are three crucial parameters in pyrolysis that have a direct influence on the product yields and product distribution. These are pyrolysis temperature, heating rate and hot vapour residence time above 200°C [19]. Consequently these parameters can be used for process control. The different pyrolysis types and typical product yield on dry



**Figure 1: Research themes in the SUPERGEN Bioenergy II Consortium [3]**

The method employed in this research project for the production of slow release fertiliser is nitrogenolysis. The term nitrogenolysis was coined by Bridgwater [4] combining the words nitrogen and pyrolysis. Nitrogenolysis is a process that aims to utilise the nitrogen in a nitrogen rich feedstock, such as rape meal or DDGS, and/or adds nitrogen during fast pyrolysis or to the fast pyrolysis products of biomass in order to produce a high nitrogen product for use as a fertiliser. An illustration of routes to produce a renewable and sustainable nitrogenous fertiliser is given in Figure 2.



**Figure 2: Routes to produce a renewable and sustainable nitrogenous fertiliser [5]**

Transport of the fast pyrolysis products within the reactor are of special interest. Beside temperature, the residence time of condensable vapours in the hot reaction zone plays an important role. It needs to be kept as short as possible to prevent unwanted secondary reactions that will convert condensable vapours into permanent gases, water vapour and char (see section 2.2.5). Additionally the presence of fast pyrolysis char, which retains all the ash components from the biomass, has an impact on the product distribution as it acts as a catalyst. Experiments that used fast pyrolysis char as a bed material in a fluidized bed reactor showed that the gas yields more than doubled [20]. At the same time the fast pyrolysis liquid yield decreased by 30 wt.% and the fast pyrolysis char yield increased [20]. Therefore it is necessary that the fast pyrolysis char is removed from the hot reaction zone as quickly as possible and separated effectively from the pyrolysis vapours. A common way in bubbling fluidized bed reactors is the use of a cyclone at the reactor outlet.

### **2.3.2 Fast pyrolysis reactor types**

The central part of the fast pyrolysis process is the reactor. Its design and its applied working principle need to meet the requirements of the fast pyrolysis process. The following main reactor types are used or have been developed [22]:

- Bubbling fluidized bed reactor
- Circulating fluidized bed and transported bed reactor
- Ablative reactor
- Entrained flow reactor
- Rotating cone reactor
- Vacuum reactor

There are several reviews published giving detailed descriptions of the different reactor types [16, 22, 23]. The review of Bridgwater and Peacocke [22] explored fast pyrolysis reactors for the production of liquids. Among the different reactor types, fluidized bed reactors are widely used in academia and are currently used in commercial production of pyrolysis liquid, e.g. Dynamotive in Canada [25]. An extensive list of all reactor types and their application was published by Bridgwater [26].

Bubbling fluidized bed reactors are used in many applications and are a proven technology. Their advantages in fast pyrolysis can be summarized as [16, 27]:

- high heat transfer rates and low temperature gradients in the reaction zone
- good temperature control of the reaction zone
- short hot vapour residence time (below 2s) above 200°C
- no moving parts inside the reactor and therefore easy to seal
- easily scalable to commercial sizes
- well established and well understood process

Due to the working principle of a bubbling fluidized bed reactor, there are several requirements that need to be met for processing. The static bed height, bed expansion and freeboard height have to be considered to avoid entrainment of bed material. The density difference between bed material and fast pyrolysis char needs to be sufficient to allow only the entrainment of the fast pyrolysis char. The fluidization velocity has to be determined so that the fast pyrolysis char is entrained, while the bed material remains in the reactor (see section 5.2).

## ***2.4 Fast pyrolysis products of biomass***

### **2.4.1 Introduction**

In this research project the fast pyrolysis and nitrogenolysis processes were used to produce fast pyrolysis liquid, fast pyrolysis char and nitrogenolysis products for use as slow release fertiliser. Therefore fast pyrolysis products of biomass are reviewed in this section to understand the characteristics and properties of the substances produced in this research project. Fast pyrolysis of biomass generally produces three different fractions [16, 27]:

- fast pyrolysis liquid consisting of mostly oxygenated organic compounds and polar compounds
- fast pyrolysis gas containing mostly carbon dioxide, carbon monoxide and methane
- fast pyrolysis char including the inorganic compounds forming the ash as solid residues of the fast pyrolysis process

The focus of this research project is on the liquid phase with a typical water content between 20 and 30wt.%.

## 2.4.2 Fast pyrolysis liquid

Fast pyrolysis liquids have been well described and characterized in the literature [19, 28-30]. They are of low viscosity, dark red to dark brown colour and a distinct smoky smell [28, 31]. They can have a high water content which results from the water content of the feedstock and water produced during fast pyrolysis [32]. Depending on the water content and the composition of the feedstock (especially high ash content), phase separation into an aqueous phase and an organic phase can occur [32].

The organic components of fast pyrolysis liquid consist mainly of a mixture of alcohols, furans, phenols, aldehydes, organic acids as well as carbohydrate [33, 34]. Hence fast pyrolysis liquid consists of several hundred components that can be grouped according to their functional groups: carboxyl-, carbonyl-, aldehyde-, ester-, acetal-, hydroxyl-groups, olefins phenols and aromatic compounds. The composition is dependent on the feedstock, production process, collection system and the storage conditions [11, 19]. Fast pyrolysis liquids are just non-miscible with hydrocarbons. They can be mixed with alcohols [35]. Mixing with water is possible up to about 45 wt.% when phase separation occurs and a tar-like product will separate from a low viscosity aqueous phase. This tar-like product is derived from the high molecular lignin products and is referred to as pyrolytic lignin in literature [36]. The water soluble fraction of phase separated fast pyrolysis liquid is mainly the product of the decomposition of cellulose and hemicellulose [11]. Fast pyrolysis liquid is acidic due to organic acids, e.g. acetic acid and formic acid. The pH-value is typically around pH 2 to 3. For most fast pyrolysis liquids the heating value on a weight basis is about 40% of the heating value of fossil fuel oils and 60% on a volume basis. The viscosity of fast pyrolysis liquids varies significantly and is dependent on the water content, content of light compounds and the storage time. During storage fast pyrolysis liquid has the tendency to undergo condensation reactions due to reactive compounds, which leads to an increasing viscosity [29]. This process is often referred to as aging. Fast pyrolysis char and elevated temperatures enhance this process and the addition of alcohol reduces this effect [35]. Skin and eye contact should be avoided as some compounds are regarded as carcinogenic [11]. Bridgwater described 26 characteristics of fast pyrolysis liquid [32]. The ones regarded as most relevant to the aim of this project are listed in Table 3.

**Table 3: Most relevant characteristics of fast pyrolysis liquid**

| Characteristic              | Cause   | Effect   | Relevance   |
|-----------------------------|---|--|---|
| Acidity or low pH           | organic acid from bio-polymer degradation                     | corrosion  | negative impact on microbial life and plant growth and possible reactions of organic acids with ammonia during nitrogenolysis |
| Aging                       | continuation of secondary reactions, including polymerization | slow increase in viscosity from secondary reactions such as condensation | key factor for the production of a solid SRF  |
| Alkali metals               | nearly all alkali metal report to char                        | deposition of solids in combustion                                       | use of char for nutrient recycling  |
| Char                        | incomplete char separation in process                         | aging of oil   | key factor for the production of a solid SRF  |
| Nitrogen                    | contaminants in biomass feed                                  | NO <sub>x</sub> in combustion  | incorporation of nitrogen in the SRF product  |
| Oxygen content is very high | biomass composition   | poor stability   | key factor for the production of SRF in terms of binding added nitrogen and producing a solid                                 |
| Temperature sensitivity     | incomplete reactions  | aging and phase separation   | key factor for the production of a solid SRF  |
| Toxicity                    | bio-polymer degradation products                              | eco-toxicity is negligible   | impact on microbial life and plant growth   |

The production of slow release fertiliser by nitrogenolysis processes uses the above stated characteristics of fast pyrolysis liquids. Especially nitrogen in the biomass feedstock is of great interest as nitrogenolysis aims to incorporate it in the SRF product (see section 1.2.3). The high oxygen content is due to oxygenated compounds, in particular functional groups such as carbonyl and carboxyl groups, which are important to potentially bind added nitrogen to the nitrogenolysis SRF (see section 2.6.2). Aging reactions and the impact of char and elevated temperatures on fast pyrolysis liquid stability are key factors for the production of a solid product by a thermal solidification process (see section 1.2.4). The aspects of acidity and alkali metals are relevant due to their impact on microbial life in soils and plant growth (see section 1.2.6).

### 2.4.3 Applications of fast pyrolysis liquids

The following figure provides examples of possible fast pyrolysis liquid applications. Applications can be categorized according to the production of energy or chemicals [11, 19].

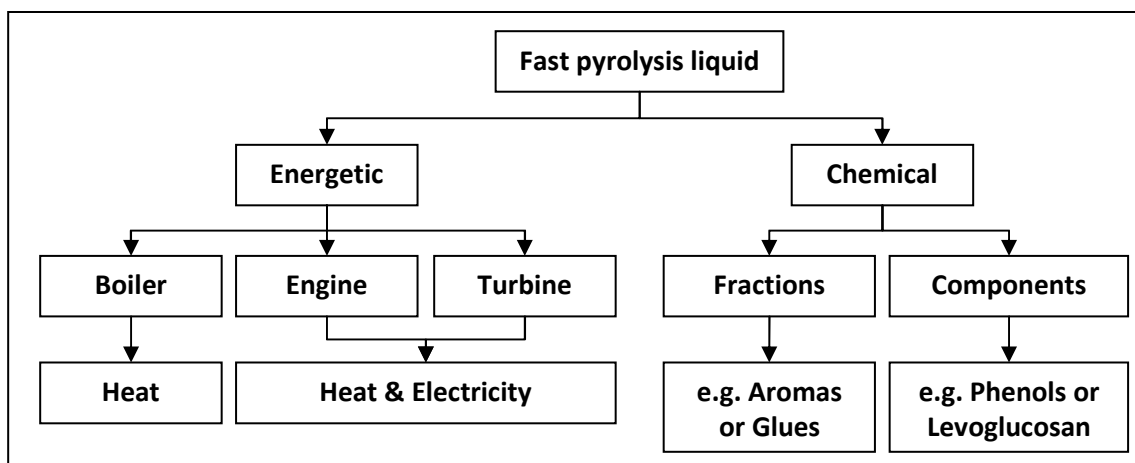


**Figure 5: Examples of applications of fast pyrolysis liquid**

Several different technologies are available for the energetic use of fast pyrolysis liquid. Details on this topic are part of many publications, such as Bridgwater [19], Czernik and Bridgwater [28] and Gerdes [11]. Alternatively fast pyrolysis liquid can also be used as a source of chemicals [16]. Examples include the use of the aqueous phase to produce liquid smoke [37], the separation of levoglucosan a product of the decomposition of cellulose [37] or the substitution of phenol and formaldehyde as adhesive in the production of chip board [38].

Another possibility is the use of the fast pyrolysis liquid in combination with a nitrogen containing compound in the nitrogenolysis process (see section 1.2.3) to produce a slow release fertiliser. The functional groups of the fast pyrolysis liquid shall therefore react with the nitrogen to form a higher molecular compound that is slowly decomposed by bacteria in the soil forming nitrate [34]. This application route is described in greater detail and discussed in section 2.6.

Regarding this research, the fast pyrolysis char is of importance for two aspects. The first is that it accelerates aging reactions in fast pyrolysis liquids (see section 2.4.2) and the second is that it contains almost all alkali metals of the feedstock that are nutrients for plant growth (see section 2.5.2).

#### **2.4.4 Fast pyrolysis gas**

Fast pyrolysis gas is the by-product of fast pyrolysis [32]. It mainly consists of carbon dioxide, carbon monoxide, some hydrogen and hydrocarbons up to C-4 [11]. In bubbling fluidized bed and circulating fluidized bed systems it can be used as fluidizing gas, either non-oxidized or oxidized to provide part of the process heat. If flue gas or inert gas is used for fluidization, the fast pyrolysis gas is heavily diluted with this gas. Fast pyrolysis gas can be used to provide a part of the necessary process heat or for pre-drying the feedstock [16]. Dynamotive in Canada uses fast pyrolysis gas as part of the heat source for their bubbling fluidized bed system and fluidization gas [25] which is supplemented with natural gas.

In this research project the fast pyrolysis gas was heavily diluted with inert nitrogen fluidization gas due to the design of the 1kg/h bubbling fluidized bed reactor (see section 5.1.1). It was not further used except for gas analysis and mass balancing purposes (see section 5.1.3).

#### **2.4.5 Fast pyrolysis char**

Fast pyrolysis char is considered a by-product in fast pyrolysis [32]. It contains almost all components forming the ash content of the biomass feedstock including the alkali metals [32]. Depending on the fast pyrolysis process it is either burned to provide process heat (e.g. rotating cone reactor) [26] or can be separated from the other products and then either be burned or used for different applications (e.g. fluidized bubbling bed reactor with cyclones) [26]. An alternative use of fast pyrolysis char is the production of activated carbon [26]. Lately the use of pyrolysis char for soil amendment (BIOCHAR) is of special interest not only for its soil improving characteristics, but also for reasons of carbon sequestration [39]. This aspect is presented in section 2.4.6.

#### **2.4.6 Pyrolysis char as soil amendment**

An alternative application for pyrolysis char is the use as soil amendment. Currently the role of char as soil amendment is investigated under two major aspects. The first one is its capability as soil conditioner; the second one is its potential to act as a carbon sink for carbon sequestration purposes.

The use of char as soil conditioner is currently being investigated by many researchers. The technique itself is not new as it had been used by indigenous people in pre Columbian times in

the Amazonian rainforest adding large amounts of char to the soil creating what is today known as Terra Preta or black soil [40]. In the relatively poor soils (like Ferralsols) the addition of char increases the ability of the soil to hold moisture and nutrients that are essential for plant growths [40, 41]. Experiments using char as soil conditioner showed that crop yields were significantly higher with added char [41].

The use of char as a carbon sink for carbon sequestration is also investigated intensively. The Terra Preta soils already show that the degradation rate of char can be very slow as these soils are several thousand years old [40]. Steinbeiss et al. [42] investigated the effect of char addition to the soil carbon balance. It was pointed out that after an initial increase the microbial activity this effect reduced and a large quantity of the added carbon remained in the soil. Cheng et al. [43] described that the molecular form and surface charge of char are changing over time. It was also pointed out that chars resulting from pyrolysis processes at about 500°C are more resistant to microbial degradation than those produced at lower temperatures [43]. Chars from fast pyrolysis processes have an atomic H:C and O:C ratio which is close to the ratios of coals. This is also illustrated in the van Krevelen diagram in Figure 6.

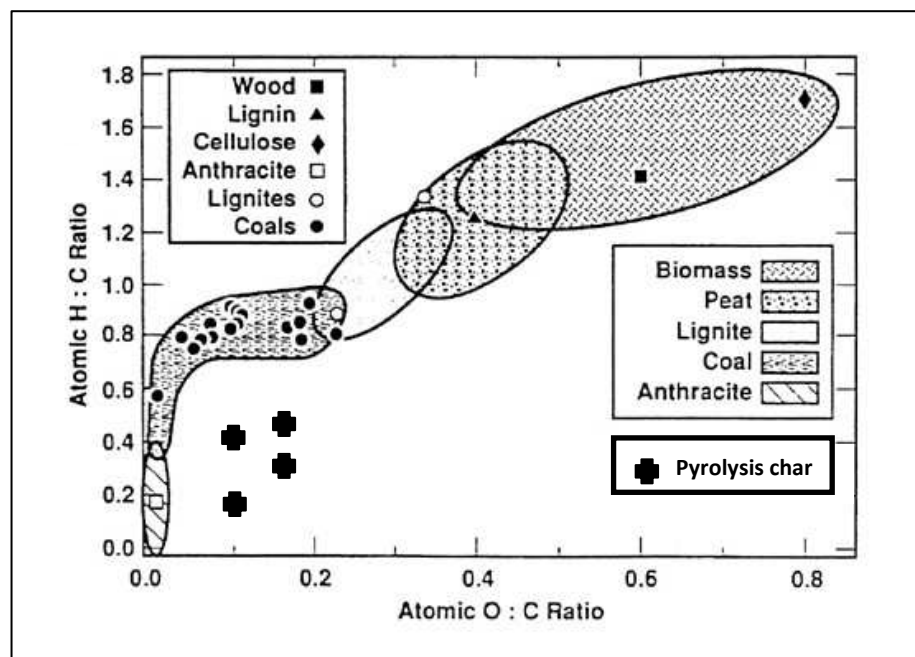


**Figure 6: van Krevelen Diagram (redrawn from [44, 45])**

Char as a soil amendment, therefore, has a great potential as a soil conditioner and a carbon sink. In terms of this research the char produced could be seen as a valuable by-product for these purposes as it is separated and not burned.

## 2.5 Plant nutrition

### 2.5.1 Introduction

One of the aims of this research is to investigate the production of slow release fertiliser by modification of the fast pyrolysis process. Therefore it is necessary to take aspects of nutrient supply and nutrient uptake by plants into consideration. The complexity of this field does not allow a very deep insight into this topic as it would exceed the possibilities given within this research. Nevertheless general aspects are summarized in this section, that are important for the understanding of this project. Due to the complexity of this field the microbial and plant test were done in close cooperation with Rothamsted Research (see section 1.2.6).

### 2.5.2 Plant nutrients

Seventeen elements have been identified as essential plant nutrients [46]. Beside carbon, hydrogen and oxygen that are provided by water and air further fourteen elements are needed. A comprehensive overview of these is illustrated in Figure 7, subdividing them into macro and micro nutrients. Although sodium is also absorbed in large quantities by plants it is not regarded as essential and it is just absorbed due to its abundance, as other elements such as aluminium or silicon.



**Figure 7: Essential plant nutrients [46]**

Another key element regarding nutrients present in soil is their availability to the plants [46]. Only part of the nutrients present is actually available to the plant and most of them are locked up in mineral or organic materials. For absorption into the plant nutrients need to be in ionic form. Metals are usually absorbed by the plants as cations, nitrogen either as  $\text{NH}_4^+$  or  $\text{NO}_3^-$ , phosphorous as  $\text{H}_2\text{PO}_4^-$  or  $\text{HPO}_4^{2-}$  and sulphur as  $\text{SO}_4^{2-}$ . All of nutrients in the soil must be dissolved in water in order to be taken up by the plants roots [46].

### 2.5.3 Nitrogen cycle / bio-degradation

As described above nitrogen is one of the macro nutrients and is commonly applied in commercial fertilisers containing nitrogen, phosphorous and potassium. Nitrogen is the key element in nitrogenolysis and is the focus of this research and therefore the natural nitrogen cycle in plant growth is presented in this section.

Figure 8 depicts an idealized nitrogen cycle by bio-degradation indicating the main cycle in bold lines [46]. There are two major stages in the cycle, the mineralization and the mobilization stage. Residues from plants and life forms containing organic nitrogen in the form of  $-NH_2$  groups are mineralized through stages of ammonification releasing nitrogen as  $NH_4^+$  and nitrification forming  $NO_3^-$  by biological activity. Part of the nitrogen is immobilized in this process due to growth of microbial population in the soil, but later released when the microbes start to decompose themselves. The mineralized nitrogen in the form of ammonium ions and nitrates are taken up by the plants and immobilized, until the plant material dies off and starts the cycle again [46].

As the additional lines in Figure 8 indicate this process is not a closed cycle, so that additional losses and gains have to be taken into consideration. Especially the removal of nitrogen from the field by harvesting is an important factor as this needs to be compensated by fertilization to keep the soil fertile.

For the aim of this research this simplified model gives a comprehensive overview why fertiliser application is necessary and in what form the nitrogen is available to the plant. Further information is available in literature, e.g. *Soils and Soil Fertility* by Troeh and Thompson [46] or *The Use of Nutrients in Crop Plants* by Fageria [47].



**Figure 8: Nitrogen cycle (main cycle in bold lines) [46]**

#### **2.5.4 Microbes**

The previous section already mentioned that microbial life in soils is a vital factor in the mineralizing process. As the SRF produced in this research was tested on its impact on microbial life in soils some key aspects are presented in this section. Microbes in soils are formed of members of the plant and animal kingdom. They can be subdivided into six groups and more detailed information can be found in literature [46]:

- Bacteria
- Actinomycetes
- Fungi
- Algae
- Protozoa
- Nematodes

All microbes play an important role in the nitrogen cycle as they are participating in the decomposition process of organic material in the soils. Microbial activity in soils is essential in the mineralization process of nutrients from dead plant and animal tissue and without it the nitrogen cycle could not work [46]. Consequently an active microbial population can be regarded as a good indicator for soil fertility and potential to stay productive. Major factors for the activity of microbial life in soils are:

- sufficient energy supply
- aeration
- water
- temperature
- pH of soil

The last factor pH is suitable for most microbes to thrive if close to neutral or slightly alkaline. An addition of lime therefore can lead to an increase in microbial activity. Also an increase in soil temperature can encourage microbial activity as it does not exceed a certain temperature and the soil does not become too dry [46].

Due to the important role of microbial life in soils, the impact of the slow release fertiliser produced via nitrogenolysis on these organisms needed to be investigated. One aspect is the toxicity of the slow release fertiliser to microbial life, another ability of the microbes to mineralize the slow release fertiliser and thereby setting free the nitrogen in the product. The reaction of microbial activity on application of the slow release fertiliser under constant growing conditions was a good indicator to its toxicity, degradability and suitability for plant tests (see section 1.2.6).

## **2.6 Nitrogenolysis and Slow release fertiliser**

### **2.6.1 Introduction**

The term nitrogenolysis was coined by Bridgwater (see section 1.1) and so far is not commonly used in literature. Nevertheless the processes described by this term have been part of investigations by Radlein, who filed a patent presented in section 2.6.2, and as part of a European project, that is presented in section 2.6.3. There are also similarities to a process called ammoxidation that is presented in section 2.6.4. As an alternative to the above stated processes state of the art commercial production processes are described in section 2.6.5.

In general slow release fertilisers (SRF) can be produced by incorporating nitrogen into more complex structures, either by chemically bonding it or coating it. During nutrient release from the SRF into the soil nitrogen compounds are converted by microbial activity to  $\text{NH}_4^+$  and by nitrification to nitrate (see Figure 8) which plants can absorb. Beside coating fertiliser granules or using special compounds containing nitrogen, several ways to bind nitrogen to a slowly degradable substrate have been investigated in past decades as described in the following section. The scope of materials reaches from the use of peat and low quality lignite, technical lignin to pyrolysis products. Also commercial production of SRF is described in the following sections.

### **2.6.2 Methods of producing organic slow-release nitrogenous fertiliser**

Radlein et al. filed an European patent EP0716056 A1 on a method of producing slow-release nitrogenous organic fertiliser from biomass [34]. The patent describes the production of organic slow release fertiliser by reacting ammonia or a related compound with the products of the fast pyrolysis process of biomass. It points out that biomass already contains about 34-44wt.% of oxygen and that it is desirable to maintain this oxygen content in the form of functional groups by using fast pyrolysis as a thermal conversion route.

The patent is based on “the discovery” that fast pyrolysis liquid readily reacts with ammonia or related nitrogen compounds. As it is a known fact that pyrolysis liquids contain relatively high concentrations of carbonyl-, carboxyl-, phenolic-groups and also aldehydes (known since wood

distillation) and that these compounds readily react with ammonia or related nitrogen compounds it is debateable if this is a discovery or an alternative application. It also states that fast pyrolysis liquids contain a substantial amount of pyrolytic lignin that is likely to be a good source of humic acid as it is supposed to have a similar structure to natural lignin [34]. The use of partially pyrolysed lignin in the production of a SRF is also included in an earlier patent by Sears et al. [48]. The claims of this patent are not extensive and allow the main processing route to be changed to fast pyrolysis and extend the reactant to ammonia and other nitrogen compounds.

Additionally the tendency of fast pyrolysis liquid to polymerize due to condensation reactions and polymerization reactions of aldehydes and ketones with primary amino compounds are mentioned in Radlein's patent in relation to the formation of a stable product.

### **2.6.2.1 Claims of Patent EP0716056 A1**

Radlein et al. make extensive claims regarding their method of producing organic slow-release nitrogenous organic fertiliser from biomass [34]. The claims can be summarized as followed:

- A process for making organic nitrogenous fertilisers from at least one starting material selected from biomass, subjecting the input material to fast pyrolysis and chemically reacting a nitrogen compound containing the  $-NH_2$  group with pyrolysis products to form organic nitrogen compounds and recovering the organic nitrogen compounds so formed.
- A process as claimed using biomass selected from agricultural waste, forestry waste, municipal solid waste, wood, grasses, algae, peat, lignite, food processing waste and beverage processing waste.
- A process as claimed including the step of adding a nitrogen compound prior to pyrolysis or adding a nitrogen compound to the liquid or vapour pyrolysis products (in-situ process).
- A process as claimed including the step of adding the nitrogen compound shortly after producing the pyrolysis products (post-processing).
- A process as claimed including the step of combining the organic nitrogen compound with an absorbent.
- A process as claimed including the step of heating the organic nitrogen compounds to remove water or to cause polymerization to occur or to cause solidification to occur.

The patent is well written in a sense that the claims include almost all possible scenarios of combination of fast pyrolysis and nitrogen, by this blocking any further development or making it part of this patent. Not all claims are well backed within the patent leaving enough factors unclear.

### 2.6.2.2 Results according to Patent EP0716056 A1

The patent includes some data on processing and results for illustration. Radlein et al. [34] state that fast pyrolysis liquids contain 6-11moles of carboxyl, carbonyl and phenolic groups depending on the feedstock (see Table 4). It is pointed out that these could react with the described nitrogen compounds and lead to 10-17wt.% of nitrogen per kg of organic fraction of liquid product.

**Table 4: Functional groups in organic fraction of liquid product [34]**



Radlein et al. [34] also show that simple aldehydes (hydroxyacetaldehyde, glyoxal, methyl glyoxal, formaldehyde and acetaldehyde) form a large fraction of the carbonyl groups which are more reactive to ammonia than ketones. The main contributors to the carboxyl groups appear to be carboxylic acids, such as formic and acetic acids. Table 5 shows some typical concentrations of some of these compounds in biomass pyrolysis liquids.

**Table 5: Concentration of compounds in wt.% of organic fraction of liquid product [34]**



The content of pyrolytic lignin in the fast pyrolysis liquids from biomass had been determined to be 20-50wt.%. The phenolic compounds in fast pyrolysis liquids are supposed to be derived from lignin. Therefore pyrolytic lignin is of interest due to its capacity to bind nitrogen and as a source for humic acids during decomposition [34].

As an example for in situ pyrolysis with nitrogen containing compounds, the example of sawdust from poplar is given. The poplar was impregnated prior to pyrolysis with an aqueous urea solution and dried. The urea content on a moisture free wood basis was 16.4wt.%. The sample was pyrolysed in a fluidized bed at 500°C and the condensed pyrolysis liquids had an organic content of 76.5wt.% on a urea and moisture free wood basis. The mass balance of 114.5wt.% on a urea and moisture free wood basis indicated that there was a significant nitrogen addition. The pyrolysis liquid was supposed to be free of urea and ammonia and consisted of 48.54wt.% carbon, 6.95wt.% hydrogen and 10.30wt.% nitrogen. Radlein et al. [34] concluded that all the added nitrogen of the urea had been incorporated as the expected uptake of nitrogen at the level of impregnation was 10wt.%. It was also concluded that any free ammonia will react directly with the hot pyrolysis vapours.

Radlein et al. also tested a fertiliser product produced from fast pyrolysis liquid and urea on beans and maize in a 80 day green house test [34]. They achieved higher crop yields when compared to non-fertilized samples and concluded that the product was not toxic and capable of releasing the nitrogen slowly. Due to the limited time frame of 80 days no statements regarding long term effect of this product could be made.

### **2.6.3 European project on slow-release fertiliser from biomass**

In 1999 the European Commission funded a collaborative project to investigate the production and recycling of agricultural materials as a novel slow-release fertiliser, FAIR-CT98-4042. The objectives were to recycle agricultural wastes and residues into a unique and valuable fertiliser that can be safely used in a range of agricultural and horticultural applications. The approach was intended to be a sustainable method of recycling agricultural materials into valuable non-food, non-fuel products. The main work objectives were the production of slow release fertiliser in an in-situ process and alternatively by post processing and testing the products

The in-situ processing route was investigated by Aston University (Birmingham, United Kingdom), but the final report is confidential and therefore little information is accessible to

the public. The post processing route was investigated by the University of Hamburg (Hamburg, Germany) and results were published as part of a doctoral thesis by Hanser in 2002 [27].

### **2.6.3.1 In-situ processing route**

The in-situ processing route is based on the principles published by Radlein et al. [34]. It combines the pyrolysis process with the process in which a nitrogen containing compound reacts with the pyrolysis products. This is achieved by the immediate reaction of the nitrogen compound with the pyrolysis products in the vapour phase. Therefore either a relatively thermally unstable nitrogen compound (urea) is added to the reactor with the biomass feedstock or ammonia gas is added to the reactor immediately. The process parameters are adapted from ordinary biomass fast pyrolysis, which means that the process takes place around 500°C. Hanser [27] points out in his doctoral thesis that this processing route using urea can lead to the formation of triazines, which he found in his in-situ experiments. Unfortunately neither method of these experiments nor results are described so that this claim cannot be verified. Triazines used to be used as pesticides and are now banned in the EU. If the in-situ processing route in combination with urea is used, it has to be investigated if triazines are formed.

### **2.6.3.2 Post processing route**

The post processing route refers to a separate process to produce slow-release fertiliser. After fast pyrolysis liquid is produced, it is used as a feedstock to produce fertiliser in a second separate process by reaction with nitrogen. Almost any type of biomass can be utilised in the pyrolysis process. Fast pyrolysis liquid is produced from biomass which contains 35-40wt.% of oxygen, which is desirable for the process. The high oxygen content of biomass is necessary to produce a large quantity of functional groups during pyrolysis [27, 34]. These functional groups react readily with the nitrogen containing compound and therefore are essential for the process. The fast pyrolysis liquid is mixed with a nitrogen containing compound and heated to start reactions between the functional groups and nitrogen compound.

Hanser [27] used urea in his experiments as a source of nitrogen to react the fast pyrolysis liquid at a temperature of 140°C. A schematic of his experimental setup is illustrated in Figure 9.



**Figure 9: Scheme of post-processing laboratory reactor setup, redrawn from [27]**

After the conversion step in a batch reactor the highly viscous product is poured in a cooled acetone bath while stirring to produce a solid stable granulate. After separation and recovery of the acetone this product can be used as slow release fertiliser (SRF). Hanser [27] optimized his process for a nitrogen content of the SRF of 13wt.% adding 23wt.% of urea to the fast pyrolysis liquid. His results indicate that a product with higher nitrogen contents would be possible (Figure 10). He concludes that there seems to be no direct link between the amount of carbonyl groups and the uptake of nitrogen in contrast to the hypothesis of Radlein et al. [34].



**Figure 10: Impact of urea addition to nitrogen content in product, redrawn from [27]**

For his experimental setup Hanser [27] determined that a urea addition of 23wt.%, a temperature of 140°C and processing time of 120min were optimal. Under these conditions 78wt.% of the input fast pyrolysis oil and urea were obtained as solid product. Regarding the nitrogen content Hanser claims that his product should contain 13wt.% of nitrogen. According to the mass balancing data published by him the final product can just contain about 11wt.% of nitrogen, if 100% of the urea had been bound in the product, see Table 6. Whether this discrepancy is due to an experimental or measurement error is unknown.

**Table 6: Balance of N in product according to Hanser’s mass balance**

|                            | g            | wt.%    |
|----------------------------|--------------|---------|
| Fast pyrolysis liquid      | 100.00       |         |
| Urea                       | 23.00        | 23.00%  |
| N in urea                  | <b>10.73</b> | 46.67%  |
|                            |              |         |
| FP liquid + urea           | 123.00       | 100.00% |
| Product                    | 95.94        | 78.00%  |
| N in product, at 13wt.% N  | <b>12.47</b> | 13.00%  |
| N in product, max possible | <b>10.73</b> | 11.19%  |

The toxicity of the product was tested on tomato plants with no indication of a toxic reaction. The effectiveness as a SRF was tested by the Danish Institute of Agricultural Sciences in pot trials with Hebe plants in comparison to an untreated sample and the commercial SRF Osmocote®. The Hebe was seeded in May and material harvested in June, July and August. In general the results indicate that the product worked well for the first two months, but showed signs of reduced fertilizing effect at the third harvest. Hanser relates this to the reduced mineralization of the nitrogen present in his product.

#### **2.6.4 Slow release fertiliser via ammoxidation**

SRFs were produced from peat and lignite in the 1960s and 1970s making use of reactions between humic acids and ammonia [49, 50]. As the amount of humic acids for the reaction is limited in these feedstocks an additional oxidation step was employed to increase the amount of humic acids resulting in a higher nitrogen content of the product. The production of SRF from peat or lignite has to be seen critical regarding its sustainability as it is still making use of a fossil fuel as input material. Furthermore the oxidation step prior to the reaction with ammonia increasing the carbon footprint of this process.

Investigations to enrich technical lignin with nitrogen were also made in the late 1960s and 1970s by Flaig [51]. Lignin was partially oxidized under pressure with oxygen and reacted with ammonia. The oxidation step was used to increase the amount of functional groups for the reaction with ammonia. This method of ammoxidation was further investigated by Meier et al. [52] and N-enriched Kraft lignin tested by Ramirez-Cano et al. [53]. The production of SRF from lignin makes use of a residue material and had been technically developed to pilot plant scale [51]. Nevertheless the necessity of air separation to provide the oxygen, an oxygen consumption of 13-15mol oxygen per kg lignin for the oxidation step and the process pressures of about 1-1.3MPa all contributed to complexity and production costs of this process [51]. Currently just one company could be identified producing artificial humus by this process. NOVIHUM is producing artificial humus and is marketing it worldwide [54].

In contrast to the above stated method of ammoxidation, that included an oxidation step to increase and/or create functional groups for the reaction with ammonia, fast pyrolysis liquid already has a high amount of these groups due to the oxygen content in biomass feedstock and the processing via pyrolysis. Therefore fast pyrolysis can be regarded as a more suitable process to create an input material for the production of a SRF, when compared to ammoxidation.

## **2.6.5 State of the art of slow release fertiliser production**

In order to achieve a controlled slow release of nutrients from a fertiliser there are currently three different principles employed [46]:

1. mineral fertilisers with low solubility
2. slow decomposing organic nitrogen compounds
3. coated fertiliser granules for slow release

Mineral fertilisers with low solubility commonly include an ammonium salt in combination with phosphorous compounds. The overall amount of nitrogen in this type of fertiliser is limited to about 10% while the phosphorous content is relatively high. The release of the nutrients depends on granule size, soil moisture content, pH and temperature [46, 55].

Slowly decomposing organic nitrogen compounds such as urea formaldehyde are used as SRF [46, 55]. These products contain up to 40% nitrogen that is made available by microbial activity

in the soil. The rate of bio-degradation depends on the chain length of the urea formaldehyde compounds, meaning that smaller chains are decomposed more readily than longer ones. Consequently the release of nutrients is linked to chain length as well as microbial activity, pH, temperature and moisture content in the soil [46, 55].

Coated fertilisers can be subdivided into a group of fertilisers being coated with sulphur, resins or thermoplastic materials. Sulphur coated urea is produced by coating urea granules with molten sulphur. The sulphur coated urea is then coated with a second layer of wax, sealing off cracks and a third layer of a conditioner. The product usually contains up to 38% of nitrogen. The release of nutrients depends on the quality of the coating. Due to the production method up to 1/3 of the granules can have cracks, leading to immediate nutrient release, and up to 1/3 may be coated too thoroughly, causing a delay in nutrient release [46, 55].

Resin coated fertilisers are produced by coating fertiliser granules with a resin forming a cross-linked, hydrophobic barrier. The two main resins used are alkyd-type resins, e.g. Osmocote®, and polyurethane coatings, e.g. Multicote®. For the alkyd-type resins the coating composition and thickness is used to control the nutrient release. The working principle is that water penetrates the coating through pores increasing the osmotic pressure in the fertiliser core, stretching the pores and releasing nutrients in this way. The polyurethane type resins do not just coat the fertiliser granule, but also react with it forming an attrition resistant SRF. The controlled release is achieved by adjusting the coating thickness and resin composition [55]. Problems are similar to sulphur coated fertilisers. The coating can either have cracks or the coating can be too thick.

Another method is to coat fertiliser granules with thermoplastic materials. The nutrient release is controlled by blending low permeability polyethylene with a high permeability polymer, e.g. ethylene-vinyl-acetate. The release rate is determined by the ratio between low permeability polyethylene and high permeability polymer [55].

Beside the problem with the cracks in the fertiliser granule coat and too thoroughly coated granule, these fertilisers have a large carbon footprint as they are produced from fossil fuels. Furthermore the multiple step coating process leads to high production costs. These costs prevent a wide use of such fertilisers.

## **3 Methods**

The following section describes the different methods used in this research project. Where applicable standardized methods were used or methods developed that are based on international standards, such as ASTM E 1131-03 [56].

### **3.1 *Sample preparation***

Of each feedstock a sufficient amount of about 50 kg was acquired in order to have sufficient material for all experiments. Two types of samples were prepared from each feedstock batch for this research project, (1) analytical samples and (2) processing samples.

(1) Analytical samples were used for TGA, Py-GC-MS and extraction experiments. The preparation procedure for the analytical samples is based on ASTM E 1757—01 [57]. The biomass feedstocks were air dried to a moisture content of less than 10wt.%. Three samples of ca. 250g were taken, mixed and ground with a cutting mill using a 2mm screen. The ground sample was sieved to a particle size fraction of 150-250 $\mu$ m. In contrast to the ASTM standard the particle size distribution was not calculated and not taken into consideration. The sieved sample was split with a riffle splitter three times discarding one of the obtained fractions each time.

(2) Processing samples were prepared for experiments on the 1 kg/h pyrolysis reactor. For the processing sample the biomass was air dried to less than 10wt.% moisture and ground in a cutting mill using a 4mm screen. The ground sample was sieved to a particle size fraction of 250 $\mu$ m to 2mm (dust free).

### **3.2 *Moisture content of biomass***

The moisture content of untreated biomass feedstock and processing samples was determined using a Sartorius MA 35 moisture analyser, which is working on similar principles as stated in ASTM standard E 871 – 82 [58]. Depending on the thermal stability of the biomass the sample was dried at 60°C or 105°C until constant weight. In each case the moisture content of three sub-samples of about 2g was determined and an average taken.

Analytical samples were either pre-dried in a temperature controlled oven before use or the moisture content was determined within the analysis procedure (e.g. TGA).

### **3.3 Ash content**

The ash content was determined based on ASTM E 1755-01 [59] with a different particle size due to the sample preparation procedure. The initial weight of the porcelain crucibles was determined after heating them to 575°C and cooling to room temperature. The samples were weighed in and heated up to 250°C for 30min to avoid flaming. After that the temperature was increased to 575°C for four hours, followed by a cooling period in a desiccator and weighing. The samples were then heated to 575°C for one hour, cooled in a desiccator and weighed again.

Alternatively the ash content of TGA samples had been determined via the combustion profile as described later in accordance with ASTM E 1131-03 [56].

### **3.4 Proximate analysis**

For the proximate analysis the results of the moisture content analysis (section 3.2), ash content analysis (section 3.3) and the thermogravimetric analysis (section 3.10) were combined. The thermogravimetric analysis contributed the results for the volatile content and fixed carbon content.

### **3.5 Elemental analysis**

Elemental analysis was performed by an external laboratory, MEDAC Ltd. (UK) certified according to BS EN ISO 9001:2008 [60]. The applied method was total oxidation using a Carlo-Erba EA 1108 Elemental Analyser. The minimum detection level for carbon, hydrogen and nitrogen was 0.1wt.%. All analyses were performed in duplicate. In case of unacceptable deviations between the results, the analyses were repeated. For further calculations averages of the results were taken. Oxygen was calculated by difference. Fast pyrolysis liquid samples were analysed as produced (meaning including the water in the pyrolysis liquid) while biomass and char were dried in a vacuum oven before analysis.

### **3.6 Extraction methods**

Two types of extractions were performed for this research project. The oil content of feedstocks was determined using an ether extraction and the content of water soluble sugar and other water soluble material in a feedstock was determined using hot water Soxhlet extraction.

The ether extraction used diethyl ether as a solvent and all extractions were performed in duplicates. The sample material was dried over night at 60°C to avoid volatilization. Approximately 4g of sample were mixed with 50ml of diethyl ether and placed in a bottle shaker for 10min. After phase separation the liquid phase was decanted and filtered through a pre-dried and weighted filter paper. The residual solid was mixed with 50ml of diethyl ether and the procedure repeated. After the third repetition all material was emptied into the filter and rinsed with ethanol. The filter paper and recovered solid sample were dried over night at 60°C. The mass loss of each sample was determined and averages calculated.

The hot water Soxhlet extraction used hot water as a solvent. The sample material was dried over night at 60°C to avoid volatilization. Approximately 4g of sample were placed into the pre-dried and weight filter thimble. The Soxhlet extractor was run for about 1 hour guaranteeing several cycles. After that the filter thimble and recovered solid sample were dried over night at 60°C. The mass loss of each sample was determined and averages calculated.

### **3.7 Higher heating value**

The Higher Heating Value (HHV) of solids and liquids was determined using the unified correlation for estimating HHV of solid, liquid and gaseous fuels published by Channiwala [61]. A wide spectrum of fuels including biomass, char, liquids and residues were taken into consideration for the derivation of this correlation. The average absolute error is claimed to be 1.45%. For these reasons this equation was chosen.

**Equation 1: Higher Heating Value according to unified correlation of Channiwala**

$$HHV = 0.3491 \times C + 1.1783 \times H + 0.1005 \times S - 0.1034 \times O - 0.0151 \times N - 0.0211 \times A$$

with

|       |   |
|-------|---|
| $HHV$ | Higher Heating Value in MJ/kg                               |
| $C$   | Carbon content in wt% on dry basis (within 0.00-92.25wt%)   |
| $H$   | Hydrogen content in wt% on dry basis (within 0.43-25.15wt%) |
| $S$   | Sulphur content in wt% on dry basis (within 0.00-94.8wt%)   |
| $O$   | Oxygen content in wt on dry basis (within 0.00-50.00wt%)    |
| $N$   | Nitrogen content in wt% on dry basis (within 0.00-5.60wt%)  |
| $A$   | Ash content in wt% on dry basis (within 0.00-71.40wt%)      |

The HHV for pyrolysis gases was calculated via the gas concentrations and the HHV of the individual gases taken from literature [62] excluding the fluidizing nitrogen on a dry gas basis.

#### Equation 2: Higher Heating Value of Pyrolysis Gas

$$HHV_{Gas} = 141.8 \times H_2 + 10.103 \times CO + 0 \times CO_2 + 55.499 \times CH_4 + 50.284 \times C_2H_4 + 51.876 \times C_2H_6 + 48.918 \times C_3H_6 + 50.345 \times C_3H_8 + 49.5 \times C_4H_{10}$$

with

|             |  |
|-------------|--|
| $HHV_{Gas}$ | Higher heating value of Pyrolysis Gas in MJ/kg |
| $H_2$       | Hydrogen content in wt% dry gas                |
| $CO$        | Carbon monoxide content in wt% dry gas         |
| $CO_2$      | Carbon dioxide content in wt% dry gas          |
| $CH_4$      | Methane content in wt% dry gas                 |
| $C_2H_4$    | Ethene content in wt% dry gas                  |
| $C_2H_6$    | Ethane content in wt% dry gas                  |
| $C_3H_6$    | Propene content in wt% dry gas                 |
| $C_3H_8$    | Propane content in wt% dry gas                 |
| $C_4H_{10}$ | n-Butane content in wt% dry gas                |

### 3.8 Water content of liquids

The water content of fast pyrolysis liquids was determined by Karl Fisher Titration according to ASTM E 203-08 [63]. The equipment used was a Metrohm 758KFD Titrino Unit and a Mettler Toledo V20 Volumetric KF titrator using Fluka HYDRANAL® Composite 5K as a titrant and Fluka

HYDRANAL® Working Medium as solvent. These reagents are especially suitable for titration in ketones and aldehydes which are present in fast pyrolysis liquids. Calibration was performed using Fluka HYDRANAL® Water Standard 10.0 before each measurement series. Three measurements were taken and an average calculated, if the measurements were within a  $\pm 1\%$  point range. Otherwise a new subsample was taken and the water content determined.

### **3.9 pH-value**

The pH-value was determined using a Sartorius PB 11 ph-meter. The ph-meter was calibrated using three calibration solutions (ph 4, 7, 11) before each measurement series. The pH of a sample was determined three times and an average taken.

The pH of fast pyrolysis liquid samples was determined directly by inserting the test electrode into the sample. For determination of the pH of solidified samples the following procedure was applied. 5g of solidified sample was mixed with 10ml of deionised water of 40°C for 10min. The Mixture was cooled down letting solid residues settle at the bottom of the vial. After that the pH of the aqueous phase was taken by inserting the test electrode.

### **3.10 Thermogravimetric Analysis**

Thermogravimetric Analysis (TGA) was performed using a Perkin Elmer Pyris 1 Thermogravimetric Analyser. The analysis was performed according to the Aston University Bioenergy Research Group (BERG) methods which are based on ASTM E 1131-03 [56]. The samples were prepared according to sample preparation method described in section 3.1 for analytical samples.

For the BERG pyrolysis method [64] approximately 3mg of each sample were analysed in duplicates according to the following program with nitrogen used as inert sample purge gas at a flow rate of 30ml/min (ATP) and a balance purge gas flow rate of 70ml/min (ATP):

- Holding 5 min at 50°C (purging with nitrogen)
- Heating at 5°C per minute until 105°C
- Holding at 105°C for 5 minutes
- Heating at 25°C per minute until 900°C
- Holding at 900°C for 15 minutes
- Cooling at 25°C per minute to 50°C

For the BERG combustion method [64] approximately 3mg of each sample were analysed in duplicates according to the following program with air used as sample purge gas and oxidizing agent at a flow rate of 30ml/min (ATP) and a balance purge gas flow rate of 70ml/min (ATP):

- Holding 5 min at 50°C (purging with air)
- Heating at 5°C per minute until 105°C
- Holding at 105°C for 5 minutes
- Heating at 5°C per minute until 575°C
- Holding at 575°C for 15 minute
- Cooling at 25°C per minute to 50°C

According to the data obtained from these two analyses the content of moisture, volatile matter, fixed carbon & ash was derived from the analytical pyrolysis. The ash content was determined by combustion. The fixed carbon content was calculated as the difference of fixed carbon & ash and ash. Furthermore temperatures for the highest conversion rate could be determined by analyzing the first derivative of the mass loss over temperature (DTG).

### ***3.11 Gas Chromatography-Mass Spectroscopy analysis of liquid samples***

For Gas Chromatography-Mass Spectroscopy (GC-MS) of liquid samples two sets of equipment were available. The first set was a PerkinElmer Autosystem XL Gas Chromatograph and TurboMass Gold Mass Spectrometer. The injector port was held at 275°C. The column used was an PerkinElmer Elite-1701 (crossbond 14% cyanopropylphenyl-85%dimethyl polysiloxane) (60m, 0.25mm i.d.,0.25µm df). The column oven was held at 45°C for 2.5min and then heated at 5°C/min to 250°C, and held for 7.5min. Helium was used as carrier gas and a split of 1:25 was applied. Mass spectra were obtained for the molecular mass range  $m/z = 35-300$ . The obtained data was analysed using TurboMass 5.0 Software and the NIST 98 Library and from literature assignments [65, 66].

The second set was a Varian GC-450 Gas Chromatograph and MS-220 Mass Spectrometer. The injector port was held at 275°C. The column used was a Varian factorFOUR® (30m, 0.25mm id., 0.25µm df). The gas chromatograph oven was held at 45°C for 2.5min and then heated at 5°C/min to 250°C, and held for 7.5min. Helium was used as carrier gas and a split of 1:20 was applied. Mass spectra were obtained for the molecular mass range  $m/z = 45-300$ . The

obtained data was analysed using Varian MS Workstation with MS Data Review Software Version 6.9.2 and the NIST 05 Library and from literature assignments [65, 66].

The fast pyrolysis liquid samples were dissolved and diluted with Ethanol (GC-grade) in a volumetric ratio of 1:4 (fast pyrolysis liquid: Ethanol) and filtered with a 22 $\mu$ m pore size syringe filter before injection. 1 $\mu$ l of diluted sample was injected in the Perkin Elmer system manually using a 1 $\mu$ l syringe and 0.5 $\mu$ l of diluted sample was injected in the Varian GC system using an auto sampler with 5 $\mu$ l syringe.

### 3.12 Pyrolysis-Gas Chromatography-Mass Spectroscopy

For Pyrolysis-Gas Chromatography-Mass Spectroscopy (Py-GC-MS) two sets of equipment were available. The first set was a CDS AS-2500 Pyroprobe<sup>®</sup> with auto sampler coupled to the above described PerkinElmer Autosystem XL Gas Chromatograph and a TurboMass Gold Mass Spectrometer. The CDS AS-2500 pyrolyser was placed on top of the GC injection port. Approximately 1mg of analytical sample was placed in a quartz glass tube as shown in Figure 11. The sample was pyrolysed at a heating rate of 1000 $^{\circ}$ C/s and a final temperature of 600 $^{\circ}$ C and dwell time of 30s. The evolving vapours were transferred via the Pyroprobe<sup>®</sup> needle assembly into the GC-MS injection port with a split ratio of 1:125. Mass spectra were obtained for the molecular mass range  $m/z = 35\text{--}300$ . The obtained data was analysed using TurboMass 5.0 Software and the NIST 98 Library and from literature assignments [65, 66].

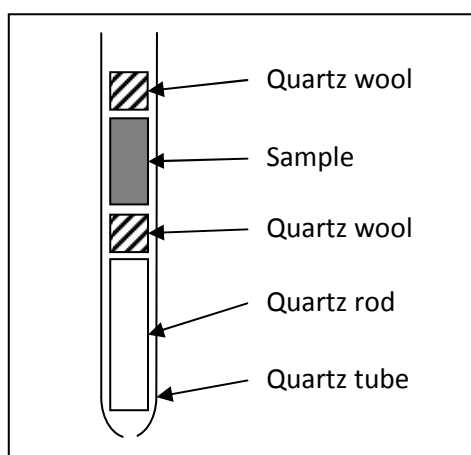


**Figure 11: Pyroprobe sample**

The second set was a CDS 5200 Pyroprobe® coupled to the above described Varian GC-450 Gas Chromatograph and MS-220 Mass Spectrometer. The devolatilised components were transferred via a heated transfer line maintained at 310°C into the Varian GC injection port. The CDS 5200 unit is capable of using reactive gases (such as ammonia, hydrogen or oxygen) adsorbing the evolving pyrolysis vapours on a Tenax-2® trap and releasing them after heating the trap up to 300°C and purging the trap with helium.

Approximately 1mg of analytical sample was placed in a quartz glass tube and held between two quartz wool plugs. The sample was pyrolysed at 550°C with a heating rate of 1000°C/s and dwell time of 30s in either inert atmosphere (helium) or in a reactive gas (10% ammonia in helium). In case of inert gas atmosphere the evolving vapours were injected into the GC-MS injection port via the heated transfer line (310°C) with a split ratio of 1:125 and analysed. In case of reactive gas atmosphere the evolving vapours were collected in a Tenax-2® trap. As soon as the pyrolysis step was completed the trap was purged with helium. Then the trap was heated to 300°C, the trapped vapours released and injected into the GC-MS injection port via the heated transfer line with a split ratio of 1:125. Mass spectra were obtained for the molecular mass range  $m/z = 45-300$ . The obtained data was analysed using Varian MS Workstation with MS Data Review Software Version 6.9.2 and the NIST 05 Library and from literature assignments [65, 66].

### **3.13 Online Gas Chromatograph**

Non condensable gases (NCG) of the pyrolysis processing experiments were analysed using a Varian Micro GC 4900CP using helium as a carrier gas. The micro GC is equipped with two channels with Thermal Conductivity Detectors (TCD). Channel A using a molecular sieve column at 80°C was used to detect hydrogen, oxygen (indicator for insufficient purging and leaks) nitrogen and carbon monoxide. Channel B using a porous polymer column at 90°C was used to detect methane, ethene, ethane, propene, propane, n-butane and carbon dioxide. The quantification of the NCG was performed via peak area using calibration curves. The calibration curves were created using 6 calibration mixtures containing the above named hydrocarbons in concentrations ranging from 0.5-25 vol.%, nitrogen and compressed air. Samples were injected for analysis every 150s, so that a virtually continuous gas sampling could be achieved with the micro GC during steady state pyrolysis operation.

### **3.14 Fourier Transform Infrared Spectroscopy**

Fourier Transform Infrared Spectroscopy (FTIR) was performed on liquid film samples and solid samples embedded in potassium bromide (KBr) salt with a PerkinElmer FT-IR Spectrometer Spectrum RXI. The spectra were analysed using the PerkinElmer software Spectrum Version 5.3.1 and additional print media [67, 68].

The solid samples were ground to a fine powder and mixed with KBr at a ratio of 5mg sample to 350mg KBr. Of this mixture a disc for analysis was formed under vacuum at a pressure of about 100MPa applied for 2 minutes. The solid samples were scanned in a range of 4000 to 400 $\text{cm}^{-1}$ , performing 32 scans with a resolution of 4.0 $\text{cm}^{-1}$  and an interval of 1.0 $\text{cm}^{-1}$ .

The liquid film was achieved by spreading one drop of sample between two polished KBr discs for liquid samples. The liquid film samples were scanned in a range of 4000 to 400 $\text{cm}^{-1}$ , performing 32 scans with a resolution of 1.0 $\text{cm}^{-1}$  and an interval of 0.5 $\text{cm}^{-1}$ .

## 4 Feedstock choice and characterization

### 4.1 Introduction

The project has investigated the pyrolysis and nitrogenolysis of biomass and biogenic residues in order to present an alternative route for the production of a sustainable slow release fertiliser (see section 1.2). The feedstocks investigated were chosen in accordance with the objective to make use of biomass and biogenic residues.

Agricultural residues with a high nitrogen content were investigated as they are usually not used as feedstock for pyrolysis in energetic applications as the feedstock nitrogen would lead to high NO<sub>x</sub> emissions if combusted. Furthermore high nitrogen feedstocks were chosen to determine the fate of the nitrogen in the feedstock during fast pyrolysis processing. The aspect of starting with a high nitrogen feedstock for the production of SRF appeared promising as the feedstock nitrogen could contribute to the nitrogen content in the SRF product and by this reduce the amount of nitrogen that would need to be added.

Agricultural and forestry residue with low nitrogen content were investigated as they would be a low cost feedstock. Neither they are usually used as pyrolysis feedstock for energetic applications due to their relatively high ash content and often phase separated fast pyrolysis liquids.

Beech wood was used as reference material, because it is known that it can be processed without difficulties and produces high liquid yields in fast pyrolysis [9, 69]. Also beech wood is virtually nitrogen free. These characteristics qualify beech wood as a reference point in terms of process parameters and performance, product yields and quality, composition of a nitrogen free fast pyrolysis liquid for the comparison with data obtained from other feedstocks and nitrogenolysis experiments.

A list of the feedstocks investigated and their origin is presented in Table 7. All feedstocks were characterized by proximate and ultimate analysis as well as thermo-gravimetric analysis (see section 4.2). Feedstocks with high oil content or added soluble fraction were also subjected to extraction methods. Selected feedstocks were analysed using pyrolysis-gas chromatography-

mass spectroscopy to get an insight into possible thermal decomposition products. All applied methods are described in detail in the method section (section 3).

**Table 7: Feedstock list**

| <b>Material</b>                              | <b>Type</b>          | <b>Origin</b>   | <b>Notes</b>  |
|--|----------------------|---|---------------|
| Anaerobic Digestion residue                  | agricultural residue | agriKomp GmbH<br>Energiepark 2<br>91732 Merkendorf, Germany   | dried residue |
| Beech wood                                   | untreated wood       | J. Rettenmaier & Söhne GmbH&Co.KG<br>73494 Rosenberg, Germany   | wood chips    |
| Dried Distillers Grains with Solubles Barley | agricultural residue | KW Alternative feeds<br>Bishopdyke Road, Sherburn - in Elmet<br>Leeds<br>LS25 6JZ, United Kingdom                                 | pellets       |
| Dried Distillers Grains with Solubles Maize  | agricultural residue | KW Alternative feeds<br>Bishopdyke Road, Sherburn - in Elmet<br>Leeds<br>LS25 6JZ, United Kingdom                                 | pellets       |
| Dried Distillers Grains with Solubles Wheat  | agricultural residue | KW Alternative feeds<br>Bishopdyke Road, Sherburn - in Elmet<br>Leeds<br>LS25 6JZ, United Kingdom                                 | pellets       |
| Pine bark                                    | forestry residue     | Aston University, BERG biomass<br>storage<br>Birmingham<br>B4 7ET, United Kingdom   | chipped       |
| Rape meal (ADM)                              | agricultural residue | ADM Trading (UK) Limited<br>Church Manorway<br>Erith, Kent<br>DA8 1DL, United Kingdom   | pellets       |
| Rape meal (GD)                               | agricultural residue | Green Dragon Fuel, New Farm<br>Mansfield Road<br>Redhill, Nottingham<br>NG5 8PB, United Kingdom                                   | Briquettes    |
| Sugar beet pulp                              | agricultural residue | British Sugar plc, Bury St Edmunds<br>Factory<br>PO Box 15<br>Hollow Road<br>Bury St Edmunds, Suffolk<br>IP32 7BB, United Kingdom | dried pulp    |
| Wheat straw                                  | agricultural residue | Aston University, BERG biomass<br>storage<br>Birmingham<br>B4 7ET, United Kingdom   | Pellets       |

## 4.2 Results of feedstock characterization and discussions

The results of the feedstock characterization are summarized in this section and compared to data from literature sources when available. All analytic methods are described in the method section, section 3. Water content, proximate and ultimate analysis, TGA and extraction experiments were performed in duplicate and ash content analysis with four samples. The data presented for the analyses are averages. The analysis of multiple samples was necessary to take the inhomogeneity of the biomass samples into consideration. It has to be noted that biomass is an inhomogeneous material and therefore relatively high deviations between literature values and those obtained are possible.

### 4.2.1 Proximate analysis

The proximate analysis was established according to the method described in section 3.4. All presented values are averages (as mentioned above) and when possible data from literature is given for comparison reasons. The data is presented in Table 8.

**Table 8: Proximate analyses of feedstocks**

| <b>Feedstock</b>           | <b>Water content</b> | <b>Volatiles</b> | <b>Fixed carbon</b> | <b>Ash</b> |
|----------------------------|----------------------|------------------|---------------------|------------|
|                            | ar, wt.%             | dry, wt.%        | dry, wt.%           | dry, wt.%  |
| Beech wood                 | 8.76                 | 86.34            | 12.61               | 1.05       |
| Beech wood, Lit. [70]      | 10.2                 | 83.00            | 16.00               | 1.00       |
| Pine Bark                  | 6.00                 | 68.43            | 28.22               | 3.35       |
| Spruce Bark, Lit. [71]     | -                    | 75.20            | 22.50               | 2.30       |
| Wheat Straw                | 9.78                 | 70.96            | 19.37               | 9.67       |
| Wheat Straw, Lit. [72]     | 11.10                | 74.90            | 18.00               | 7.10       |
| Wheat DDGS                 | 4.11                 | 80.95            | 14.37               | 4.69       |
| Barley DDGS                | 4.60                 | 80.16            | 15.50               | 4.34       |
| Maize DDGS                 | 4.27                 | 85.41            | 9.52                | 5.07       |
| DDGS, Lit. [73]            | 8.90                 | 78.20            | 14.70               | 7.10       |
| Green Dragon rape meal     | 5.52                 | 83.30            | 11.05               | 5.65       |
| ADM rape meal              | 6.21                 | 74.56            | 18.28               | 7.16       |
| Rape meal, Lit. [74]       | -                    | 67.00            | 25.80               | 7.20       |
| AD-residue                 | 9.99                 | 66.82            | 13.57               | 19.61      |
| AD-residue, Lit. [75]      | 8.52                 | 74.79            | 22.86               | 2.35       |
| Sugar beet pulp            | 2.69                 | 61.14            | 30.26               | 8.60       |
| Sugar beet pulp, Lit. [76] | 6.10                 | 79.02            | 17.79               | 3.19       |

The proximate analysis results generally are in good agreement with the data published in the literature. The deviations can be regarded as part of the inhomogeneous nature of the

material biomass used. The significantly higher volatile content of Green Dragon rape meal results from a very high content of residual oil, which was determined by extraction experiments (section 4.2.3). The high differences in the ash content of the AD-residue samples are caused by the wide range of input materials used in anaerobic digestion and the sampling method. While the AD-residue in the literature source was solid material floating in the digester fed with cow manure, the AD-residue investigated was taken from the solid residues of the digestion of a mixture of agricultural residues, like maize stalk, and manure after pressing and air drying in a barn. Therefore the ash content was expected to be higher and the sample could also contain contamination from the barn, e.g. dust.

The results for DDGS are in good agreement with literature and DDGS from different grains are relatively constant in their content of volatiles, fixed carbon and ash. Sugar pulp again shows differences between the sample investigated and the literature, which are most likely due to different production methods during sugar extraction.

Beech wood, pine bark and wheat straw are in good correspondence with the literature data. In general all residues show a relatively high content of ash, when compared to a woody biomass like beech wood.

#### **4.2.2 Ultimate analysis**

The ultimate analysis was established according to the methods described in section 3.5 and is presented below on dry, ash free basis. All presented values are averages of duplicate analyses and when possible data from literature is given for comparison. The data is shown in Table 9.

For almost all feedstocks the results of the ultimate analysis are in good agreement to the data published in the referenced literature sources. One exception is Green Dragon rape meal, which is caused by the high content of residual oil in this sample (see section 4.2.3). The residual oil with its fatty acids causes higher carbon and hydrogen contents of this material when compared to ADM rape meal or the rape meal in the literature source. Of greater importance are the relatively high nitrogen contents in rape meals and DDGSs with more than 5.5wt.% (daf). Proteins are the main source of this nitrogen in these feedstocks. ADM rape meal contains approximately 36% of proteins [77] and barley DDGS approximately 26% [78]. Therefore rape meal and DDGS are commonly used as animal feed. Also important is the fact that AD-residue and sugar beet pulp do not containing large amounts of nitrogen (less than

2wt.% (daf)). For AD-residue this is likely due to the fact that the nitrogenous compounds are separated with the liquid residual phase and therefore the solid residue just contains minor quantities of nitrogen. Although sugar beet pulp is used as an animal feed for its residual sugar content (around 6% [79]) and protein content (around 9% [79]), the values obtained for the nitrogen content show that in terms of nitrogen it is not a high nitrogen feedstock. As expected pine bark and wheat straw have a low nitrogen content of less than 1wt.% (daf).

**Table 9: Ultimate analyses of feedstocks**

| <b>Feedstock</b>           | <b>C</b>             | <b>H</b>  | <b>N</b>    | <b>O*</b> |
|----------------------------|----------------------|-----------|-------------|-----------|
|                            | daf, wt.%            | daf, wt.% | daf, wt.%   | daf, wt.% |
| Beech wood                 | 53.6                 | 5.42      | <b>bdl.</b> | 40.98     |
| Beech wood, Lit. [70]      | 49.3                 | 6.10      | 0.14        | 44.46     |
| Pine Bark                  | 52.26                | 5.58      | 0.12        | 42.04     |
| Spruce bark, Lit. [71]     | 51.07                | 6.04      | 0.41        | 42.48     |
| Wheat Straw                | 48.14                | 6.08      | 0.69        | 45.09     |
| Wheat Straw, Lit. [72]     | 49.30                | 6.40      | 0.48        | 43.82     |
| Wheat DDGS                 | 50.24                | 6.78      | <b>5.55</b> | 37.43     |
| Barley DDGS                | 50.01                | 6.19      | <b>5.70</b> | 38.10     |
| Maize DDGS                 | 54.21                | 6.55      | <b>5.59</b> | 33.65     |
| DDGS, Lit. [73]            | 52.24                | 6.72      | <b>4.80</b> | 36.24     |
| Green Dragon rape meal     | 55.51                | 7.25      | <b>5.63</b> | 31.61     |
| ADM rape meal              | 48.49                | 6.19      | <b>6.10</b> | 39.22     |
| Rape meal, Lit. [74]       | 46.60                | 6.50      | <b>6.03</b> | 40.87     |
| AD-residue                 | 48.85                | 6.36      | 1.95        | 42.85     |
| AD-residue, Lit. [75]      | 47.60                | 7.06      | 1.99        | 43.35     |
| Sugar beet pulp            | 41.76                | 5.63      | 1.70        | 50.91     |
| Sugar beet pulp, Lit. [76] | 43.40                | 6.30      | 1.40        | 48.90     |
| O*                         | Oxygen by difference |           |             |           |

Additionally the ultimate analysis shows that the nitrogen content in the beech wood used is below detection level and it is therefore justified to regard this material as virtually nitrogen free and use it as reference material for this aspect.

### 4.2.3 Extraction experiments

Rape meal and DDGS are residues that contain residual oils and/or added sugars from their production process. As these oils and sugars are pyrolysed and their decomposition products are contributing to the liquid fast pyrolysis product, it is of interest how much oils and sugars are present in the feedstock samples. Therefore extraction experiments were performed on rape meal and DDGS samples according to the methods described in section 3.6. The oil

content of the samples was determined by ether extraction and the water soluble fraction by a separate hot water Soxhlet extraction. The data is presented in Table 10.

**Table 10: Ether and hot water extraction results**

|                                | Unit | Rape Meal<br>G. Dragon | Rape Meal<br>ADM | DDGS<br>Wheat | DDGS<br>Barley | DDGS<br>Maize |
|--------------------------------|------|------------------------|------------------|---------------|----------------|---------------|
| Ether extraction mass loss     | wt.% | 23.50                  | 2.60             | 5.00          | 6.48           | 12.79         |
| Hot water extraction mass loss | wt.% | 12.60                  | 12.94            | 31.61         | 28.16          | 40.65         |

The extraction experiments show that the oil content of rape meal is heavily dependent on the source and the extraction method employed at the oil mill. Green Dragon rape meal is produced by a small company without the use of any chemical extraction method and therefore contains 23.5wt.% of residual oil. In contrast ADM rape meal provided by a large scale producer has a residual oil content of just 2.6wt.%. This difference is significant, because the high oil content of Green Dragon rape meal caused problems during the fast pyrolysis experiments that led to the exclusion of this feedstock (see section 6.8 for details). ADM rape meal in contrast was processed without problems.

The hot water extraction was particularly interesting for the Dried Distiller's Grains with Solubles (DDGS) feedstocks to determine the amount of solubles added to the dried distiller's grains. The dried distiller's grains are largely composed of fibre from the grain and insoluble protein [80]. The solubles result from added thin stillage, which contains residual oligosaccharides, organic acids and by-products of the fermentation [80]. It can be seen that up to 40.7wt.% hot water soluble components were present in the samples. It was expected that these components were contributing to the fast pyrolysis liquid yield. In contrast to the high oil content in Green Dragon rape meal, the high content of hot water soluble material in DDGS samples were processed without problems.

#### **4.2.4 Thermogravimetric Analysis**

Thermogravimetric analyses of the feedstocks were performed according to the methods described in section 3.10. The results obtained contributed to the proximate analysis and gave information about the thermo-chemical decomposition behaviour of the feedstocks under pyrolysis conditions. In this section the TGA curves (Figure 12 and Figure 14) are presented, although their main information about feedstock moisture volatiles, fixed carbon and ash are

already presented as part of the proximate analysis (see section 4.2.1). The first derivatives of the mass loss over temperature of the samples (DTG curves) are presented indicating the rate of mass loss or thermal decomposition of samples. The curves presented indicate the temperatures of major mass loss and the temperature range the decomposition reactions are taking place (Figure 13 and Figure 15).

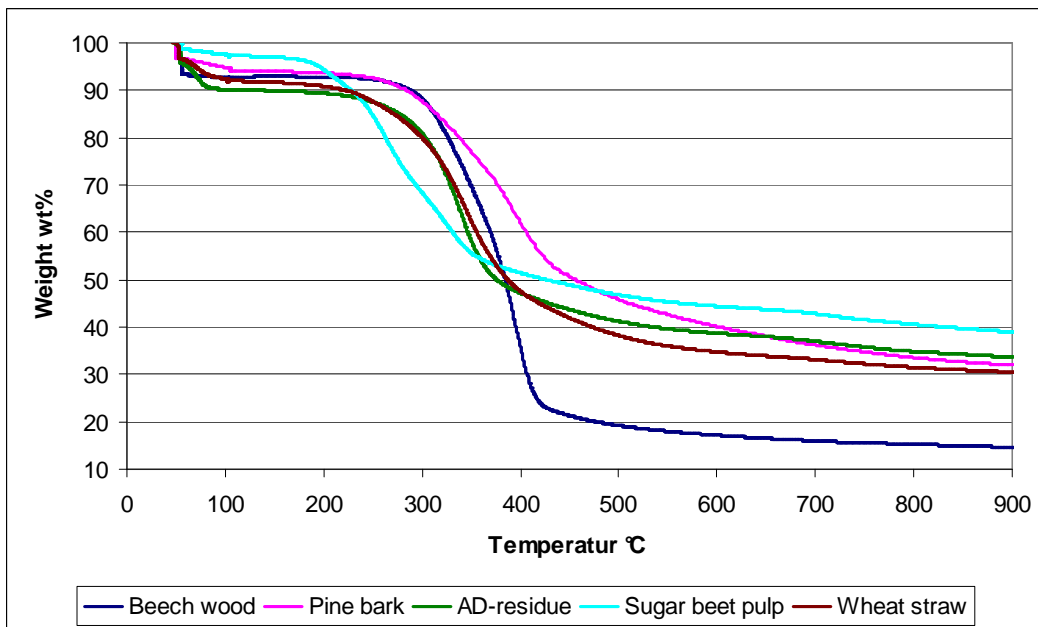


**Figure 12: Pyrolysis TGA curve of selected feedstocks I**

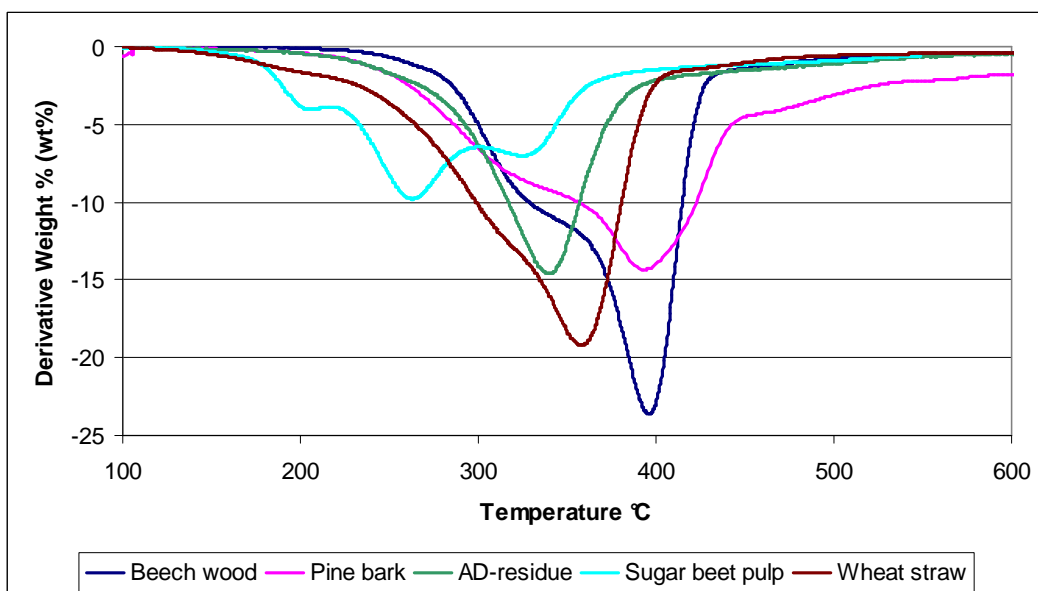


**Figure 13: Pyrolysis DTG of selected feedstocks I**

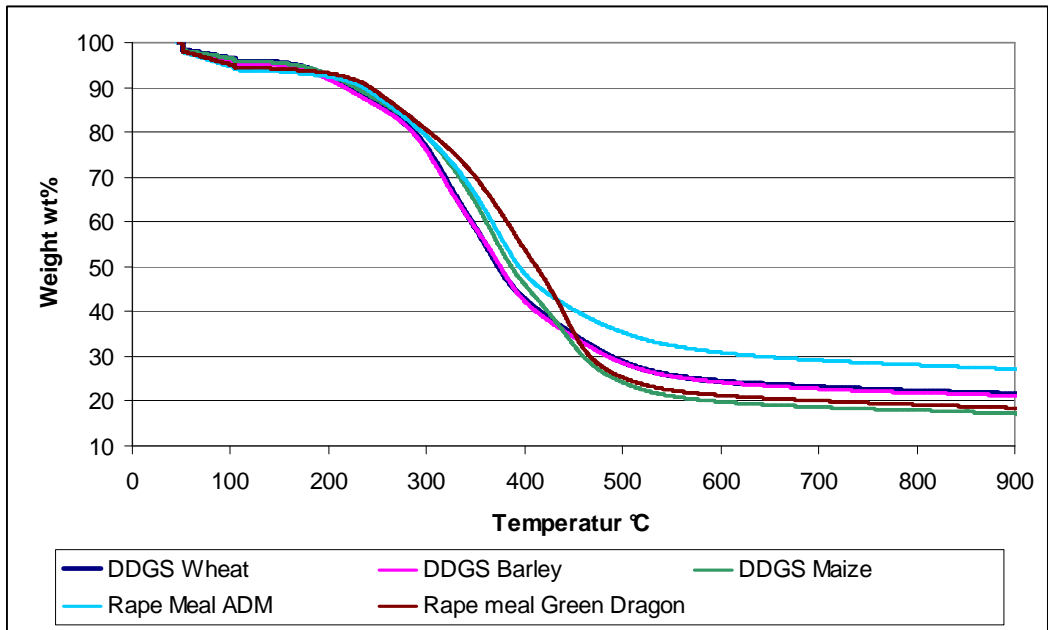


**Figure 14: Pyrolysis TGA curve of selected feedstocks II**

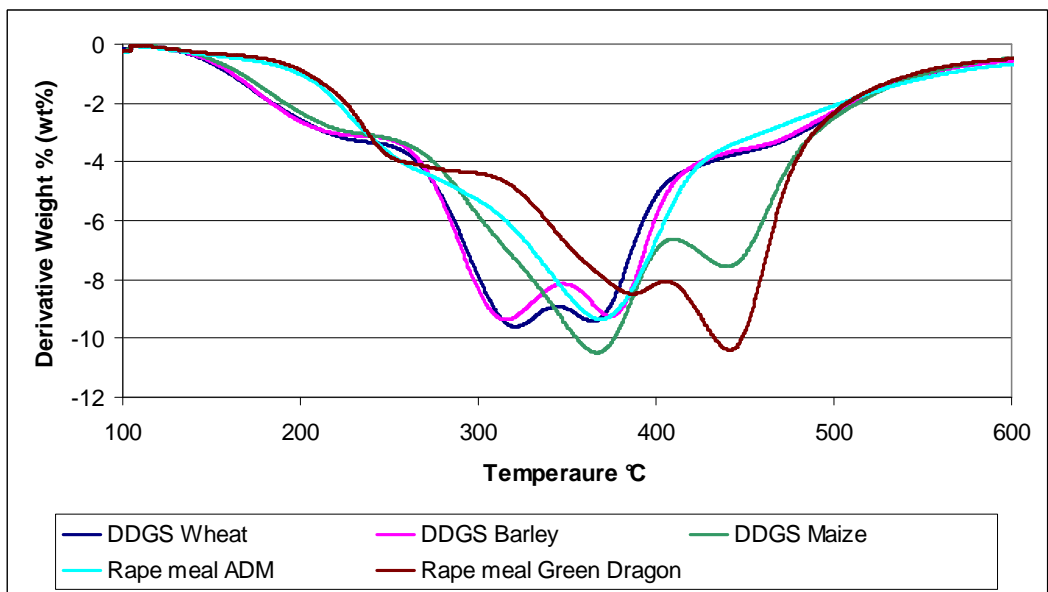


**Figure 15: Pyrolysis DTG of selected feedstocks II**

The DTG curves clearly show the different decomposition behaviours of the 10 presented feedstocks. DDGS, rape meal and sugar beet pulp, show similar decomposition patterns, wide decomposition temperature range and multiple decomposition peaks. The DDGS feedstocks wheat and barley DDGS are almost identical. All three DDGSs show a shoulder two major peaks in their rate of mass loss. The shoulder is usually attributed to readily decomposing materials such as hemicellulose. The wide decomposition temperature range indicates that the different components decompose continuously over the whole temperature interval investigated. The first decomposition peak is likely to indicate an increased decomposition of sugars while the

second one is most likely linked to fibrous material. Sugar beet pulp shows a similar behaviour, but in general peaks are at lower temperatures. ADM containing no added sugars and a small amount of oils just shows one larger peak at 369°C indicating the fibrous material. Green dragon rape meal having a high oil content has a small peak at 387°C linked to fibrous material and a larger one at 440°C indicating an increased decomposition of oils. Beech wood, AD-residue pine bark and wheat straw differ in their decomposition behaviour when compared to the materials above. These materials just show a shoulder and a one major decomposition peak. This is due to the fact that these materials do not contain relevant amounts of added sugars or residual oils. Beech wood shows the typical decomposition behaviour of a woody biomass (see section 2.2.5). The shoulder at 330°C indicates the decomposition of hemicellulose and the peak at 396°C the decomposition peak of cellulose, while the lignin decomposes over the whole investigated temperature range. Wheat straw and AD-residue behave similar, though decomposition peak temperatures are lower. This is most likely due to catalytic reactions caused by alkaline metals in these materials. As shown by Nowakowski et al. alkaline metals react as catalyst during pyrolysis [15]. Pine bark also contains a high amount of ash and alkaline metals. Although the decomposition peak temperature is 393°C the peak itself is more broad and the decomposition rate not as high as for beech wood. This is most likely linked to the catalytic effect of the alkaline metals. The temperatures of major decomposition peaks are summarized in Table 11.

**Table 11: Decomposition peaks of DTG analysis of selected feedstocks**

| Feedstock              | Decomposition Peaks* |                      |                      |
|------------------------|----------------------|----------------------|----------------------|
|                        | Shoulder             | 1 <sup>st</sup> peak | 2 <sup>nd</sup> peak |
|                        | °C                   | °C                   | °C                   |
| DDGS Wheat             | 240                  | <b>321</b>           | 364                  |
| DDGS Barley            | 240                  | <b>316</b>           | 380                  |
| DDGS Maize             | 240                  | <b>368</b>           | 440                  |
| Rape meal ADM          | 270                  | <b>369</b>           |                      |
| Rape meal Green Dragon | 260                  | 387                  | <b>440</b>           |
| Sugar beet pulp        | 206                  | <b>263</b>           | 327                  |
| AD-residue             |                      | <b>340</b>           |                      |
| Beech wood             | 330                  | <b>396</b>           |                      |
| Pine bark              | 325                  | <b>393</b>           |                      |
| Wheat Straw            |                      | <b>358</b>           |                      |
| *major peak in bold    |                      |                      |                      |

Table 11 shows that the major decomposition peak temperatures for all material are below 500°C. The DTG curves indicate that the decomposition reactions are significantly reducing at

about 500°C and have almost stopped at about 600°C. In terms of processing the materials investigated these information indicate that a fast pyrolysis temperature of 500°C or above would be suitable to pyrolyse these feedstocks achieving a high degree of conversion.

#### 4.2.5 Py-GC-MS

The high nitrogen feedstocks, DDGSs and rape meals, were investigated in an initial step using Py-GC-MS to determine possible pyrolysis products. The methods applied are described in section 3.12. For these experiments the CDS 2500 Pyrolyser® and PerkinElmer GC-MS were used. Of particular interest was which products are formed during the decomposition of high nitrogen feedstocks. In Figure 16 the chromatogram of the pyrolysis vapours for barley DDGS is presented and suggested peak assignments are listed in Table 12 mainly for peaks with a relative abundance of more than 20%. The chromatograms of the pyrolysis vapours of all feedstocks investigated by Py-GC-MS and tables with suggested peak assignments are attached in appendix A. A presentation of these in the main text was not seen as beneficial, because the example of barley DDGS allows to present all relevant features.

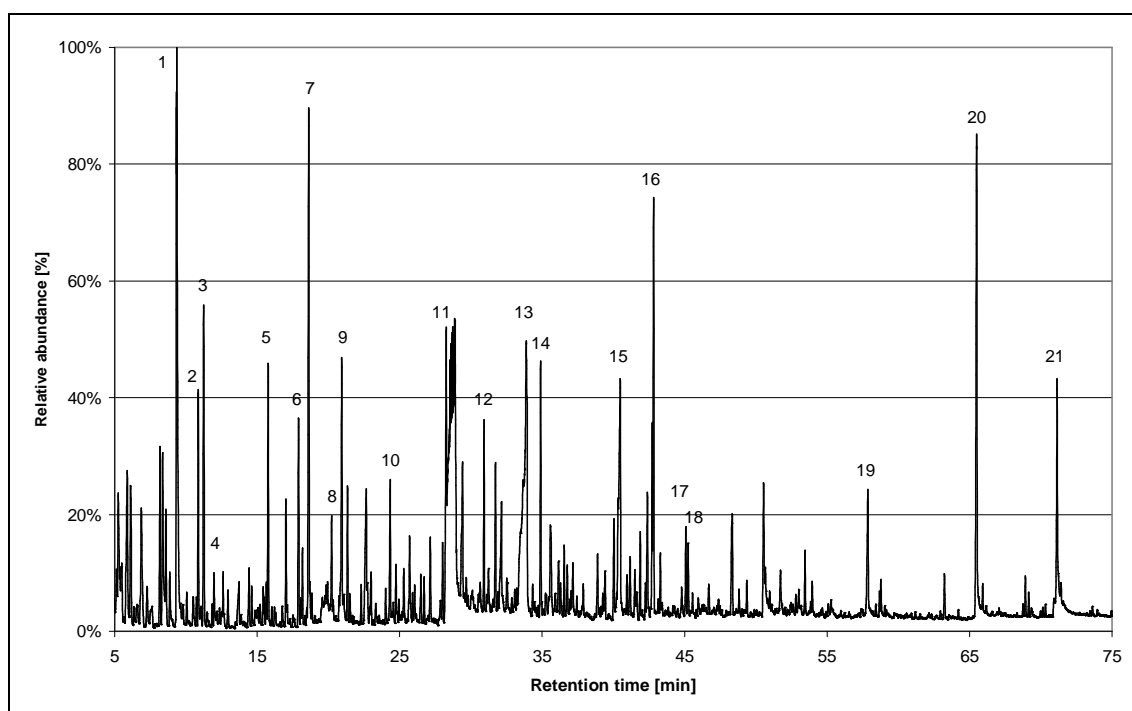


Figure 16: Example of Py-GC-MS Chromatogram of barley DDGS

**Table 12: Suggested peak assignments of barley DDGS chromatogram**

| Peak #                                | RT [min] | Base Peak [m/z] | MW [g/mol] | Peak assignment                       |
|---------------------------------------|----------|-----------------|------------|---------------------------------------|
| 1                                     | 9.360    | 45              | 60         | Acetic Acid                           |
| 2                                     | 10.860   | 43              | 74         | 1-Hydroxy-2-propanone                 |
| 3                                     | 11.243   | 91              | 92         | Toluene                               |
| 4                                     | 11.970   | 79              | 79         | <b>Pyridine</b>                       |
| 5                                     | 15.762   | 67              | 67         | <b>Pyrrrole</b>                       |
| 6                                     | 17.903   | 43              | 102        | Acetic anhydride                      |
| 7                                     | 18.625   | 96              | 96         | Furfural                              |
| 8                                     | 20.220   | 80              | 79         | <b>3-Methyl-1H-Pyrrrole</b>           |
| 9                                     | 20.942   | 41              | 98         | 2-Furfuryl alcohol                    |
| 10                                    | 24.329   | 98              | 99         | 2-Hydroxy-2-Cyclopentene-1-one        |
| 11                                    | 28.272   | 58              | 114        | <b>3,4-Dihydro-2-methoxy-2H-pyran</b> |
| 12                                    | 30.913   | 94              | 94         | Phenol                                |
| 13                                    | 33.881   | 61              | 92         | Glycerine                             |
| 14                                    | 34.890   | 107             | 108        | Methylphenol (Cresol)                 |
| 15                                    | 40.480   | 95              | 95         | <b>3-Pyridinol</b>                    |
| 16                                    | 42.832   | 150             | 150        | 4-Vinyl-Guaiacol                      |
| 17                                    | 45.084   | 85              | 154        | Syringol                              |
| 18                                    | 45.240   | 117             | 117        | <b>Indole</b>                         |
| 19                                    | 57.862   | 60              | 162        | Levoglucofan                          |
| 20                                    | 65.500   | 214             | 214        | Fatty acid                            |
| 21                                    | 71.140   | 41              | 280        | Fatty acid                            |
| Nitrogen containing compounds in bold |          |                 |            |                                       |

The Py-GC-MS results show typical decomposition products for biomass. For each feedstock more than 80 peaks in each pyrolysis vapour chromatogram were investigated and the majority of peaks could be assigned to specific compounds. DDGS feedstocks and rape meals showed most of the decomposition products of cellulose, hemicellulose and lignin that had been identified by Faix et al. [65, 66]. These are the most abundant ones in all feedstock samples. Also glycerine and fatty acids have been identified from residual oils in the feedstocks. In addition the high nitrogen feedstocks show different nitrogen compounds resulting from the thermal decomposition of proteins, such as pyridine and pyrrole. These compounds are of interest as these could contribute to the nitrogen content of a possible fertiliser via nitrogenolysis.

## 5 Processing by fast pyrolysis and nitrogenolysis

### 5.1 General – Bubbling fluidized bed reactors

Bubbling fluidized bed reactors are a proven technology in fast pyrolysis and are used from laboratory scale to commercial scale (see section 2.3.2). The present research project employed the 1kg/h bubbling fluidized bed reactor in the Aston University Bioenergy Research Group. The technical features of this unit as well as general process parameters used are described in this section.

#### 5.1.1 1kg/h bubbling fluidized bed reactor

The bubbling fluidized bed reactor at Aston University including the condensation train is illustrated in Figure 17.

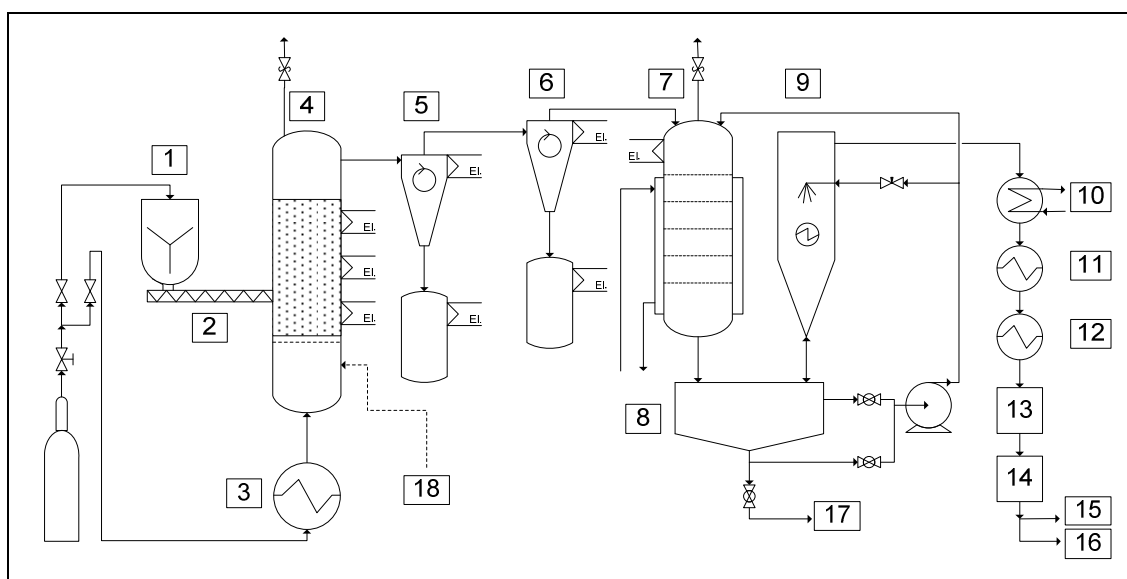


**Figure 17: Flow diagram of fast pyrolysis reactor with condensation train (numbers are explained in the text that follows)**

The unit is designed for a maximum processing capacity of 1kg biomass feedstock per hour. A description of the components including the modifications follows:

The feedstock is filled into the volumetric feeder hopper which is fitted with an agitator and twin metering screws (K-Tron K2M-T20) (#1). Feed is dropped by gravity into the inlet of a

single fast screw (#2). The feeding system is constantly purged with nitrogen to prevent backflow of pyrolysis gases and support feedstock transport. This fast screw is cooled by a water jacket to prevent pyrolysis in the feeding system and transports the feedstock rapidly into the middle of the fluidized bed. The fluidizing gas is nitrogen, electrically heated in a heat exchanger (#3) integrated into the lower half of the reactor upstream of the distribution plate and used on a single pass basis. The reactor (#4) is tubular and electrically heated on its outside by three ceramic knuckle heaters. 1 kg of quartz sand with particle sizes between 600 and 850 $\mu$ m is used as bed material (see section 5.2.2). The pyrolysis vapours, gases and char particles are entrained by the fluidizing gas and leave the reactor at the top. The char particles are separated in two cyclones in series. Cyclone 1 fitted with char pot 1 (#5 cyclone and char pot 1) separates coarse char particles and cyclone 2 fitted with char pot 2 (#6 cyclone and char pot 2) separates fine char particles. The pipes and cyclones upstream of the quench column inlet are trace heated to approximately reactor temperature to avoid condensation of pyrolysis vapours that would lead to deposits in the piping. The vapours are condensed in a quench column (#7) using ISOPAR™ as the quenching media at 30°C, which is recycled from the common tank (#8). The quench column has a water cooled jacket to cool the ISOPAR™ and quenched products. The aerosols are separated in a wet electrostatic precipitator (ESP) (#9) flushed with ISOPAR™. Both condensates are collected in the common tank (#8) and are referred to as fast pyrolysis liquid. The ISOPAR™ is skimmed off the top of this tank and recycled to the quench and electrostatic precipitator processes. The remaining light condensable vapours which pass through the quench and ESP are condensed in a water cooled heat exchanger (#10) at 10°C followed by two dry ice/acetone cooled heat exchangers (#11 & 12) at -70°C. The liquids collected are referred to as secondary condensates. The non-condensable gases (NCG) pass through a cotton wool filter (#13) and are metered by a diaphragm gas meter (#14). They are analysed every 150s by a Varian Micro GC for NCGs and hydrocarbons up to C4 (gas outlet #15) and the excess gas is vented into a fume hood (gas outlet #16). Fast pyrolysis liquid is removed at the bottom of the common tank (outlet #17). Temperatures are measured and recorded using K-Type thermocouples linked to a Microlink 751 ADC Unit combined with Windmill data logging software. To monitor and regulate the pyrolysis temperature, the temperatures of the fluidizing gas before the distribution plate, at the bottom of the bed, the middle of the bed, the freeboard above the bed, the electric nitrogen pre-heater and the electric ceramic knuckle heaters are measured. The overall system pressure and the pressure differences between the distribution plate and at the top of the reactor, between the reactor outlet and the quench column inlet, between the quench column inlet and the ESP outlet and between the ESP outlet and the gas meter outlet are monitored by

analogue instrumentation. They are used to determine if any part of the unit is starting to get blocked and if fluidized bed is operating within suitable parameters.

## **5.1.2 Modifications to the unit**

The unit was critically reviewed and discussions held with previous users. In order to improve the unit in terms of reliability, handling and process control a number of modifications were implemented which are discussed below.

### **5.1.2.1 Temperature control bed heaters**

The reactor bed is heated by three ceramic knuckle heaters placed on the outside of the reactor tube. Initially these heaters were controlled by one PID controller with one K-type thermocouple. This led to a significant temperature difference between the two bottom heaters and the top heater of up to 30°C. This was caused by the different power output levels. To overcome this layout issue and to achieve a more homogenous temperature profile, a second PID controller with K-type thermocouple was added to control the top bed heater. The temperature difference was reduced to 5°C as a consequence. The temperature among the heaters and reactor was more homogenous and reduced their thermal stress and tendency to overheat.

### **5.1.2.2 Temperature control trace heaters**

A similar situation was found for the trace heating bands of the three heating zones between the reactor top and the quench column inlet. Cyclone 1 (zone 1), cyclone 2 (zone 2) and the pipe trace heating between cyclones and quench column (zone 3) were controlled by only one PID controller with one K-type thermocouple. Due to different power output levels of the heating bands used and the different heat demands of zone 1, 2 and 3 this led to temperature differences of up to 50°C between zone 1 and zone 2 and 3. Separating zone 1 from zone 2 and 3 using a second PID controller and K-type thermocouple reduced the temperature difference to 10°C. This reduced overheating of the trace heating bands. Furthermore local hot spots leading to coke formation inside the piping were reduced.

### **5.1.2.3 Data-Logging**

The data logging system was replaced to allow more analogue input signals and improve operation by being able to monitor the temperatures more closely and accurately. Furthermore the old, partially damaged cabling was replaced and a new computer installed. A Microlink 751 USB analogue digital converter (ADC) was used in combination with a 593 isothermal thermocouple connection box providing 16 analogue inputs. The visualization and data logging was realized using a Windmill data acquisition software version 7. The recorded data was imported to Microsoft Office Excel for further analysis and interpretation. This setup allowed the creation of temperature profiles for all measurement points during an experiment and their analysis.

### **5.1.2.4 Additional water cooled heat exchanger**

The water vapour load in the pyrolysis gas after the electrostatic precipitator (ESP) frequently led to blockages from excessive ice accumulation in the dry ice/acetone cooled heat exchangers during experiments lasting longer than one hour. A water cooled heat exchanger was added in the vapour/gas stream downstream of the ESP and upstream of the dry ice/acetone cooled heat exchangers to condense the majority of the water vapour. Since this modification no blockages of the dry ice cooled heat exchangers occurred.

### **5.1.3 Mass balancing scheme**

The mass balance of the process is determined gravimetrically. In order to obtain a good mass balance closure an extensive mass balancing procedure was followed. A good mass balance closure is important to draw conclusions from the product yields obtained and to define if the experiments are actually suitable to draw conclusions with an acceptable error. Most components of the 1kg/h bubbling fluidized bed rig are not suitable to be measured directly as disassembling them would be too time consuming and a weighing balance with high maximum capacity as well as high sensitivity would be needed. The mass balancing scheme employed for this research is presented in Table 13 giving information about the material being measured, in which part of equipment it is present and how it is measured. This scheme allowed mass balance closure of up to 97wt.%. Possible errors influencing the mass balance were caused by problems in product recovery and hold up, gas measurement errors, losses of water vapour due to non-condensed vapours and dissolution of some fast pyrolysis products in the ISOPAR™.

**Table 13: Mass balancing scheme for 1kg/h bubbling fluidized bed rig**

| <b>Material</b>                     | <b>Equipment</b>                           | <b>Method</b>   |
|-------------------------------------|--|---|
| <b>Input materials:</b>             |  |   |
| Biomass                             | feed hopper                                | difference between weight of material filled in and material removed from feed hopper   |
| Sand                                | reactor                                    | difference between weight of input sand and bed material after the experiment reduced by the weight of coarse and fine char in bed as described below |
| <b>Char product:</b>                |  |   |
| coarse char                         | reactor                                    | weight of char particles sieved from the recovered bed material after experiment with a larger particle size than the sand                            |
| fine char and char coating the sand | reactor                                    | mass loss of recovered bed material after removal of coarse char, before and after burning off char in oven and removal of ash by sieving             |
| Char                                | 1 <sup>st</sup> cyclone and char pot       | direct measurement of the product mechanically removed from the 1 <sup>st</sup> cyclone and char pot  |
| Char                                | 2 <sup>nd</sup> cyclone and char pot       | direct measurement of the product mechanically removed from the 2 <sup>nd</sup> cyclone and char pot  |
| Char                                | metal pipes                                | direct measurement of the product mechanically removed from the pipes   |
| <b>FP liquid product:</b>           |  |   |
| fast pyrolysis liquid               | quench column                              | direct measurement of product after removal and phase separation from ISOPAR™   |
| fast pyrolysis liquid hold up       | quench column                              | estimate according to results of hold up experiments  |
| secondary condensate                | Water cooled heat exchanger                | difference between weight of washing acetone input and recovered material   |
| secondary condensate                | Water cooled heat ex. collection flask     | difference in weight before and after experiment  |
| secondary condensate                | Dry ice cooled heat exchanger 1            | difference in weight before and after experiment  |
| secondary condensate                | Dry ice cooled heat ex. 1 collection flask | difference in weight before and after experiment  |
| secondary condensate                | Dry ice cooled heat exchanger 2            | difference in weight before and after experiment  |
| secondary condensate                | Dry ice cooled heat ex. 2 collection flask | difference in weight before and after experiment  |
| secondary condensate                | glass pipes                                | difference in weight before and after experiment  |
| secondary condensate                | cotton wool filter                         | difference in weight before and after experiment  |
| <b>FP gas product:</b>              |  |   |
| total gas output                    | diaphragm gas meter                        | direct measurement of total gas volume flow before and after the experiment   |
| pyrolysis gas                       | Varian Mirco GC                            | on-line measurement of gas composition and determination of pyrolysis gas mass by average gas composition and total gas volume flow                   |

In order to determine the total amount of reaction water formed during the experiment, the moisture content of the feedstock was determined by a Sartorius MA 35 moisture analyzer (see section 3.2) and the water content of the fast pyrolysis liquid and secondary condensates was determined by Karl Fisher Titration (see section 3.8). The difference between the sum of water in the fast pyrolysis liquids and the water added to the process by the feedstock moisture was regarded as reaction water.

Errors in the mass balance were mostly caused by insufficient product recovery, especially fast pyrolysis liquid, but also char. The detected gases were limited to the calibrated gases. Furthermore the gases were heavily diluted in fluidizing nitrogen usually accounting for more than 95% of the analysed gas stream. Consequently small errors in the detected gases had a big impact on the gas balance. Loss of water vapour due to incomplete condensation was also identified as a possible source for mass balancing error. A simulation with ASPEN plus was made to estimate the amount of water possibly carried out with the product gas by saturating nitrogen gas with water. 0°C and 0.1MPa were chosen as conditions at the exit of the second dry ice/acetone heat exchanger. 2.91g of water per 1m<sup>3</sup> nitrogen (ATP) would be carried out under these conditions. At a nitrogen flow rate of 50l/min (ATP) and a run time of 3hours a total of 13.71g of water would have been lost in terms of mass balancing. Compared to a liquid yield of about 1000g in such an experiment (see section 6.2.1) this accounts to about 1.4wt% of liquid product.

## **5.2 Process parameters**

The process parameters that were measured or calculated for the pyrolysis and in-situ nitrogenolysis experiments are listed below and discussed in succeeding sections:

- Fluidization velocity
- Bed material and particle size
- Pyrolysis reactor temperature
- Residence time of hot vapours
- Feeding rate
- Feedstock moisture
- Quench liquid temperature and flow rate

## 5.2.1 Minimum fluidization velocity

The minimum fluidization velocity was determined theoretically and empirically. The values obtained were compared and the empirical data evaluated according to the literature [81].

### 5.2.1.1 Theoretical minimum fluidization velocity

The minimum fluidization velocity describes the gas velocity in the empty reactor tube at the point when the downward gravitational forces of the bed material and the forces caused by the upward flowing fluidization gas reaches an equilibrium and the particles start to be fluidized. In order to calculate the minimum fluidization velocity the ERGUN equation [82] (Equation 3) and the equation for the pressure drop of the bed (Equation 4) [81] are used.

#### Equation 3: ERGUN equation

$$\frac{\Delta p}{\Delta L} = 150 \frac{(1-\psi)^2}{\psi^3} \frac{v_f \rho_f v}{\bar{d}_p^2} + 1.75 \frac{(1-\psi)}{\psi^3} \frac{\rho_f v^2}{\bar{d}_p}$$

#### Equation 4: Pressure drop of reactor bed

$$\Delta p = (\rho_s - \rho_f)(1-\psi)g\Delta L$$

with

|             |                              |
|-------------|------------------------------|
| $\Delta p$  | pressure drop bed            |
| $\Delta L$  | length of bed                |
| $\psi$      | porosity                     |
| $v_f$       | kinematic viscosity of fluid |
| $\rho_s$    | density solid                |
| $\rho_f$    | density fluid                |
| $v$         | fluid velocity               |
| $\bar{d}_p$ | Sauter particle diameter     |
| $g$         | gravitational acceleration   |

WEN and YU [83] suggested Equation 5 as an approximation for the minimum fluidization velocity using empirically determined factors for the usually missing factor of porosity at point of fluidization.

### Equation 5: WEN and YU equation

$$Re_{mf} = 33,7\sqrt{1+3,6\times 10^{-5} Ar} - 1$$

$$Re_{mf} = \frac{v_{mf} \bar{d}_p}{\nu_f}$$

$$Ar = \frac{(\rho_s - \rho_f)g(\bar{d}_p)^3}{\rho_f \nu_f^2}$$

with

- Re Reynolds number
- Ar Archimedes number
- $\nu_f$  kinematic viscosity of fluid
- $\rho_s$  density solid
- $\rho_f$  density fluid
- $v_{mf}$  mean fluid velocity
- $\bar{d}_p$  Sauter particle diameter
- $g$  gravitational acceleration

Equation 5 was used for determining the theoretical value for the minimum fluidization velocity in this work. Table 14 shows the input data, minimum fluidization velocity and corresponding fluidization gas flow rates for two sand particle size ranges that were used (see section 5.2.2).

**Table 14: Minimum fluidization data**

| Data                                   |                                    | Case 1        | Case 2        |
|--|------------------------------------|---------------|---------------|
| Reactor temperature                    | °C                                 | 500           | 500           |
| Sand particle size range               | µm                                 | 600-710       | 710-850       |
| Density sand                           | kg/m <sup>3</sup>                  | 2530          | 2530          |
| Density nitrogen at 500°C              | kg/m <sup>3</sup>                  | 0.436         | 0.436         |
| Kinematic viscosity nitrogen at 500°C  | 10 <sup>-5</sup> m <sup>2</sup> /s | 8.048         | 8.048         |
| Archimedes number (Ar)                 |                                    | 2471.581      | 4173.830      |
| Reynolds number (Re)                   |                                    | 1.464         | 2.438         |
| Minimum fluidization velocity at 500°C | m/s                                | <b>0.180</b>  | <b>0.252</b>  |
| Minimum fluidization gas flow (ATP)    | l/min                              | <b>17.084</b> | <b>23.889</b> |

#### 5.2.1.2 Empirical determination of minimum fluidization velocity

The minimum fluidization velocity was also determined empirically by observing the correlation between fluidization gas flow rate and pressure drop over the distribution plate and bed. The reactor was heated to 500°C for these measurements to simulate operating conditions. The feeding system purge gas flow rate was held constant at 17l/min (ATP)

(ordinary set point for experiments) while the nitrogen fluidization gas flow rate was varied between 0 and 70l/min (ATP) in 5l/min increments. For 600-710 $\mu$ m sand, the pressure drop of the bed increased almost linear to 4981Pa from 0 to 20l/min (ATP). Starting from 25l/min the pressure drop increased at a lower rate due to the dynamic pressure drop caused by the distribution plate. For 710-850 $\mu$ m sand similar observations were made, except that the pressure drop increased almost linearly until 5230Pa at 25l/min.

Additionally the amount of sand entrained out of the reactor was measured for the above stated gas flow rates to determine a suitable gas flow rate range for operation. The system was heated to operating temperature, the feeding system purge gas flow rate held constant at 17l/min (ATP) and each flow rate maintained for 10min before the amount of sand in the first char pot was measured. For 600-710 $\mu$ m sand no sand entrainment was observed until a fluidization gas flow rates of 60l/min (ATP). At 65l/min (ATP) 3.51g were measured and at 70l/min (ATP) 3.88g. For 710-850 $\mu$ m sand particle size no sand was entrained for the fluidization gas flow rates investigated.

Based on these findings and the statements of previous users of this reactor the fluidization gas flow rate was chosen to be around 40l/min for 600-710 $\mu$ m sand and 55l/min for 710-850 $\mu$ m sand.

### **5.2.1.3 Evaluation of fluidization velocity**

The empirically determined fluidization velocities and input data were used to calculate Froude and Reynolds number and the results entered in the diagram published by Reh [81]. Reh used dimensionless numbers to describe the different states of fluidization and his diagram is commonly applied in process engineering. The Reh diagram and the calculated data points are displayed in Figure 18. It can be seen that the fluidization velocities determined are all in the area of bubbling fluidized bed, although at the lower part of the fluid bed regime, not far from the fixed bed regime. Consequently the chosen gas flow rates are suitable for the experiments, but should not be further reduced.

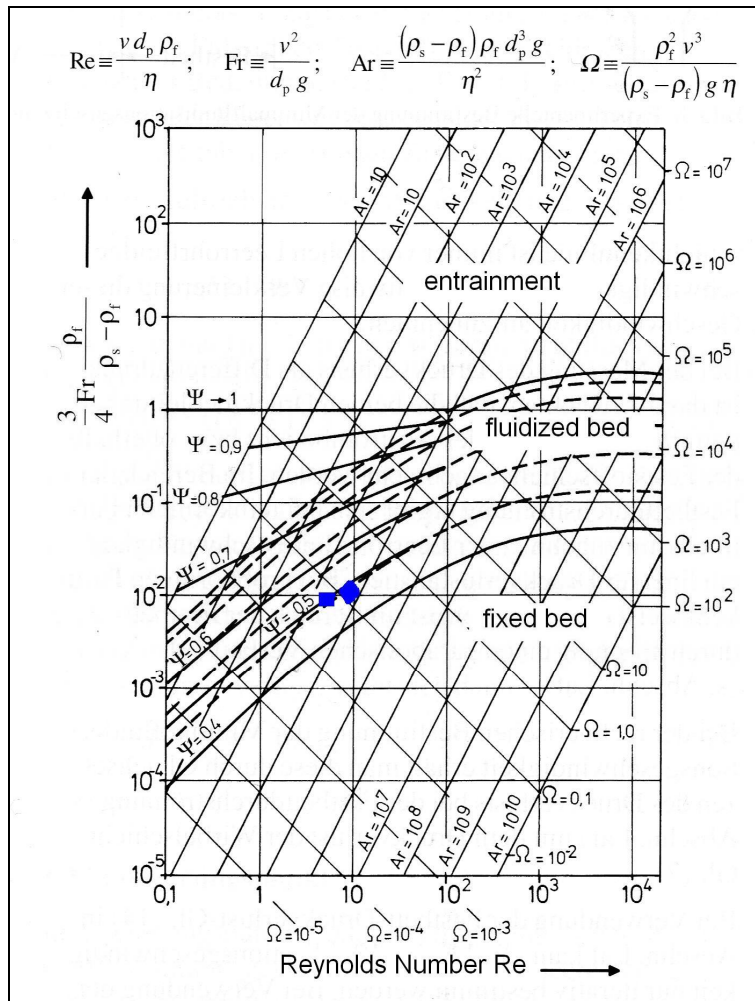


Figure 18: Reh diagram [81] with recalculated results indicated

## 5.2.2 Bed material and particle size

Silica sand was chosen as the inert bed material. It guarantees good heat transfer rates in the reactor bed, is mechanically robust, cheap and thermally stable. The latter is important as char coating the sand after an experiment is burned off. The particle size ranges employed were 600-710 $\mu\text{m}$  for biomass such as beech wood, pine bark and straw and 710-850 $\mu\text{m}$  for biomass such as DDGS, sugar beet pulp and rape meal. This is due to the different char particle densities of these materials.

The minimum particle size was determined by the hole diameter in the distribution plate of 500 $\mu\text{m}$ . The particle size ranges were chosen according to three aspects: previous parameters used with this unit [84], good fluidization of bed material at moderate nitrogen gas consumption and good char particle entrainment. Based on previous practice at the Aston University Bioenergy Research Group [84] it was known that a sand particle size range 600-

710 $\mu\text{m}$  was suitable for most biomass feedstocks at a moderate nitrogen gas consumption of about 50l/min (ATP). For feedstocks such as rape meal or DDGS it was found that a sand particle size range 710-850 $\mu\text{m}$  was more suitable due to the fact that a higher fluidization velocity was needed to entrain the char particles. This was found out during the first experiments with this feedstocks. At the same time the bigger sand size range prevented entrainment of the bed material itself (see section 5.2.1.2).

### 5.2.3 Pyrolysis reactor temperature

In order to reduce the number of process parameters that have an impact on product yields and improve the comparability of the experiments, a fixed pyrolysis reactor temperature of 500°C was chosen. According to Bridgwater et al. [22] fast pyrolysis produces maximum liquid yields at processing temperatures around 500°C displayed in Figure 19. The SRF produced via nitrogenolysis is either the product of fast pyrolysis liquid from high nitrogen feedstock or fast pyrolysis vapours reacting with ammonia or fast pyrolysis liquid reacting with a nitrogen compound. In either case the SRF is based on the condensed fast pyrolysis vapours. Therefore a high yield of product was assumed to be one of the aims in order to produce SRF. Furthermore it was expected that higher reactor temperatures could possibly lead to the formation of more stable nitrogen compounds during in-situ nitrogenolysis that are not bio-degradable. Temperatures lower than 450°C were not regarded as promising as the reaction rates of fast pyrolysis become very slow. Unfortunately due to time constrains this aspect could not be investigated in this research and therefore is part of the recommendations (see section 11).



**Figure 19: Fast pyrolysis yields of Aspen Poplar at different temperatures [16]**

## 5.2.4 Hot vapour residence time

The hot vapour residence time within the hot reaction zone needs to be minimised to reduce secondary reactions that decrease the liquid yield as described in section 2.2.5. The hot vapour residence time is directly dependent on the fluidization gas flow rate and the design of a given set of equipment. The maximum hot vapour residence time ( $t_{\max}$ ) can be calculated as followed:

### Equation 6: Maximum hot vapour residence time

$$t_{\max} = \frac{V_{\text{system,hot}}}{\dot{V}_{\text{gas,hot}}}$$

with

$t_{\max}$  maximum hot vapour residence time [seconds]

$V_{\text{system,hot}}$  Volume of system's hot reaction zone [liter]

$\dot{V}_{\text{gas,hot}}$  Volumetric flow of fluidizing gas at operating temperature [liter per second]

$t_{\max}$  does not take into consideration the evolving water vapour from the wet feedstock, nor the pyrolysis vapours produced and therefore the actual residence time will be a little shorter.  $t_{\max}$  is displayed for sample process parameters in Table 15. The hot zone reaches from the reactor until the inlet of the quench column, where the vapours are cooled rapidly below 200°C.

**Table 15: Calculation of maximum hot vapour residence time**

| <b>Volume of hot reaction zone</b>                 |        |       |
|--|--------|-------|
| Volume reactor above distribution plate            | 1.676  | l     |
| Volume sand (to be deducted)                       | -0.395 | l     |
| Volume pipe to cyclone 1                           | 0.015  | l     |
| Volume cyclone 1                                   | 0.966  | l     |
| Volume pipe to cyclone 2                           | 0.016  | l     |
| Volume cyclone 2                                   | 0.264  | l     |
| Volume pipe to quench column                       | 0.068  | l     |
| Total volume of hot reaction zone                  | 2.609  | l     |
| <b>Fluidizing gas flow rate (Nitrogen)</b>         |        |       |
| Bottom flow rate at 20°C and 0.1MPa                | 40     | l/min |
| Feeder flow rate at 20°C and 0.1MPa                | 15     | l/min |
| Total flow rate at 20°C and 0.1MPa                 | 55     | l/min |
| Total flow rate at 500°C and 0.1MPa                | 145.06 | l/min |
| Total flow rate at 500°C and 0.1MPa                | 2.418  | l/s   |
| <b>Maximum residence time in hot reaction zone</b> |        |       |
| Maximum. residence time                            | 1.08   | s     |

### **5.2.5 Feed rate of biomass**

The biomass feed rate was limited by several factors. The lower limit was determined by the minimum revolutions per minute of the volumetric screw feeder (36RPM) and the bulk density of the material. Furthermore it was not desirable to run the 1kg/h pyrolysis unit at feeding rates lower than 0.4kg/h, because for feeding rates up to 400g/h a smaller test reactor was available and the impact of hold ups and losses proportionally increased at low feeding rates. The upper limit of the biomass feed rate was determined by the design of the unit, especially the limitations in heating power and heat transfer. The nominal maximum feeding rate was 1kg/h, although this was dependent on the feedstock characteristics, including moisture content or oil content in the case of rape meal. The feeding rates used were up to 1kg/h for woody biomass and forestry residue and 0.4 to 0.8kg/h for agricultural residues.

### **5.2.6 Feedstock moisture**

It is generally recommended that the feedstock moisture is less than 10wt.% [19] as any feedstock moisture contributes to the water content in the liquid fast pyrolysis product leading to a lower heating value and even to phase separation. Furthermore more energy is needed for the evaporation of the water. The impact of feedstock moisture on pyrolysis product yield beech wood has been investigated by Gerdes [11]. His work on beech wood showed that the impact of feedstock moisture on the liquid product yield on a dry feedstock basis is limited for moisture contents between 0 and 11wt.%. The liquid yields in his experiments were around 63wt.% on a dry feedstock basis. Nevertheless it has to be noted that decreasing feedstock moisture leads to changes in the properties of the liquid obtained, such as an increase in viscosity and higher heating value.

Due to this limited impact the feedstocks used were not pre-dried as long as the moisture content was less than 12wt.%. Furthermore a small biomass moisture content helps to reduce the risk of unwanted pyrolysis reactions within the fast feeding screw as the energy consumed by the heating up and evaporation of water is reducing the possibility of pyrolysis taking place.. For processing on a larger scale, removing a drying step to achieve moisture contents significantly below 10wt.% prior to pyrolysis would also reduce the energy demand of the whole process.

## 5.2.7 Quench system and liquid

The quench system consist of a quench column with a water cooled cooling jacket in which the fast pyrolysis vapours are in direct contact with the quench medium ISOPAR™ V. ISOPAR™ V is an iso-paraffinic hydrocarbon which is not miscible with fast pyrolysis liquid [11, 16]. Its major characteristics are presented in Table 16.

**Table 16: Product data ISOPAR™ V [85]**



12 litres of the quench medium were re-circulated in the system at a flow rate of approximately 10l/min and the temperature of the ISOPAR™ V was maintained at 30°C for all experiments by regulating the cooling water flow rate manually. After the experiment the ISOPAR™ V and fast pyrolysis liquid were put in a separation funnel and were left to phase separate and the separated liquids recovered.

## 5.3 *In-situ Nitrogenolysis*

The in-situ nitrogenolysis experiments used the same experimental setup and process parameters as described above to enable a comparison between pyrolysis and in-situ nitrogenolysis experiments. The only alteration was the addition of ammonia gas as a nitrogen compound as described below.

### 5.3.1 Nitrogen compound, injection point and preheating

Ammonia gas was chosen as the nitrogen containing compound for the experiments for the following reasons. Preliminary experiments with ammonia salts mixed with the biomass feedstock showed that due to the difference in particle size and density the mixture had the tendency to segregate in the volumetric feed hopper due to the movement of the agitator over time. Additionally it was known from the FAIR project (see section 2.6.3) that urea as a nitrogen compound formed urea dimers and trimers during co-pyrolysis and probably re-combined after dissociation. Soaking biomass in aqueous ammonia salt solutions proved to be

not suitable for biomass with high residual oil content, because it did not penetrate the sample. It was possible to soak beech wood in aqueous ammonia salt solution, but drying the sample afterwards took very long and ammonia was released in this process. Some properties of Ammonia gas are listed in Table 17.

**Table 17: Properties of Ammonia [86]**



It was possible to add ammonia gas at a constant rate to the process. Also no decomposition reactions of ammonia salts had to take place prior to reacting with the pyrolysis vapours as ammonia gas is already in a reactive form. The injection point for the ammonia gas was chosen to be after the nitrogen pre-heater and before the distribution plate (see Figure 17, #18). Injection before the distribution plate ensured a good mixture of the ammonia gas with the fluidizing nitrogen before entering the reactor. The additional heat load to preheat the ammonia gas was provided by the fluidization gas. The heat load was calculated (see example Table 18) taking into consideration the heat capacities of nitrogen and ammonia and the set point for the nitrogen pre-heater was increased from 500°C to 525°C to maintain the fluidization gas temperature at 500°C, see example in Table 18.

**Table 18: Calculation of new nitrogen pre-heater set point**

|                                     | Nitrogen      | Ammonia  | Unit                    |
|-------------------------------------|---------------|----------|-------------------------|
| Density [86, 87]                    | 1.15          | 0.71     | kg/m <sup>3</sup> (ATP) |
| Volumetric flow rate                | 40.00         | 2.00     | l/min (ATP)             |
|                                     | 6.67E-04      | 3.33E-05 | m <sup>3</sup> /s       |
| Mass flow rate                      | 7.67E-04      | 2.36E-05 | kg/s                    |
| Temperature of Stream               | <b>525.00</b> | 20.00    | °C                      |
|                                     | 798.15        | 293.15   | K                       |
| Specific heat capacity, cp [86, 87] | 7.89          | 2.16     | kJ/(kg K)               |
| Temp. of mixture (fluidizing gas)   | 793.93        |          | K                       |
|                                     | <b>500.78</b> |          | °C                      |

### 5.3.2 Nitrogen addition rate

The heterogeneity of biomass feedstock made it necessary to determine a common base on which the nitrogen addition to the process should be calculated. The carbon content of the feedstock on a dry feedstock basis was chosen as a base for these calculations as it is the major component of biomass and varies within well defined limits. The nitrogen addition rate was calculated as a mass percentage of elemental nitrogen on the base of the carbon content of dry feedstock. In combination with the feeding rate of the feedstock as received, the moisture content of the feedstock, the relative amount of nitrogen in ammonia gas and the density of ammonia gas at 0.1MPa and 20°C (ATP) the ammonia gas flow rate could be calculated (see Equation 7). A range from 0 to 20wt.%C nitrogen addition on dry feedstock carbon content basis was tested with beech wood to investigate if there is a limit in uptake of nitrogen. As mainly the functional groups are expected to react [34] it was expected that the nitrogen uptake would be limited.

#### Equation 7: Calculation of ammonia gas addition flow rate

$$F_{Am} = M_F \times (1 - C_M) \times C_C \times A_N \times \frac{1}{C_N} \times \frac{1}{D_{Am}} \times \frac{1}{60}$$

with

- $F_{Am}$  flow rate ammonia gas at ATP [l/min]
- $M_F$  feed rate feedstock as received [g/h]
- $C_M$  moisture content feedstock [wt.%] as received
- $C_C$  carbon content feedstock [wt.%] dry basis
- $A_N$  elemental nitrogen addition rate [wt.%C]
- $C_N$  elemental nitrogen content in ammonia [wt.%]
- $D_{Am}$  density ammonia at ATP [g/l]

## **6 Pyrolysis and in-situ nitrogenolysis experiments**

### ***6.1 Introduction***

A wide range of different feedstocks were processed on the 1kg/h pyrolysis rig in order to investigate and evaluate their thermal processing behaviour. The experiments were used to test process parameters and obtain data on product yields. Furthermore the pyrolysis products obtained were analysed to form a data base for comparison between pyrolysis and in-situ nitrogenolysis experiments. Based on the results of the pyrolysis experiments two feedstocks were selected for the in-situ nitrogenolysis experiments. This reduction of feedstocks was mainly due to time constrains.

In this section, the results of the pyrolysis and in-situ nitrogenolysis experiments are presented and discussed. Table 19 gives an overview of the experiments with mass balance on the 1kg/h unit and preliminary experiments on the 300g/h unit. The experiments marked as cooperation were performed with fellow researchers. The ones performed to support the work of fellow researchers are not reported and discussed and just listed to give a complete overview. Technically unsuccessful / aborted experiments are presented in section 6.8 presenting the problems in general and suggesting solutions to the problems.

**Table 19: List of pyrolysis and in-situ nitrogenolysis experiments**

| <b>Exp. No.</b> | <b>Date</b> | <b>Name</b>       | <b>Feedstock</b>      | <b>Remark</b> |
|-----------------|-------------|-------------------|-----------------------|---------------|
| 001             | 24.10.2008  | Beech I           | Beech wood            | cooperation   |
| 002             | 05.03.2009  | Beech II          | Beech wood            | successful    |
| 003             | 01.06.2009  | Beech III         | Beech wood            | successful    |
| 004             | 06.10.2010  | Beech IV          | Beech wood            | successful    |
| 005             | 10.11.2010  | Beech V           | Beech wood            | successful    |
| 006             | 03.08.2010  | Beech NH3 I       | Beech wood + Ammonia  | successful    |
| 007             | 15.09.2010  | Beech NH3 II      | Beech wood + Ammonia  | successful    |
| 008             | 26.10.2010  | Beech NH3 III     | Beech wood + Ammonia  | successful    |
| 009             | 24.11.2010  | Beech NH3 IV      | Beech wood + Ammonia  | successful    |
| 010             | 09.02.2011  | Beech NH3 V       | Beech wood + Ammonia  | successful    |
| 011             | 23.02.2011  | Beech NH3 VI      | Beech wood + Ammonia  | successful    |
| 012             | 03.03.2011  | Beech NH3 VII     | Beech wood + Ammonia  | successful    |
| 013             | 15.07.2009  | Barley DDGS       | DDGS Barley           | successful    |
| 014             | 08.11.2010  | DDGS NH3 I        | DDGS Barley + Ammonia | successful    |
| 015             | 05.04.2011  | DDGS NH3 II       | DDGS Barley + Ammonia | successful    |
| 016             | 07.04.2011  | DDGS NH3 III      | DDGS Barley + Ammonia | successful    |
| 017             | 04.05.2011  | DDGS NH3 IV       | DDGS Barley + Ammonia | successful    |
| 018             | 28.07.2009  | ADM Rape Meal II  | Rape meal ADM         | low closure   |
| 019             | 25.08.2009  | ADM Rape Meal III | Rape meal ADM         | successful    |
| 020             | 25.11.2009  | AD-Residue        | AD residue            | successful    |
| 021             | 09.06.2009  | Bark              | Bark                  | successful    |
| 022             | 20.11.2008  | Straw             | Wheat straw           | cooperation   |
| 023             | 15.02.2011  | Sugar beet pulp   | Sugar beet pulp       | cooperation   |
| 024             | 29.09.2008  | Soft wood I       | Mixed soft wood       | 300g/h unit   |
| 025             | 01.10.2008  | Soft wood II      | Mixed soft wood       | 300g/h unit   |
| 026             | 29.01.2009  | Willow I          | Willow SRC            | cooperation   |
| 027             | 18.03.2009  | Willow II         | Willow SRC            | cooperation   |
| 028             | 30.06.2009  | Miscanthus I      | Miscanthus            | cooperation   |
| 029             | 02.07.2009  | Miscanthus II     | Miscanthus            | cooperation   |
| 030             | 06.08.2009  | Miscanthus III    | Miscanthus            | cooperation   |
| 031             | 24.06.2009  | Eucalyptus        | Eucalyptus            | cooperation   |

## 6.2 Pyrolysis of beech wood

Beech wood was chosen as a reference material as it is virtually nitrogen free and can be processed without difficulties by fast pyrolysis. 5 successful experiments with beech wood were performed to establish data for product yields and characteristics and to demonstrate the repeatability of the experiments. The results for three experiments are given in the following sections.

### 6.2.1 Results

The process parameters were held constant for the three pyrolysis experiments (see Table 20). All experiments were performed around the previously discussed 500°C (see section 5.2.3) with actual feeding rates between 787 and 900g/h. The processing times were 3 hours or more in order to obtain a high mass balance closure and reduce the effect of hold ups and losses. The beech wood was pyrolysed without any difficulties and the fast pyrolysis liquid obtained was a in a single phase and did not phase separate even after up to 2 years of storage at room temperature.

**Table 20: Process parameters beech wood**

| Experiment number                     |       | 002         | 004         | 005         |
|---------------------------------------|-------|-------------|-------------|-------------|
| Feedstock                             |       | Beech wood  | Beech wood  | Beech wood  |
| Reactor temperature (nominal)         | °C    | 500.00      | 500.00      | 500.00      |
| Reactor temperature (average)         | °C    | 507.50      | 510.46      | 509.62      |
| Bed material                          |       | Silica sand | Silica sand | Silica sand |
| Bed material particle size            | µm    | 600-710     | 600-710     | 600-710     |
| Bed material mass                     | g     | 1000.00     | 1000.00     | 1000.00     |
| Duration                              | h:min | 3:21        | 3:00        | 3:00        |
| Feeder nitrogen flow rate (ATP)       | l/min | 15.00       | 15.00       | 15.00       |
| Fluidization nitrogen flow rate (ATP) | l/min | 35.00       | 35.00       | 35.00       |
| Feed rate (nominal)                   | g/h   | 913.32      | 900.00      | 896.70      |
| Feed rate (average)                   | g/h   | 821.20      | 787.08      | 899.67      |
| Total feed (as received)              | g     | 2751.02     | 2361.23     | 2699.01     |

The long processing times and the extensive mass balancing scheme (see section 5.1.3) allowed mass balance closures between 93 and 99% (dfb) for these experiments. Table 21 summarizes the mass balance results and Figure 20 shows the pyrolysis product yields on a dry feedstock basis.

**Table 21: Mass balance beech wood**

| <b>Experiment number</b>                   | <b>002</b>     |                | <b>004</b>     |                | <b>005</b>     |                |
|--|----------------|----------------|----------------|----------------|----------------|----------------|
| Feedstock                                  | Beech wood     |                | Beech wood     |                | Beech wood     |                |
| Unit                                       | g              | %              | g              | %              | g              | %              |
| <b>Input:</b>                              |                |                |                |                |                |                |
| Feedstock (ar)                             | 2751.02        |                | 2361.23        |                | 2699.01        |                |
| Feedstock moisture (ar)                    | 287.48         | 10.45%         | 256.67         | 10.87%         | 271.43         | 10.06%         |
| <b>Feedstock (dry)</b>                     | <b>2463.54</b> | <b>100.00%</b> | <b>2104.56</b> | <b>100.00%</b> | <b>2427.58</b> | <b>100.00%</b> |
| <b>Output:</b>                             |                |                |                |                |                |                |
| <b>Total FP char yield (dry)</b>           | <b>419.27</b>  | <b>17.02%</b>  | <b>364.43</b>  | <b>17.32%</b>  | <b>336.42</b>  | <b>13.86%</b>  |
| FP Char in reactor and piping (dry)        | 48.44          | 1.97%          | 61.57          | 2.93%          | 59.66          | 2.46%          |
| FP Char in 1st cyclone (dry)               | 367.09         | 14.90%         | 301.84         | 14.34%         | 276.52         | 11.39%         |
| FP Char in 2nd cyclone (dry)               | 3.73           | 0.15%          | 1.02           | 0.05%          | 0.24           | 0.01%          |
| <b>Total FP liquid yield (excl. water)</b> | <b>1323.73</b> | <b>53.73%</b>  | <b>995.48</b>  | <b>47.30%</b>  | <b>1180.33</b> | <b>48.62%</b>  |
| FP liquid yield (incl. water)              | 1700.52        |                | 1308.51        |                | 1513.04        |                |
| FP liquid yield (excl. water)              | 1296.35        | 52.62%         | 979.39         | 46.54%         | 1136.83        | 46.83%         |
| Secondary condensate yield (incl. water)   | 186.26         |                | 228.38         |                | 226.03         |                |
| Secondary condensate yield (excl. water)   | 27.38          | 1.11%          | 16.09          | 0.76%          | 43.50          | 1.79%          |
| <b>Calculated Reaction water</b>           | <b>275.57</b>  | <b>11.19%</b>  | <b>284.74</b>  | <b>13.53%</b>  | <b>287.31</b>  | <b>11.84%</b>  |
| Water in FP liquid                         | 404.17         |                | 329.12         |                | 376.21         |                |
| Water in secondary condensate              | 158.88         |                | 212.29         |                | 182.53         |                |
| <b>FP gas yield (excl. N2)</b>             | <b>428.86</b>  | <b>17.41%</b>  | <b>406.40</b>  | <b>19.31%</b>  | <b>453.72</b>  | <b>18.69%</b>  |
| Error of mass balance                      |                | 0.65%          |                | 2.54%          |                | 6.99%          |

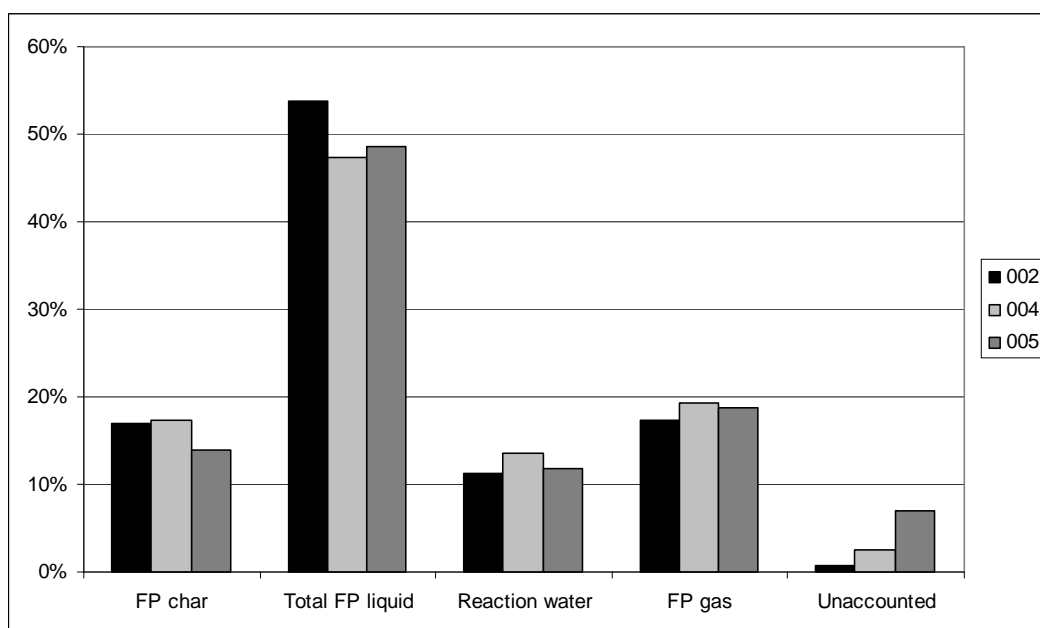


**Figure 20: Fast pyrolysis product yields for beech wood pyrolysis experiments (dfb)**

The fast pyrolysis gas composition in weight percent is given in Table 22. It excludes the fluidizing nitrogen. The higher heating value of the pyrolysis gas was calculated based on the higher heating values of the gas components published in literature [62] and its mass fraction (see section 3.7). It should be noted that the experiment number 002 has a 8% point higher carbon dioxide level and low C2-C4 levels and therefore a lower heating value. As the product yields for fast pyrolysis char and fast pyrolysis liquid are within the ordinary range and the amount of reaction water a bit lower than average, this is most likely due to a measurement error on the B-Channel of the Varian Micro GC (see section 3.13) and not due to insufficient purging of the system and oxidation of products.

**Table 22: Fast pyrolysis gas composition beech wood excluding fluidization nitrogen**

| Experiment No.  | 002        | 004        | 005        |
|-----------------|------------|------------|------------|
| Feedstock       | Beech wood | Beech wood | Beech wood |
| Hydrogen        | 0.27%      | 0.34%      | 0.37%      |
| Carbon monoxide | 35.91%     | 32.47%     | 33.90%     |
| Carbon dioxide  | 56.45%     | 48.26%     | 48.04%     |
| Methane         | 4.36%      | 4.41%      | 4.75%      |
| Ethene          | 0.90%      | 2.25%      | 2.10%      |
| Ethane          | 0.69%      | 2.42%      | 2.18%      |
| Propene         | 0.72%      | 2.80%      | 2.64%      |
| Propane         | 0.56%      | 3.39%      | 2.94%      |
| n-Butane        | 0.14%      | 3.65%      | 3.08%      |
| Sum             | 100.00%    | 100.00%    | 100.00%    |
| HHV [MJ/kg]     | 7.95       | 13.48      | 13.07      |

Elemental analysis data (for method see section 3.5) for the fast pyrolysis char and fast pyrolysis liquid are presented in Table 23 (oxygen is calculated by difference) together with data published in the literature and higher heating values calculated with the equation published by Channiwala (see section 3.7).

**Table 23: Elemental analysis of beech wood fast pyrolysis products**

|             | Beech char           | Beech char  | Beech oil | Beech oil   |
|-------------|----------------------|-------------|-----------|-------------|
|             |                      | Source [88] |           | Source [88] |
| C (daf)     | 76.34%               | 78.81%      | 54.24%    | 51.00%      |
| H (daf)     | 3.41%                | 3.03%       | 6.90%     | 5.90%       |
| N (daf)     | bdl.                 | n.d.        | bdl.      | n.d.        |
| O* (daf)    | 20.25%               | 18.16%      | 38.86%    | 43.10%      |
| HHV [MJ/kg] | 26.79                | 28.92       | 23.05     | 20.30       |
| O*          | Oxygen by difference |             |           |             |

## 6.2.2 Analysis and discussion

The fast pyrolysis experiments of beech wood show that the process parameters chosen are suitable for the production of fast pyrolysis liquid with high liquid yields. The average liquid yield is 61wt.% based on dry feedstock. This value is lower than the possible maximum of 75wt.% on dry feedstock basis reported by Bridgwater [16], but is in good correspondence with findings of Gerdes [11] who was using a comparable setup. Also the average yields for char (16wt.% (dfb)) and gas (18wt.% (dfb)) are within the expected ranges (see section 2.3.1).

As shown in Figure 20, the variation in the product yields is small and the overall mass balance closures have an average of 96wt.% (dfb). Therefore it can be stated that the repeatability of the experiments with the chosen setup and mass balancing scheme is given and suitable for the aims of this project.

The elemental composition of the pyrolysis char and oil are in good agreement with the results published by Guillain et al. as shown in Table 23. These results also support the choice for beech wood as virtually nitrogen free feedstock, because nitrogen levels in the products are below detection level. Consequently it can be regarded as nitrogen free for the purpose of comparison with later findings.

### 6.3 Fast pyrolysis of agricultural residues with a high nitrogen content

Agricultural residues with a high nitrogen content have been investigated by fast pyrolysis at the chosen standard conditions. The nitrogen in these materials is mostly in the form of proteins and therefore these feedstocks are commonly used as animal feed. The aim was to investigate how these materials will behave during fast pyrolysis and to obtain information on product yields and nitrogen content in the fast pyrolysis products. A high nitrogen content in the feedstock was seen as beneficial for the production of a slow release fertiliser, as nitrogen is already present and in principle less of it would needed to be added to the process.

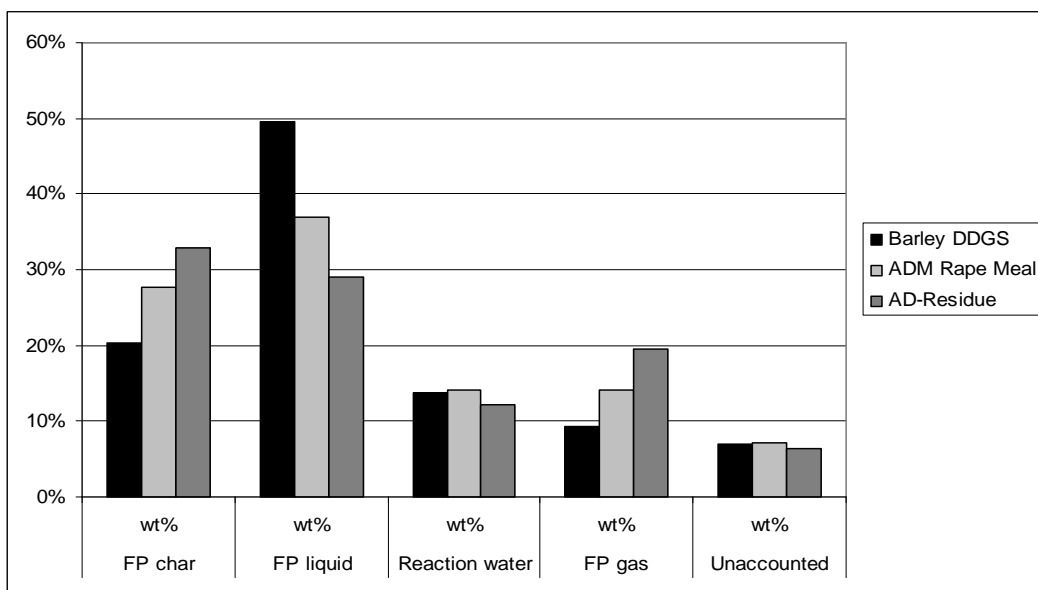
#### 6.3.1 Results

Table 24 lists the process parameters. These were kept constant except for the particle size and fluidizing nitrogen flow rate due to different char densities. As described in section 5.2.2 the higher char particle density of some feedstocks made it necessary to alter these parameters.

**Table 24: Process parameters high N feedstocks**

| Date                                  |       | 013         | 019           | 020         |
|---------------------------------------|-------|-------------|---------------|-------------|
| Feedstock                             |       | Barley DDGS | ADM Rape Meal | AD-Residue  |
| Reactor temperature (nominal)         | °C    | 500.00      | 500.00        | 500.00      |
| Reactor temperature (average)         | °C    | 506.00      | 505.00        | 515.98      |
| Bed material                          |       | Silica sand | Silica sand   | Silica sand |
| Bed material particle size            | µm    | 650-710     | 710-850       | 650-710     |
| Bed material mass                     | g     | 1000.00     | 1000.00       | 1000.00     |
| Duration                              | h:min | 1:09        | 1:42          | 2:00        |
| Feeder nitrogen flow rate (ATP)       | l/min | 17.00       | 17.00         | 17.00       |
| Fluidization nitrogen flow rate (ATP) | l/min | 45.00       | 65.00         | 38.00       |
| Feed rate (nominal)                   | g/h   | 442.80      | 723.30        | 480.00      |
| Feed rate (average)                   | g/h   | 427.46      | 707.37        | 464.55      |
| Total feed (as received)              | g     | 491.58      | 754.53        | 929.09      |

Table 25 shows the mass balance and Figure 21 illustrates the product yields. It can be seen that the liquid yields for these feedstocks vary between 41 and 63wt.% (dfb). Especially AD-residue has a significantly lower liquid yield of 41wt.% if compared to an average of 61wt.% of beech wood. An observation made during these experiments was that the char particles of rape meal and DDGS had a higher density making it necessary to increase both the fluidization gas flow rate and sand particle size of the bed material in order to entrain the char particles out of the reactor, while not entraining the bed material.



**Figure 21: Fast pyrolysis product yields of high N feedstocks**

Table 25: Mass balance high N feedstocks

| Experiment number                          | 013           |                | 019           |                | 020           |                |
|--|---------------|----------------|---------------|----------------|---------------|----------------|
| Feedstock                                  | Barley DDGS   |                | ADM Rape Meal |                | AD-Residue    |                |
| Unit                                       | g             | %              | g             | %              | g             | %              |
| <b>Input:</b>                              |               |                |               |                |               |                |
| Feedstock (ar)                             | 491.58        |                | 754.53        |                | 929.09        |                |
| Feedstock moisture (ar)                    | 39.77         | 8.09%          | 67.91         | 9.00%          | 87.24         | 9.39%          |
| <b>Feedstock (dry)</b>                     | <b>451.81</b> | <b>100.00%</b> | <b>686.62</b> | <b>100.00%</b> | <b>841.85</b> | <b>100.00%</b> |
| <b>Output:</b>                             |               |                |               |                |               |                |
| <b>Total FP char yield (dry)</b>           | <b>91.80</b>  | <b>20.32%</b>  | <b>189.99</b> | <b>27.67%</b>  | <b>276.88</b> | <b>32.89%</b>  |
| FP Char in reactor and piping (dry)        | 46.42         | 10.27%         | 67.04         | 9.76%          | 46.71         | 5.55%          |
| FP Char in 1st cyclone (dry)               | 45.07         | 9.98%          | 120.03        | 17.48%         | 225.18        | 26.75%         |
| FP Char in 2nd cyclone (dry)               | 0.31          | 0.07%          | 2.92          | 0.43%          | 4.99          | 0.59%          |
| <b>Total FP liquid yield (excl. water)</b> | <b>224.24</b> | <b>49.63%</b>  | <b>253.26</b> | <b>36.88%</b>  | <b>243.65</b> | <b>28.94%</b>  |
| FP liquid yield (incl. water)              | 257.30        |                | 282.42        |                | 261.98        |                |
| FP liquid yield (excl. water)              | 218.68        | 48.40%         | 240.22        | 34.99%         | 220.6         | 26.20%         |
| Secondary condensate yield (incl. water)   | 68.89         |                | 136.20        |                | 171.26        |                |
| Secondary condensate yield (excl. water)   | 5.56          | 1.23%          | 13.04         | 1.90%          | 23.05         | 2.74%          |
| <b>Calculated Reaction water</b>           | <b>62.18</b>  | <b>13.76%</b>  | <b>97.45</b>  | <b>14.19%</b>  | <b>102.35</b> | <b>12.16%</b>  |
| Water in FP liquid                         | 38.62         |                | 42.20         |                | 41.38         |                |
| Water in secondary condensate              | 63.33         |                | 123.16        |                | 148.21        |                |
| <b>FP gas yield (excl. N2)</b>             | <b>42.26</b>  | <b>9.35%</b>   | <b>97.24</b>  | <b>14.16%</b>  | <b>164.92</b> | <b>19.59%</b>  |
| Error of mass balance                      |               | 6.93%          |               | 7.09%          |               | 6.42%          |

The elemental analyses of the feedstock and the pyrolysis products are shown in Table 26 (for method see section 3.5). The nitrogen content is of great importance. It can be seen that Barley DDGS and ADM rape meal have high nitrogen content in the feedstock and in the pyrolysis liquids.

**Table 26: Elemental analyses and yields for high N feedstocks and fast pyrolysis products**

|                      |                      | Feedstock    | FP char      | FP liquids   | FP gas<br>(calculated) | MB error |
|----------------------|----------------------|--------------|--------------|--------------|------------------------|----------|
| <b>Barley DDGS</b>   |                      |              |              |              |                        |          |
| C                    | dfb                  | 47.84%       | 57.28%       | 48.22%       | 35.10%                 |          |
| H                    | dfb                  | 6.87%        | 2.62%        | 7.75%        | 1.70%                  |          |
| N                    | dfb                  | <b>4.49%</b> | <b>3.42%</b> | <b>5.21%</b> | n.d.                   |          |
| O*                   | dfb                  | 36.08%       | 15.91%       | 38.83%       | 63.20%                 |          |
| Ash                  | dfb                  | 4.73%        | 20.78%       | n.d.         | -                      |          |
| Input/Yield          | dfb                  | 100.00%      | 20.32%       | 63.39%       | 9.35%                  | 6.93%    |
| <b>ADM rape meal</b> |                      |              |              |              |                        |          |
| C                    | dfb                  | 45.01%       | 55.76%       | 50.74%       | 33.05%                 |          |
| H                    | dfb                  | 6.60%        | 2.64%        | 13.65%       | 1.32%                  |          |
| N                    | dfb                  | <b>5.66%</b> | <b>3.68%</b> | <b>5.88%</b> | n.d.                   |          |
| O*                   | dfb                  | 34.97%       | 15.14%       | 29.74%       | 65.63%                 |          |
| Ash                  | dfb                  | 7.76%        | 22.78%       | n.d.         | -                      |          |
| Input/Yield          | dfb                  | 100.00%      | 27.67%       | 51.08%       | 14.16%                 | 7.09%    |
| <b>AD residue</b>    |                      |              |              |              |                        |          |
| C                    | dfb                  | 40.42%       | 57.76%       | 55.44%       | 34.82%                 |          |
| H                    | dfb                  | 5.26%        | 2.83%        | 8.88%        | 1.43%                  |          |
| N                    | dfb                  | <b>1.61%</b> | <b>1.06%</b> | <b>2.88%</b> | nd.                    |          |
| O*                   | dfb                  | 35.64%       | 4.69%        | 32.80%       | 63.75%                 |          |
| Ash                  | dfb                  | 17.25%       | 33.67%       | n.d.         | -                      |          |
| Input/Yield          | dfb                  | 100.00%      | 32.89%       | 41.10%       | 19.59%                 | 6.42%    |
| O*                   | Oxygen by difference |              |              |              |                        |          |

Figure 22 correlates the nitrogen content to the product yields and shows the distribution of the nitrogen contained in the feedstock within the products. The nitrogen content of the gas phase was calculated by difference between the nitrogen in feedstock and nitrogen in solid and liquid fast pyrolysis products as the used Varian Micro GC could not quantify gaseous nitrogen compounds (see section 3.13) and contains the mass balancing error. Therefore the presented data can just represent a pseudo-mass balance.

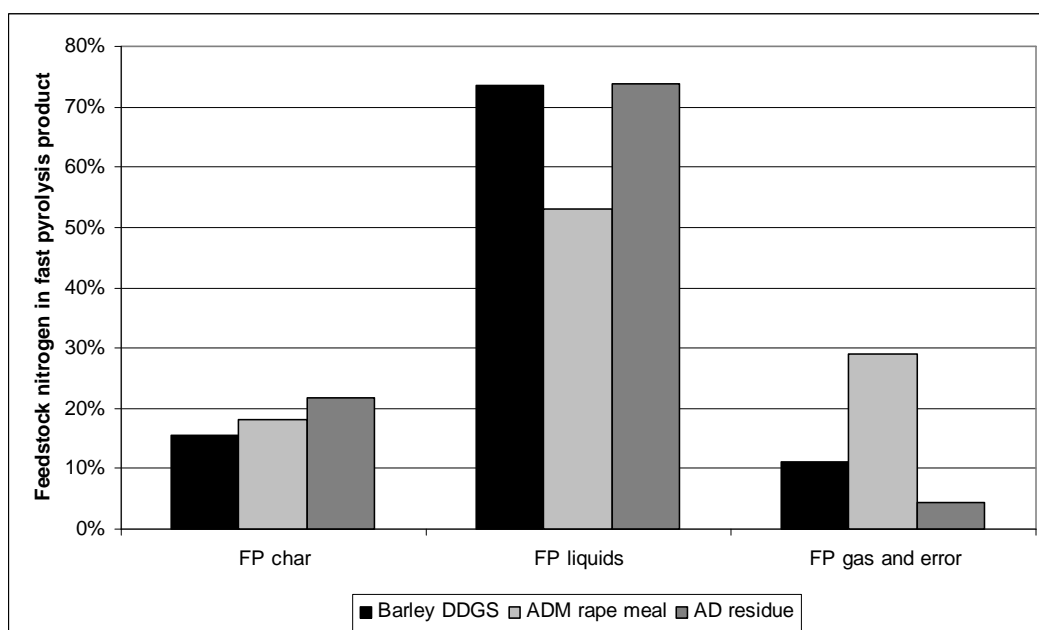


**Figure 22: Feedstock nitrogen distribution in fast pyrolysis products**

### 6.3.2 Analysis and discussion

The fast pyrolysis experiments with high nitrogen feedstocks show that the chosen process parameters are suitable for the production of fast pyrolysis liquid with high liquid yields in the case of barley DDGS and ADM rape meal. Particularly the liquid yield of 63wt.% of barley DDGS is comparable to the liquid yield of 61wt.% of beech wood. The lower liquid yield of AD-residue is most likely caused by the relatively high ash content of this feedstock (see Table 8) leading to higher char and gas yields due to the catalytic behaviour of elements in the ash. The mass balance closures of these experiments are slightly lower than for the beech wood experiments, but still above 90% which is a good result for the chosen experimental setup. Reasons for the lower mass balance closure are likely to be losses during recovery and to a limited extent the inability of the Micro GC to identify nitrogen compounds in the gas phase.

The elemental analysis shows that the feedstock nitrogen appears to be slightly concentrated in the liquid pyrolysis products as it can be seen in Table 26. In combination with the higher product yields for fast pyrolysis liquids the concentration of nitrogen in the fast pyrolysis liquid leads to the conclusion that more than 70wt.% of the nitrogen present in Barley DDGS feedstock and AD-residue feedstock and more than 50wt.% of the nitrogen presenting ADM-rape meal feedstock can be found in the pyrolysis liquid as shown in Figure 22. In terms of the production of a slow release fertiliser from pyrolysis liquids this can only be regarded as

beneficial, as the amount of nitrogen that would need to be added to the pyrolysis liquid could be reduced.

## **6.4 Pyrolysis of agricultural and forestry residue with low N**

An agricultural residue (wheat straw) and a forestry residue (pine bark), both low in nitrogen, were investigated as these are low value feedstocks that are not commonly used in fast pyrolysis for fast pyrolysis liquid production. Also these materials contain relatively high amounts of alkaline metals belonging to the group of plant nutrients (see section 2.5.2). The aim was to test process parameters and obtain data on product distribution and yield to evaluate if these two feedstocks are promising for the in-situ nitrogenolysis experiments.

### **6.4.1 Results**

The pyrolysis conditions are listed in Table 27 and the mass balance in Table 28. The corresponding product yields are presented in Figure 23.

**Table 27: Process parameters low N feedstocks**

| Experiment number                     |       | 022             | 021         |
|---------------------------------------|-------|-----------------|-------------|
| Feedstock                             |       | Wheat Straw     | Bark        |
| Reactor temperature (nominal)         | °C    | 500.00          | 500.00      |
| Reactor temperature (average)         | °C    | recording error | 504.00      |
| Bed material                          |       | Silica sand     | Silica sand |
| Bed material particle size            | µm    | 600-710         | 600-710     |
| Bed material mass                     | g     | 1000.00         | 1000.00     |
| Duration                              | h:min | 7:00            | 3:05        |
| Feeder nitrogen flow rate (ATP)       | l/min | 15.00           | 17.00       |
| Fluidization nitrogen flow rate (ATP) | l/min | 38.00           | 43.00       |
| Feed rate (nominal)                   | g/h   | 956.82          | 890.70      |
| Feed rate (average)                   | g/h   | 993.71          | 1049.52     |
| Total feed (as received)              | g     | 6956.00         | 3236.01     |

**Table 28: Mass balance low N feedstocks**

| Experiment number                          | 022            |                | 021            |                |
|--|----------------|----------------|----------------|----------------|
| Feedstock                                  | Wheat Straw    |                | Bark           |                |
| Unit                                       | g              | %              | g              | %              |
| <b>Input:</b>                              |                |                |                |                |
| Feedstock (ar)                             | 6956.00        |                | 3236.01        |                |
| Feedstock moisture (ar)                    | 706.03         | 10.15%         | 571.48         | 17.66%         |
| <b>Feedstock (dry)</b>                     | <b>6249.97</b> | <b>100.00%</b> | <b>2664.53</b> | <b>100.00%</b> |
| <b>Output:</b>                             |                |                |                |                |
| <b>Total FP char yield (dry)</b>           | <b>1912.65</b> | <b>30.60%</b>  | <b>1003.65</b> | <b>37.67%</b>  |
| FP Char in reactor and piping (dry)        | 113.28         | 1.81%          | 83.60          | 3.14%          |
| FP Char in 1st cyclone (dry)               | 1799.37        | 28.79%         | 884.94         | 33.21%         |
| FP Char in 2nd cyclone (dry)               | na.            | na.            | 35.11          | 1.32%          |
| <b>Total FP liquid yield (excl. water)</b> | <b>2286.75</b> | <b>36.59%</b>  | <b>904.48</b>  | <b>33.95%</b>  |
| FP liquid yield (incl. water)              | 3144.26        |                | 1436.03        | 53.89%         |
| FP liquid yield (excl. water)              | 2244.37        | 35.91%         | 895.82         | 33.62%         |
| Secondary condensate yield (incl. water)   | 168.29         |                | 310.55         | 11.65%         |
| Secondary condensate yield (excl. water)   | 42.38          | 0.68%          | 8.66           | 0.33%          |
| <b>Calculated Reaction water</b>           | <b>319.77</b>  | <b>5.12%</b>   | <b>270.62</b>  | <b>10.16%</b>  |
| Water in FP liquid                         | 899.89         |                | 540.21         |                |
| Water in secondary condensate              | 125.91         |                | 301.89         |                |
| <b>FP gas yield (excl. N2)</b>             | <b>1156.18</b> | <b>18.50%</b>  | <b>385.06</b>  | <b>14.45%</b>  |
| Error of mass balance                      |                | 9.19%          |                | 3.78%          |

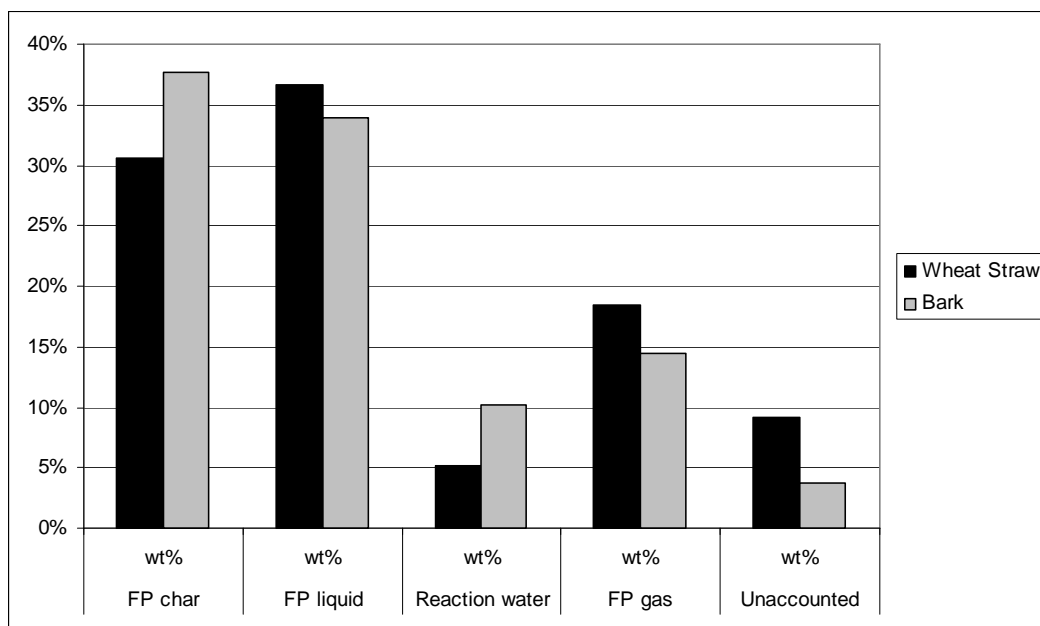


**Figure 23: Fast pyrolysis product yields of low N feedstocks**

Both feedstocks have a high fast pyrolysis char yield at the expense of liquids produced. Furthermore the fast pyrolysis liquids from the collection tank of both feedstocks were phase separated consisting of an aqueous top phase and a viscous bottom phase. The elemental analyses of both feedstocks and their chars are displayed in Table 29.

**Table 29: Elemental analysis of low N feedstocks and FP chars**

| Element | Basis                | Bark      |         | Wheat straw |         |
|---------|----------------------|-----------|---------|-------------|---------|
|         |                      | feedstock | FP char | feedstock   | FP char |
| C       | dfb                  | 50.51%    | 66.74%  | 43.49%      | 52.25%  |
| H       | dfb                  | 5.40%     | 2.90%   | 5.50%       | 2.44%   |
| N       | dfb                  | 0.12%     | 0.06%   | 0.62%       | 0.50%   |
| O*      | dfb                  | 40.63%    | 19.64%  | 40.73%      | 13.14%  |
| Ash     | dfb                  | 3.35%     | 10.67%  | 9.67%       | 31.67%  |
| O/C     | daf                  | 0.60      | 0.22    | 0.70        | 0.19    |
| H/C     | daf                  | 1.28      | 0.52    | 1.52        | 0.56    |
| O*      | Oxygen by difference |           |         |             |         |

## 6.4.2 Analysis and discussion

The low nitrogen content of the feedstocks of less than 1wt.% in combination with the low liquid yields and the phase separation of the fast pyrolysis liquids can only be seen as a disadvantage for the aim of this project to produce a slow release fertiliser from the liquid fast pyrolysis product.

The low yields are most likely linked to the higher ash content in the feedstocks (see Table 8). Investigations have shown that alkaline metals in the ash act as a catalyst in pyrolysis (see section 2.2.5) that lead to cracking of vapours and an increased gas and char yield.

The O/C and H/C ratios of the fast pyrolysis char are as expected in the area of coals (see van Krevelen diagram section 2.4.6). Combined with the alkaline metals bound in the FP char, the FP char of these feedstocks might be suitable as a soil amendment feeding back these metals to the soil and providing a carbon sink due to the slow degradation rates reported for black carbon [40]. The later aspect is currently investigated by many researchers, but not further investigated here as it is beyond the scope of this research. Information on this topic has been presented in section 2.4.6.

## ***6.5 In-situ nitrogenolysis of beech wood at different N addition rates***

In this experimental series beech wood was pyrolysed at different nitrogen (in form of ammonia) addition rates for in-situ nitrogenolysis. The series was performed to investigate the relationship between nitrogen addition and nitrogen content in the liquid in-situ nitrogenolysis product. It was expected that the capability of the liquid fast pyrolysis product to bind nitrogen is limited as suggested by Radlein (see section 2.6.2).

Four in-situ nitrogenolysis experiments were performed with nominal nitrogen addition levels as ammonia between 5 and 20wt.%C nitrogen addition based on dry feedstock carbon content. Beech wood was chosen for these experiments, because it was clear that all nitrogen in the product was added in the process from ammonia addition.

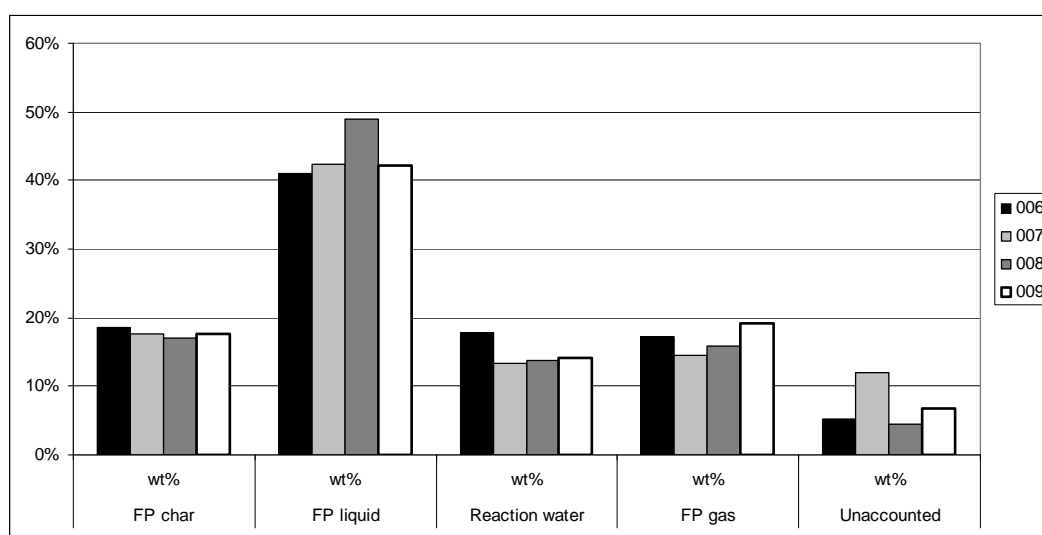
### **6.5.1 Results**

Table 30 lists the process parameters. These were kept constant throughout the series and are the same as for the reference experiments (see section 6.2). The level of nitrogen addition was calculated based on the nominal feed rate and carbon content of the dry beech wood used adjusting the ammonia gas flow to the closest 0.1l/min that could be indicated by the rotameter used for dosing the ammonia gas (see Equation 7). After the experiment the actual nitrogen addition was calculated using the average feed rate and the used ammonia gas flow rate, which is shown in Table 30.

**Table 30: Process parameters for beech wood with different N addition rates**

| Experiment number                     |       | 006         | 007         | 008         | 009         |
|---------------------------------------|-------|-------------|-------------|-------------|-------------|
| Feedstock                             |       | Beech wood  | Beech wood  | Beech wood  | Beech wood  |
| Reactor temperature (nominal)         | °C    | 500.00      | 500.00      | 500.00      | 500.00      |
| Reactor temperature (average)         | °C    | 507.26      | 508.36      | 505.47      | 511.38      |
| Bed material                          |       | Silica sand | Silica sand | Silica sand | Silica sand |
| Bed material particle size            | µm    | 600-710     | 600-710     | 600-710     | 600-710     |
| Bed material mass                     | g     | 1000.00     | 1000.00     | 1000.00     | 1000.00     |
| Duration                              | h:min | 1:30        | 1:41        | 2:00        | 2:00        |
| Feeder nitrogen flow rate (ATP)       | l/min | 18.00       | 18.00       | 18.00       | 18.00       |
| Fluidization nitrogen flow rate (ATP) | l/min | 35.00       | 35.00       | 35.00       | 35.00       |
| Ammonia flow rate (ATP)               | l/min | 1.50        | 2.50        | 0.60        | 1.00        |
| Nitrogen addition                     | wt.%C | 12.02%      | 22.57%      | 5.86%       | 9.21%       |
| Feed rate (nominal)                   | g/h   | 913.32      | 823.50      | 843.90      | 863.70      |
| Feed rate (average)                   | g/h   | 821.20      | 812.86      | 753.04      | 795.51      |
| Total feed (as received)              | g     | 2751.02     | 1354.77     | 1506.07     | 1591.01     |

The mass balance is displayed in Table 31 and the product yields in Figure 24. The product yields were calculated on a dry feedstock basis excluding the added ammonia gas to allow comparison between pyrolysis and in-situ nitrogenolysis experiments. It can be seen that the liquid yields for the experiments vary between 56 and 63wt.% (dfb).



**Figure 24: In-situ nitrogenolysis product yields for beech wood according to N addition rates**

**Table 31: Mass balance for beech wood with different N addition rates**

| Experiment number                          | 006            |                | 007            |                | 008            |                | 009            |                |
|--|----------------|----------------|----------------|----------------|----------------|----------------|----------------|----------------|
| Feedstock                                  | Beech wood     |                | Beech wood     |                | Beech wood     |                | Beech wood     |                |
| Nitrogen addition [wt%C]                   | 12.02%         |                | 22.57%         |                | 5.86%          |                | 9.21%          |                |
| Unit                                       | g              | %              | g              | %              | g              | %              | g              | %              |
| <b>Input:</b>                              |                |                |                |                |                |                |                |                |
| Feedstock (ar)                             | 1377.23        |                | 1354.77        |                | 1506.07        |                | 1591.01        |                |
| Feedstock moisture (ar)                    | 145.16         | 10.54%         | 139.59         | 10.30%         | 158.64         | 10.53%         | 161.17         | 10.13%         |
| <b>Feedstock (dry)</b>                     | <b>1232.07</b> | <b>100.00%</b> | <b>1215.18</b> | <b>100.00%</b> | <b>1347.43</b> | <b>100.00%</b> | <b>1429.84</b> | <b>100.00%</b> |
| <b>Output:</b>                             |                |                |                |                |                |                |                |                |
| <b>Total FP char yield (dry)</b>           | <b>229.91</b>  | <b>18.66%</b>  | <b>214.80</b>  | <b>17.68%</b>  | <b>229.55</b>  | <b>17.04%</b>  | <b>250.74</b>  | <b>17.54%</b>  |
| FP Char in reactor and piping (dry)        | 50.21          | 4.08%          | 60.77          | 5.00%          | 51.07          | 3.79%          | 74.16          | 5.19%          |
| FP Char in 1st cyclone (dry)               | 176.38         | 14.32%         | 151.20         | 12.44%         | 176.26         | 13.08%         | 14.68          | 1.03%          |
| FP Char in 2nd cyclone (dry)               | 3.32           | 0.27%          | 2.83           | 0.23%          | 2.22           | 0.16%          | 1.90           | 0.13%          |
| <b>Total FP liquid yield (excl. water)</b> | <b>505.62</b>  | <b>41.04%</b>  | <b>514.62</b>  | <b>42.35%</b>  | <b>660.75</b>  | <b>49.04%</b>  | <b>604.56</b>  | <b>42.28%</b>  |
| FP liquid yield (incl. water)              | 729.35         |                | 657.89         |                | 861.80         |                | 805.07         |                |
| FP liquid yield (excl. water)              | 488.28         | 39.63%         | 487.31         | 40.10%         | 643.12         | 47.73%         | 567.19         | 39.67%         |
| Secondary condensate yield (incl. water)   | 141.13         |                | 158.66         |                | 141.50         |                | 162.88         |                |
| Secondary condensate yield (excl. water)   | 17.34          | 1.41%          | 27.31          | 2.25%          | 17.63          | 1.31%          | 37.37          | 2.61%          |
| <b>Calculated Reaction water</b>           | <b>219.70</b>  | <b>17.83%</b>  | <b>162.34</b>  | <b>13.36%</b>  | <b>183.91</b>  | <b>13.65%</b>  | <b>202.22</b>  | <b>14.14%</b>  |
| Water in FP liquid                         | 241.07         |                | 170.58         |                | 218.68         |                | 237.88         |                |
| Water in secondary condensate              | 123.79         |                | 131.35         |                | 123.87         |                | 125.51         |                |
| <b>FP gas yield (excl. N2)</b>             | <b>213.28</b>  | <b>17.31%</b>  | <b>177.01</b>  | <b>14.57%</b>  | <b>213.63</b>  | <b>15.85%</b>  | <b>275.25</b>  | <b>19.25%</b>  |
| Error of mass balance                      |                | 5.16%          |                | 12.05%         |                | 4.42%          |                | 6.79%          |

An important observation for the whole beech wood series was that the in-situ nitrogenolysis liquid obtained from the tank was phase separated forming an aqueous top phase and viscous bottom phase. The mass ratio between top and bottom phase is about 30:70. The phases are not separately reported in Table 31 to keep the results comparable to the pyrolysis experiments. The bottom phase changed to a hard rubber like mass within hours when stored at room temperature. Furthermore the secondary condensates and cotton wool filter had a significant ammonia smell after all runs due to surplus ammonia that was carried through the system with the gas stream. Figure 26 illustrated the relative amount of nitrogen bound in the products.

The elemental analyses of nitrogenolysis liquid phases and chars are displayed in Table 32. The nitrogenolysis char contains levels of nitrogen of less than 1.49wt.%, while the liquid product contains up to 7.26wt.% in the bottom phase and 7.53wt.% in the top phase.

**Table 32: Elemental analysis of nitrogenolysis products at different N addition rates**

|                |   |   |   |   |
|----------------|---|---|---|---|
| Feedstock      | Beech wood                              | Beech wood                              | Beech wood                              | Beech wood                              |
| Exp. No.       | 006                                     | 007                                     | 008                                     | 009                                     |
| N addition     | 5.86%                                   | 9.21%                                   | 12.02%                                  | 22.57%                                  |
| <b>Product</b> | <b>Char</b>                             | <b>Char</b>                             | <b>Char</b>                             | <b>Char</b>                             |
| C (af)         | 84.66%                                  | 85.75%                                  | 82.41%                                  | 77.26%                                  |
| H (af)         | 3.47%                                   | 3.65%                                   | 3.28%                                   | 5.11%                                   |
| N (af)         | 0.43%                                   | 0.46%                                   | 0.52%                                   | 1.49%                                   |
| O* (af)        | 11.44%                                  | 10.14%                                  | 13.79%                                  | 16.14%                                  |
| <b>Product</b> | <b>Nitrogenolysis liq. top phase</b>    |
| C (af)         | 26.63%                                  | 24.39%                                  | 25.01%                                  | 26.83%                                  |
| H (af)         | 9.80%                                   | 10.18%                                  | 9.46%                                   | 9.53%                                   |
| N (af)         | 4.29%                                   | 5.15%                                   | 6.30%                                   | 7.53%                                   |
| O* (af)        | 59.29%                                  | 60.29%                                  | 59.24%                                  | 56.12%                                  |
| <b>Product</b> | <b>Nitrogenolysis liq. bottom phase</b> |
| C (af)         | 50.90%                                  | 55.45%                                  | 51.17%                                  | 52.51%                                  |
| H (af)         | 8.22%                                   | 7.58%                                   | 8.03%                                   | 7.83%                                   |
| N (af)         | 4.18%                                   | 5.36%                                   | 6.93%                                   | 7.26%                                   |
| O* (af)        | 36.72%                                  | 31.62%                                  | 33.88%                                  | 32.40%                                  |
| O*             | Oxygen by difference                    |   |   |   |

The distribution of feedstock nitrogen in the nitrogenolysis products and losses are displayed in Figure 25. In Figure 26 the nitrogen content in the top phase and bottom phase is plotted over the rate of nitrogen addition. It clearly indicates that the nitrogen incorporated in both phases is limited as the nitrogen content does not increase at the same rate as the nitrogen addition.

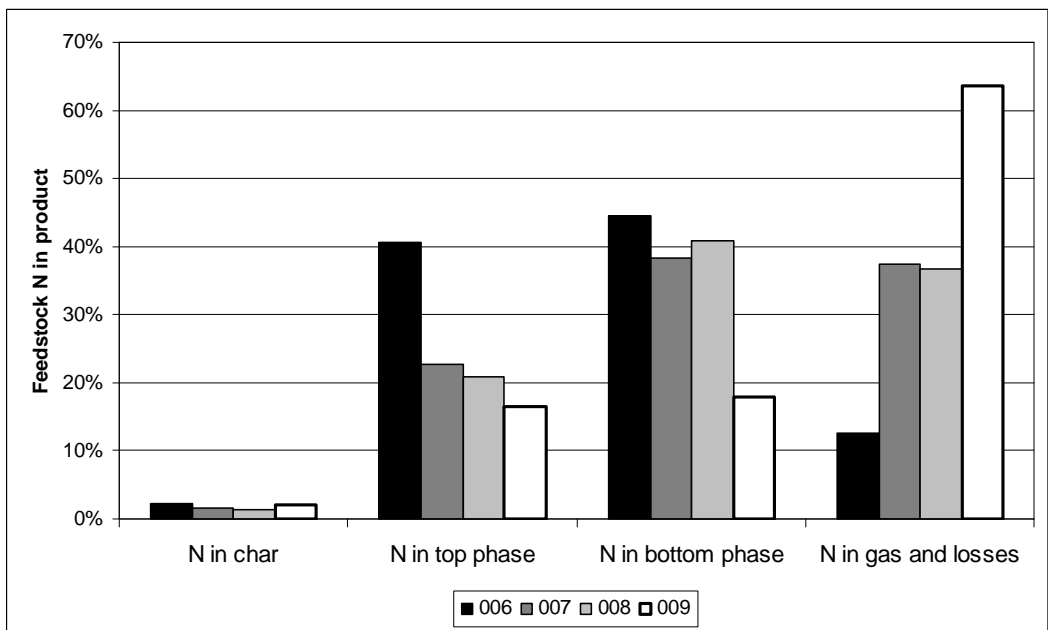


Figure 25: Distribution of feedstock nitrogen in nitrogenolysis products and losses

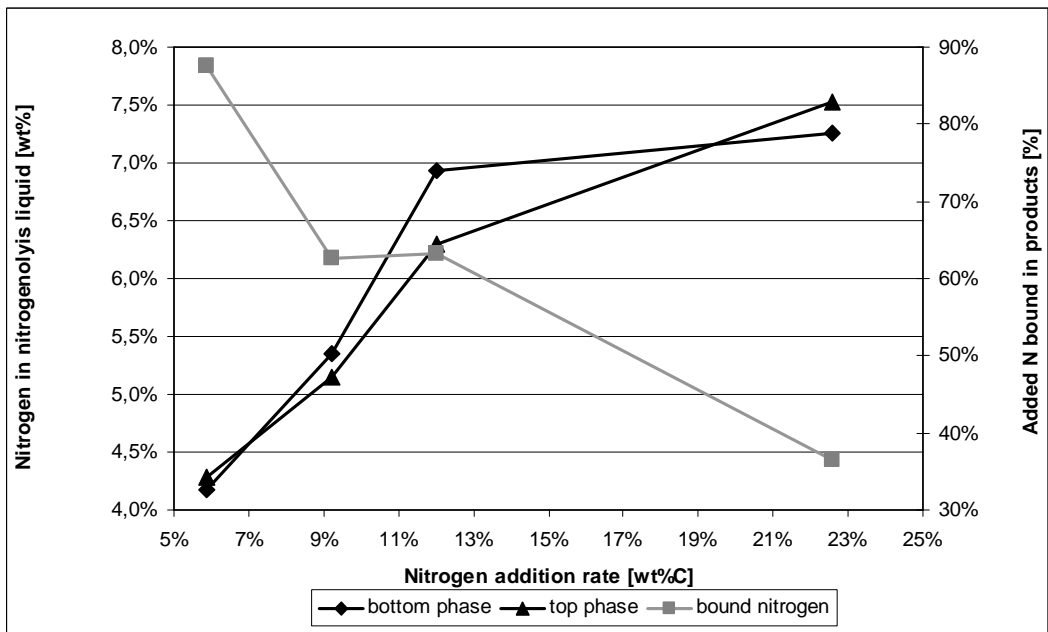
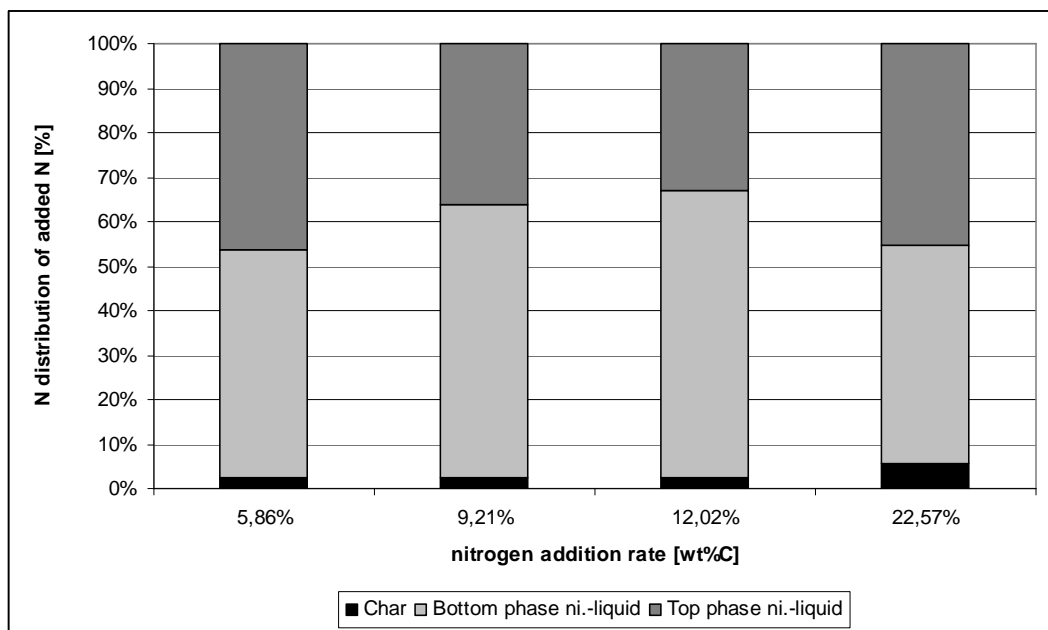


Figure 26: N content in nitrogenolysis liquids (black lines) and relative amount of N bound in nitrogenolysis products (grey line)

Figure 25 shows that with increasing the nitrogen addition rate the relative amount of nitrogen added to the char is relatively constant, the relative amount added to the top phase is decreasing and the relative amount of feed nitrogen added to the bottom phase and the losses are increasing. Additionally in Figure 26 it can be seen that the relative amount of nitrogen bound in liquid and solid nitrogenolysis products over the amount of nitrogen added to the process decreases with higher nitrogen addition rates, meaning that in the case of the 22.57wt.%C nitrogen addition experiment less than 40% of the added nitrogen actually is bound in the products. In contrast for the lowest addition rate of 5.86wt.%C more than 85% of the added nitrogen were bound in the products.

The distribution of the added nitrogen bound in the nitrogenolysis products is shown in Figure 27. It emphasises that hardly any of the added nitrogen is bound in the char. More than half of the nitrogen is bound in the bottom phase of the nitrogenolysis liquid.



**Figure 27: Nitrogen distribution of added nitrogen in nitrogenolysis char and liquids**

## 6.5.2 Analysis and discussion

The liquid product yields indicate that the total amount of liquid products is lower when compared to the reference beech wood experiments. Also the aspect of added nitrogen has to be taken into consideration here as the mass balance excludes the ammonia gas for comparison reasons, although the added nitrogen contributes to the mass balance. It can be

concluded that the addition of ammonia gas has a direct impact on the condensable vapour phase and reduces the amount of liquids obtained from the process.

The char yields are similar to the reference experiments with an average of 18wt.% (see Figure 24). It is interesting to note that the nitrogen uptake by the char is significantly lower than the uptake by the oil and does not exceed 1.5wt.%. It can be concluded that the ammonia gas mainly reacts with the vapour phase and not with the solid. This can also be seen in Figure 27 above indicating that less than 6% of the added nitrogen is contained in the char for all samples and is typically 2.6 wt.% for lower N additions. Whether the nitrogen in the char is chemically bound or just adsorbed was not investigated. This should be done if the char is considered as nitrogen containing soil amendment or fuel (see section 11) due to possible emissions.

The most significant and obvious change was observed with the nitrogenolysis liquid products. In contrast to the reference experiments it phase separates forming an aqueous top phase and a viscous bottom phase. Additionally the bottom phase readily polymerized and became hard like rubber within a week if stored at room temperature. This phenomenon is thought to be caused by the ammonia causing a shift to longer chain condensation products and enhancing polymerization reactions.  $\text{NH}_2$ - groups in urea are known to react with phenols and aldehydes to form urea resins [34]. In order to understand this phenomenon further investigations were performed that are described in section 8.

Figure 25 and Figure 26 clearly indicate that the nitrogen uptake in the liquid bottom phase product is limited. Radlein [34] already suggested this, linking it to the limited amount of functional groups of 6-11mol/kg fast pyrolysis liquid, see section 2.6.2. Although Hanser [27] objected to the theory that the nitrogen uptake was simply limited to by the amount of functional groups, he also observed a limitation in nitrogen uptake in his post processing experiments (see Figure 10). The limited uptake is also underlined by the actual amount of nitrogen bound in the nitrogenolysis products at different addition rates (Figure 27). While the amount nitrogen added is increased in the experimental series, just part of the additional nitrogen reacts and the rest passes the system un-reacted as losses.

For the distribution of the added nitrogen in the nitrogenolysis char and liquids it is an interesting result that the bottom phase has the highest uptake of nitrogen among the in-situ nitrogenolysis products, except for the very high nitrogen addition rate. The latter is most

likely due to the higher partial pressure of ammonia gas in that experiment leading to a higher amount of ammonia dissolved in the aqueous phase. As this ammonia is likely not chemically bound, it could be recovered and reused in the nitrogenolysis process. This aspect was not investigated further, but recommendations are presented in section 11.

As a consequence of the results presented the nitrogen addition rate for the slow release fertiliser production experiments was determined to be 12wt.%C based on dry feedstock carbon content. A higher addition rate did not show a significant increase in added nitrogen in the liquid product that the slow release fertiliser was derived from. Already at this addition rate an excess of about 40% non-reacted ammonia gas was expected that would need to be recycled in a continuous process.

## ***6.6 In-situ nitrogenolysis of beech wood – SRF production experiments***

The experimental series of pyrolysing beech wood in the presence of ammonia gas – in-situ nitrogenolysis – at a nitrogen addition rate of nominal 12wt.%C (as determined in section 6.5) was conducted in order to produce sufficient amounts of the product, nitrogenolysis liquid bottom phase, for further analysis (section 8), thermal solidification experiments (section 7) and microbial and plant testing (section 9). The process parameters were determined in the experiments that are described in section 6.2 and 6.5 for a suitable nitrogen addition rate.

### **6.6.1 Results**

The nitrogenolysis experiments were conducted with the process parameters listed in Table 33. All parameters were kept constant in order to get repeatable and comparable results and constant product quantity and quality. In order to obtain enough material for the following investigations two 3 hour and one 2 hour run were performed. No problems occurred during these runs.

**Table 33: Process parameters for beech wood nitrogenolysis production runs**

| Experiment number                     |       | 010         | 011         | 012         |
|---------------------------------------|-------|-------------|-------------|-------------|
| Feedstock                             |       | Beech wood  | Beech wood  | Beech wood  |
| Reactor temperature (nominal)         | °C    | 500.00      | 500.00      | 500.00      |
| Reactor temperature (average)         | °C    | 517.48      | 515.15      | 517.63      |
| Bed material                          |       | Silica sand | Silica sand | Silica sand |
| Bed material particle size            | µm    | 600-710     | 600-710     | 600-710     |
| Bed material mass                     | g     | 1000.00     | 1000.00     | 1000.00     |
| Duration                              | h:min | 3:00        | 3:00        | 2:00        |
| Feeder nitrogen flow rate (ATP)       | l/min | 18.00       | 18.00       | 18.00       |
| Fluidization nitrogen flow rate (ATP) | l/min | 35.00       | 35.00       | 35.00       |
| Ammonia flow rate (ATP)               | l/min | 2.00        | 1.80        | 1.80        |
| Nitrogen addition                     | wt.%C | 15.13%      | 16.73%      | 14.16%      |
| Feed rate (nominal)                   | g/h   | 1105.80     | 1049.10     | 994.50      |
| Feed rate (average)                   | g/h   | 962.63      | 784.84      | 931.17      |
| Total feed (as received)              | g     | 2887.91     | 2354.52     | 1862.35     |

The mass balances are displayed in Table 34 and the product distributions are shown in Figure 28. From the mass balances it can be seen that the actual nitrogen addition was around the nominal 15wt.%C. The product yields are calculated on dry feedstock basis and exclude the ammonia gas. The three experiments have a very high closure of around 99wt.%, which will be discussed later. Figure 28 clearly shows that the product distribution of the three runs was very similar.

**Table 34: Mass balance for beech wood nitrogenolysis production runs**

| Experiment number                          | 010            |                | 011            |                | 012            |                |
|--|----------------|----------------|----------------|----------------|----------------|----------------|
| Feedstock                                  | Beech wood     |                | Beech wood     |                | Beech wood     |                |
| Nitrogen addition [wt%C]                   | 15.13%         |                | 16.73%         |                | 14.16%         |                |
| Unit                                       | g              | %              | g              | %              | g              | %              |
| <b>Input:</b>                              |                |                |                |                |                |                |
| Feedstock (ar)                             | 2887.91        |                | 2354.52        |                | 1862.35        |                |
| Feedstock moisture (ar)                    | 277.91         | 9.62%          | 229.41         | 9.74%          | 188.53         | 10.12%         |
| <b>Feedstock (dry)</b>                     | <b>2610.00</b> | <b>100.00%</b> | <b>2125.11</b> | <b>100.00%</b> | <b>1673.81</b> | <b>100.00%</b> |
| <b>Output:</b>                             |                |                |                |                |                |                |
| <b>Total FP char yield (dry)</b>           | <b>563.85</b>  | <b>21.60%</b>  | <b>380.04</b>  | <b>17.88%</b>  | <b>303.82</b>  | <b>18.15%</b>  |
| FP Char in reactor and piping (dry)        | 222.48         | 8.52%          | 57.05          | 2.68%          | 55.89          | 3.34%          |
| FP Char in 1st cyclone (dry)               | 339.66         | 13.01%         | 320.95         | 15.10%         | 245.07         | 14.64%         |
| FP Char in 2nd cyclone (dry)               | 1.71           | 0.07%          | 2.04           | 0.10%          | 2.86           | 0.17%          |
| <b>Total FP liquid yield (excl. water)</b> | <b>1303.84</b> | <b>49.96%</b>  | <b>1073.72</b> | <b>50.53%</b>  | <b>826.26</b>  | <b>49.36%</b>  |
| FP liquid yield (incl. water)              | 1712.09        |                | 1398.19        |                | 1074.01        |                |
| FP liquid yield (excl. water)              | 1248.36        | 47.83%         | 1023.78        | 48.18%         | 791.83         | 47.31%         |
| Secondary condensate yield (incl. water)   | 248.21         |                | 223.94         |                | 188.18         |                |
| Secondary condensate yield (excl. water)   | 55.48          | 2.13%          | 49.93          | 2.35%          | 34.43          | 2.06%          |
| <b>Calculated Reaction water</b>           | <b>378.55</b>  | <b>14.50%</b>  | <b>319.01</b>  | <b>15.01%</b>  | <b>247.40</b>  | <b>14.78%</b>  |
| Water in FP liquid                         | 463.73         |                | 374.41         |                | 282.18         |                |
| Water in secondary condensate              | 192.73         |                | 174.01         |                | 153.75         |                |
| <b>FP gas yield (excl. N2)</b>             | <b>359.97</b>  | <b>13.79%</b>  | <b>334.28</b>  | <b>15.73%</b>  | <b>283.39</b>  | <b>16.93%</b>  |
| Error of mass balance                      |                | 0.15%          |                | 0.85%          |                | 0.77%          |

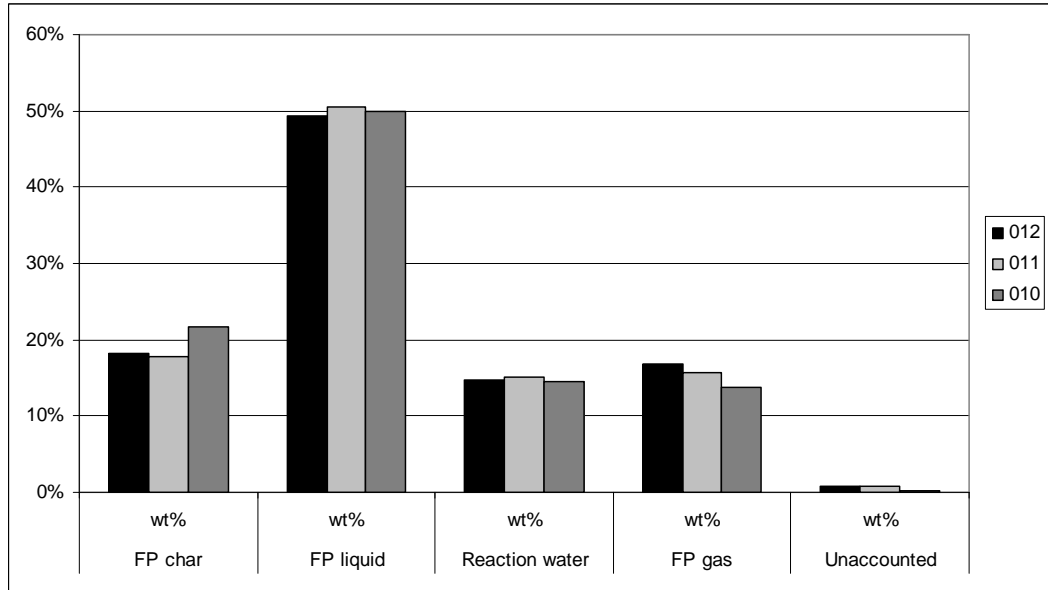


**Figure 28: Product distribution of beech wood nitrogenolysis production runs**

## 6.6.2 Analysis and discussion

Although slight deviations in terms of average reactor temperature average feeding rate and resulting average nitrogen addition on carbon basis occurred, the mass balances and product yields show the repeatability of the production experiments. By the three experiments sufficient amount of product for further testing was produced and the repeatability was shown. The high mass balance closure of about 99% is due to the fact that it is calculated on a dry feedstock basis excluding the ammonia gas, although the added ammonia contributes to the mass balance. When compared to the reference experiments (see section 6.2) this indicates that nitrogen was added to the product as the reference experiments had a closure between 93 and 97wt.%.

Most important is the relatively high yield of liquid products at about 65wt.%. This yield has to be subdivided into the aqueous top phase and viscous bottom phase. The mass ratio between top and bottom phase is about 30:70.

The top phase has a high water content with an average Karl Fischer titration water content of 49wt.%. It has a distinct ammonia smell. Whether the ammonia is actually chemically bound or just dissolved in the aqueous phase was not determined. The latter is expected and would give the opportunity to recover ammonia from this phase by a stripping process to enhance the overall system performance. This aspect is part of the recommendations in section 11. For

the thermal solidification step investigated (section 7) the phase separation is beneficial as a large proportion of the water is separated with the top phase.

The bottom phase is highly viscous and changes into a hard rubber like substance within a week if stored at room temperature. It contains approximately 10wt.% of water. An exact value could not be determined due to the nature of the sample. The bottom phase is of special interest as the nitrogen in this phase is supposed to be chemically bound. This is investigated in section 8. Furthermore this phase was converted in a thermal solidification step into a solid slow release fertiliser that is the desired final product. The analysis of this phase and the thermal conversion are included in sections 8.3 and 7.6.

## ***6.7 Nitrogenolysis of DDGS – SRF production experiments***

Barley DDGS was used for nitrogenolysis with the same process parameters as the experimental series of pyrolysing beech wood in the presence of ammonia. The nominal nitrogen addition was kept at 12wt.%C as used for beech and determined in section 6.5. The barley DDGS series was conducted in order to produce sufficient amounts of fast pyrolysis liquid bottom phase, for further analysis (section 8), thermal solidification experiments (section 7) and microbial and plant testing (section 9).

### **6.7.1 Results**

The nitrogenolysis experiments were conducted with the process parameters listed in Table 35. All parameters were kept constant in order to get repeatable results and constant product quantity and quality. No problems occurred during these runs.

**Table 35: Process parameters for Barley DDGS nitrogenolysis production runs**

| Experiment number                     |       | 015         | 016         | 017         |
|---------------------------------------|-------|-------------|-------------|-------------|
| Feedstock                             |       | Barley DDGS | Barley DDGS | Barley DDGS |
| Reactor temperature (nominal)         | °C    | 500.00      | 500.00      | 500.00      |
| Reactor temperature (average)         | °C    | 526.16      | 530.87      | 527.46      |
| Bed material                          |       | Silica sand | Silica sand | Silica sand |
| Bed material particle size            | µm    | 710-850     | 710-850     | 710-850     |
| Bed material mass                     | g     | 1000.00     | 1000.00     | 1000.00     |
| Duration                              | h:min | 1:26        | 4:00        | 3:11        |
| Feeder nitrogen flow rate (ATP)       | l/min | 17.00       | 17.00       | 17.00       |
| Fluidization nitrogen flow rate (ATP) | l/min | 47.00       | 52.00       | 52.00       |
| Ammonia flow rate (ATP)               | l/min | 1.50        | 1.50        | 1.50        |
| Nitrogen addition                     | wt.%C | 22.98%      | 21.39%      | 21.75%      |
| Feed rate (nominal)                   | g/h   | 565.00      | 570.00      | 550.00      |
| Feed rate (average)                   | g/h   | 554.02      | 596.60      | 550.37      |
| Total feed (as received)              | g     | 784.86      | 2386.41     | 1742.83     |

The mass balances are provided in Table 36 and the product distributions are shown in Figure 29. From the process parameters (Table 35) it can be seen that the actual nitrogen addition was above the nominal 12wt.%C, around 22wt.%C which was caused by the low feedstock feeding rates and set minimum flow rate of ammonia. The product yields are calculated on dry feedstock basis and are excluding the ammonia gas. The three experiments have a very high closure of around 95wt.%, which will be explained later. Figure 29 shows that the product distribution of the three runs was very similar, although the first run has a lower mass balance closure.

**Table 36: Mass balances of Barley DDGS nitrogenolysis production runs**

| Experiment number                          | 015           |                | 016            |                | 017            |                |
|--|---------------|----------------|----------------|----------------|----------------|----------------|
| Feedstock                                  | Barley DDGS   |                | Barley DDGS    |                | Barley DDGS    |                |
| Nitrogen addition [wt%C]                   | 22.98%        |                | 21.39%         |                | 21.75%         |                |
| Unit                                       | g             | %              | g              | %              | g              | %              |
| <b>Input:</b>                              |               |                |                |                |                |                |
| Feedstock (ar)                             | 784.86        |                | 2386.41        |                | 1742.83        |                |
| Feedstock moisture (ar)                    | 64.96         | 8.28%          | 202.61         | 8.49%          | 148.66         | 8.53%          |
| <b>Feedstock (dry)</b>                     | <b>719.90</b> | <b>100.00%</b> | <b>2183.80</b> | <b>100.00%</b> | <b>1594.17</b> | <b>100.00%</b> |
| <b>Output:</b>                             |               |                |                |                |                |                |
| <b>Total FP char yield (dry)</b>           | <b>120.87</b> | <b>16.79%</b>  | <b>397.72</b>  | <b>18.21%</b>  | <b>289.97</b>  | <b>18.19%</b>  |
| FP Char in reactor and piping (dry)        | 37.99         | 5.28%          | 11.89          | 0.54%          | 9.36           | 0.59%          |
| FP Char in 1st cyclone (dry)               | 81.23         | 11.28%         | 382.29         | 17.51%         | 277.04         | 17.38%         |
| FP Char in 2nd cyclone (dry)               | 1.65          | 0.23%          | 3.54           | 0.16%          | 3.57           | 0.22%          |
| <b>Total FP liquid yield (excl. water)</b> | <b>337.58</b> | <b>46.89%</b>  | <b>1071.49</b> | <b>49.07%</b>  | <b>797.62</b>  | <b>50.03%</b>  |
| FP liquid yield (incl. water)              | 401.62        |                | 1233.01        |                | 924.22         |                |
| FP liquid yield (excl. water)              | 323.09        | 44.88%         | 1000.59        | 45.82%         | 746.18         | 46.81%         |
| Secondary condensate yield (incl. water)   | 95.33         |                | 362.82         |                | 266.97         |                |
| Secondary condensate yield (excl. water)   | 14.49         | 2.01%          | 70.90          | 3.25%          | 51.43          | 3.23%          |
| <b>Calculated Reaction water</b>           | <b>94.41</b>  | <b>13.11%</b>  | <b>321.73</b>  | <b>14.73%</b>  | <b>244.92</b>  | <b>15.36%</b>  |
| Water in FP liquid                         | 78.53         |                | 232.42         |                | 178.04         |                |
| Water in secondary condensate              | 80.84         |                | 291.92         |                | 215.54         |                |
| <b>FP gas yield (excl. N2)</b>             | <b>102.47</b> | <b>14.23%</b>  | <b>317.80</b>  | <b>14.55%</b>  | <b>225.61</b>  | <b>14.15%</b>  |
| Error of mass balance                      |               | 8.97%          |                | 3.44%          |                | 2.26%          |

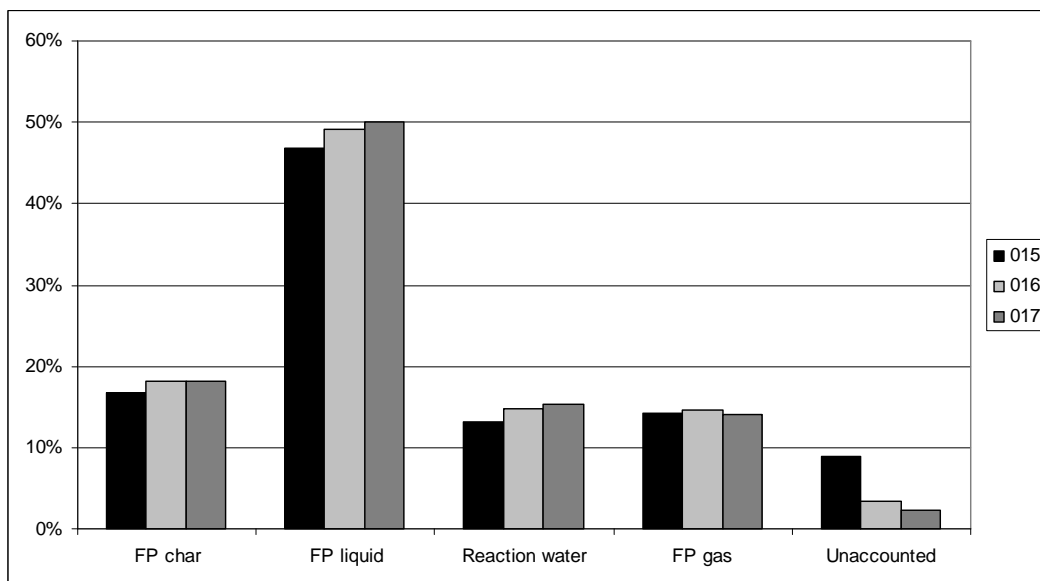


**Figure 29: Product distribution of barley DDGS nitrogenolysis production runs**

## 6.7.2 Analysis and discussion

The average reactor temperature was kept higher during the barley DDGS experiments and the average feeding rate was kept relatively low to ensure that the feedstock is fully pyrolysed. As DDGS contains fatty acids and sugars it behaves differently during nitrogenolysis than beech wood requiring a higher heat input. The average nitrogen addition on carbon basis was not the planned 15wt.%C, but around 22wt.%C due to the above mentioned low feeding rate and set gas flow on the rotameter.

The mass balance closure of the first experiment with 91wt.% is lower (see Figure 29) than the closures of the second experiment (97wt.%) and third run (98wt.%). This was caused by difficulties during the removal of the nitrogenolysis liquids due to their high viscosity. This problem was overcome by draining them warm. In general the mass balance closures indicate the uptake of nitrogen into the product as they are higher than the comparable pyrolysis experiment closures, just as it was the case for the beech wood experiments. The total yield of liquid product is 63wt.% on dry feedstock basis, so almost as high as the yield for barley DDGS in the pyrolysis experiments (see Table 26).

The liquid nitrogenolysis product obtained did not readily phase separate from the quenching medium ISOPAR™. Centrifuging samples at 4000RPM for 15min for liquid GC-MS analysis showed that even after this procedure the samples still contained ISOPAR™ as chromatograms

obtained showed. Although the incomplete phase separation did not prevent a successful thermal solidification of the obtained liquid, a more suitable quenching medium would need to be found for a continuous production process (see section 11). The reasons for the incomplete phase separation could not be identified.

## **6.8 Trouble shooting**

This section is dedicated to the description of problems that occurred while operating the 1kg/h bubbling fluidized bed reactor rig and how these problems were solved or mitigated. In this context general aspects are presented and not individual experiments discussed.

In section 5.1.2 the modifications implemented on the 1kg/h rig are described. The aim of these was to improve the reliability, handling and process control of the rig. The process measurement and control components were identified as a source for problems while operating the rig. The measurement and control components do not form an integrated system, but consist of individual components. In case of the bed heaters and trace heaters up to three heaters with different power output levels were controlled by one PID-controllers leading to high temperature differences between the heaters. This created local hot spots and caused excessive wear and heat damage to the ceramic knuckle heaters and heating bands. Additional control circuits were added to overcome these problems (see section 5.1.2).

The old data recording system operated unreliable due to malfunctions of the analogue-digital-converter (ADC) unit and electrical faults in the thermocouple wiring. A new ADC unit was installed including new software and a new computer and all measurement lines rewired with new shielded cables.

As described in section 5.1.2 the water vapour in the gas/vapour stream after the electrostatic precipitator (ESP) lead to excessive ice accumulation in the dry ice cooled heat exchangers blocking them. A water cooled heat exchanger was added after the ESP to condense the majority of water vapour prior to the dry ice cooled heat exchangers. The ice build up was reduced significantly and no further blockages at this place occurred.

Another source for problems during processing was the fast screw feeding system (see section 5.1.1). Certain materials have the tendency to start pyrolysing within the fast screw causing blockages. This effect is even amplified if the fast screw tip is ground down by the bed

material. To avoid such blockages three basic measures were taken. The purge gas flow rate had to be maintained at a sufficient level (above 15l/min ATP) to prevent sand and vapours from entering the fast screw and acting as a coolant to a certain extent. Moist feedstock (water content approx. 10wt.%) was used as the water in the feedstock prevented pre-pyrolysis due to the energy uptake of the water and evaporation of it. The fast screw was checked and polished in frequent intervals (every 3 experiments) to prevent/remove deposits. Worn fast screws were replaced if necessary.

The fluidizing velocity was and proved to be a crucial factor when operating the 1kg/h rig (see section 5.2.1). It needs to guarantee a proper fluidization of the bed material while entraining the char particles produced without entraining the bed material. The experiments with rape meal and DDGS quickly showed that the fluidization gas stream and bed material particle size needed to be adjusted to the higher density of char particles of these feedstocks. By this char accumulation in the reactor forming a second fluidized char bed above the sand bed could be avoided.

Additionally the feedstock Green Dragon rape meal caused severe problems during processing. The bed heaters were not able to provide enough energy to stabilize the bed temperature at 500°C even at a low feeding rate of 0.5kg/h. Furthermore the char had the tendency to agglomerate and was not entrained properly. These effects are most likely caused by the very high oil content of this feedstock. In contrast ADM rape meal, having a low oil content, did not cause such problems. As an alternative rape meal feedstock was available and an additional oil extraction step for Green Dragon rape meal was not seen as feasible Green Dragon rape meal was abandoned as a feedstock.

The removal of the highly viscous fast pyrolysis and in-situ nitrogenolysis liquids from the quench column collection tank proved to be difficult. Although it was common practice before to remove the liquid after letting the 1kg/h rig cool down, the liquid was drained while still being warm (approx. 30°C). To prevent oxygen from entering the system a purge gas flow was maintained during this procedure and an additional fume extraction placed near the outlet of the quench column collection tank.

Beside the described problems other issues with and while operating the 1kg/h rig were mitigated or prevented by extensive and laborious maintenance work after each experiment performed.

## **7 Solidification and modification of liquid products**

### ***7.1 Introduction***

The aim of this research is to present an alternative route for the production of a slow release fertiliser (SRF) from biomass. Also it was defined that the product should be solid for better storage and handling. Therefore, a conversion process of the highly viscous in-situ nitrogenolysis product into a solid is needed (see section 1.2.4). A thermal solidification process was chosen due to the specific characteristics of fast pyrolysis liquid; as presented in section 2.4.2, fast pyrolysis liquid ages at elevated temperatures due to polymerization and other reactions. This aging behaviour was seen as the key factor for the production of a solid SRF as a thermal conversion can make use of this behaviour. Additionally temperatures above 100°C would also lead to the evaporation of water and even higher temperatures up to 150°C would also lead to the evaporation of low molecular weight organic compounds such as organic acids improving the acidity of the product.

Additionally the aspect of nitrogenolysis via modification of fast pyrolysis liquid from the collection tank (see section 1.2.5) was investigated. This was done by reacting fast pyrolysis liquid derived from beech wood with a nitrogen containing compound in combination with the solidification process.

Due to restrictions in time and equipment a batch process was developed for these processes. A continuous process including spray drying would have been a preferable solution, but the additional time necessary for the development of a suitable reactor with pump and spraying nozzles for a product like fast pyrolysis / nitrogenolysis liquids would have exceeded the available timeframe. The developed procedure is described below in section 7.2.

## 7.2 Batch reactor

For the thermal solidification of liquid pyrolysis and in-situ nitrogenolysis products a batch reactor experimental setup was developed. A flow diagram is provided in Figure 30.

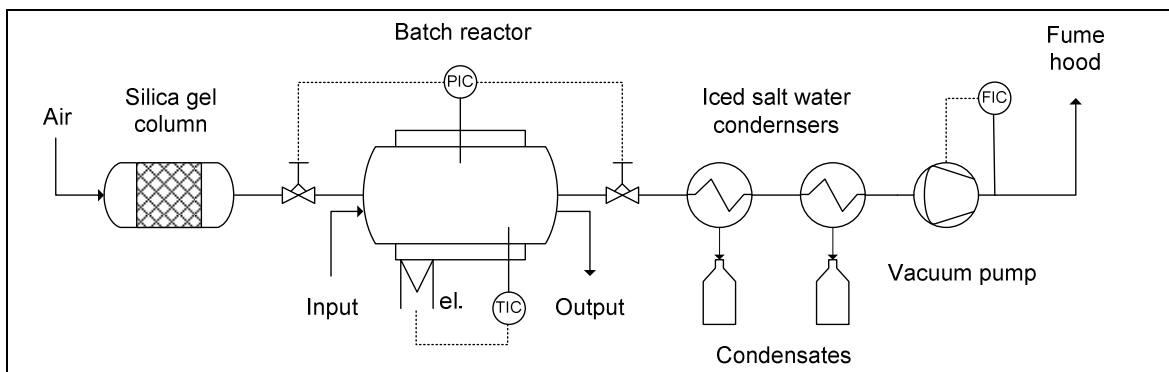


**Figure 30: Batch reactor setup**

The batch reactor consists of a Technico OVA 031 oven, which is electrically heated and gives the possibility to apply a vacuum. The available space allowed to place the samples in three Petri dishes in the oven. Evolving gases and vapours from these samples were purged from the reactor chamber by a constant flow of pre-dried air (see also next paragraph). For this purpose air was sucked through a silica gel packed column and through the inlet valve of the batch reactor, leaving it by the outlet valve with the gases and vapours. Upon leaving the batch reactor the vapour and gas stream passed through a cascade of two finger condensers emerged in iced salt water solution (NaCl) at  $-15^{\circ}\text{C}$  in order to condense the majority of vapours. The remaining gas stream of air and non-condensable gases (NCGs) passed through a cotton wool filter (pre-dried cotton wool) before being sucked through a vacuum pump. The outlet stream was vented into a fume hood. The process parameters are described in section 7.3.

The constant purge gas flow prevented an accumulation of potentially combustible and/or harmful vapours in the batch reactor. Furthermore the purge gas flow was used to transport the evolving vapours into the condensation train minimizing the risk of condensation within the batch reactor. The purge gas, vapours and NCGs were sucked through the experimental setup to eliminate the risk of leakage to the laboratory environment.

### **7.3 Process parameters**

The process parameters were mainly determined by the design of the experimental setup and materials used in the experiments and are described in the following sections.

#### **7.3.1 Temperature**

The temperature was limited between room temperature (20°C) and the maximum stable operating temperature of the Technico OVA 031 oven (170°C). Other restrictions resulted from materials used in the experiments. As fast pyrolysis and nitrogenolysis liquids contain a relatively large amount of water, temperatures just above the boiling point of water were regarded as promising (100°C at 1013.25hPa). Furthermore fast pyrolysis liquid also contains organic acids, such as formic acid and acetic acid. Although these are supposed to react during nitrogenolysis or solidification due to different reactions, it was seen as reasonable to consider a temperature above their boiling points to drive off excess acids and improve the acidity of the final product (boiling point acetic acid: 118°C at 1013.25hPa). For these reasons all experiments were performed within the temperature interval of 120°C and 170°C, when operated at ambient pressure.

#### **7.3.2 Pressure**

The experimental setup allowed the pressure in the reaction chamber to be regulated between ambient pressure (1013.25hPa) and an applied vacuum of -500hPa (gauge), which was possible with the chosen setup. Although an applied vacuum would lower the boiling point of compounds present in the investigated materials, it was expected that the impact on the process would be marginal. This expectation was backed by some preliminary experiments performed as part of a Master of Engineering project. Consequently all experiments were performed at ambient pressure.

#### **7.3.3 Processing time**

The processing time has to be subdivided into the time for heating up the sample and actual time for the solidification at processing temperature. As the experimental setup did not provide the possibility to determine the time needed for heating up, but the sample amount was rather small with a large surface area, it was assumed that the heating up time would be less than 5min. Nevertheless all times are given as processing times, meaning the time

between placing the sample in the preheated batch reactor and removing them from it in hot state.

Another restriction resulting from the chosen experimental setup was that the sample could not be checked for the degree of solidification during the experiment, as this would have interfered with the mass balance. Therefore samples were removed from the oven in hot state after a set time, cooled down in desiccator and analysed, rather than measuring the time until a solid sample was produced. A general processing time of 1 hour was chosen for the experiments due to these factors and restrictions in laboratory time and equipment.

#### **7.3.4 Catalyst**

Catalysts are widely used in industry to reduce processing times and/or temperatures. For the conversion process the use of a catalyst that is cheap and can remain in the final product would be beneficial. Pyrolysis char is known to act as a catalyst in fast pyrolysis liquid ageing reactions [35] due to its large surface area (similar to activated carbon) and the inorganic compounds present in the char especially alkali metals (see section 2.4.2). As it is a by-product of the fast pyrolysis and nitrogenolysis process and is also used as soil amendment (see section 2.4.6), it is a suitable candidate for a catalyst to reduce either the temperature or the processing time or both.

#### **7.3.5 Mass balances**

The experimental oven allowed placing 3 samples in Petri dishes simultaneously in it. The weight of each Petri dish was determined before and after the experiment allowing conclusions of the conversion rate from liquid to solid for each sample. In contrast the vapours were collected and measured for all samples together. Consequently the mass balance could just be established for all three Petri dishes together. The NCGs and very light vapours were determined by difference, including any error made. A mass balancing scheme is listed in Table 37.

**Table 37: Mass balancing scheme of batch reactor setup**

| Material         | Equipment           | Method   |
|------------------|---------------------|--|
| 3 input samples  | Petri dishes        | weight of input material and Petri Dish  |
| 3 output samples | Petri dishes        | weight of output material and Petri Dish   |
| condensate I     | finger condenser I  | difference in weight before and after experiment of the finger condenser 1 without/with liquid |
| condensate II    | finger condenser II | difference in weight before and after experiment of the finger condenser 2 without/with liquid |
| condensate II    | cotton wool filter  | difference in weight before and after experiment   |

## 7.4 Solidification experiments – fast pyrolysis liquid

Solidification experiments were performed with beech wood fast pyrolysis liquid to determine suitable process parameters for producing a solid product. Experiments with beech wood fast pyrolysis liquid without and with the addition of fast pyrolysis char were done. The experimental series consisted of five experiments as listed in Table 38. The addition rate of char was based on the weight of fast pyrolysis with its water content subtracted. The temperatures chosen for the experiment were 130°C, 150°C and 170°C, although 130°C was finally not used, because the liquid did not solidify at 150°C.

**Table 38: Conversion experiments with beech wood FP liquid**

| Experiment | Sample material                        | Temperature | Duration |
|------------|--|-------------|----------|
| 1          | Beech wood FP liquid                   | 150°C       | 1h       |
| 2          | Beech wood FP liquid                   | 170°C       | 1h       |
| 3          | Beech wood FP liquid + 1wt.% FP char   | 150°C       | 1h       |
| 4          | Beech wood FP liquid + 2.5wt.% FP char | 150°C       | 1h       |
| 5          | Beech wood FP liquid + 5wt.% FP char   | 150°C       | 1h       |

### 7.4.1 Results and discussion

The results of this series of experiments are summarized in Table 39. Although 3 individual Petri dishes with sample were placed in the batch reactor and measured individually, the masses for liquid sample and product are given as a sum, because the condensates were measured as one total as well. The differences between the individual samples in terms of conversion rate were minor, so that it was assumed that all samples reacted similar to the conversion.

As it can be seen in Table 39, row Total Output measured, the solid product and the condensate account for more than 87wt.% of the mass balance for all experiments. The

absolute numbers for the amount of water indicate that some water was not condensed in the finger condensers, because the amount of water in the condensate is smaller than the amount of water in the FP liquid and the solid product is supposed to be free of water. If polycondensation reactions are taking place during the conversion, the amount of water measured after conversion should have been a bit higher than the amount of water introduced into the system by the FP liquid. The amount of organics in the condensate is low when compared to the water. All condensate samples had a slight vinegar smell indicating the presence of acetic acid.

**Table 39: Results of solidifying beech wood fast pyrolysis liquid**

| Experiment                   | 1     |              | 2     |              | 3     |              | 4     |        | 5     |              |
|------------------------------|-------|--------------|-------|--------------|-------|--------------|-------|--------|-------|--------------|
| Unit                         | g     | wt.%         | g     | wt.%         | g     | wt.%         | g     | wt.%   | g     | wt.%         |
| Total input (measured)       | 54.80 | 100.00       | 58.65 | 100.00       | 56.47 | 100.00       | 56.48 | 100.00 | 60.49 | 100.00       |
| FP liquid (dry basis)        | 41.17 | 75.13        | 44.07 | 75.14        | 42.06 | 74.48        | 41.45 | 73.39  | 43.38 | 71.71        |
| Water in FP liquid           | 13.63 | 24.87        | 14.58 | 24.86        | 13.98 | 24.76        | 13.72 | 24.29  | 14.36 | 23.74        |
| FP char (dry basis)          | 0.00  | 0.00         | 0.00  | 0.00         | 0.43  | 0.76         | 1.31  | 2.32   | 2.75  | 4.55         |
| Total output (measured)      | 49.43 | <b>90.20</b> | 52.00 | <b>88.66</b> | 50.05 | <b>88.63</b> | 51.82 | 91.75  | 52.92 | <b>87.49</b> |
| Product, solid (dry basis)   | 31.55 | 57.57        | 29.57 | 50.42        | 31.63 | 56.01        | 33.07 | 58.55  | 34.37 | 56.82        |
| Condensate (dry basis)       | 5.03  | 9.18         | 8.83  | 15.06        | 5.01  | 8.87         | 5.51  | 9.76   | 5.43  | 8.98         |
| Water in condensate          | 12.85 | 23.45        | 13.60 | 23.19        | 13.41 | 23.75        | 13.24 | 23.44  | 13.12 | 21.69        |
| NCGs + error (by difference) | 5.37  | 9.80         | 6.65  | 11.34        | 6.42  | 11.37        | 4.66  | 8.25   | 7.57  | 12.51        |
| Solidified                   |       | No           |       | Yes          |       | No           |       | Yes    |       | Yes          |

When experiment 1 and 2 are compared it can be seen that the higher temperature produces a lower product output and more organic compounds in the condensate indicating that more organic material is evaporating and is not bound in the product as it would be expected.

Regarding the aspect of obtaining a solid, the samples without char addition showed that just the experiment at 170°C was producing a solid. The addition of char as a catalyst improved the conversion process in terms of solidification as the additions of 2.5wt.% and 5wt.% of char lead to a solid brittle product at 150°C. The results indicate that either the time could be shortened or the temperature lowered for the addition of 5wt.% of char. Taking the FP liquid modification and solidification experiments (see section 7.5.1) into consideration it was decided that the char addition should be limited due to difficulties in sample preparation at

high char addition rate. Therefore the process parameters were kept at 150°C and 1hour and further experiments performed with a char addition of 2.5wt.%.

## ***7.5 Nitrogenolysis via fast pyrolysis liquid modification***

Nitrogenolysis by reacting fast pyrolysis liquid with a nitrogen compound was investigated in experiments that combined the conversion process and solidification process. The products were investigated in terms of total nitrogen added to the product and how water soluble the nitrogen in the product would be. The chosen experimental setup is different from the method described by Hanser [27], as he was reacting the fast pyrolysis liquid and nitrogen compound in a heated closed reactor with stirrer keeping it in a liquid state prior to solidification (see section 2.6.3.2).

### **7.5.1 Fast pyrolysis liquid modification and solidification experiments**

The setup of the fast pyrolysis liquid modification and solidification experiments was based on the solidification experiments for fast pyrolysis liquid using the same process parameters. The only difference was that an additional nitrogen containing reactant was added. As the reactant for the experiments the following nitrogen compounds were taken in to consideration:

- ammonium nitrate
- ammonium carbonate
- ammonium chloride
- ammonium phosphate
- urea

Ammonium nitrate was ruled out due to safety concerns as it can form explosive mixtures. Ammonium carbonate has a very low decomposition temperature of 60°C and was expected to decompose too quickly, losing the ammonia into the gas phase too quickly without reacting. Ammonium chloride and ammonium phosphate were both suitable for their thermal decomposition behaviour. The latter was chosen for the experiments as conventional fertilisers contain phosphorus (NPK fertilisers). Ammonium phosphate starts to decompose at 130°C [89] setting free ammonia, which is in the temperature range of the conversion experiments.

Urea was used as it is easy to handle, has two NH<sub>2</sub> groups and was also used by Hanser in his experiments (see section 2.6.3.2). As the temperature for these experiments is significantly lower than during in-situ nitrogenolysis, the formation of urea dimers and trimers was not expected. According to Schaber et al. [90] biuret is formed during the decomposition of urea between 160°C and 190°C. As biuret is toxic to plants in moderate and high concentrations [91] the formation of biuret had to be avoided by keeping the process temperatures below 160°C.

The addition rate of urea and ammonium phosphate dibasic was based on the amount of functional groups present in fast pyrolysis liquid. Radlein et al. pointed out that fast pyrolysis liquid contains 6-11mole of functional groups per kg of fast pyrolysis liquid on a dry basis [34]. As an average 8 mole was assumed for calculating the addition rate. Urea and ammonium phosphate dibasic have both two nitrogen groups. Consequently 24wt.% urea and 53wt.% ammonium phosphate dibasic were added to the fast pyrolysis liquid on a dry basis.

The addition of char had been shown to support the solidification process (see section 7.4). Therefore two experiments with an addition of the nitrogen compound and 2.5wt.% fast pyrolysis char were performed. The experiments are listed in Table 40.

**Table 40: Post processing experiments with fast pyrolysis liquid**

| Experiment | Sample material   | Temp. | Time |
|------------|---|-------|------|
| 6          | Beech wood FP liquid + urea                             | 150°C | 1h   |
| 7          | Beech wood FP liquid + ammonium phosphate dibasic       | 150°C | 1h   |
| 8          | Beech wood FP liquid + urea + 2.5wt.% FP char           | 150°C | 1h   |
| 9          | BW FP liquid + ammonium phosphate di. + 2.5wt.% FP char | 150°C | 0.5h |

## 7.5.2 Results and discussion

The results of this experimental series are summarized in Table 41. Although 3 individual Petri dishes with sample were placed in the batch reactor and individually measured, the masses for liquid sample and product are given as a sum, because the condensates were measured as one total. The differences between the individual samples were minor, so that it was assumed that all samples reacted.

**Table 41: Results of modifying and solidifying beech wood FP liquid**

| Experiment                   | 6     |              | 7     |              | 8     |              | 9     |              |
|------------------------------|-------|--------------|-------|--------------|-------|--------------|-------|--------------|
| Unit                         | g     | wt.%         | g     | wt.%         | g     | wt.%         | g     | wt.%         |
| Total input                  | 76.92 | 100.00       | 79.82 | 100.00       | 78.40 | 100.00       | 80.81 | 100.00       |
| FP liquid (dry basis)        | 42.39 | 55.11        | 41.62 | 52.14        | 42.45 | 54.15        | 41.45 | 51.29        |
| Water in FP liquid           | 14.03 | 18.24        | 13.77 | 17.25        | 14.05 | 17.92        | 13.72 | 16.98        |
| N compound (dry basis)       | 20.50 | 26.65        | 24.43 | 30.61        | 20.58 | 26.25        | 24.30 | 30.07        |
| FP char (dry basis)          | 0.00  | 0.00         | 0.00  | 0.00         | 1.32  | 1.68         | 1.34  | 1.66         |
| Total output (measured)      | 69.27 | 90.05        | 74.26 | 93.03        | 72.52 | 92.50        | 76.23 | 94.33        |
| Product, solid (dry basis)   | 53.91 | <b>70.09</b> | 58.75 | <b>73.60</b> | 53.45 | <b>68.18</b> | 63.37 | <b>78.42</b> |
| Condensate (dry basis)       | 1.99  | 2.59         | 1.17  | 1.47         | 2.46  | 3.14         | 0.99  | 1.23         |
| Water in condensate          | 13.37 | 17.38        | 14.34 | 17.97        | 16.61 | 21.19        | 11.87 | 14.69        |
| NCGs + error (by difference) | 7.65  | 9.95         | 5.56  | 6.97         | 5.88  | 7.50         | 4.58  | 5.67         |
| Solid                        |       | No           |       | Yes          |       | Yes          |       | Yes          |

Table 41 shows the solid product and the condensate account for more than 90wt.% in the mass balance for all experiments. The absolute numbers for the amount of water indicate that for experiments 6 and 9 the amount of water measured in the condensate was slightly lower than in the input fast pyrolysis liquid, although in experiment 7 and 8 it was slightly higher. Although mass balancing errors have to be taken into consideration, this could indicate that more reaction water is formed during the modification and solidification, e.g. by condensation reactions, than in the solidification experiments 7.4.1. The amount of organics in the condensate is lower when compared to the experiments without reactant (see 7.4.1) with less than 3.2wt.%. In contrast to the previous experiments the condensates had no particular smell and did not have a characteristic vinegar smell.

The experiments 7, 8 and 9 produced a brittle solid. The experiment with ammonium phosphate dibasic (experiment 7) produced a solid without char addition after a processing time of 1 hour. Therefore the processing time for the experiment with char addition (experiment 9) was reduced to 30min, which was sufficient to produce a solid. As in solidification experiments (see 7.4.1) the addition of char improved the solidification process when experiment 6 and 8 are compared.

The solid product in experiment 7, 8 and 9 accounted for more than 68wt.% of all input materials. The samples with ammonium phosphate achieved slightly higher solid product yields than the sample with urea. The mass balance indicates that the main fraction of the

material driven off during the treatment is water. Vice versa the results also show that less than 14wt.% of the initial dry sample material is lost during the conversion meaning that a good conversion rate is achieved by this method.

The amount of nitrogen incorporated in the solid product and the solubility of the compounds formed was investigated in washing experiments, which are described in section 7.5.3.

### **7.5.3 Modification and solidification product washing experiments**

The two most promising products of the modification and solidification experiments, the products of experiments 8 and 9, were investigated regarding their content of nitrogen by elemental analysis and were subjected to a cold and hot water washing process. As urea and ammonium phosphate dibasic are both water soluble the washing experiments were performed in order to determine the amount of nitrogen that is soluble in cold water (20°C) and in hot water (60°C). After the washing procedure the samples were analysed for their carbon, hydrogen and nitrogen content. This relatively simple procedure allowed drawing conclusions, whether the nitrogen in the solidified sample would be released slowly or not. The amount of nitrogen washed out by cold water would be immediately available and indicated that the reactant is not bound in the fast pyrolysis liquid matrix. The amount of nitrogen washed out by hot water would be available in mid term and it also indicates that no microbial activity is needed to make it water soluble. Nevertheless it would still offer a slower nutrient release.

The steps in the washing experiments were:

1. Mixing 0.5g of product with 10ml of cold (20°C) or hot (60°C) deionised water
2. Placing the sample in a heated Grant Ultrasonic bath for 5min to achieve a good level of agitation
3. Centrifuging the sample in a Eppendorf 5702 centrifuge at 2.5 relative centrifugal force for 5min
4. Removal of aqueous phase
5. Drying of sample at 20°C over night to avoid volatilization, which could take place at higher temperatures
6. Weighing washed and dried sample
7. Analysing sample for C, H, N content

## 7.5.4 Results and discussion

The samples of experiments 8 and 9 of section 7.5.2 were washed as described above, a mass balance was established and the washed and dried samples were analysed for their nitrogen content. The results of these washing experiments and the prior solidification process (see Table 41) are summarized in Table 42. The results indicate that the samples resulting from the urea experiments have higher nitrogen contents (see Table 42), when compared to the ammonium phosphate dibasic experiments. On the other hand the urea samples also have a significant higher mass loss during each experimental step.

**Table 42: Recovered solids and nitrogen contents [in wt.%]**

| <b>Experiment</b>  |                  | <b>Recovered solid after Solidification</b> | <b>Recovered solid after Cold wash</b> | <b>Recovered solid after Hot wash</b> |
|--------------------|------------------|---|--|---------------------------------------|
| 8<br>(urea+char)   | recovered mass   | 68.18%                                      | 68.80%                                 | 57.80%                                |
|                    | nitrogen content | 17.30%                                      | 9.28%                                  | 9.33%                                 |
| 9<br>(AmPhos+char) | recovered mass   | 78.42%                                      | 84.40%                                 | 82.81%                                |
|                    | nitrogen content | 6.02%                                       | 4.34%                                  | 4.41%                                 |

The Sankey diagram in Figure 31 illustrates the fate of nitrogen during the combined modification and solidification step (conversion) and washing steps of the fast pyrolysis liquid to solid process with urea and char added. It can be seen that just 3.72wt.% of nitrogen added as urea is lost during conversion, but 60.75wt.% during the cold washing step and an additional 5.52wt.% during the hot washing step.

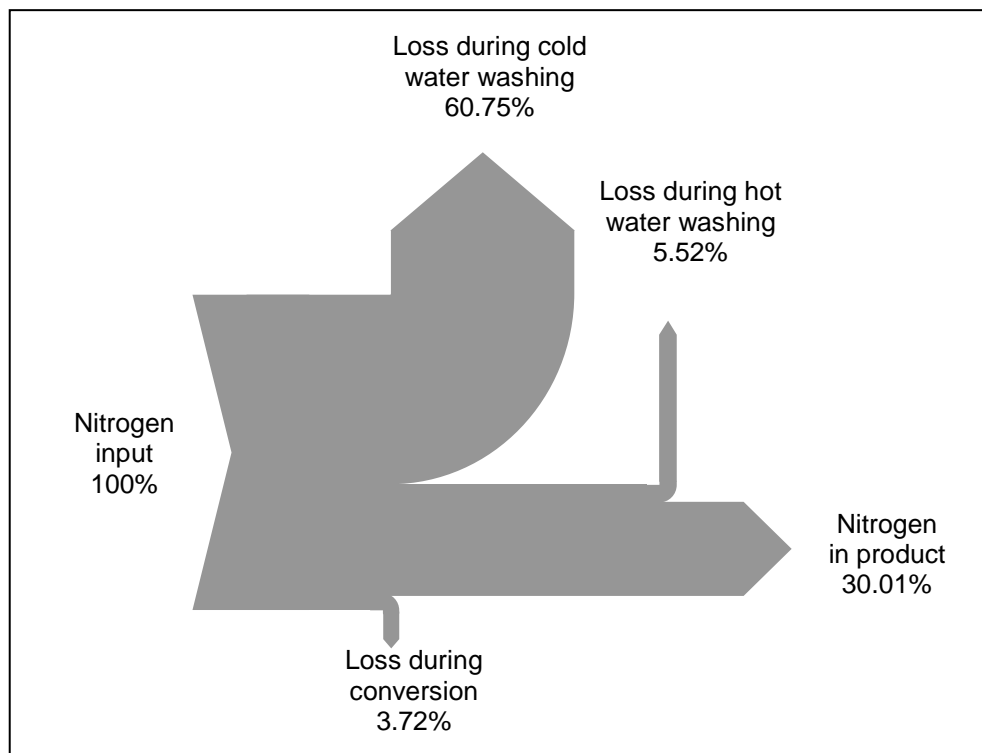


**Figure 31: Fate of nitrogen in urea sample, experiment 8**

The Sankey diagram indicates that just a minor amount of the nitrogen in urea was lost to the gas phase during conversion and that the majority of the added nitrogen stayed in the solid product. The washing process revealed that most of the nitrogen in the solidified product is water soluble indicating that it is not bound in complex structures and therefore would be available immediately for plant growth. This implies that there would not be a slow release effect and being prone to leaching. It is likely that most of the urea did not react under the chosen conditions and that most of the nitrogen washed out of the sample was in its original form.

Figure 32 shows the fate of nitrogen during the combined modification and solidification step (conversion) and washing steps of the fast pyrolysis liquid to solid process with ammonium phosphate dibasic and char addition. It can be seen that 25.98wt.% of nitrogen is lost during the conversion step, 28.98wt.% during the cold washing step and just 0.14wt.% during the hot washing step.

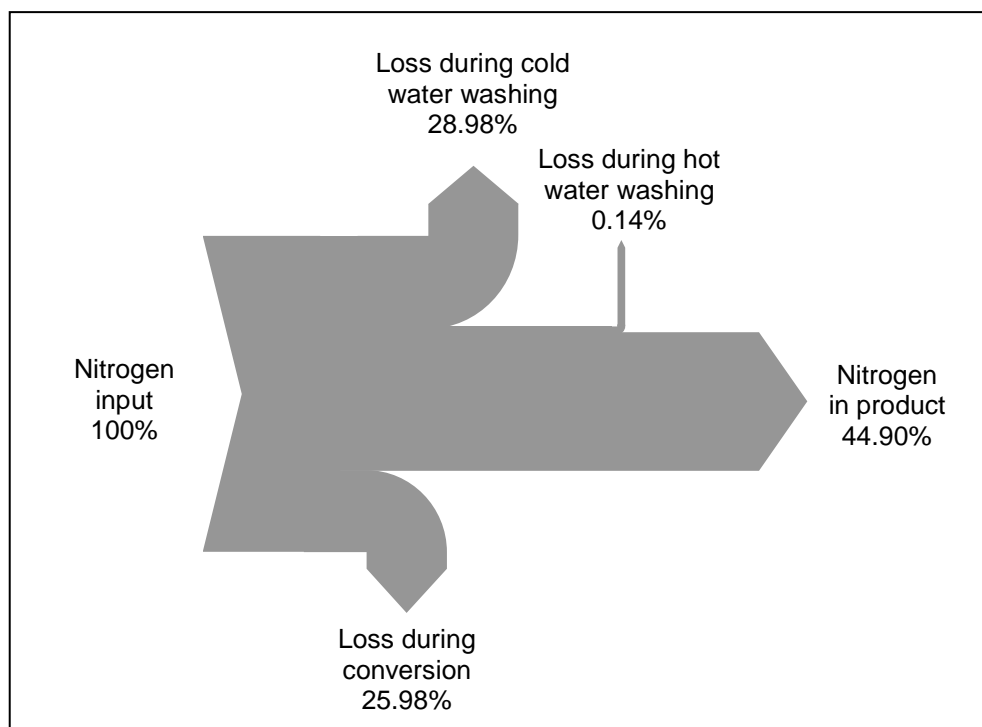


**Figure 32: Fate of nitrogen in ammonium phosphate sample, experiment 9**

Compared to the urea sample the ammonium phosphate sample shows higher losses of nitrogen during the conversion step, indicating that the ammonium phosphate decomposed releasing ammonia into the gas phase. In contrast to the urea sample, the losses during the washing steps are significantly lower leading to a product with 44.9wt.% of the input nitrogen compared to 30.1wt.% with urea. The results indicate that the nitrogen of the ammonium phosphate has been incorporated into the fast pyrolysis liquid matrix in a way that makes it less water soluble. Therefore the product obtained is more likely to have a slow release effect for nitrogen and is less prone to leaching, when compared to the urea experiment product.

The mass and nitrogen balances for both samples indicate that although the chosen setup is capable of producing solid nitrogen enriched products, the products do not appear to have the necessary characteristics for a slow release fertiliser. The losses of nitrogen during the combined modification and solidification step and especially the relatively high losses during the washing experiments lead to the conclusion that the combined modification and solidification route is not suitable for the sustainable production of a slow release fertiliser in this way.

## 7.6 Solidification experiments of in-situ nitrogenolysis liquid

Solidification experiments with in-situ nitrogenolysis liquids of beech wood (see section 6.6) and Barley DDGS (see section 6.7) were performed in order to obtain mass balancing data. The setup for the solidification experiments of nitrogenolysis liquid was based on the solidification experiments for fast pyrolysis liquid using the same process parameters, but without the addition of any nitrogen compounds. Addition of char to the samples was planned, but turned out to be impossible due to the extremely high viscosity of the nitrogenolysis liquids. The experiments and process parameters are listed in Table 43.

**Table 43: Conversion experiments with nitrogenolysis liquids**

| Experiment | Sample material                               | Temperature | Time |
|------------|---|-------------|------|
| 10         | Beech wood nitrogenolysis liquid bottom phase | 150°C       | 1h   |
| 11         | Barley DDGS nitrogenolysis liquid             | 150°C       | 1h   |

### 7.6.1 Results and discussion

The results of the experiments are summarized in Table 44. Although 3 individual Petri dishes with sample were placed in the batch reactor and the masses determined individually, the masses for liquid sample and product are given as a sum, because the condensates were measured as one total. The differences between the individual samples in terms of conversion rate were minor, so that it was assumed that all samples reacted similar to the conversion.

**Table 44: Results of conversion of nitrogenolysis products**

| Experiment                        | 10    |               | 11    |               |
|-----------------------------------|-------|---------------|-------|---------------|
|                                   | g     | wt.%          | g     | wt.%          |
| Total Input                       | 31.65 | 100.00%       | 34.09 | 100.00%       |
| Nitrogenolysis liquid (dry basis) | 28.49 | 90.00%        | 30.68 | 90.00%        |
| Water in nitrogenolysis liquid    | 3.17  | 10.00%        | 3.41  | 10.00%        |
| Total Output (measured)           | 28.31 | <b>89.44%</b> | 30.30 | <b>88.88%</b> |
| Product (dry basis)               | 25.58 | <b>80.82%</b> | 27.20 | <b>79.79%</b> |
| Condensate (dry basis)            | 0.05  | 0.17%         | 0.06  | 0.18%         |
| Water in condensate               | 2.68  | 8.45%         | 3.04  | 8.91%         |
| NCGs + error (by difference)      | 3.34  | 10.56%        | 3.79  | 11.12%        |
| Solid                             |       | Yes           |       | Yes           |

The solid product and the condensate account for about 89wt.% in the mass balance for both experiments. The absolute numbers for the amount of water indicate that some water was not condensed in the finger condensers. If condensation reactions are taking place during the

solidification, the amount of water should even be a bit higher. At the same time the amount of organics in the condensate is very low. The condensates did not have any particular smell, like the ones from the fast pyrolysis liquid experiments. With a solid product output of about 80wt.% (see Table 44) for both nitrogenolysis liquids the rate of conversion is rather high. This is most likely due to the fact that the nitrogenolysis liquid was already partially polymerized and just the highly viscous material was used for solidification. The solidified product was hard and brittle and could be ground to a fine powder. In terms of the production of solid slow release fertiliser the thermal solidification process seems to be suitable for liquid in-situ nitrogenolysis products to achieve this product.

## **7.7 Summary**

The results of the solidification and combined modification and solidification experiments showed that the batch reactor was capable of producing a solid product that can also be enriched with nitrogen. It was demonstrated that thermal solidification of fast pyrolysis and in-situ nitrogenolysis liquids is possible and can produce a solid brittle product. Furthermore the role of fast pyrolysis char as a catalyst in this process was established, showing that solidification processing times and temperatures could be reduced by the addition of 2.5wt.% of fast pyrolysis char.

The combined modification and solidification experiments of fast pyrolysis liquid showed that a nitrogen enrichment of fast pyrolysis liquid in combination with solidification is possible. It appears that the solid products produced do not have the necessary characteristics of a slow release fertiliser when produced with this experimental setup.

Regarding the solidification process, it can be stated that mainly water is driven off the fast pyrolysis liquid during solidification. Consequently the achieved conversion rates varied between 50wt.% and 80wt.% of the input material, depending on its water content. Taking this into consideration and the energy demand for the evaporation of water, an input material with low water content is favourable although handling of the intermediate highly viscous product is more difficult. A highly organic and viscous bottom phase of a phase separated fast pyrolysis or in-situ nitrogenolysis liquid would therefore be preferable for the thermal solidification process.

## **8 Analysis of fast pyrolysis and in-situ nitrogenolysis liquids**

### ***8.1 Introduction***

The development of the in-situ nitrogenolysis process and the determination of suitable process parameters as well as the investigations into the solidification process were all related to the processing part of this research.

This section is dedicated to the analysis of the products resulting from the fast pyrolysis, in-situ nitrogenolysis and solidification processes. Although elemental analysis gives information about the total amount of nitrogen in the products, it can neither give information about the type of nitrogen compound nor about the bond type nitrogen has with the supporting matrix. For this reason, analytical methods like Py-GC-MS, GC-MS and FTIR were applied to selected samples to get a better insight into these aspects.

### ***8.2 Analytical Py-GC-MS in inert and reactive gas***

This section is dedicated to a comparative study via analytical Pyrolysis-Gas Chromatography-Mass Spectroscopy in inert and reactive gas atmosphere. The aim of this study is to identify possible pyrolysis and in-situ nitrogenolysis products in order to point out differences and investigate if the addition of ammonia gas or ammonium carbonate has an immediate impact on the decomposition products during analytical pyrolysis.

The materials used for this study were cellulose, Xylan (for hemicellulose), Organosolv lignin and beech wood. As biomass is composed of cellulose, hemicellulose and lignin these three basic substances were pyrolysed in an initial step to analyze and record decomposition products and their retention times. Furthermore the experimental setup was tested with these experiments.

Virtually nitrogen free beech wood was pyrolysed in an inert and reactive atmosphere using 10% ammonia in helium. Consequently any nitrogen containing compound must be the result from the addition of ammonia. Also a mixture of beech wood and ammonium carbonate were

co-pyrolysed. Ammonium carbonate was chosen due to its low decomposition temperature (around 60°C) and the decomposition by-product carbon dioxide that does not interfere with the experimental setup.

### 8.2.1 Method

The employed equipment was a CDS 5200 Pyroprobe® with trap coupled to a Varian GC-450 Gas Chromatograph and MS-220 Mass Spectrometer via a heated transfer line held at 310°C (see section 3.12).

In a quartz glass tube approximately 1mg of analytical sample (see section 3.1) was prepared, held between two quartz wool plugs. For beech wood and ammonium carbonate a sample of 1mg beech wood and 0.25mg ammonium carbonate were used. The Py-GC-MS experiments were performed with the following sequence:

**Table 45: Py-GC-MS analysis sequence**

| Inert gas   | Reactive gas   | Ammonium carbonate   |
|---|--|--|
| purge with helium   | purge with helium  | purge with helium  |
|   | purge with reactive gas for 3min heating to 350°C  |  |
| pyrolysing at a heating rate of 1000°C/s and a final temperature of 550°                                      | pyrolysing sample at a heating rate of 20°C/msec to a final temperature of 550°C and holding it 15sec at 550°C while adsorbing the volatile pyrolysis products in a trap | pyrolysing sample at a heating rate of 20°C/msec to a final temperature of 550°C and holding it 15sec at 550°C while adsorbing the volatile pyrolysis products in a trap |
|   | purging residual reactive gas from system with helium  | purging residual reactive gas from system with helium  |
| sending the volatile pyrolysis products to the GC-MS with helium as carrier gas                               | desorbing pyrolysis products from trap by heating the trap to 300°C for 2 min and sending the volatile pyrolysis products to the GC-MS with helium as carrier gas        | desorbing pyrolysis products from trap by heating the trap to 300°C for 2 min and sending the volatile pyrolysis products to the GC-MS with helium as carrier gas        |
| injection into the GC-MS injection port via the heated transfer line with a split ratio of 1:125 and analysis | injection into the GC-MS injection port via the heated transfer line with a split ratio of 1:125 and analysis  | injection into the GC-MS injection port via the heated transfer line with a split ratio of 1:125 and analysis  |

## 8.2.2 Results

The chromatograms and tables of identified compound for cellulose, Xylan (for hemicellulose) and lignin were obtained in order to test the setup and form a data base. Therefore they are not presented in the main text, but are part of appendix B. In general the results proved that the setup is suitable and that characteristic key markers were identified.

The chromatograms of beech wood pyrolysed in inert and reactive atmosphere (ammonia and ammonium carbonate) are presented in this section. In Figure 33, Figure 34 and Figure 35 the chromatograms of each experiment are presented individually. In order to emphasize the findings, the three chromatograms are plotted superimposed and the presented retention times are split. To give greater detail the chromatograms for the retention time from 1-18min are presented in Figure 36 and from 18-55min in Figure 37. Peaks with high abundances are not fully shown to be able to show less abundant peaks as well.

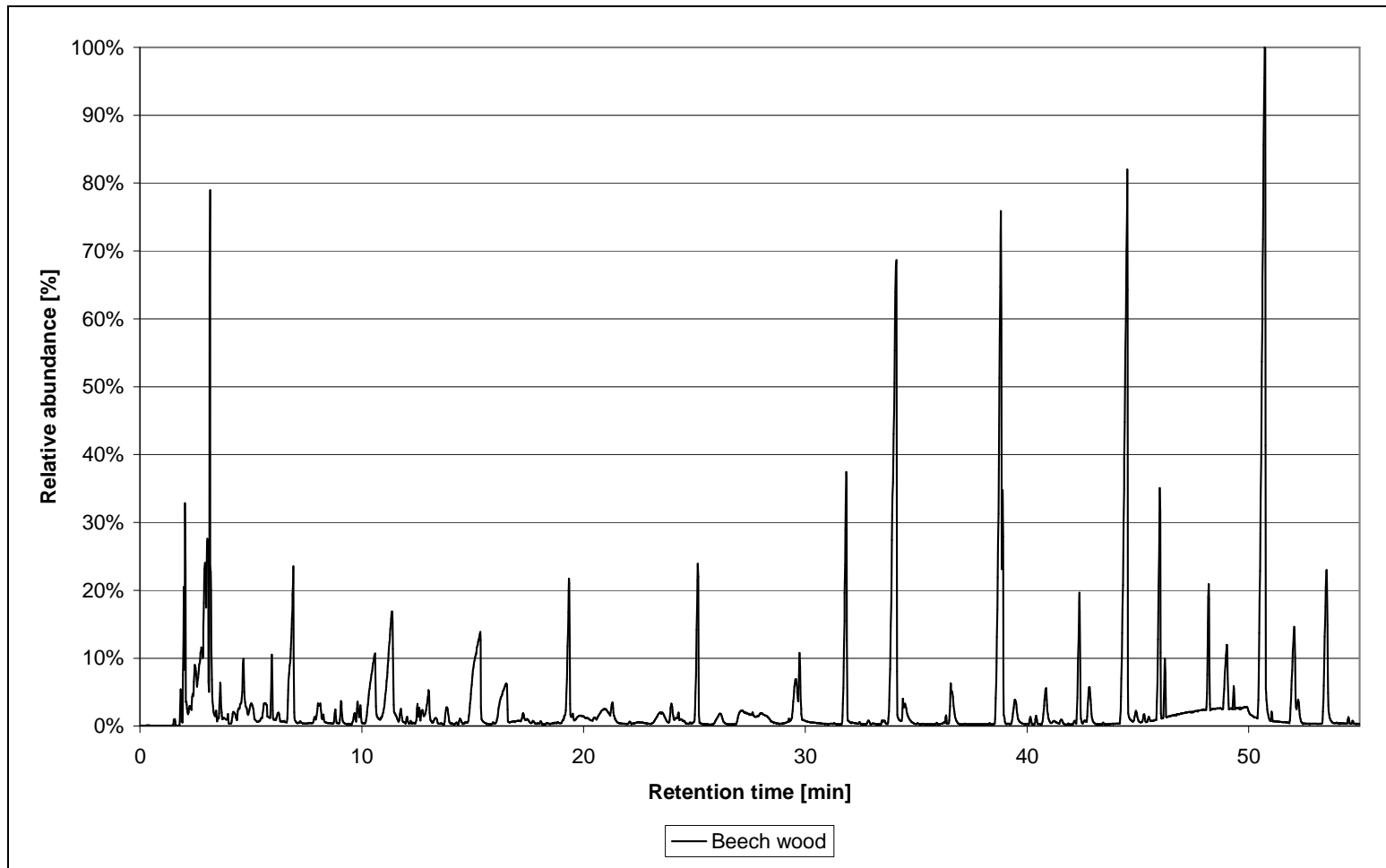


Figure 33: Chromatogram of beech wood analytical pyrolysis in inert atmosphere

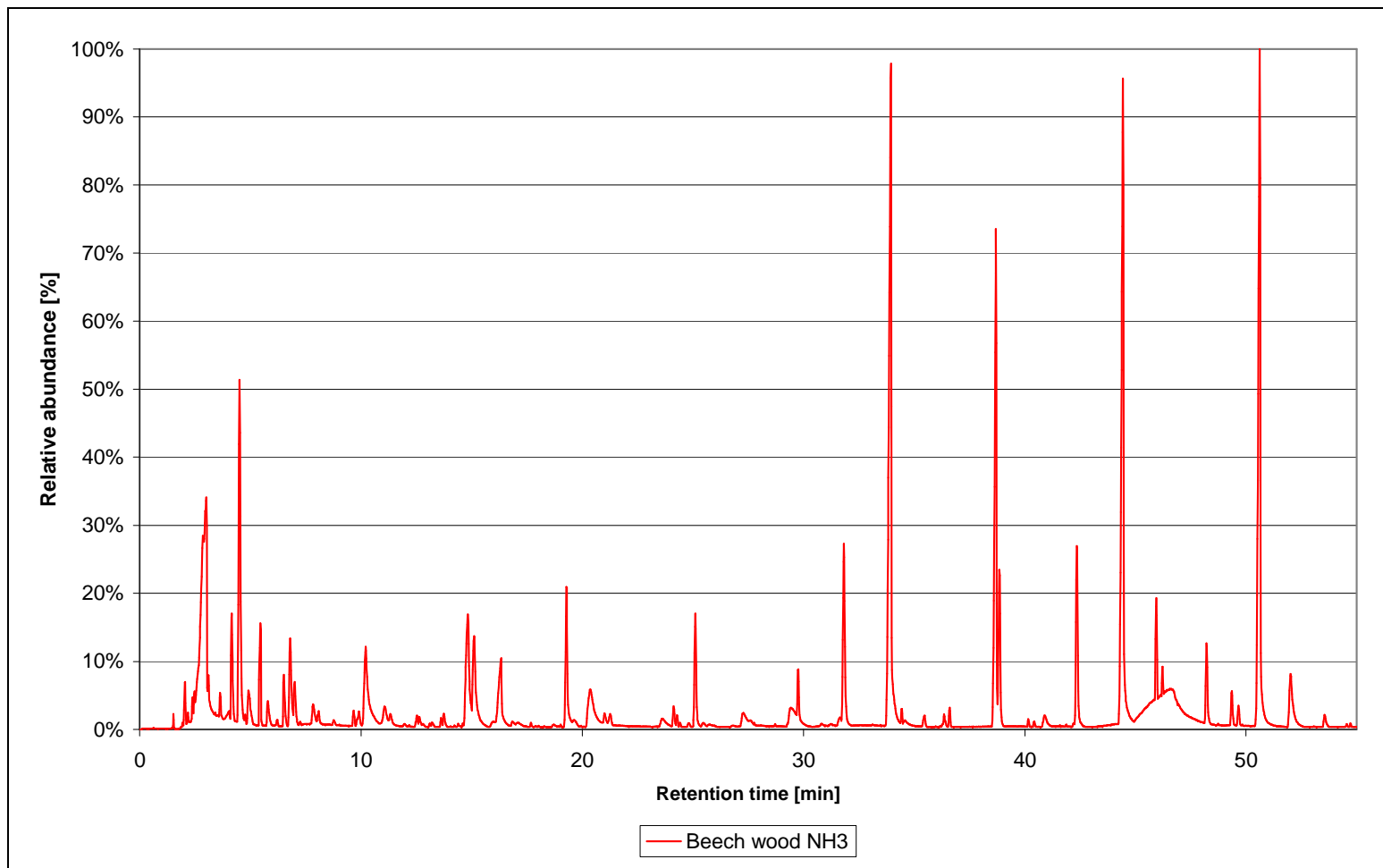


Figure 34: Chromatogram of beech wood analytical pyrolysis in ammonia atmosphere

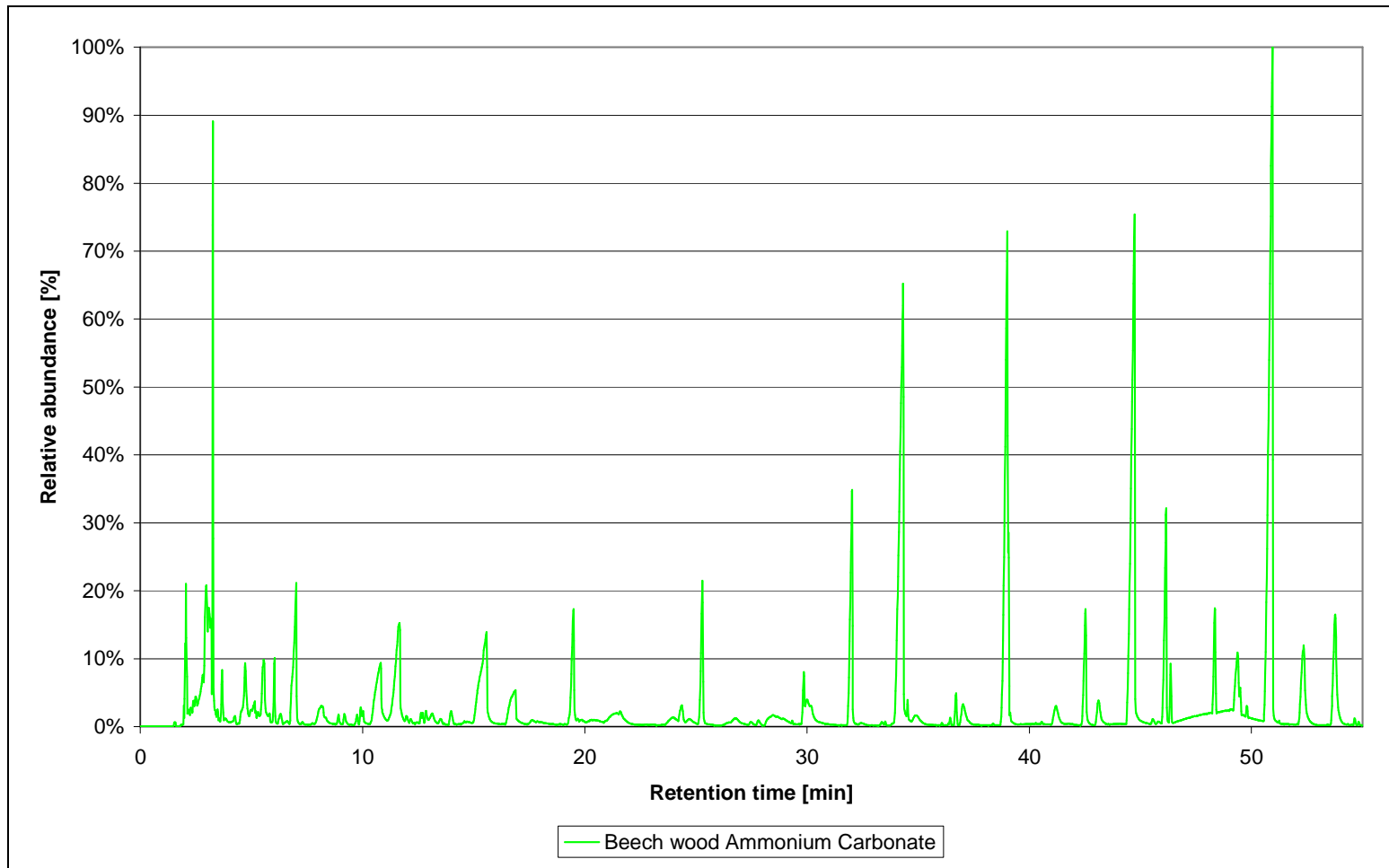


Figure 35: Chromatogram of beech wood analytical pyrolysis with ammonium carbonate

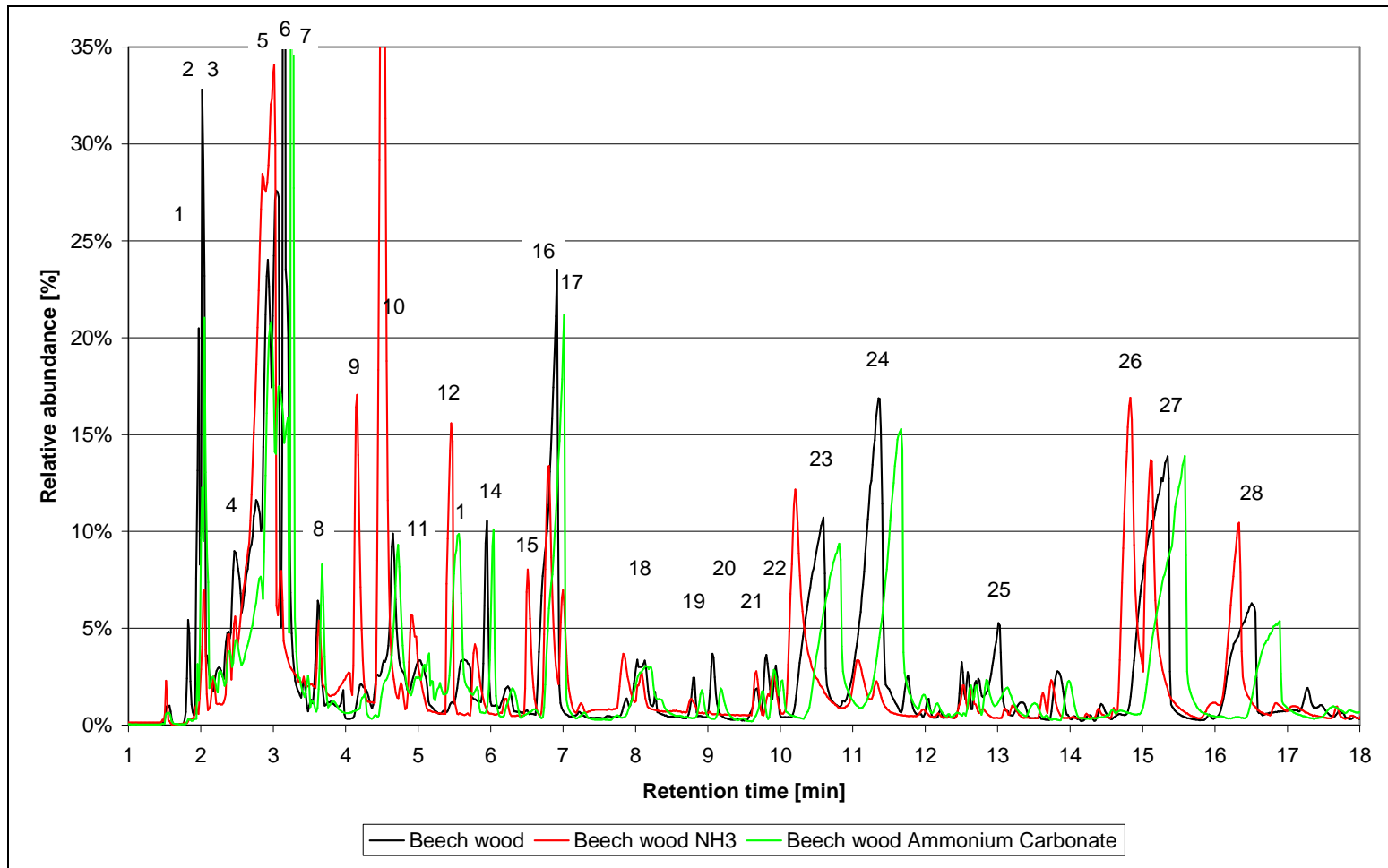


Figure 36: Chromatogram of beech wood analytical pyrolysis in inert and reactive atmosphere, RT 1-18min

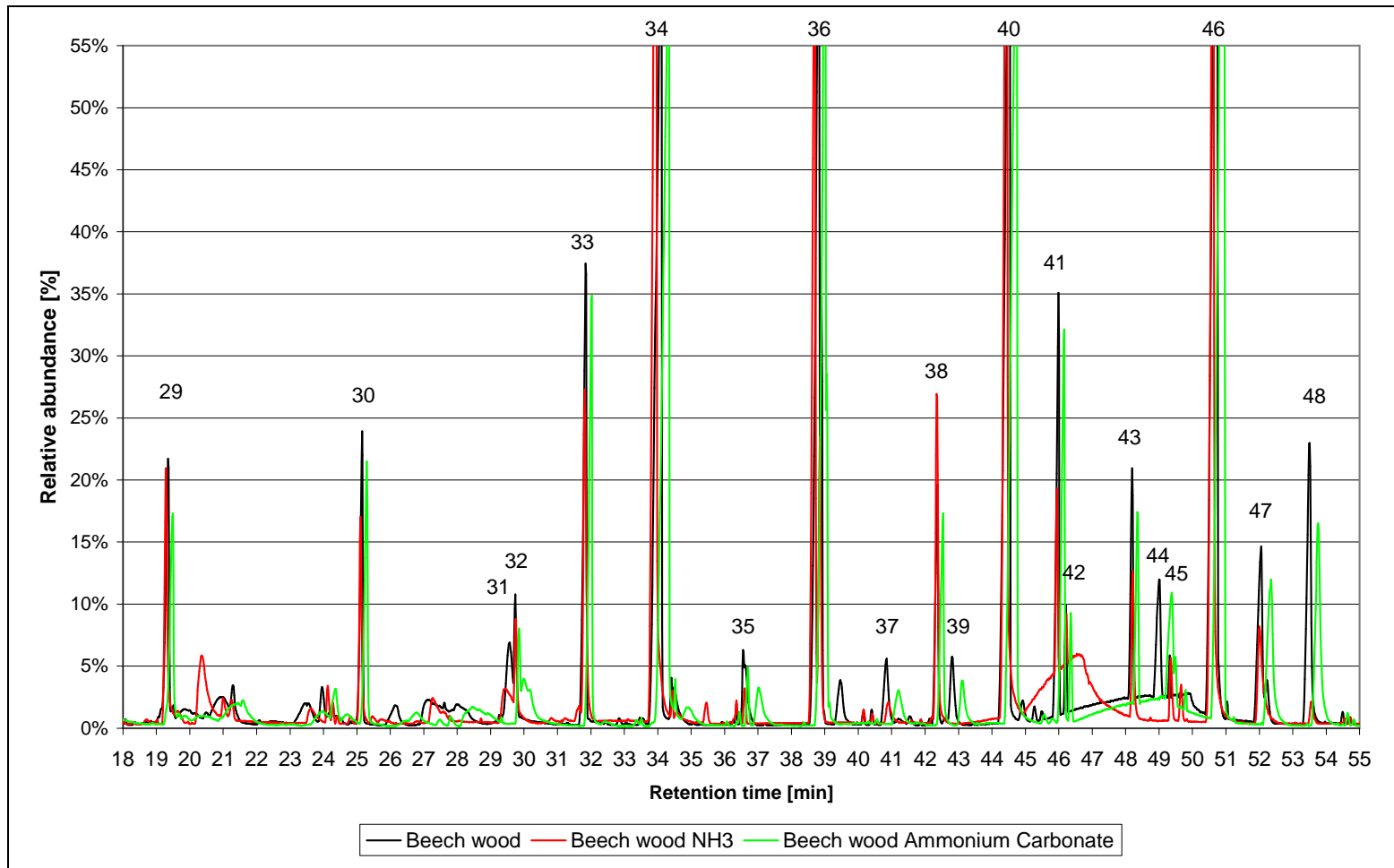


Figure 37: Chromatogram of beech wood analytical pyrolysis in inert and reactive atmosphere, RT 18-55min

The suggested peak assignments for the analysed peaks in the chromatograms are listed in Table 46 for retention time from 1-18min and in Table 47 for retention time 18-55min.

**Table 46: Assigned Peaks in Py-GC-MS chromatogram for beech wood runs, RT 1-18min**

|        | Beech wood untr., clean 22 | Beech wood NH3, clean 37 | Beech wood Am.Carb., clean 39 |           |                 |  |
|--------|----------------------------|--------------------------|-------------------------------|-----------|-----------------|--|
| Peak # | RT [min]                   | RT [min]                 | RT [min]                      | M [g/mol] | Base Peak [m/z] | Assigned compound                      |
| 1      | 1.969                      |                          | 2.019                         | 68        | 68              | (Furan)                                |
| 2      | 2.019                      |                          | 2.052                         | 60        | 43              | (Acetic acid)                          |
| 3      |                            | 2.034                    |                               | 75        | 44              | (2-Amino-1-propanol)                   |
| 4      | 2.464                      |                          |                               |           |                 | Unknown                                |
| 5      | 3.074                      |                          | 2.973                         |           |                 | Unknown                                |
| 6      |                            | 2.997                    |                               |           |                 | Unknown                                |
| 7      | 3.156                      |                          | 3.266                         | 74        |                 | Acetic acid methyl ester               |
| 8      | 3.612                      | 3.631                    | 3.676                         | 86        | 43              | Butandione                             |
| 9      |                            | 4.155                    |                               | 81        | 80              | 2-Methyl-1H-Pyrrole                    |
| 10     | 4.654                      | 4.515                    | 4.721                         | 86        | 55              | 2-Propenoic acid methyl ester          |
| 11     |                            | 4.955                    |                               |           |                 | Unknown                                |
| 12     |                            | 5.458                    |                               | 118       | 45              | Propanoic acid, 2-hydroxy-,ethyl ester |
| 13     |                            |                          | 5.545                         | 88        | 87              | 1,3-Dioxane                            |
| 14     | 5.949                      | 5.783                    | 6.039                         | 84        | 84              | (3H)-Furan-2-one                       |
| 15     |                            | 6.510                    |                               | 94        | 94              | Methylpyrazine                         |
| 16     | 6.915                      | 6.805                    | 6.952                         | 96        | 96              | Furfural                               |
| 17     |                            | 7.000                    |                               | 95        | 80              | 2-Ethyl-1H-pyrrole                     |
| 18     | 8.027                      | 7.844                    | 8.182                         | 98        | 98              | Furfuryl alcohol                       |
| 19     | 8.815                      | 8.759                    | 8.915                         | 96        | 42              | 4-Cyclopentene-1,3-dione               |
| 20     | 9.078                      |                          | 9.192                         |           |                 | Unknown                                |
| 21     | 9.663                      | 9.668                    | 9.765                         | 96        | 67              | 2-Methyl-Cyclopenten-1-one             |
| 22     |                            | 9.896                    | 10.026                        | 110       | 95              | 2-Ethyl-5-methylfuran                  |
| 23     | 10.597                     | 10.189                   | 10.814                        |           |                 | Unknown                                |
| 24     | 11.355                     | 11.070                   | 11.649                        | 98        | 98              | 1,3-Cyclopentandione                   |
| 25     | 13.011                     |                          |                               | 86        | 42              | Butyrolactone                          |
| 26     |                            | 14.833                   | 14.833                        | 114       | 114             | Unknown                                |
| 27     | 15.345                     | 15.111                   | 15.501                        | 114       | 114             | 4-Hydroxy-5,6-dihydro-(2H)-pyran-2-one |
| 28     | 16.442                     | 16.335                   | 16.859                        | 112       | 112             | 2-Hydroxy-1-methyl-1-cyclopenten-3-one |

**Table 47: Assigned Peaks in Py-GC-MS chromatogram for beech wood runs, RT 18-55min**

|        | Beech wood untr., clean 22 | Beech wood NH3, clean 37 | Beech wood Am.Carb., clean 39 |           |                 |                               |
|--------|----------------------------|--------------------------|-------------------------------|-----------|-----------------|-------------------------------|
| Peak # | RT [min]                   | RT [min]                 | RT [min]                      | M [g/mol] | Base Peak [m/z] | Assigned compound             |
| 29     |                            | 20.356                   |                               |           |                 | Unknown                       |
| 30     | 25.530                     | 25.112                   | 25.228                        | 138       | 123             | Guaiacol, 3-methyl-           |
| 31     | 29.560                     | 29.432                   |                               | 140       | 140             | Catechol, 3-methoxy-          |
| 32     | 29.742                     | 29.740                   | 29.867                        | 152       | 137             | Guaiacol, 4-ethyl-            |
| 33     | 31.827                     | 31.821                   | 31.964                        | 150       | 150             | Guaiacol, 4-vinyl-            |
| 34     | 34.083                     | 33.950                   | 34.326                        | 154       | 154             | Syringol                      |
| 35     | 36.556                     |                          | 36.705                        | 164       | 164             | Eugenol                       |
| 36     | 38.824                     | 38.699                   | 38.982                        | 168       | 168             | Syringol, 4-methyl-           |
| 37     | 40.836                     |                          |                               | 166       | 151             | Acetoguaiacone                |
| 38     | 42.366                     | 42.363                   | 42.520                        | 182       | 182             | Syringol, 3-ethyl-            |
| 39     | 42.794                     |                          |                               | 180       | 137             | Hydroxyisoeugenol             |
| 40     | 44.504                     | 44.438                   | 44.725                        | 180       | 180             | Syringol, 4-vinyl-            |
| 41     | 45.987                     | 45.946                   | 46.146                        | 194       | 194             | Syringol, 4-allyl-            |
| 42     |                            | 46.228                   | 46.360                        | 196       | 167             | Syringol, 4-propyl-           |
| 43     | 48.193                     | 48.206                   | 48.347                        | 194       | 194             | Syringol, 4-propenyl- (cis)   |
| 44     | 49.003                     |                          | 49.397                        | 182       | 182             | Syringaldehyde                |
| 45     | 49.333                     | 49.354                   | 49.479                        | 192       | 192             | unknown, likely C11H12O3      |
| 46     | 50.736                     |                          | 50.945                        | 194       | 194             | Syringol, 4-propenyl- (trans) |
| 47     | 52.051                     | 50.616                   | 52.349                        | 196       | 181             | Acetosyringone                |
| 48     | 53.510                     | 52.009                   | 53.750                        | 210       | 167             | Syringyl acetone              |

### 8.2.3 Analysis and discussion

Figure 36 and Figure 37 clearly show that there are just small differences between smaller peaks the chromatograms of the analytical pyrolysis of beech wood in inert and reactive atmospheres. Especially Figure 37 depicts mostly the peaks typical for lignin derived decomposition products and Table 47 listing these compounds is almost identical for all three experiments. This can be interpreted that in the chosen setup the reactive gases have no impact on the decomposition of lignin in beech wood and do not react with the lignin decomposition products in primary reactions. As the reaction time between pyrolysis and capturing the vapours in the Tenax-2® trap is extremely limited, the setup is not likely to allow any secondary reactions between ammonia gas and the decomposition products.

Also Figure 36 and Table 5 indicate that there is hardly any change in the decomposition products of beech wood. The retention time between 1min and 18min being characteristic for lighter decomposition products of cellulose and hemicellulose do not show much change

except for very light compounds. As well as for the lignin derived compounds also here it is suspected that except for very light compounds no primary reactions occur between ammonia and the decomposition products. The immediate “freezing” of the products on the trap appears to prevent further reactions. Only few compounds containing nitrogen were identified such as 2-Methyl-1H-pyrrole, Methylpyrazine or 2-Ethyl-1H-pyrrole.

The obtained results indicate that the added ammonia to the analytical pyrolysis does not alter the decomposition products of beech wood under the experimental conditions. They suggest that the reaction between ammonia and pyrolysis decomposition products occur in a secondary reaction after the pyrolysis step. That in general ammonia is reacting with pyrolysis products has been shown by Radlein [34] as well as within this research work.

### **8.3 GC-MS analysis of pyrolysis and in-situ nitrogenolysis liquids**

This section is dedicated to a comparative study of pyrolysis liquids obtained via fast pyrolysis in a bubbling fluidized bed reactor from beech wood and barley DDGS and in-situ nitrogenolysis liquids of the same feedstocks obtained under the same processing parameters.

The investigated fast pyrolysis and in-situ nitrogenolysis liquids have been produced within this research project as presented in section 6. The elemental analysis of the liquids is presented in Table 48.

**Table 48: Elemental analysis of investigated liquids**

| Element | Basis                | Unit | Beech wood       |                                    | Barley DDGS      |                       |
|---------|----------------------|------|------------------|------------------------------------|------------------|-----------------------|
|         |                      |      | Pyrolysis liquid | Nitrogenolysis liquid bottom phase | Pyrolysis liquid | Nitrogenolysis liquid |
| C       | daf                  | wt.% | 54.24%           | 56.86%                             | 56.73%           | 43.86%                |
| H       | daf                  | wt.% | 6.90%            | 7.68%                              | 7.15%            | 9.96%                 |
| N       | daf                  | wt.% | bdl.             | 7.70%                              | 6.13%            | 9.96%                 |
| O*      | daf                  | wt.% | 38.86%           | 27.76%                             | 29.99%           | 36.22%                |
| O*      | Oxygen by difference |      |                  |                                    |                  |                       |

The fast pyrolysis liquid of beech wood is virtually nitrogen free as it can be seen in Table 48. In contrast the in-situ nitrogenolysis liquid of beech wood contains 7.70wt.% of nitrogen indicating that nitrogen has been added during nitrogenolysis. Barley DDGS fast pyrolysis liquid

contains 6.13wt.% nitrogen and nitrogenolysis liquid 9.96wt.%, indicating an uptake of 3.83wt.%.

The point of interest in this study is to investigate in what way the added nitrogen is present in the in-situ nitrogenolysis liquids. Therefore the pyrolysis and in-situ nitrogenolysis liquids are investigated using GC-MS for liquid samples in order to point out the differences and identify possible nitrogenolysis products.

### **8.3.1 Method**

The equipment used was a Varian GC-450 Gas Chromatograph and MS-220 Mass Spectrometer (see section 3.11). The fast pyrolysis and in-situ nitrogenolysis liquids were dissolved and diluted with ethanol (GC-grade) in a volumetric ratio of 1:4 (fast pyrolysis liquid: ethanol) and filtered with a 22µm pore size syringe filter before injection. 0.5µl of diluted sample was injected into the Varian system by an auto sampler.

### **8.3.2 Results**

The chromatograms of beech wood fast pyrolysis and in-situ nitrogenolysis liquids are presented to show the differences and similarities. In Figure 38, Figure 39 and Figure 40 the chromatograms of each experiment are presented individually. In order to present the results more clearly the chromatograms are plotted superimposed and the chromatograms for beech liquids are split and presented in Figure 41 for retention times from 4-19min and in Figure 42 for retention times from 19-36min. The identified peaks are presented in Table 49 and Table 50.

For barley DDGS pyrolysis and nitrogenolysis liquids the chromatograms are presented individually in Figure 43 and Figure 44. In Figure 45 they are presented superimposed for the same reasons as stated above. The assigned peaks are listed in Table 51.

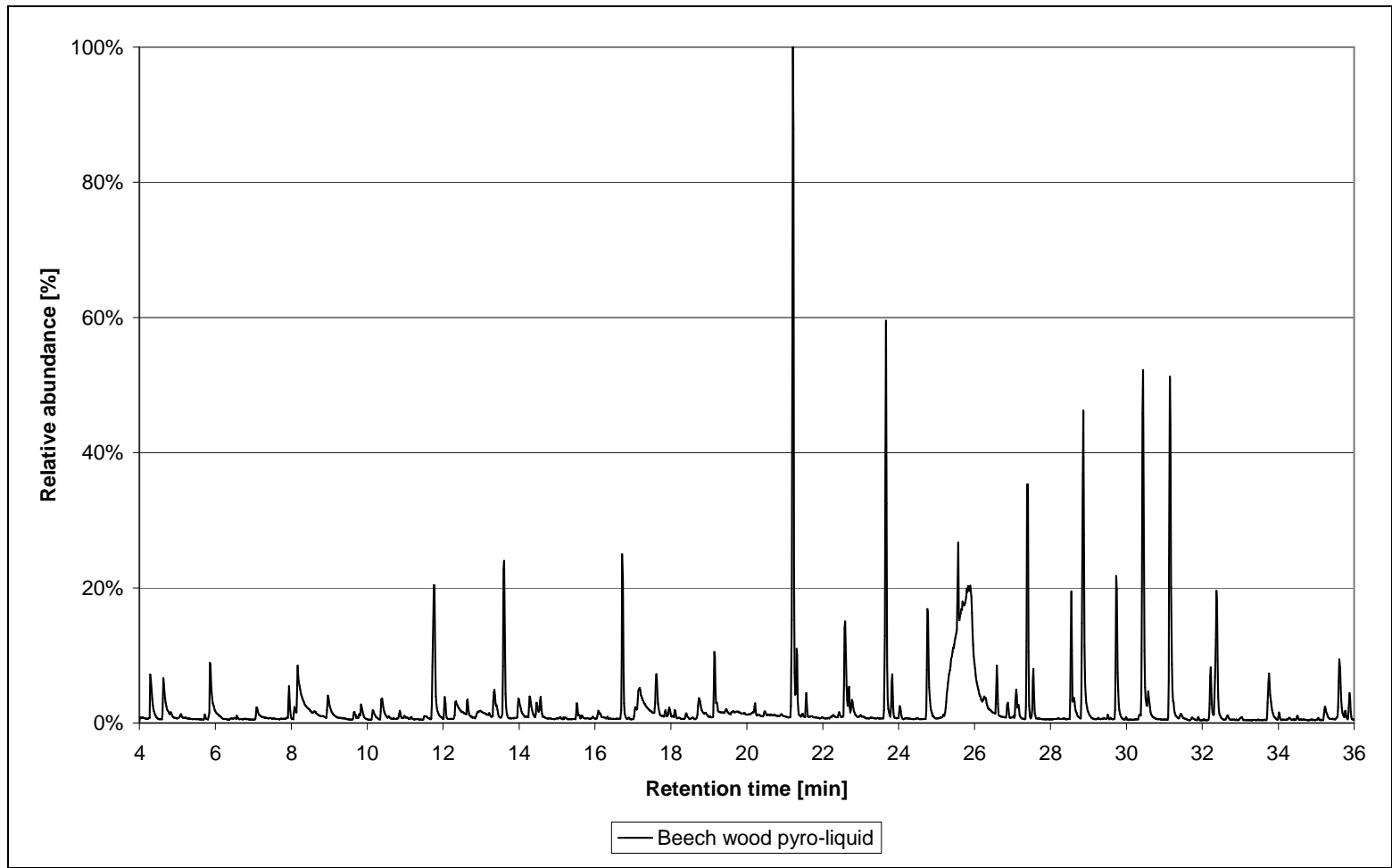


Figure 38: Chromatogram of beech wood pyrolysis liquid

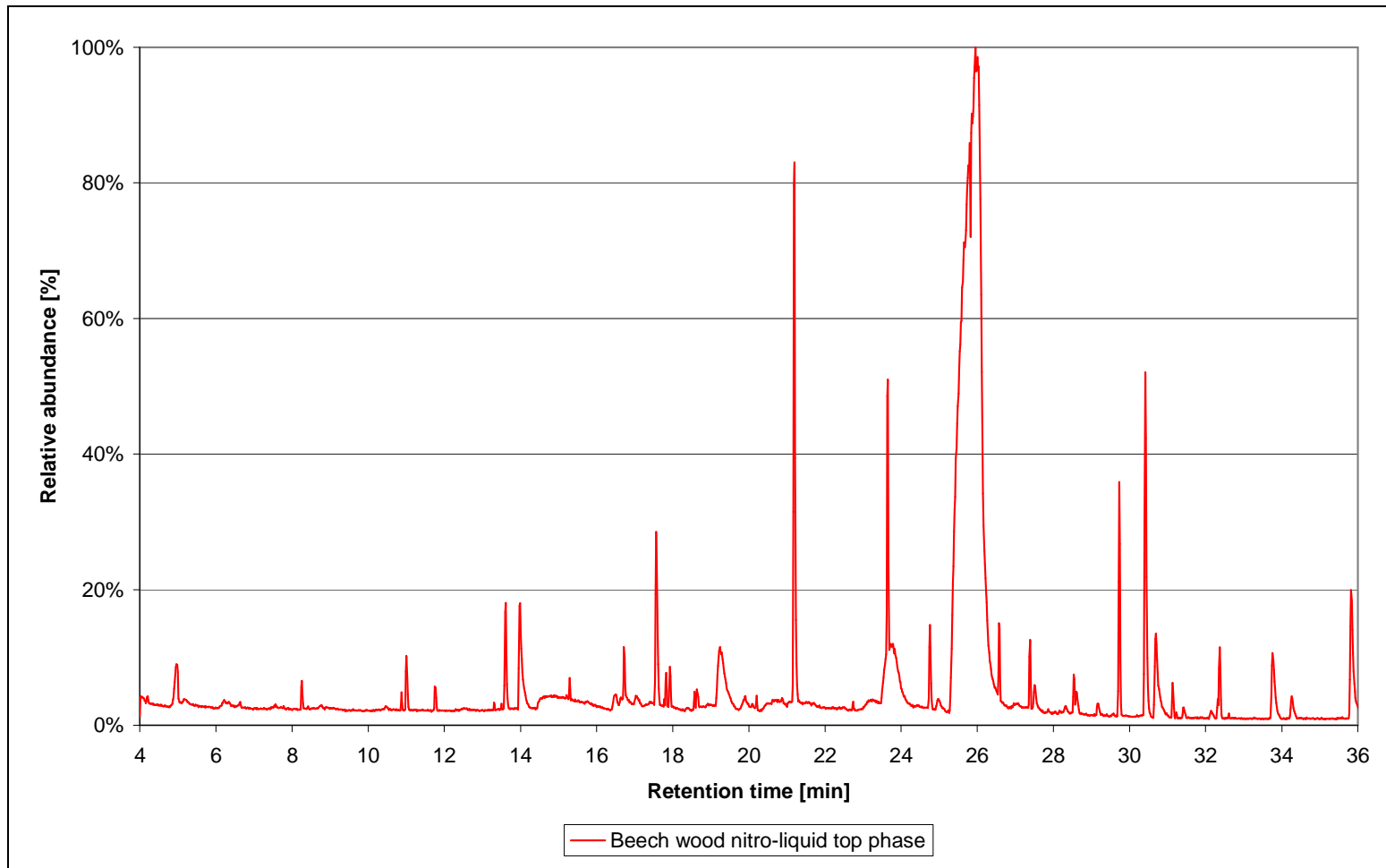


Figure 39: Chromatogram of beech wood nitrogenolysis liquid top phase

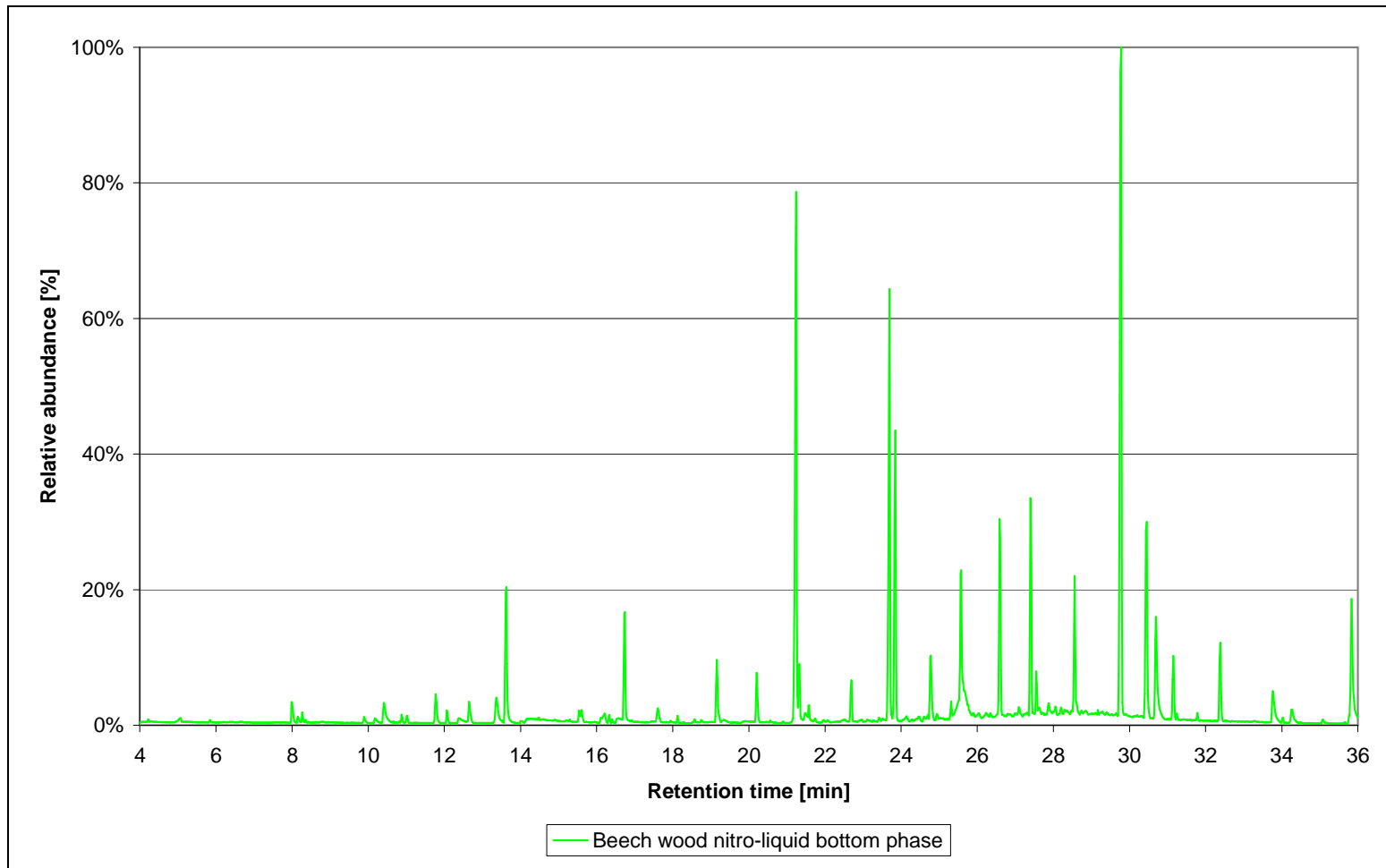


Figure 40: Chromatogram of beech wood nitrogenolysis liquid bottom phase

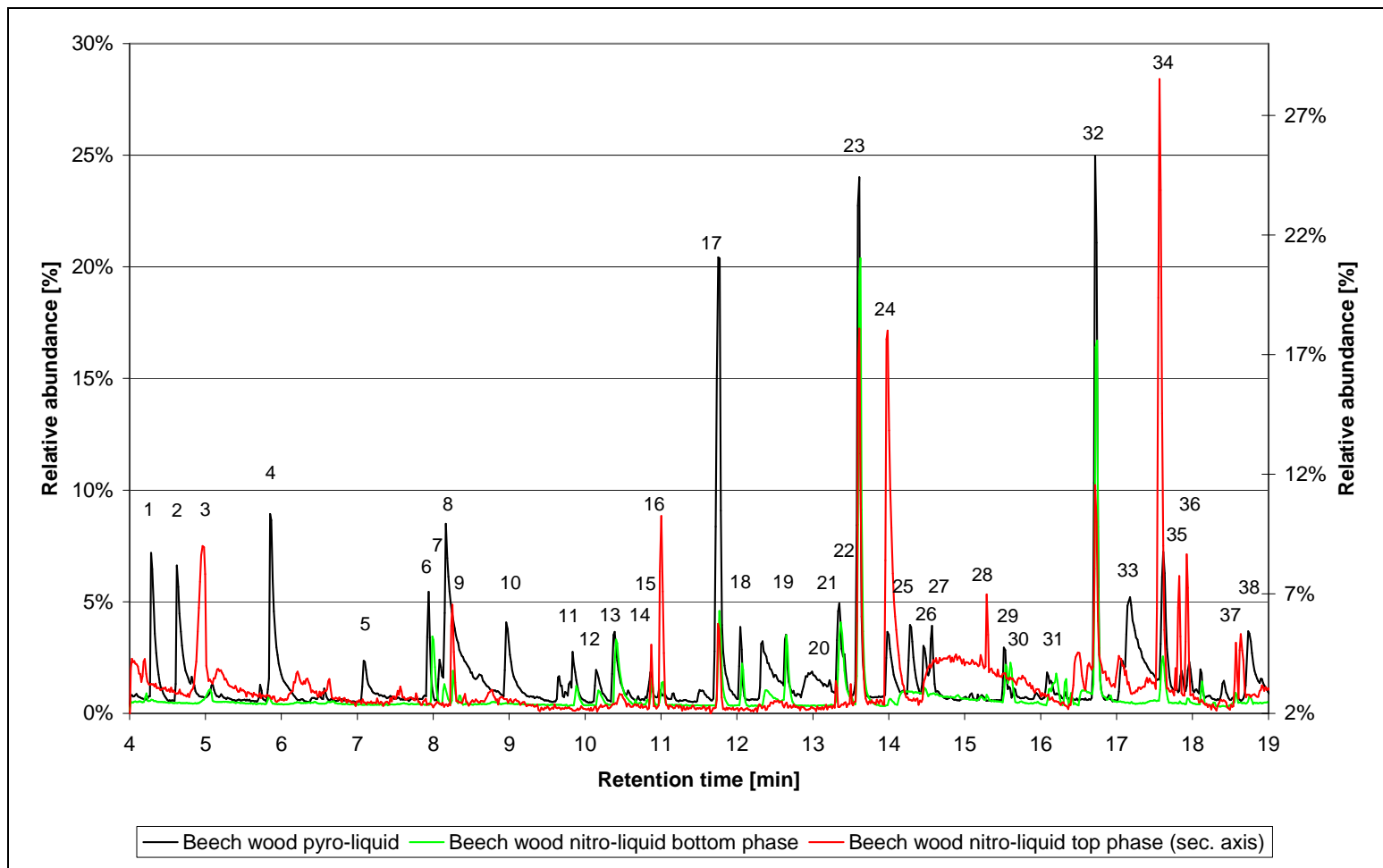


Figure 41: Chromatogram of beech wood pyrolysis and nitrogenolysis liquids, RT 4-19min

**Table 49: Assigned peaks for beech wood pyrolysis and nitrogenolysis liquids, RT 4-19min**

| Peak # | Beech w. py.-liquid, untreated<br>RT [min] | Beech w. ni.-liquid top phase<br>RT [min] | Beech w. ni.-liquid bottom phase<br>RT [min] | M [g/mol] | Base Peak [m/z] | Assigned compound                           |
|--------|--|---|--|-----------|-----------------|---|
| 1      | 4.286                                      |   |  | 86        | 41/57           | 2-Methyl-Butanal or 3-Pentanone             |
| 2      | 4.624                                      |   |  | 86        | 57/41           | 3-Pentanone or 2-Methyl-Butanal             |
| 3      |  | 4.98                                      |  | 88        | 60              | Butanoic acid                               |
| 4      | 5.87                                       |   |  | 96        | 96              | 2,5-Dimethylfural                           |
| 5      | 7.083                                      |   |  |           |                 | unknown                                     |
| 6      | 7.937                                      |   | 7.988  | 96        | 67              | 2-Methyl-2-cyclopenten-1-one                |
| 7      |  |   | 8.149  | 110       | 95              | 2-Acetylfuran                               |
| 8      | 8.167                                      |   |  | 84        | 55              | (5H)-Furan-2-one                            |
| 9      |  | 8.255                                     | 8.261  | 108       | 108             | 4,6-Dimethyl-pyrimidine                     |
| 10     | 8.962                                      |   |  | 98        | 43              | 5-Methyl-2(5H)-Furanone                     |
| 11     | 9.836                                      |   | 9.885  | 96        | 96              | 3-Methyl-2-cyclopenten-1-one                |
| 12     | 10.145                                     |   | 10.177                                       | 98        | 69              | 4-Methyl-5H-furan-2-one                     |
| 13     | 10.389                                     | 10.467                                    | 10.406                                       | 94        | 94              | Phenol                                      |
| 14     | 10.66                                      |   |  | 112       | 69              | 2,5-dihydro-3,5-dimethyl-2-furanone         |
| 15     |  | 10.873                                    | 10.878                                       | 122       | 121             | 2-Ethyl-6-methyl-pyrazine                   |
| 16     |  | 11.003                                    | 11.009                                       | 122       | 122             | 3,6-Dimethyl-2-pyridinamine                 |
| 17     | 11.77                                      | 11.75                                     | 11.77  | 112       | 112             | 2-Hydroxy-1-methyl-1-cyclopenten-3-one      |
| 18     | 12.045                                     |   | 12.064                                       | 110       | 67              | 2,3-Dimethyl-2-cyclopenten-1-one            |
| 19     | 12.647                                     |   | 12.648                                       | 108       | 108             | o-Cresol                                    |
| 20     |  | 13.303                                    |  | 136       | 135             | 2-Ethyl-3,5-dimethyl-pyrazine               |
| 21     | 13.348                                     |   | 13.366                                       | 108       | 107             | m-Cresol                                    |
| 22     |  | 13.497                                    |  | 136       | 135             | 3-Ethyl-2,5-dimethyl-pyrazine               |
| 23     | 13.609                                     | 13.613                                    | 13.626                                       | 124       | 109             | Guaiacol                                    |
| 24     | 13.999                                     | 13.987                                    |  | 148       | 57              | (1,4-Dioxane-2,5-dimethanol)                |
| 25     | 14.155                                     |   |  | 126       | 126             | Maltol                                      |
| 26     | 14.276                                     |   |  | 122       | 107             | Phenol, 2-ethyl                             |
| 27     | 14.569                                     |   |  | 126       | 126             | 3-Ethyl-2-hydroxy-2-cyclopenten-1-one       |
| 28     |  | 15.289                                    |  | 134       | 119             | (5H-5Methyl-6,7-dihydrocyclopenta-pyrazine) |
| 29     |  |   | 15.535                                       | 122       | 107             | Phenol, 3-ethyl                             |
| 30     | 15.516                                     |   | 15.6   | 122       | 107             | Phenol, 4-ethyl                             |
| 31     | 16.083                                     |   |  | 138       | 138             | (Guaiacol, 4-methyl)                        |
| 32     | 16.718                                     | 16.718                                    | 16.742                                       | 138       | 123             | Guaiacol, 3-methyl-                         |
| 33     | 17.16                                      |   |  | 110       | 110             | Catechol                                    |
| 34     | 17.614                                     | 17.563                                    | 17.608                                       | 144       | 69              | 1,4:3,6-Dianhydro-à-d-glucofuranose         |
| 35     |  | 17.825                                    |  | 144       | 43              | 4,4-Anhydro-d-galactosan                    |
| 36     |  | 17.922                                    |  | 144       | 43              | 3,4-Anhydro-d-galactosan                    |
| 37     |  | 18.636                                    |  |           |                 | unknown                                     |
| 38     | 18.733                                     |   |  | 140       | 140             | Catechol, 3-methoxy-                        |

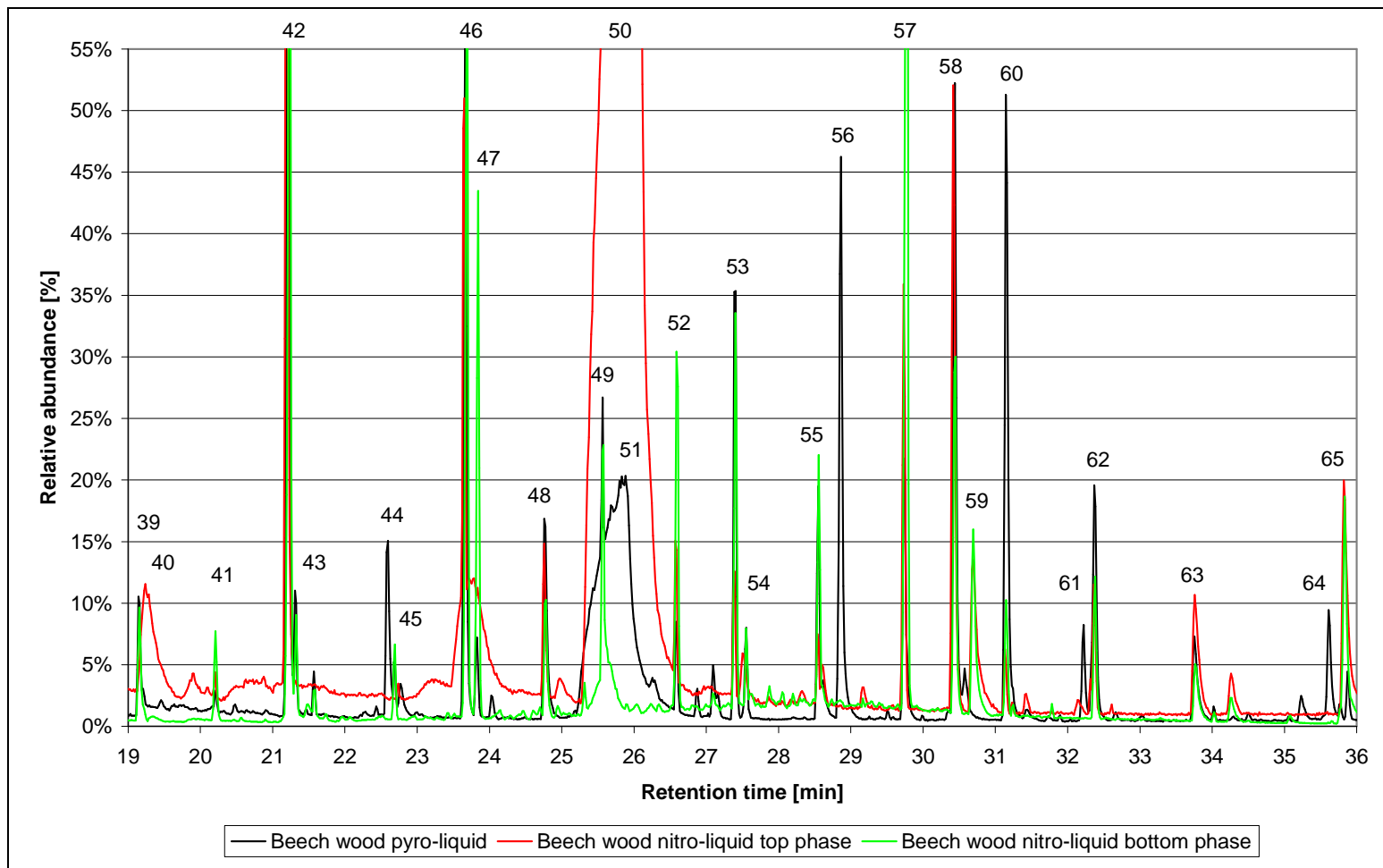


Figure 42: Chromatogram of beech wood pyrolysis and nitrogenolysis liquids, RT 19-36min

**Table 50: Assigned peaks for beech wood pyrolysis and nitrogenolysis liquids, RT 19-36min**

|        | Beech w.<br>py.-liquid,<br>untreated | Beech w.<br>ni.-liquid<br>top<br>phase | Beech w.<br>ni.-liquid<br>bottom<br>phase |              |                       |                                  |
|--------|--------------------------------------|--|---|--------------|-----------------------|----------------------------------|
| Peak # | RT [min]                             | RT [min]                               | RT [min]                                  | M<br>[g/mol] | Base<br>Peak<br>[m/z] | Assigned compound                |
| 39     | 19.144                               |  | 19.155                                    | 152          | 137                   | Guaiacol, 4-ethyl-               |
| 40     |                                      | 19.223                                 |   |              |                       | unresolved peak                  |
| 41     |                                      |  | 20.208                                    | 150          | 150                   | Guaiacol, 4-vinyl-               |
| 42     | 21.211                               | 21.183                                 | 21.242                                    | 154          | 154                   | Syringol                         |
| 43     | 21.308                               |  | 21.324                                    | 164          | 164                   | Eugenol                          |
| 44     | 22.594                               |  |   | 152          | 151                   | Isovanillin                      |
| 45     |                                      |  | 22.69                                     | 164          | 164                   | Isoeugenol (trans)               |
| 46     | 23.665                               | 23.654                                 | 23.694                                    | 168          | 168                   | Syringol, 4-methyl-              |
| 47     | 23.829                               | 23.819                                 | 23.842                                    | 164          | 164                   | Isoeugenol                       |
| 48     | 24.758                               | 24.757                                 | 24.765                                    | 166          | 151                   | Acetoguaiacone                   |
| 49     | 25.565                               |  | 25.579                                    | 182          | 167                   | Syringol, 4-ethyl-               |
| 50     | 25.749                               |  |   | 180          | 137                   | (Hydroxyisoeugenol)              |
| 51     |                                      | 25.985                                 |   | 162          | 60                    | Levoglucosan                     |
| 52     | 26.583                               | 26.571                                 | 26.583                                    | 180          | 165                   | 1-(2,5-dimethoxyphenyl)-ethanone |
| 53     | 27.387                               | 27.389                                 | 27.387                                    | 194          | 194                   | Syringol, 4-propenyl- (cis)      |
| 54     | 27.552                               | 27.519                                 | 27.549                                    | 196          | 167                   | (Syringol, 4-propyl-)            |
| 55     | 28.551                               | 28.539                                 | 28.558                                    | 194          | 194                   | Syringol, 4-propenyl- (trans)    |
| 56     | 28.863                               |  |   | 182          | 182                   | Syringol, 3-ethyl-               |
| 57     | 29.751                               | 29.731                                 | 29.782                                    | 194          | 194                   | Syringol, 4-allyl-               |
| 58     | 30.442                               | 30.414                                 | 30.448                                    | 196          | 181                   | Acetosyringone                   |
| 59     |                                      | 30.694                                 | 30.694                                    | 180          | 137                   | Hydroxyisoeugenol                |
| 60     | 31.145                               | 31.132                                 | 31.151                                    | 210          | 167                   | Syringyl acetone                 |
| 61     | 32.221                               |  |   | 210          | 167                   | Sinapyl alcohol                  |
| 62     | 32.367                               | 32.367                                 | 32.383                                    | 210          | 181                   | Propiosyringone                  |
| 63     | 33.755                               | 33.757                                 | 33.765                                    | 212          | 167                   | Dihydrosinapyl alcohol           |
| 64     | 35.611                               |  |   | 208          | 208                   | Sinapaldehyde                    |
| 65     | 35.873                               | 35.822                                 | 35.832                                    | 210          | 167                   | Syringyl alcohol                 |

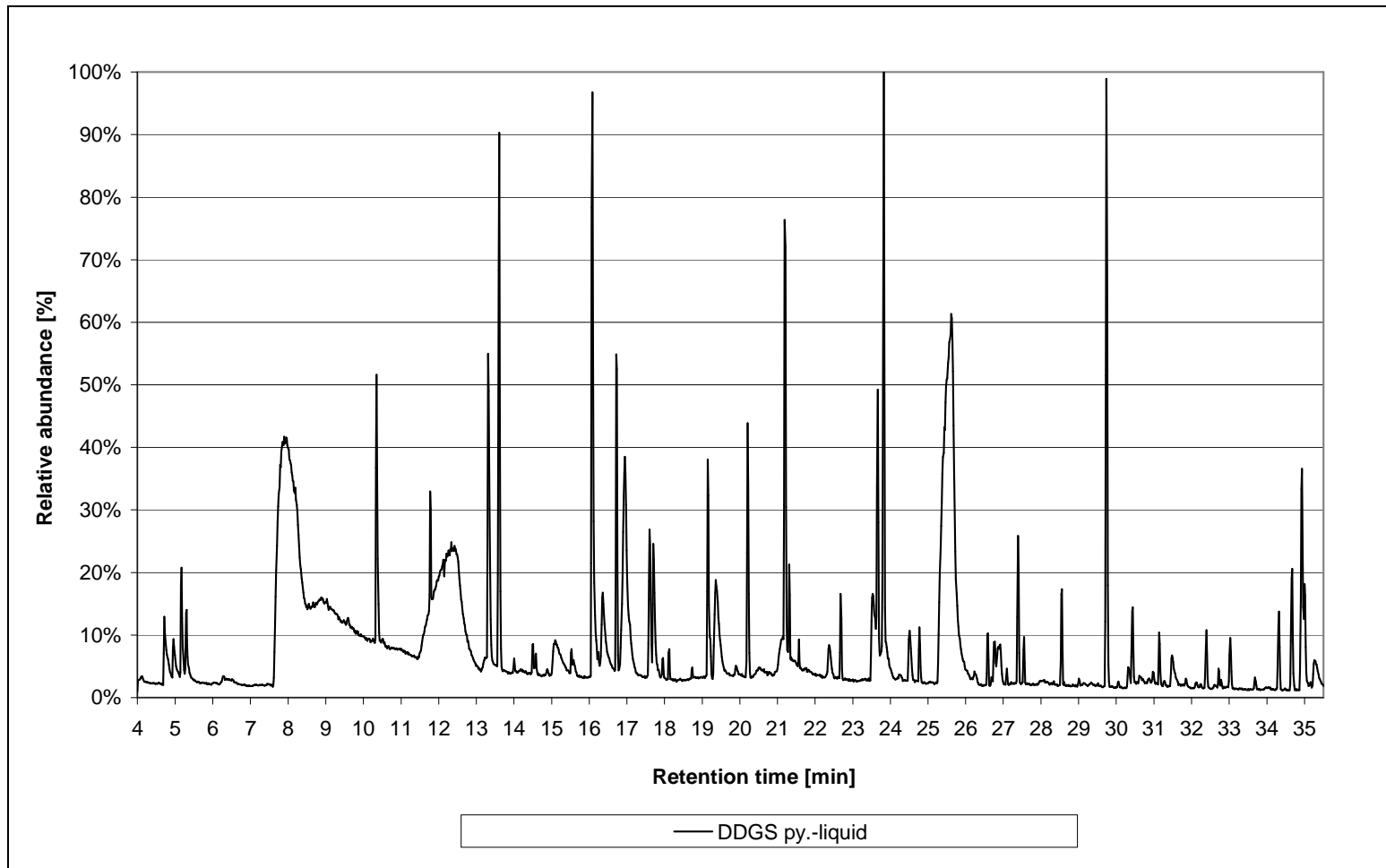


Figure 43: Chromatogram of barley DDGS pyrolysis liquid

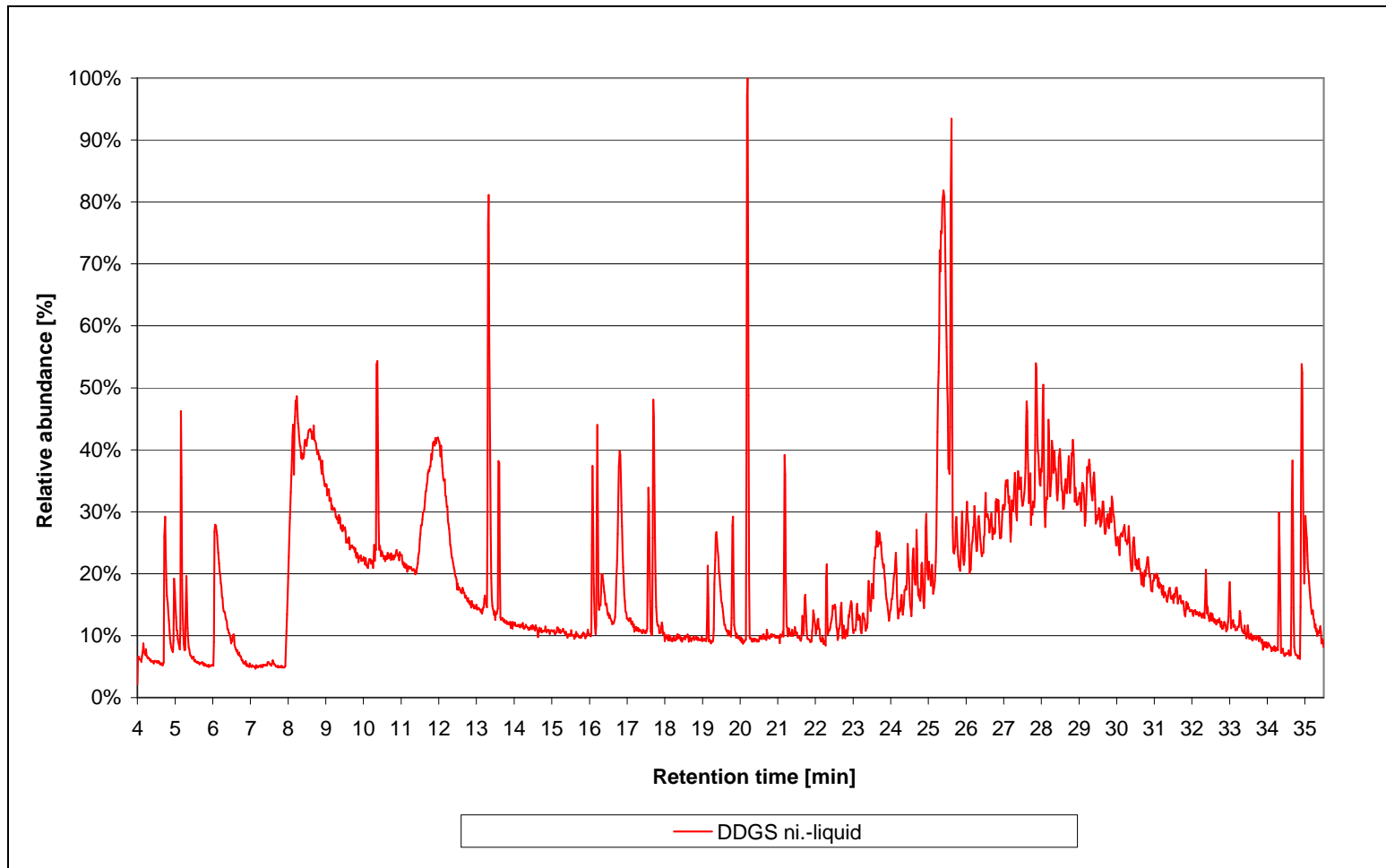


Figure 44: Chromatogram of barley DDGS nitrogenolysis liquid

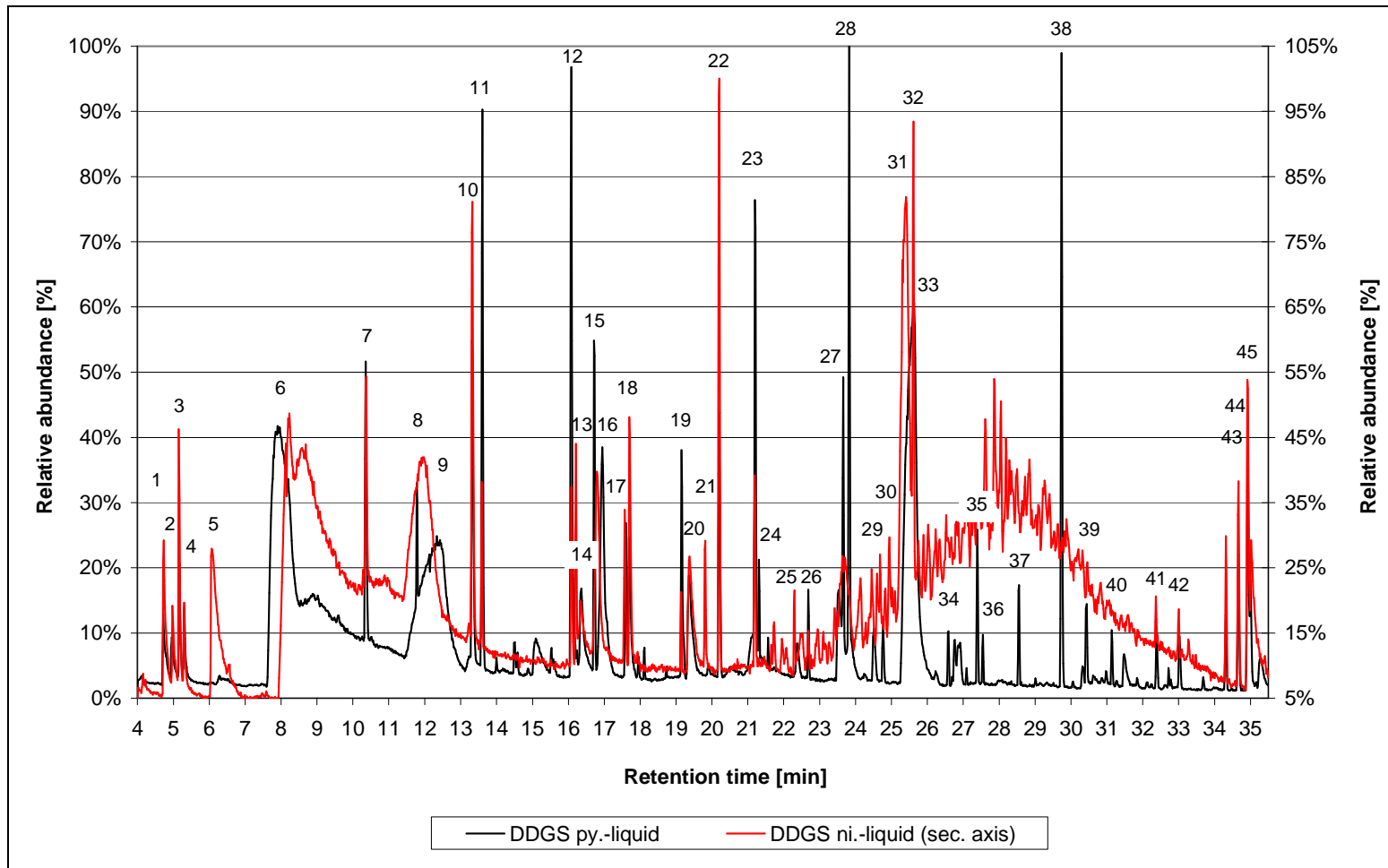


Figure 45: Chromatogram of barley DDGS pyrolysis and nitrogenolysis liquids, RT 4-36min

**Table 51: Assigned peaks for barley DDGS pyrolysis and nitrogenolysis liquids, RT 19-36min**

| Peak # | DDGS py.-<br>liquid<br>RT [min] | DDGS ni.-<br>liquid<br>RT [min] | M<br>[g/mol] | Base<br>Peak<br>[m/z] | Assigned compound                            |
|--------|---------------------------------|---------------------------------|--------------|-----------------------|--|
| 1      | 4.713                           | 4.734                           | 90           | 45                    | (2,3-Butanediol)                             |
| 2      | 4.958                           | 4.974                           | 88           | 45                    | (3-Methyl-2-butanol)                         |
| 3      | 5.17                            | 5.151                           |              |                       | column bleed                                 |
| 4      | 5.302                           | 5.295                           |              |                       | unknown                                      |
| 5      |                                 | 6.065                           | 86           | 57                    | Formic acid, 2-propenyl ester                |
| 6      | 7.966                           | 8.246                           |              |                       | unresolved peak                              |
| 7      | 10.352                          | 10.352                          | 94           | 94                    | Phenol                                       |
| 8      | 11.774                          |                                 | 112          | 112                   | 2-Hydroxy-1-methyl-1-cyclopenten-3-one       |
| 9      | 12.454                          | 12.061                          |              |                       | unresolved peak                              |
| 10     | 13.314                          | 13.327                          | 108          | 107                   | p-Cresol                                     |
| 11     | 13.607                          | 13.585                          | 124          | 109                   | Guaiacol                                     |
| 12     | 16.085                          | 16.084                          | 122          | 107                   | Phenol, 4-ethyl-                             |
| 13     |                                 | 16.215                          | 142          | 142                   | unknown                                      |
| 14     | 16.377                          |                                 | 122          | 107                   | Phenol, 3-ethyl-                             |
| 15     | 16.718                          |                                 | 138          | 123                   | Guaiacol, 3-methyl-                          |
| 16     | 16.946                          | 16.801                          |              |                       | unknown, sugar derived                       |
| 17     | 17.602                          | 17.567                          | 144          | 69                    | 1,4:3,6-Dianhydro- $\alpha$ -D-glucopyranose |
| 18     | 17.699                          | 17.697                          | 120          | 120                   | Phenol, 4-vinyl-                             |
| 19     | 19.15                           | 19.144                          | 152          | 137                   | Guaiacol, 4-ethyl-                           |
| 20     | 19.362                          | 19.373                          |              |                       | unknown, sugar derived                       |
| 21     |                                 | 19.813                          | 117          | 117                   | Indole                                       |
| 22     | 20.204                          | 20.206                          | 150          | 150                   | Guaiacol, 4-vinyl-                           |
| 23     | 21.195                          | 21.186                          | 154          | 154                   | Syringol                                     |
| 24     | 21.309                          |                                 | 164          | 164                   | Eugenol                                      |
| 25     |                                 | 22.302                          | 131          | 131                   | Indole, 4-methyl-                            |
| 26     | 22.68                           |                                 | 164          | 164                   | Isoeugenol (cis)                             |
| 27     | 23.66                           | 23.647                          | 168          | 168                   | Syringol, 4-methyl                           |
| 28     | 23.823                          | 23.809                          | 164          | 164                   | Isoeugenol (trans)                           |
| 29     | 24.524                          |                                 |              |                       | unknown                                      |
| 30     | 24.767                          |                                 | 166          | 151                   | Acetoguaiacone                               |
| 31     |                                 | 25.389                          | 162          | 60                    | Levogluconan                                 |
| 32     | 25.563                          |                                 | 182          | 167                   | Syringol, 4-ethyl                            |
| 33     |                                 | 25.615                          |              |                       | unknown, likely fatty acid                   |
| 34     | 26.589                          | 26.573                          | 180          | 180                   | Syringol, 4-vinyl-                           |
| 35     | 27.386                          | 27.381                          | 194          | 194                   | Syringol, 4-allyl-                           |
| 36     | 27.55                           |                                 | 196          | 167                   | Syringol, 4-propyl-                          |
| 37     | 28.554                          |                                 | 194          | 194                   | Syringol, 4-propenyl- (cis)                  |
| 38     | 29.738                          | 29.729                          | 194          | 194                   | Syringol, 4-propenyl- (trans)                |
| 39     | 30.435                          | 30.422                          | 196          | 181                   | Acetosyringone                               |
| 40     | 31.139                          |                                 | 210          | 167                   | Syringyl acetone                             |
| 41     | 32.391                          | 32.367                          |              | 154/70                | unknown, protein derived                     |
| 42     | 33.024                          | 33.008                          |              | 70/154                | unknown, protein derived                     |
| 43     | 34.637                          | 34.314                          |              | 154/70                | unknown, protein derived                     |
| 44     | 34.673                          | 34.672                          |              | 154/70                | unknown, protein derived                     |
| 45     | 34.933                          | 34.917                          |              | 70/154                | unknown, protein derived                     |

Figure 41 and Figure 42 show, that the differences between pyrolysis and in-situ nitrogenolysis liquids of beech wood are limited. The main observation is that the chromatograms have changed due to the phase separation of the nitrogenolysis liquids. Therefore water soluble products appear to be more abundant in the aqueous top phase and organic ones in the bottom phase of the nitrogenolysis liquids.

The identified compounds are mainly present in all three liquids. Especially the lignin derived higher molecular weight components appear to be unaltered by the addition of ammonia (see Table 50). Just four nitrogen containing compounds were assigned and few peaks remained unassigned that are not already present in the nitrogen free beech wood pyrolysis liquid (see Table 49).

Figure 45 shows the chromatograms of barley DDGS pyrolysis and in-situ nitrogenolysis liquids. Unfortunately the in-situ nitrogenolysis liquid contains residual ISOPAR™ that did not phase separate even after centrifuging the sample at 4000RPM for 5min. Therefore the quality of the chromatogram is limited. Nevertheless Figure 45 shows that just as for beech wood the differences between the chromatograms are minor. The identified compounds (see Table 51) are mainly present in both liquids. Beside nitrogen compounds resulting from protein decomposition just few others were identified.

### **8.3.3 Analysis and discussion**

The results obtained show that it was not possible to identify the nitrogen compounds formed during nitrogenolysis by means of GC-MS for liquid samples and the applied method. The fact that nitrogen is present is proven by the elemental analysis, but in what type of compounds remains unknown. It remains unclear, if:

1. the nitrogen is present in very light compounds being flushed undetected from the system with the solvent or
2. the concentration of the formed compounds is too low to be detected beside the pyrolysis products or
3. if the formed nitrogen compounds are long chain compounds that polymerize in the protection liner of the injection port of the GC held at 275°C upon injection.

As beech wood in-situ nitrogenolysis liquid bottom phase polymerizes readily after production the later possibility could be one reason. The aqueous phase in contrast might contain light compounds that could be flushed with the solvent.

Although barley DDGS in-situ nitrogenolysis liquid is single phased, the above stated possibilities might also apply here. Also the barley DDGS product polymerizes at elevated temperatures and might contain light compounds in the aqueous part of the emulsion.

#### ***8.4 Analysis of solidified fast pyrolysis and in-situ nitrogenolysis liquids via FTIR***

This section is dedicated to a comparative study of solidified fast pyrolysis and in-situ nitrogenolysis liquids of beech wood and barley DDGS, produced via fast pyrolysis in a bubbling fluidized bed reactor and thermally solidified, via Fourier Transformed Infrared Spectroscopy.

The analysis of solidified fast pyrolysis and in-situ nitrogenolysis liquids via FTIR can give general information about bond types in functional groups present in the sample. As liquid fast pyrolysis and in-situ nitrogenolysis samples contain a considerable amount of water, solidified samples were analysed using FTIR avoiding that the water is contributing to the obtained spectra. Additionally a solid product is one of the aims of this research project to produce a slow release fertiliser.

The obtained spectra were transformed using Kubelka-Munk transformation. In order to allow a qualitative comparison between the solidified fast pyrolysis and in-situ nitrogenolysis liquids and illustrate the differences the corresponding pairs were plotted head to tail and normalized.

Information about characteristic IR spectra and frequencies of bond types in functional groups were obtained from literature [67, 68]. The most important frequencies and bond types in functional groups that are expected to be present in fast pyrolysis liquid and nitrogen containing functional groups are summarized in Table 52.

**Table 52: IR frequencies of specific bond types in functional groups [67, 68]**



Fast pyrolysis and in-situ nitrogenolysis liquids are a mixture of several hundred compounds (see section 2.4.2) and therefore the spectra of their solidified samples are expected to be a sum of the spectra of all these compounds. Consequently no specific compound can be clearly identified by this analysis. Nevertheless characteristic regions of bond types in functional groups can be identified and conclusions drawn based upon this.

#### 8.4.1 Method

The employed equipment was a PerkinElmer FT-IR Spectrometer Spectrum RXI. The solid samples were ground to a fine powder and mixed with KBr at a ratio of 5mg sample to 350mg KBr. Of this mixture a disc for analysis was formed under vacuum at a pressure of about 100MPa applied for 2 minutes (for method see section 3.14).

#### 8.4.2 Results

Although the obtained spectra of the solidified fast pyrolysis and in-situ nitrogenolysis liquids cannot be readily interpreted, the key elements of a possible interpretation have been summarized in Table 53. As it can be seen in Figure 46 and Figure 47 the four samples show similar spectra and consequently similar bonds and corresponding functional groups were identified.

All four samples show a broad peak between  $3550\text{-}3200\text{cm}^{-1}$  related to O-H stretching in alcohols and phenols and O-H stretching in carboxylic acids between  $3300\text{-}2500\text{cm}^{-1}$ . Also all spectra show peaks for C-H stretching between  $3000\text{-}2850\text{cm}^{-1}$  related to alkanes and alkyl groups. In the region between  $2260\text{-}2100\text{cm}^{-1}$  no peaks were detected in all samples, indicating that no nitriles, isocyanates, isothiocyanates, diimides or azides were present at a detectable level. Differences in the spectra occur in the region of  $1760\text{-}1665\text{cm}^{-1}$  that are related to C=O stretching in carbonyl groups. Beech wood solidified fast pyrolysis liquid is showing a clear peak at  $1710\text{cm}^{-1}$  and barley DDGS solidified pyrolysis liquid peaks at  $1708$  and  $1723\text{cm}^{-1}$  that are related to C=O stretching in carboxylic acids, ketones, aldehydes or esters. Furthermore barley DDGS solidified fast pyrolysis liquid shows a significant peak at  $1672\text{cm}^{-1}$  interpreted as the C=O stretching in amides.

In contrast in beech wood solidified in-situ nitrogenolysis liquid no peak is detected as in the solidified fast pyrolysis liquid, but a peak at  $1162\text{cm}^{-1}$  being interpreted as C=O stretching in

amides. In barley DDGS solidified in-situ nitrogenolysis liquid just one significant peak is left at  $1668\text{cm}^{-1}$  being interpreted as the C=O stretching in amides.

All samples show peaks in the region of  $1610\text{-}1450\text{cm}^{-1}$  being interpreted as C-C in ring stretching and indicating the presence of aromatic compounds. Between  $1470\text{-}1450\text{cm}^{-1}$  a peak for C-H bending is indicating the presence of alkanes or alkyl groups in all four samples. In the region between  $1390\text{-}1000\text{cm}^{-1}$  all spectra show peaks being interpreted as C-O stretching in phenols, carboxylic acids, esters or ethers.

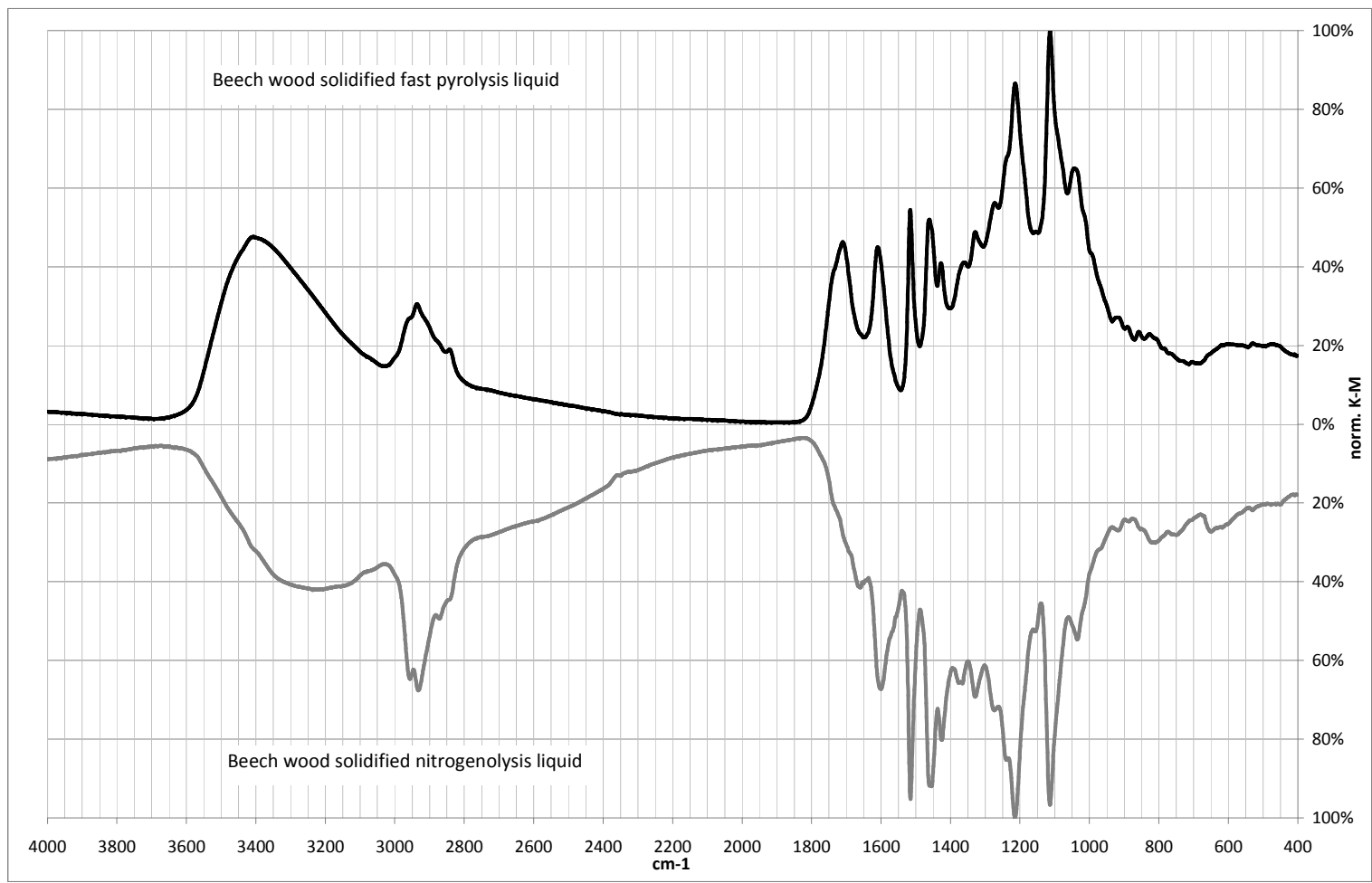


Figure 46: IR spectra of beech wood solidified fast pyrolysis and nitrogenolysis liquid

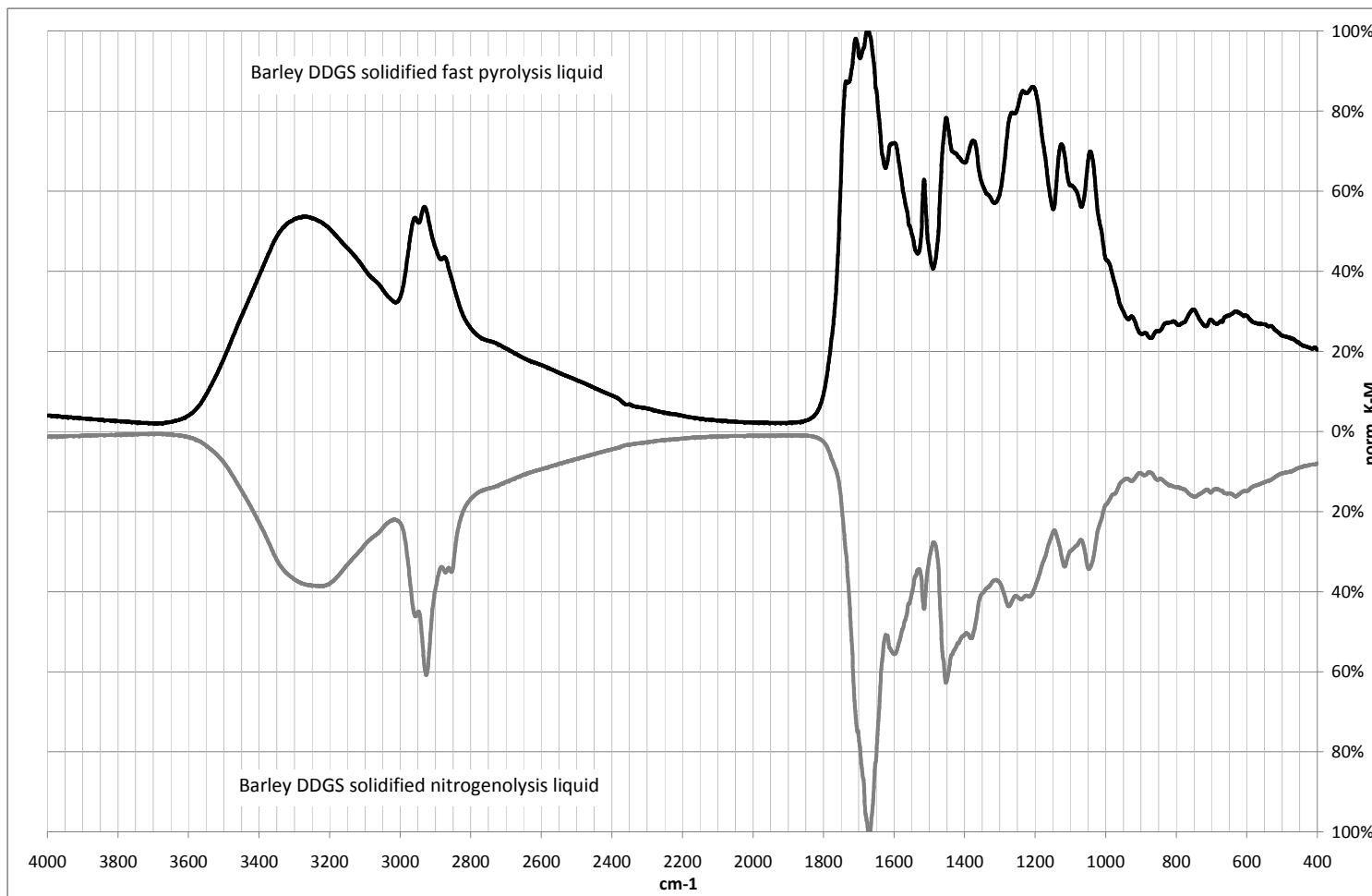


Figure 47: IR spectra of barley DDGS solidified fast pyrolysis and nitrogenolysis liquid

**Table 53: Interpretation of IR spectra**

| frequency region, cm <sup>-1</sup> | bond   | functional group                               | Beech wood solidified fast pyrolysis liquid | Beech wood solidified in-situ nitrogenolysis liquid | Barley DDGS solidified fast pyrolysis liquid | Barley DDGS solidified in-situ nitrogenolysis liquid |
|------------------------------------|--|--|---|---|--|--|
| 3550-3200                          | O-H stretch  | alcohols, phenols                              | broad peak                                  | broad peak  | broad peak                                   | broad peak   |
| 3400-3250                          | N-H stretch  | amines, amides                                 | no N in sample                              | overlaid by O-H stretch                             | overlaid by O-H stretch                      | overlaid by O-H stretch                              |
| 3300-2500                          | O-H stretch  | carboxylic acids                               | broad peak                                  | broad peak  | broad peak                                   | broad peak   |
| 3000-2850                          | C-H stretch  | alkanes, alkyl                                 | strong peak                                 | strong peak   | strong peak                                  | strong peak  |
| 2260-2240                          | C≡N stretch  | nitriles                                       | no peak, below detection level              | no peak, below detection level                      | no peak, below detection level               | no peak, below detection level                       |
| 2270-2100                          | -N=C=O, -N=C=S<br>-N=C=N-, -<br>N=N <sup>+</sup> =N <sup>-</sup> | isocyanates, isothiocyanates, diimides, azides | no peak, below detection level              | no peak, below detection level                      | no peak, below detection level               | no peak, below detection level                       |
| 1760-1665                          | C=O stretch  | carboxylic acid, ketone, aldehydes, esters     | peak at 1710                                |   | peak at 1708 & 1723                          |  |
| 1695-1650                          | R-(C=O)-NH <sub>3</sub>  | amides   |   | peak at 1662  | significant peak at 1672                     | significant peak at 1668                             |
| 1610-1585                          | C-C stretch (in ring)  | aromatics                                      | peak at 1610                                | peak at 1601  | peak at 1599                                 | peak at 1599   |
| 1525-1450                          | C-C stretch (in ring)  | aromatics                                      | peak at 1514                                | peak at 1515  | peak at 1515                                 | peak at 1515   |
| 1470-1450                          | C-H bend   | alkanes, alkyl                                 | peak at 1461                                | peak at 1456  | peak at 1452                                 | peak at 1453   |
| 1390-1330                          | C-O stretch  | phenols in pellets                             | peak at 1329                                | peak at 1329  | peak at 1376                                 | peak at 1381   |
| 1320-1000                          | C-O stretch  | carboxylic acids, esters, ethers               | peaks at 1214, 1113,1044                    | peaks at 1214, 1114,1035                            | peaks at 1300-1200, 1125,1044                | peaks at 1300-1200, 1116, 1048                       |

### 8.4.3 Analysis and discussion

As mentioned in section 2.4.2, fast pyrolysis liquids contain hundreds of compounds, among them alcohols, organic acids and phenolic compounds. The later ones result from the thermal decomposition of lignin and are expected to form a major part of the solidified products after thermal solidification. Other compounds such as alcohols and organic acids are suspected to have reacted forming esters and ethers or have evaporated during thermal solidification.

For these reasons it is likely to have significant peaks for C-C in ring stretching and C-O stretching as well as O-H stretching as all samples showed in their spectra. The absence of any peaks indicating nitriles, cyanates, diimides or azides can only be seen positively as these compounds are not regarded as beneficial for the use of the products as slow release fertiliser. The spectra do not indicate that these potentially harmful or toxic nitrogen compounds are present in detectable amounts in the samples.

The most interesting part of all spectra is the region between  $1760\text{-}1650\text{cm}^{-1}$ . For beech wood and barley DDGS products a clear change in the spectra can be seen. Peaks indicating carboxylic acids in the solidified fast pyrolysis liquids are no longer present in the solidified in-situ nitrogenolysis liquids spectra. Instead a peak indicating the presence of amides is appearing in the case of beech wood product and in the case of the barley DDGS spectrum the amide peak is even stronger. This can be interpreted as the consequence of the addition of ammonia during in-situ nitrogenolysis causing the carboxylic acid groups to react forming amides. This would be highly beneficial for the aim of the project as this reaction is binding nitrogen in the slow release fertiliser matrix and at the same time reduces the acidity of the product.

Although the investigated samples are not ideal for being analysed by FTIR, the spectra obtained allow the interpretation that no nitriles, cyanates, diimides or azides are present in detectable amounts and that carboxylic acid groups seem to react with ammonia forming amides during the process chain. Also the spectra show that the product appears to contain a significant amount of aromatics that might not be beneficial for a slow release fertiliser.

## **8.5 Summary**

The performed studies via Py-GC-MS, GC-MS for liquid samples and FTIR have shown the complexity and difficulty in analysing fast pyrolysis and in-situ nitrogenolysis products. Although none of the applied techniques was able to deliver non-ambiguous results, general information regarding possible reactions during nitrogenolysis and nitrogenolysis products composition could be deducted. Further analysis would be needed to identify the compounds formed during in-situ nitrogenolysis. Nuclear magnetic resonance spectroscopy could be a possible option for this (see section 11).

The comparative study via Py-GC-MS in inert and reactive gas atmosphere revealed that the identified products were almost the same for all experiments. This indicates that the ammonia present during reactive gas analytical pyrolysis did not alter the decomposition pathways or immediately reacted during pyrolysis. It was concluded that the reaction between ammonia and pyrolysis vapours occurs in a secondary reaction, which was inhibited by the very short residence time and the “freezing” of the evolving vapours on the Tenax-2® trap.

The comparative study via GC-MS for liquid samples of the fast pyrolysis and in-situ nitrogenolysis liquids showed that the predominant compounds identified in all products were the fast pyrolysis decomposition products. Unfortunately this analytical technique was not able to identify the nitrogen compounds formed during in-situ nitrogenolysis (with few exceptions). Whether this was due to too low concentrations or problems with the experimental setup or method could not be identified. Possible explanations are presented in the corresponding section.

The comparative study via FTIR of solidified fast pyrolysis and in-situ nitrogenolysis samples produced spectra that were a sum of the spectra of all compounds present in the products. Nevertheless it showed that there was no indication for nitriles, cyanates, diimides or azides to be present in detectable amounts, which was seen as unsuitable for a slow release fertiliser. The spectra also indicated that carboxylic acid groups appear to react with ammonia forming amides during nitrogenolysis. Another observation was that all spectra showed the highly aromatic nature of the products.

## **9 Microbial and plant testing**

### ***9.1 Introduction***

Beside the technical and chemical aspects in the development of a slow release fertiliser it is important to investigate the actual biological compatibility of the developed products. Consequently this section is dedicated to a study on the impact on microbial life in soils and to plant tests of pyrolysis and nitrogenolysis products.

In order to guarantee a high level of quality, all investigations were performed in close cooperation with Rothamsted Research, Harpenden (UK), being specialized in plant and soil sciences. The tasks were shared as described in section 1.2.6.

The investigated key questions were, (1) if fast pyrolysis liquid and solidified fast pyrolysis liquid can be used as a substrate for soil microbial biomass and if the nitrogen present in these products is slowly mineralized by microbial activity and (2) if the in-situ nitrogenolysis slow release fertiliser enhances plant growth over a period of time and if the plants show any visual sign of negative reaction to the application of the in-situ nitrogenolysis slow release fertiliser.

### ***9.2 Study on the impact of solidified fast pyrolysis products on microbial life in soil***

In order to determine the impact of fast pyrolysis liquid and solidified fast pyrolysis liquid a study on the effect of these substances on microbial life in soils was carried out. Research partner and performing this study was the institute for Sustainable Soils and Grassland Systems at Rothamsted Research, Harpenden UK.

In cooperation with Rothamsted Research the questions were investigated if fast pyrolysis liquid and solidified fast pyrolysis liquid can be used as a substrate for soil microbial biomass and if the nitrogen present in these products is slowly mineralized by microbial activity. The results were also interpreted in terms of toxicity of the provided fast pyrolysis products.

An initial discussion and screening of the provided fast pyrolysis liquid and solidified fast pyrolysis product revealed that the liquid product was not suitable for testing as the pH was too low and it was impossible to distinguish between the impact of the low pH and a possible toxicity on soil microbial biomass. Therefore the following study was carried out for solidified fast pyrolysis liquid derived from rape meal via fast pyrolysis in a bubbling fluidized bed reactor and thermal solidification.

### 9.2.1 Methods

The solidified pyrolysis liquid derived from rape meal contained 59% carbon and 9% nitrogen. The soil used for the experiments was an arable fine, silty clay loam, pH 5.8, from the Hoosfield strip at Rothamsted Research [92] collected and prepared according to Kemmitt et al. [93]. The soil samples were incubated at 25°C in a dark room with sufficient ventilation and controlled humidity level for up to 112 days. The solidified fast pyrolysis liquid was added as shown in Table 54 and samples without treatment and with ryegrass used as references. The addition is based on  $\mu\text{g}$  carbon added per gram of soil.

**Table 54: Samples for microbial biomass study**



The microbial activity and carbon content in microbial biomass were determined by  $\text{CO}_2$  evolution [93] and fumigation extraction technique [94] measuring the carbon content in a soil sample. The initial carbon content in the soil samples was determined as  $58 \pm 1 \mu\text{g C/g}$  soil [95]. The nitrogen was determined by measuring  $\text{NO}_3$  evolution and  $\text{NH}_4$  present on soil samples taken [95].

### 9.2.2 Results

The key findings of the study are illustrated in Figure 48 to Figure 55. The addition of solidified fast pyrolysis liquid lead to a rapid increase of microbial activity as it can be seen in Figure 48 in terms of  $\text{CO}_2$  evolution. Despite this general trend an initial phase of reduced  $\text{CO}_2$  evolution

was observed for the Bio-oil 5000 treatment [95]. Figure 49 shows that biomass carbon increased in the Bio-oil 5000 treatment up to 400% during the first 12 days of incubation while the Bio-oil 2000 treatment only measured a noticeable increase after 32 days and the Bio-oil 500 treatment just stayed slightly above the control sample.



**Figure 48: CO<sub>2</sub> evolution of microbial study samples [95]**



**Figure 49: Microbial biomass carbon in microbial study samples [95]**

The degree of mineralization of the carbon added with the solidified fast pyrolysis product was calculated from the accumulated CO<sub>2</sub> evolution taking a priming effect into account. Figure 50 presents the degree of carbon mineralization based on the fraction of carbon added. It can be seen that the mineralization appears to be quicker initially and slows down over the investigated period of 112 days. The concentration of the solidified fast pyrolysis liquid does not appear to affect the degree of mineralization and the treatments show a degree of mineralization of 13-14% after 112 days.



**Figure 50: Bio-oil carbon degree of mineralization in microbial study samples [95]**

The addition of solidified pyrolysis liquid shows some interesting results in terms of mineralization of nitrogen. As it is shown in Figure 51 and Figure 52 the Bio-oil 500 treatment mainly set free  $\text{NO}_3$  as it is expected [95]. In contrast the Bio-oil 5000 treatment mainly set free nitrogen as  $\text{NH}_4$  and the Bio-oil 2000 treatment setting free both types.



**Figure 51:  $\text{NO}_3$  evolution of microbial study samples [95]**



**Figure 52: NH<sub>4</sub> evolution of microbial study samples [95]**

The total amount of nitrogen mineralized is presented in Figure 53. The degree of mineralization was based on the amount of nitrogen mineralized and added. The values range between 12 and 20% after 32 days and increase slowly to 20.5 to 25% after 112 days for the treatments.



**Figure 53: Degree of N mineralization of microbial study samples [95]**

Figure 54 compares the CO<sub>2</sub> evolution of the Bio-oil 5000 treatment to the reference, ryegrass and combined treatment. It clearly shows higher CO<sub>2</sub> evolution, so higher microbial activity for the ryegrass treatment. In case of the combined treatment the microbial activity the CO<sub>2</sub> evolution was reduced for the first two days compared to just ryegrass [95]. Figure 55 depicts the biomass carbon after 84 days indicating a high increase of 380% for ryegrass, while biomass carbon is hardly increased in the Bio-oil 5000 treatment when compared to the reference treatment as well.



**Figure 54: CO<sub>2</sub> evolution in different treatments in microbial study samples [95]**



**Figure 55: Biomass carbon in different treatments of microbial study samples [95]**

### **9.2.3 Analysis and discussion**

The increases in CO<sub>2</sub> evolution clearly indicate that solidified fast pyrolysis liquid was used by the microbial soil organisms, although at a lower rate than ryegrass. The initial reduction of CO<sub>2</sub> evolution in the Bio-oil 5000 samples indicates a period of adjustment for the microbial life forms. This can be interpreted that some species are not able to tolerate solidified fast pyrolysis liquid at such a high application rate.

Interesting findings are regarding the mineralization products of the samples with high solidified fast pyrolysis liquid concentrations. Especially the high  $\text{NH}_4$  values for the Bio-oil 5000 treatment indicate that the mineralization route has changed. It could mean that the microbial community structure has changed in that way, that more stress sensitive nitrifying bacteria are reduced [95].

The presented data indicates that microbial life in soil can thrive on solidified fast pyrolysis liquid, although some microbial species seem to have a reduced activity at very high concentrations. The nitrogen in the fast pyrolysis product is mineralized up to 25% after 112 days. To evaluate the suitability of the fast pyrolysis product as a slow release fertiliser, it would need to be investigated, how much nitrogen will be mineralized after 112 days and how much is unavailable.

### ***9.3 Study on the effect of in-situ nitrogenolysis derived SRF on plant growth***

This section is dedicated to a study on the effect of in-situ nitrogenolysis derived slow release fertiliser on plant growth. The focus of this study is, if the in-situ nitrogenolysis slow release fertiliser enhances plant growth over a period of time and, if the plants show any visual sign of negative reaction to the application of in-situ nitrogenolysis slow release fertiliser.

This study was performed in cooperation with and at the Centre for Bio-energy and Climate Change, PIE Department Rothamsted Research, Harpenden (UK). The tasks were shared as described in section 1.2.6. In order to investigate the performance and suitability of in-situ nitrogenolysis slow release fertiliser the experimental setup and methods were developed and are described in the following.

#### **9.3.1 Experimental setup and methods**

The focus of this study was the availability of nitrogen for plant growth that is supplied by fertiliser, in case of a slow release fertiliser in a controlled way over a longer period of time. Therefore the impact of other nutrients (as described in section 2.5.2) was excluded from this study by providing them in sufficient amounts to the experiment.

A key factor in mobilizing/mineralizing nitrogen from the in-situ nitrogenolysis SRF is an active microbial community in the soil. How the microbial life in soil contributes to nitrogen mineralization is described in sections 2.5.3 and 2.5.4 and that it can thrive on fast pyrolysis products has been shown in the study presented in section 9.2. For this reason sandy loam soil from the Woburn site of Rothamsted Research was chosen for the study that is known to show good microbial activity.

The plant chosen for the study was ryegrass. Ryegrass is relatively fast growing, has a quite constant demand for nitrogen and can be cut in frequent intervals. These factors were seen as important for a long term study to collect information on the slow release fertilizing effect and plant yields.

For the planting pots with a 20 cm diameter were chosen. These were placed in a fenced area under a canopy with saucer pans. This setup was chosen in order to eliminate the factor rain and nutrient leaching, while still simulating outside weather conditions and soil temperatures that have an impact on microbial activity and plant growth. The experimental setup included in-situ nitrogenolysis SRFs, conventional fertilisers, fast pyrolysis char and an untreated sample as reference. The different treatments and are listed in Table 55.

**Table 55: Plant test treatments**

| Sample name | Treatment type                 | Nitrogen content [wt.%] | Application rate |         |
|-------------|--------------------------------|-------------------------|------------------|---------|
|             |                                |                         | [kgN/ha]         | [g/pot] |
| untreated   | no addition                    | 0.00%                   | 0                | 0.00    |
| Beech SRF   | nitrogenolysis beech wood SRF  | 7.09%                   | 350              | 15.51   |
| DDGS SRF    | nitrogenolysis barley DDGS SRF | 9.45%                   | 350              | 11.64   |
| Osmocote®   | conventional SRF Osmocote®     | 19.00%                  | 350              | 5.79    |
| Am. nitrate | ammonium nitrate fertiliser    | two additions           | Σ 350            | -       |
| FP char     | fast pyrolysis char            | -                       | -                | 20.00   |

In-situ nitrogenolysis derived SRFs from beech wood and from barley DDGS were chosen to investigate if there is any difference between a product with all nitrogen added during the process and a product with nitrogen that partially had been in the original feedstock. Osmocote® was chosen to compare the performance of the in-situ nitrogenolysis SRFs with a conventional SRF. Ammonium nitrate was used to compare the effect of SRFs and conventional multiple fertilizing with a mineral fertiliser. The char sample was used to investigate the often discussed effect of the addition of char. The blank sample should indicate the performance of the untreated soil used in the study.

Each treatment was set up 5 times in order to get average data and identify inconsistencies. The application rate was determined to be 350 kg of nitrogen per hectare, so 3.5mgN/cm<sup>2</sup> (see Table 55). The 30 pots were randomized to eliminate the factor of position in the test plot. The rye grass was seeded and cut after 47 days, 89 days and 131 days. Of each cut the dry harvested matter was determined.

### 9.3.2 Results

The rye grass seeds germinated for all treatments without any visible sign of inhibited or delayed germination. Before the first harvest the rye grass showed sufficient growth for all treatments, although differences in terms of yields and shade of green of the foliage were visible (see Figure 56 to Figure 58).



Figure 56: Randomized plant tests before the 1<sup>st</sup> harvest



Figure 57: Untreated soil sample, light green foliage



Figure 58: SRF sample, darker green foliage

The above ground dry matter plant yields of the three harvests are shown in Figure 59. In general the yield data of all 5 repetitions of each treatment were consistent and Figure 59 displays the average as a bar and fluctuation range as a line. The untreated and fast pyrolysis char samples showed relative constant low yields. The fertiliser samples showed higher yields with the general tendency to lower yields in the 3<sup>rd</sup> harvest and Osmocote® achieving the overall highest yields.

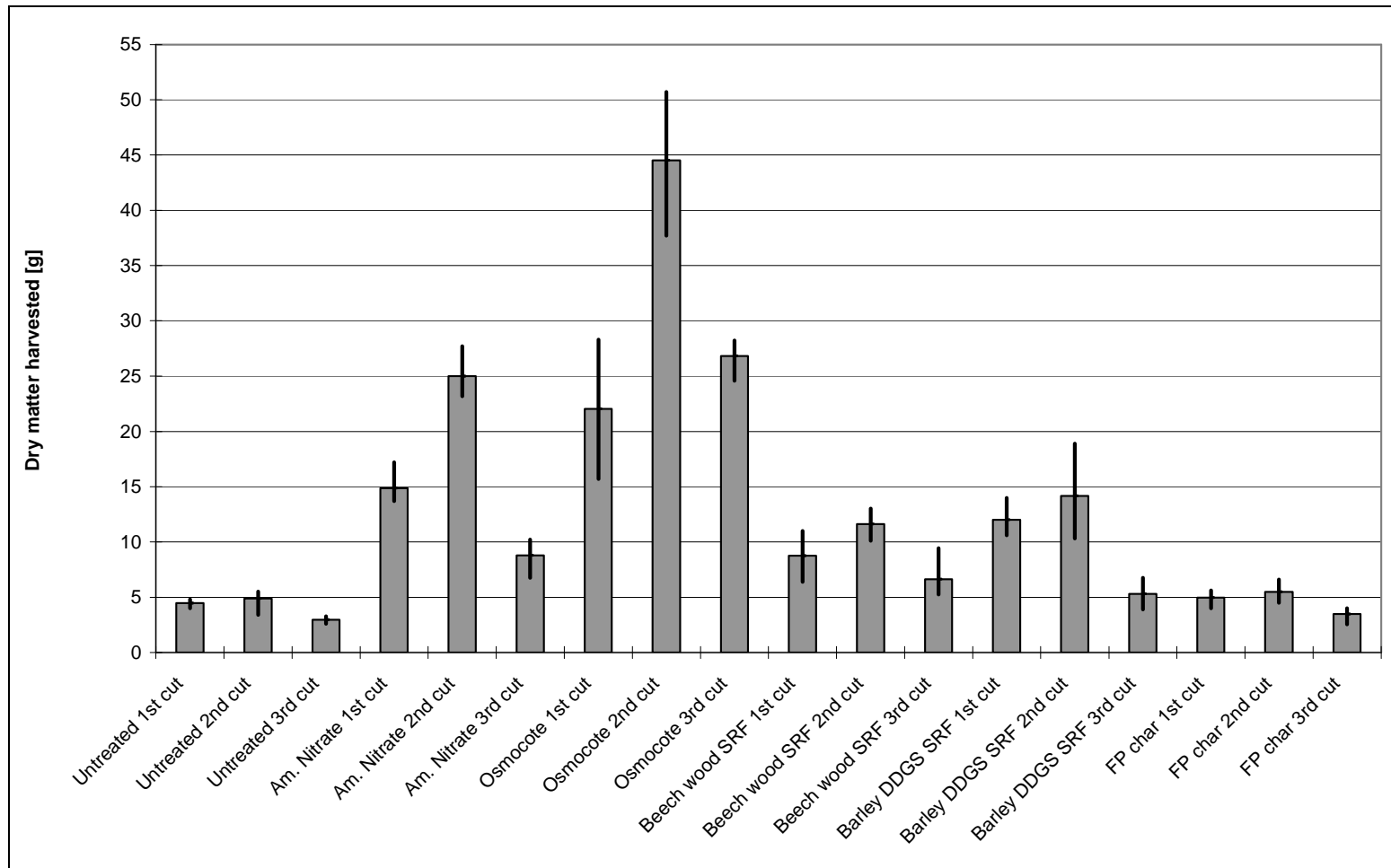


Figure 59: Dry matter harvest yields of plant experiments

The dried plant materials of the 1<sup>st</sup> harvest was also analysed for their elemental composition. For each treatment equal amounts of dry harvested material from each sample were mixed and prepared as analytical sample according to the method described in section 3.1. The elemental composition was determined in duplicate according to the method described in section 3.5. Table 56 is showing the averages of the elemental analysis for each treatment. It can be seen that the untreated sample and fast pyrolysis char sample have significant lower nitrogen in the dry matter than the samples treated with fertiliser.

**Table 56: Elemental analysis of dry matter samples of 1<sup>st</sup> harvest**

| Element | Unit                 | Untreated sample | Beech Wood SRF | Barley DDGS SRF | Osmocote® SRF | Ammonium nitrate | Fast Pyrolysis. char |
|---------|----------------------|------------------|----------------|-----------------|---------------|------------------|----------------------|
| C       | wt.%                 | 41.27%           | 41.35%         | 42.01%          | 41.99%        | 42.90%           | 41.43%               |
| H       | wt.%                 | 5.70%            | 5.72%          | 5.93%           | 5.79%         | 5.87%            | 5.92%                |
| N       | wt.%                 | 1.28%            | 3.12%          | 2.53%           | 4.59%         | 3.99%            | 1.48%                |
| O*      | wt.%                 | 51.75%           | 49.81%         | 49.53%          | 47.63%        | 47.24%           | 51.17%               |
| O*      | Oxygen by difference |                  |                |                 |               |                  |                      |

### 9.3.3 Analysis and Discussion

The observations made indicate that the SRFs produced by in-situ nitrogenolysis do not have a negative impact on germination of the ryegrass seeds used in the experimental setup. Furthermore the darker green foliage of the SRF samples, when compared to the untreated soil samples, indicate a higher amount of chlorophyll in the ryegrass leaves, which indicates a higher uptake of nitrogen into the plant. This observation is supported by the results of the elemental analysis of the dry plant matter. The nitrogen content of the untreated soil sample and fast pyrolysis char samples are significantly lower than the samples with fertiliser, indication a lack in nitrogen supply.

Regarding the harvested dry matter it can be stated that all samples with fertiliser achieved higher yields than untreated samples. Additionally for all samples with fertiliser addition there is the general trend that the highest yields were achieved for the 2<sup>nd</sup> harvest and that there is a noticeable reduction in productivity for the 3<sup>rd</sup> harvest. For the ammonium nitrate treatment this was expected as the fertiliser was given in two steps. For the slow release fertilisers a certain peak at the beginning of the testing period was also expected. In case of the SRFs produced by in-situ nitrogenolysis this is likely due to readily available components formed in the production process. In case of Osmocote® it is expected that the coating of a part of the coated fertiliser granules is deficient leading to an almost imminent fertiliser release. For the

SRFs produced by in-situ nitrogenolysis the reduction in productivity for the 3<sup>rd</sup> harvest appears to be more significant than for Osmocote®, as the yields achieved are almost as low as the yields of the treatment without fertiliser. A possible reason for this phenomenon can be the nitrogen components formed during the in-situ nitrogenolysis process. The observed yields indicate that part of the nitrogen is bound in components that cannot be mineralized by the microbial activity in the soil within the experimental time frame. Hanser observed a similar behaviour for the fertiliser he produced in his post processing experiments [27]. He also concluded that his product includes nitrogen compounds that are not mineralized in a short or mid term time range. Radlein et al. stopped their plant tests after 80 days, so before the observed reduction in productivity [34]. As Hanser's preparation method for the SRF is comparable to Radlein et al., a similar behaviour is likely. If the nitrogen in these components will be broken down over a longer period of time, by this providing a long term slow release effect, or if the nitrogen is locked in these components and is not mineralized could not be clarified with this study.

The included fast pyrolysis char treatment in this study showed that the impact of fast pyrolysis char without additional fertiliser is marginal in combination with the sandy loam soil from the Woburn site. These results should not be compared to other studies with char performed in the Amazonian area, as the circumstances are significantly different. The soil used in this study is a rich soil, more capable of holding nutrients than a Ferrasols soil, and the factor of nutrient leaching was excluded by placing the experimental setup under a canopy. In this specific experimental setup the used fast pyrolysis char just showed, that it does not have any negative effect on germination of the rye grass seeds, but also no direct effect on the achieved product yields. The added carbon to the soil did not show a negative effect on plant growths.

## **9.4 Summary**

The findings of the microbial study and plant study indicate that the solidified products derived from fast pyrolysis/in-situ nitrogenolysis liquids do not show any negative impact on the microbial life in soils, germination of seeds or plant growths. The results show that microbial life in soil can thrive on solidified fast pyrolysis liquid, although some microbial species seem to have a reduced activity at very high concentrations. Both studies indicate that there is a reduction in nitrogen mineralization and consequently nitrogen availability for plant growth after a period of around 90-100days. This is likely due to nitrogen bound in compounds that

cannot be mineralized in short or medium term by soil microbes. If this nitrogen will be mineralized in the long run providing a long term slow release effect, or is locked up in the slow release fertiliser matrix could not be identified and would need to be investigated.

## 10 Conclusions

The overall aim of this research project was to investigate fast pyrolysis and nitrogenolysis of biomass and biogenic residues as an alternative route to produce a sustainable slow release fertiliser. This overall aim was subdivided into 6 subtasks that have been investigated and presented in this report.

A variety of biomass and biogenic residues were investigated and characterized for their potential use as feedstocks in the fast pyrolysis and nitrogenolysis processes. It was concluded that the high nitrogen feedstocks DDGSs and rape meal have the greatest potential in the nitrogenolysis process as they contain a relatively high amount of nitrogen (around 5.7wt.%, daf) and a relatively high amount of volatiles (around 80.9wt.%, dry). It was also shown that beech wood is suitable as a reference material as its nitrogen content was below detection level and volatiles were around 86.3wt.% (dry). The Pyrolysis-Gas Chromatography-Mass Spectroscopy results of the high nitrogen feedstocks showed that the main decomposition products from these feedstocks identified were the ones from cellulose, hemicellulose and lignin and some decomposition products of proteins.

The fast pyrolysis processing experiments showed that the 1kg/h bubbling fluidized bed reactor was suitable for the experiments in terms of processing capacity and in terms of reliability after the implementation of some modifications. Regarding the process parameters, suitable fluidizing gas velocities, bed material particle sizes, feeding rates and pyrolysis/reactor temperatures (around 500°C were established. Data regarding fast pyrolysis product yields and basic characteristics of fast pyrolysis products for several feedstocks were obtained. The DDGSs, ADM rape meal and beech wood were confirmed as suitable fast pyrolysis feedstocks for later processing via in-situ nitrogenolysis. Green Dragon rape meal was excluded from the feedstock list as no stable operation conditions could be reached while processing. This phenomenon was linked to the relatively high residual oil content of Green Dragon rape meal. Pine bark, AD-residue and wheat straw were ruled out as possible feedstocks for the in-situ nitrogenolysis experiments, although fast pyrolysis processing was possible. This was due to the low liquid yields of these feedstocks (around 35wt.%, dfb) and high char and gas yields. As the slow release fertiliser produced by nitrogenolysis is based on the liquid product, a high liquid yield was seen as necessary for an efficient production.

The focus of the nitrogenolysis experiments was on the in-situ nitrogenolysis processing experiments. This means that high nitrogen feedstocks and beech wood as a reference material were subjected to fast pyrolysis with the addition of ammonia gas to the reactor. Ammonia gas was chosen due to the fact that it could be dosed and fed more easily and steadily into the reactor than an ammonia salt and that no decomposition step had to take place to produce reactive ammonia gas. Experiments for the optimal nitrogen addition rate were performed with beech wood and an addition of 15 wt.%C of elemental nitrogen on a feedstock carbon base was determined as the most suitable nitrogen addition rate. In-situ nitrogenolysis production runs of more than 2 hours were performed and mass balances established. The products were characterized and showing that the main addition of nitrogen is to the liquid in-situ nitrogenolysis product. Taking into consideration the nitrogen concentration in the in-situ nitrogenolysis product and the product yields of solids and liquids almost all nitrogen was present in the liquid products.

Beside the processing experiments by fast pyrolysis and in-situ nitrogenolysis analytical studies were performed. A comparative study via Pyrolysis-Gas chromatography-Mass Spectroscopy with inert and reactive gas revealed that the presence of ammonia gas during pyrolysis did not appear to have any direct impact on the decomposition products of beech wood under the chosen experimental conditions. The chromatograms obtained and the suggested peak assignments showed almost no differences between inert and ammonia experiments. This was explained by the experimental setup "freeing" the decomposition products almost instantly by adsorbing them in a trap and thereby preventing secondary reactions between the pyrolysis vapours and the added ammonia.

The comparative study via Fourier Transformed Infrared Spectroscopy of solidified fast pyrolysis and in-situ nitrogenolysis products showed that there was some alteration in the spectra obtained. Significant was the shift in frequencies indicating C=O stretches typically related to the presence of carboxylic acids to C=O stretches related to amides. Furthermore the study showed that the products were highly aromatic and did not contain nitriles, cyanates, diimides or azides in detectable amounts. These nitrogen compounds would have been problematic in a slow release fertiliser product.

A batch reactor process was developed to thermally solidify the liquid fast pyrolysis and in-situ nitrogenolysis products. The experiments showed that a brittle solid product could be

obtained via thermal solidification at 150°C and 1h processing time. It was also established that an addition of 2.5wt.% fast pyrolysis char enhanced the solidification process.

The same batch reactor setup was also used for the post-processing nitrogenolysis experiments. In these experiments fast pyrolysis liquids were modified and solidified in a combined process by adding urea or ammonium phosphate in combination with fast pyrolysis char to produce a nitrogen enriched solid product. The solids produced were subjected to a cold and hot water washing procedure to determine the amount of cold and hot water soluble compounds in the product. This was seen as an indicator for the availability of nitrogen compounds with cold water soluble ones for short term availability and hot water soluble ones for short to mid term availability. The experiments revealed that after the washing procedure just 30wt.% of the added nitrogen remained in the washing residue for urea and 45% of added nitrogen for ammonium phosphate. It was concluded that the combined modification and solidification with this experimental regime was not suitable to produce a slow release fertiliser.

The impact of solidified fast pyrolysis liquids and nitrogenolysis liquids on microbial life in soils and plant growth was tested in cooperation with Rothamsted Research, Harpenden UK. The microbial tests indicated that microbes can thrive on solidified fast pyrolysis and nitrogenolysis liquids, although some microbial species seem to have a reduced activity at very high concentrations. The nitrogen in the products is mineralized up to 25% after 112 days. If the remaining nitrogen would be mineralized or if it is locked up permanently, could not be clarified with these experiments.

The test on the impact on plant growth with rye grass showed that the application of slow release fertiliser produced via in-situ nitrogenolysis had no negative impact on germination or plant growth. The fertilizing effect was proven by the obtained dry matter yields in three harvests, which were all higher than the untreated reference sample, but lower than the conventionally produced slow release fertiliser yields. A drop in the productivity for all samples with added fertiliser was observed at the third harvest. The dry matter yield for samples with nitrogenolysis slow release fertiliser almost dropped to the level of untreated samples. The cause for this could not be investigated due to time constraints, but it is expected that this is linked to the mineralization rate of the nitrogen compounds in the nitrogenolysis SRF. If the nitrogen is mineralized at a very slow rate or locked up would need to be investigated.

The relatively wide scope of this research project and restrictions in terms of equipment, high time demand to run the 1kg/h fluidized bed reactor and man power set limitations to some aspects in this research. Also the cooperation with a very helpful external partner did not improve the situation regarding time consumption. Consequently the lack of time led to the fact that some investigations could not be made and therefore are part of the recommendations.

The overall aim of this research project was reached. It was possible to demonstrate an alternative route for the production of a slow release fertiliser via nitrogenolysis from biomass and biogenic residues. It was also shown that the products obtained had the actual capability of acting as a slow release fertiliser in plant tests. Unfortunately it could not be clarified in which form the nitrogen is present in the slow release fertiliser produced. The use of ammonia, which has a large carbon footprint, was due to practicality reasons and should be replaced by another more eco friendly nitrogen compound, if that is possible. Nevertheless it was also shown that the feedstock nitrogen can be incorporated in the in-situ nitrogenolysis slow release fertiliser product, so that less nitrogen would need to be added during the process.

## 11 Recommendations

This section is dedicated to recommendations regarding the research project pyrolysis and nitrogenolysis of biomass and biogenic residues. In the first part specific recommendations resulting from the research are given and in the second part more general recommendations are suggested. Most of the recommendations are closely linked to the research carried out and result from time constraints.

The impact of reactor temperature for the in-situ nitrogenolysis process should be investigated to investigate if the amount of nitrogen bound in the products is linked to the processing temperature (see section 5.2.3).

In combination with this aspect the biodegradability of the nitrogen compounds formed at different temperatures would need to be investigated. It would be beneficial to investigate if the nitrogen in the fast pyrolysis char is chemically bound, adsorbed or absorbed (see section 6.5.2) to evaluate if nitrogen could be driven off in the form of ammonia and recycled in the nitrogenolysis process.

The same aspect should be investigated for the aqueous top phase of some liquid in-situ nitrogenolysis products, in order to evaluate if ammonia could be stripped from this liquid and recycled in the process (see sections 6.5.2 and 6.6.2).

The question of a more suitable quenching medium would need to be raised as phase separation between ISOPAR™ and barley DDGS in-situ nitrogenolysis liquid did not readily occur (see section 6.7.2).

An important question is which nitrogen compounds are actually formed during the in-situ nitrogenolysis process. The analytical techniques available were not able to answer this question in a satisfactory way (see section 8.5). Therefore further investigations are necessary. One option could be the CDS 5200 Pyroprobe® with the additional high pressure reactor. This setup would allow simulation of the nitrogenolysis process on an analytical scale more accurately, because it would allow the reaction time to be regulated between pyrolysis vapours and ammonia. The setup used did not allow this (see section 8.2.3). Another option would be the use of Nuclear Magnetic Resonance Spectroscopy for liquid and solid samples.

Whether this technique would be able to deliver unambiguous results would need to be tested. Also the question of calibrating for possible N compounds would need to be solved. Hanser employed this technique in an attempt to analyse his post-processing nitrogenolysis products and was able to identify some nitrogen compounds formed [27].

For the microbial life in soil tests it should be investigated, which type of microbes show reduced activity, when solidified in-situ nitrogenolysis products are applied at high concentrations (see section 9.2.3). That might also answer the question why samples treated with pyrolysis products released more  $\text{NH}_4^+$  and not  $\text{NO}_3$ . Furthermore it would be recommended that the microbial and plant tests are done for a longer period of time than in this project to investigate if the nitrogen in the in-situ nitrogenolysis slow release fertiliser, which is left after the investigated 112days, is mineralized at a very slow rate or locked up in the product (see section 0).

The in-situ nitrogenolysis process should be modelled and energy balances obtained to be able to make a life cycle analysis. This would be helpful in evaluating the actual benefit of the slow release fertiliser produced in this way, when compared to a conventionally produced slow release fertiliser.

A techno-economic feasibility study should be performed based on the findings of this research project and the suggested modelling work to establish the costs for the in-situ nitrogenolysis slow release fertiliser.

Finally the outcome of this research project in combination with the recommended additional investigations should give the necessary information to give a full evaluation of the in-situ nitrogenolysis process and its potential for commercialisation.

## 12 References

1. von Carlowitz, H.C. (1713). *Sylvicultura oeconomica : Anweisung zur wilden Baumzucht*. Leipzig: Braun (Reprint Freiberg: TUBA & Akad. Buchh.,2000): 284 pages
2. Apodaca, L.E. (2011). *Nitrogen (Fixed) / Ammonia*, in *Mineral Commodity Summaries 2011*, Survey, U.S.G. (Ed.), Reston (Virginia-USA): U.S. Geological Survey: p. 112-113
3. Bridgwater, A.V. and Jones, J. (2007). *SUPERGEN Bioenergy Continuation*, in *British Bio Energy News - SUPERGEN Issue 6*, Fenton, R. (Ed.), Birmingham (UK): Bioenergy Research Group, Aston University: p. 2-3
4. Bridgwater, A.V. (2009). *Sustainability Research at Aston University Bioenergy Research Group*, in *European Bioenergy News - Bioenergy NOE Volume 5*, Watkinson, I. (Ed.), Birmingham (UK): Bioenergy Research Group, Aston University: p. 8
5. Bridgwater, A.V. and Harms, A.B. (2009). *Sustainable fertilisers*, in *IEA Bioenergy Task 34 - PyNe Newsletter Issue 26*, Burrowes, S. (Ed.), Birmingham (UK): Bioenergy Research Group, Aston University: p. 6-7
6. Carpita, N. and McCann, M. (2000). *The cell wall*, in *Biochemistry and Molecular Biology of Plants*, Buchanan, B., Gruissem, W., Jones, R. (Ed.), Rockville, Maryland: American Society of Plant Physiologists: p. 52-108
7. Dung, N.N.X., Manh, L.H., Uden, P. (2002). *Tropical fibre sources for pigs— Digestibility, digesta retention and estimation of fibre digestibility in vitro*. *Animal Feed Science and Technology*, **102** (1-4): p. 109-124.
8. Ucar, S. and Ozkan, A.R. (2008). *Characterization of products from the pyrolysis of rapeseed oil cake*. *Bioresource Technology*, **99** (18): p. 8771-8776.
9. Wang, Y., Wu, L., Wang, C., Yu, J., Yang, Z. (2011). *Investigating the influence of extractives on the oil yield and alkane production obtained from three kinds of biomass via deoxy-liquefaction*. *Bioresource Technology*, **102** (14): p. 7190-7195.
10. Alén, R., Kuoppala, E., Oesch, P. (1996). *Formation of the main degradation compound groups from wood and its components during pyrolysis*. *Journal of Analytical and Applied Pyrolysis*, **36** (2): p. 137-148.
11. Gerdes, C. (2001). *Pyrolyse von Biomasseabfall: Thermochemische Konversion mit dem Hamburger Wirbelschichtverfahren*. Dr. Thesis, Hamburg: Universität Hamburg.
12. Hellwig, M. (1988). *Zum Abbrand von Holzbrennstoffen unter besonderer Berücksichtigung der zeitlichen Abläufe*. Dr. Thesis, München: Technische Universität München.

13. Meier, D. (2001). *Thermochemische Umwandlung - Pyrolyse*, in *Energie aus Biomasse - Grundlagen, Techniken und Verfahren*, Kaltschmitt, M. and Hartmann, H. (Ed.), Berlin, Heidelberg, New York: Springer Verlag: p. 477-494
14. Müller Hagedorn, M. (2004). *Charakterisierung der Pyrolyse von Biomasse am Beispiel von Nadel- und Laubbaumholz*. Dr. Thesis, Karlsruhe: Universität Karlsruhe.
15. Nowakowski, D.J. and Jones, J.M. (2008). *Uncatalysed and potassium-catalysed pyrolysis of the cell-wall constituents of biomass and their model compounds*. *Journal of Analytical and Applied Pyrolysis*, **83** (1): p. 12-25.
16. Bridgwater, A.V. (2007). *The production of biofuels and renewable chemicals by fast pyrolysis of biomass*. *International Journal of Global Energy Issues* **27** (2): p. 60-203.
17. Raab, K., Eltrop, L., Deimling, S., Kaltschmitt, M. (2006). *Möglichkeiten der energetischen Umwandlung*, in *Leitfaden Bioenergie*, FNR (Ed.), Gülzow: Fachagentur Nachwachsende Rohstoffe e.V.: p. 17-23
18. Albright, L.F., Crynes, B.L., Corcoran, W.H. (1983). *Pyrolysis, theory and industrial practice*. New York: Academic Press: 482 pages
19. Bridgwater, A.V. (2007). *IEA Bioenergy 27th update - Biomass pyrolysis*. *Biomass & Bioenergy*, **31** (4): p. VII-XVIII.
20. Piskorz, J., Radlein, D., Majerski, P., Scott, D.S. (1996). *The Waterloo Fast Pyrolysis Process*, in *Bio-oil Production & Utilization: Proceedings of the 2nd EU-Canada Workshop on Thermal Biomass Processing*, Bridgwater, A.V. and Hogan, E. (Ed.), CPL Press: p. 335-342
21. Nowakowski, D.J., Jones, J.M., Brydson, R.M.D., Ross, A.B. (2007). *Potassium catalysis in the pyrolysis behaviour of short rotation willow coppice*. *Fuel*, **86** (15): p. 2389-2402.
22. Bridgwater, A.V. and Peacocke, G.V.C. (2000). *Fast pyrolysis processes for biomass*. *Renewable & Sustainable Energy Reviews*, **4** (1): p. 1-73.
23. Kaltschmitt, M. and Hartmann, H. (2001). *Energie aus Biomasse - Grundlagen, Techniken und Verfahren*. Berlin, Heidelberg, New York: Springer Verlag: 770 pages
24. Kaltschmitt, M. and Baumbach, G. (2001). *Grundlagen Festbrennstoffnutzung - Grundlagen der thermochemischen Umwandlung*, in *Energie aus Biomasse - Grundlagen, Techniken und Verfahren*, Kaltschmitt, M. and Hartmann, H. (Ed.), Berlin, Heidelberg, New York: Springer Verlag: p. 272-280
25. Dynamotive Energy Systems (2012). *Dynamotive Energy Systems - Fast pyrolysis*, Available from: <http://www.dynamotive.com/technology/fast-pyrolysis/> [Accessed 20.01.2012]

26. Bridgwater, A.V. (2012). *Review of fast pyrolysis of biomass and product upgrading*, *Biomass and Bioenergy*. Biomass & Bioenergy, **38** p. 68-94.
27. Hanser, C. (2002). *Strukturelle Untersuchungen Reaktionen und Anwendung von Flash-Pyrolyseölen aus Biomasse*. Dr. Thesis, Hamburg: Universität Hamburg.
28. Czernik, S. and Bridgwater, A.V. (2004). *Overview of applications of biomass fast pyrolysis oil*. *Energy & Fuels*, **18** (2): p. 590-598.
29. Oasmaa, A. and Czernik, S. (1999). *Fuel Oil Quality of Biomass Pyrolysis Oils State of the Art for the End Users*. *Energy & Fuels*, **13** (4): p. 914-921.
30. Oasmaa, A. and Peacocke, C. (2001). *A guide to physical property characterization of biomass-derived fast pyrolysis liquids*. Espoo: VTT Publications 731: 79 p. + app. 46 p. pages
31. Bridgwater, A.V., Czernik, S., Piskorz, J. (2001). *An overview of Fast Pyrolysis*, in *Progress in thermochemical biomass conversion - Volume 2*, Bridgwater, A.V. (Ed.), Blackwell Science: p. 977-997
32. Bridgwater, A.V. (2011). *Upgrading Fast Pyrolysis Liquids*, in *Thermochemical Processing of Biomass: Conversion Into Fuels, Chemicals and Power*, Brown, R.C. (Ed.), Chichester (UK): John Wiley & Sons: p. 155-199
33. Garcia-Perez, M., Chaala, A., Pakdel, H., Kretschmer, D., Roy, C. (2007). *Characterization of bio-oils in chemical families*. *Biomass & Bioenergy*, **31** (4): p. 222-242.
34. Radlein, D.S.A.G., Piskorz, J.K., Majerski, P.A. (2000). *Method of producing slow-release nitrogenous organic fertilizer from biomass*, European Patent: EP 0716056
35. Diebold, J.P. and Czernik, S. (1997). *Additives To Lower and Stabilize the Viscosity of Pyrolysis Oils during Storage*. *Energy & Fuels*, **11** (5): p. 1081-1091.
36. Radlein, D.S.T.A.G., Piskorz, J., Scott, D.S. (1987). *Lignin derived oils from the fast pyrolysis of poplar wood*. *Journal of Analytical and Applied Pyrolysis*, **12** (1): p. 51-59.
37. Briens, C., Piskorz, J., Berruti, F. (2008). *Biomass valorization for fuel and chemicals production - A review*. *International Journal of Chemical Reactor Engineering*, **6** (Review R2): p. 1-49.
38. Panagiotis, N. (1998). *Binders for the wood industry made with pyrolysis oil*, in *Newsletter of the PyNe-Network*, Humphreys, C. (Ed.), Birmingham (UK): Bioenergy Research Group - Aston University: p. 6-7
39. Gaunt, J.L. and Lehmann, J. (2008). *Energy balance and emissions associated with biochar sequestration and pyrolysis bioenergy production*. *Environmental Science & Technology*, **42** (11): p. 4152-4158.

40. Glaser, B. (2007). *Prehistorically modified soils of central Amazonia: a model for sustainable agriculture in the twenty-first century*. Philosophical Transactions of the Royal Society B: Biological Sciences, **362** (1478): p. 187-196.
41. Steiner, C., Teixeira, W.G., Lehmann, J., Nehls, T., de Macedo, J.L.V., Blum, W.E.H., Zech, W. (2007). *Long term effects of manure, charcoal and mineral fertilization on crop production and fertility on a highly weathered Central Amazonian upland soil*. Plant and Soil, **291** (1-2): p. 275-290.
42. Steinbeiss, S., Gleixner, G., Antonietti, M. (2009). *Effect of biochar amendment on soil carbon balance and soil microbial activity*. Soil Biology and Biochemistry, **41** (6): p. 1301-1310.
43. Cheng, C.H., Lehmann, J., Engelhard, M.H. (2008). *Natural oxidation of black carbon in soils: Changes in molecular form and surface charge along a climosequence*. Geochimica Et Cosmochimica Acta, **72** (6): p. 1598-1610.
44. Energy Research Centre of the Netherlands (2011). *Phyllis - Database for biomass and waste (Char)*, Available from: <http://www.ecn.nl/phyllis> [Accessed 28.12.2011]
45. Hustad, J. and Barrio, M. (2000). *IFRF Online Combustion Handbook - What is biomass?*, Available from: <http://www.handbook.ifrf.net/handbook/cf.html?id=23> [Accessed 28.12.2011]
46. Troeh F.R. and Thompson L.M. (2005). *Soils and Soil Fertility*. 6, Oxford: Blackwell Publishing: 489 pages
47. Fageria, N.K. (2009). *The use of nutrients in crop plants*. Boca Raton: CRC Press - Taylor & Francis Group: 430 pages
48. Sears, K.D. and Herrick, F.W. (1977). *Soil conditioners and fertilizers from spent sulfite liquor*, USA: US4002457
49. Coca, J., Alvarez, R., Fuertes, A.B. (1984). *Production of a Nitrogenous Humic Fertilizer by the Oxidation Ammoniation of Lignite*. Industrial & Engineering Chemistry Product Research and Development, **23** (4): p. 620-624.
50. Hakli, O., Dumanli, A.G., Nalbant, A., Okyay, F., Yurum, Y. (2009). *The Conversion of Low-rank Kilyos Coal to Nitrogenous Fertilizers*. Energy Sources Part A-Recovery Utilization and Environmental Effects, **33** (2): p. 164-170.
51. Flaig, W. (1972). *Verwertung eines Abfallproduktes der Zellstoffindustrie als Düngemittel - ein Beitrag zur umweltfreundlichen Technik*. Landbauforschung Völkenrode, **Sonderheft** (014): p. 86-93.

52. Meier, D., Zunigapartida, V., Ramirezcano, F., Hahn, N.C., Faix, O. (1994). *Conversion of Technical Lignins into Slow-Release Nitrogenous Fertilizers by Ammoxidation in Liquid-Phase*. *Bioresource Technology*, **49** (2): p. 121-128.
53. Ramírez-Cano, F., Ramos-Quirarte, A., Faix, O., Meier, D., González-Alvarez, V., Zúñiga-Partida, V. (2001). *Slow-release effect of N-functionalized kraft lignin tested with Sorghum over two growth periods*. *Bioresource Technology*, **76** (1): p. 71-73.
54. NOVIHUM (2012). *Entstehung von NOVIHUM durch die oxidative Ammonialyse*, Available from: [http://www.novihum.de/press/studies/graphic\\_entstehung.jpg](http://www.novihum.de/press/studies/graphic_entstehung.jpg) [Accessed 08.08.2012]
55. Avi, S. (2001). *Advances in controlled-release fertilizers*. *Advances in Agronomy*, **71**, p. 1-49.
56. ASTM International (2003). *Standard Test Method for Compositional Analysis by Thermogravimetry (E 1131 – 03)*, West Conshohocken (USA): ASTM Int.
57. ASTM International (2001). *Standard Practice for Preparation of Biomass for Compositional Analysis (E 1757 – 01)*, West Conshohocken (USA): ASTM Int.
58. ASTM International (1982). *Standard Method for Moisture Analysis of Particulate Wood Fuels (E 871 – 82 (Reapproved 1998))*, West Conshohocken (USA): ASTM Int.
59. ASTM International (2001). *Standard Test Method for Ash in Biomass (E 1755 – 01)*, West Conshohocken (USA): ASTM Int.
60. British Standard Institute (2008). *Quality management systems. Requirements (BS EN ISO 9001:2008)*, London: BSI
61. Channiwala, S.A. and Parikh, P.P. (2002). *A unified correlation for estimating HHV of solid, liquid and gaseous fuels*. *Fuel*, **81** (8): p. 1051-1063.
62. Brandt, F. (2000). *Brennstoffe und Verbrennungsrechnung. FDBR-Fachbuchreihe 3rd*, Essen: Vulkan Verlag: 166 pages
63. ASTM International (2001). *Standard Test Method for Water Using Volumetric Karl Fischer Titration (E 203 – 01)*, West Conshohocken (USA): ASTM Int.
64. Greenhalf, C.E., Nowakowski, D.J., Harms, A.B., Titiloye, J.O., Bridgwater, A.V. (2012). *Sequential pyrolysis of willow SRC at low and high heating rates - Implications for selective pyrolysis*. *Fuel*, **93** p. 692-702.
65. Faix, O., Fortmann, I., Bremer, J., Meier, D. (1991). *Thermal degradation products of wood - Gas chromatographic separation and mass spectrometric characterization of polysaccharide derived products*. *Holz als Roh- und Werkstoff*, **49** (5): p. 213-219.

66. Faix, O., Meier, D., Fortmann, I. (1990). *Thermal-Degradation Products of Wood - Gas-Chromatographic Separation and Mass-Spectrometric Characterization of Monomeric Lignin Derived Products*. Holz als Roh- und Werkstoff, **48** (7-8): p. 281-285.
67. Pretsch, E., Bühlmann, P., Badertscher, M. (2009). *Structure Determination of Organic Compounds - Tables of Spectral Data*. 4th, Berlin Heidelberg: Springer-Verlag 436 pages
68. Silverstein, R.M., Morrill, T.C., Bassler, G.C. (1981). *Spectrometric Identification of Organic Compounds*. 4th, New York: John Wiley & Sons: 442 pages
69. Harms, A.B., Nowakowski, D.J., Bridgwater, A.V. (2010). *Fast Pyrolysis Processing of Agricultural and Forestry Residues: Nitrogen Recycling and Carbon Sequestration*, in *Proceedings of the bioten conference of biomass, bioenergy and biofuels 2010*, Bridgwater, A.V. (Ed.), Newbury: CPL Press: p. 525-532
70. Energy Research Centre of the Netherlands (2011). *Phyllis - Database for biomass and waste (Beech Wood)*, Available from: <http://www.ecn.nl/phyllis> [Accessed 28.12.2011]
71. Oasmaa, A., Kuoppala, E., Solantausta, Y. (2003). *Fast Pyrolysis of Forestry Residue. 2. Physicochemical Composition of Product Liquid*. Energy & Fuels, **17** (2): p. 433-443.
72. Energy Research Centre of the Netherlands (2011). *Phyllis - Database for biomass and waste (Wheat Straw)*, Available from: <http://www.ecn.nl/phyllis> [Accessed 28.12.2011]
73. Giuntoli, J., de Jong, W., Arvelakis, S., Spliethoff, H., Verkooijen, A.H.M. (2009). *Quantitative and kinetic TG-FTIR study of biomass residue pyrolysis: Dry distiller's grains with solubles (DDGS) and chicken manure*. Journal of Analytical and Applied Pyrolysis, **85** (1-2): p. 301-312.
74. Barz, M. and Heinisch, R. (1999). *Biomasse für die Wirbelkammerfeuerung : Ergebnisse eines Forschungsprojektes zur thermischen Nutzung von Rapsextraktionsschrot*. BKW - Das Energie-Fachmagazine, **51** p. 48-50.
75. Yuan, X., Shi, X., Zeng, S., Wei, Y. (2010). *Activated carbons prepared from biogas residue: Characterization and methylene blue adsorption capacity*. Journal of Chemical Technology & Biotechnology, **86** (3): p. 361-366.
76. Yilgin, M., Deveci Duranay, N., Pehlivan, D. (2010). *Co-pyrolysis of lignite and sugar beet pulp*. Energy Conversion and Management, **51** (5): p. 1060-1064.
77. ADM Trading (U.K.) Limited (2008). *Product Summary - Rapeseed meal*, Available from: <http://www.admworld.com/euen/ahn/summary.asp> [Accessed 08.12.2008]

78. KW alternative feeds (2012). *Scottish Distillers Barley Pellets*, Available from: <http://www.kwalternativefeeds.co.uk/products/view-products/scottish-distillers-barley-pellets/> [Accessed 24.01.2012]
79. Trident Feeds (2012). *Pressed Sugar Beet Pulp*, Available from: <http://www.tridentfeeds.co.uk/products/pressed-sugar-beet-pulp/> [Accessed 24.01.2012]
80. Kim, Y., Mosier, N.S., Hendrickson, R., Ezeji, T., Blaschek, H., Dien, B., Cotta, M., Dale, B., Ladisch, M.R. (2008). *Composition of corn dry-grind ethanol by-products: DDGS, wet cake, and thin stillage*. *Bioresource Technology*, **99** (12): p. 5165-5176.
81. Wirth, K.-E. (2006). *Strömungszustände und Druckverlust in Wirbelschichten*, in *VDI-Wärmeatlas. Berechnungsunterlagen für Druckverlust, Wärme- und Stoffübergang*, VDI-Gesellschaft Verfahrenstechnik und Chemieingenieurwesen (GVC) (Ed.), 10, Berlin, Heidelberg, New York: Springer-Verlag p. Lcb 1-11
82. Wirth, K.-E. (2006). *Druckverlust bei Strömungen durch Schüttungen*, in *VDI-Wärmeatlas. Berechnungsunterlagen für Druckverlust, Wärme- und Stoffübergang*, VDI-Gesellschaft Verfahrenstechnik und Chemieingenieurwesen (GVC) (Ed.), 10, Berlin, Heidelberg, New York: Springer-Verlag p. Laf 1-5
83. Wen, C.Y. and Yu, Y.H. (1966). *A generalized method for predicting the minimum fluidization velocity*. *AIChE Journal*, **12** (3): p. 610-612.
84. Sitzmann, J. (2009). *Upgrading of Fast Pyrolysis Oils by Hot Filtration*. PhD Thesis, Birmingham, UK: Aston University.
85. Multisol Limited (2008). *ISOPAR™ SERIES ISOPARAFFINIC HYDROCARBONS*, Available from: <http://www.multisolgroup.com/Isopar-Series-Typical-Properties.pdf> [Accessed 06.08.2009]
86. Krauss, R. (2006). *Stoffwerte von Ammoniak*, in *VDI-Wärmeatlas. Berechnungsunterlagen für Druckverlust, Wärme- und Stoffübergang*, VDI-Gesellschaft Verfahrenstechnik und Chemieingenieurwesen (GVC) (Ed.), 10, Berlin, Heidelberg, New York: Springer-Verlag p. Dbf 1-17
87. Krauss, R. (2006). *Stoffwerte von Stickstoff*, in *VDI-Wärmeatlas. Berechnungsunterlagen für Druckverlust, Wärme- und Stoffübergang*, VDI-Gesellschaft Verfahrenstechnik und Chemieingenieurwesen (GVC) (Ed.), 10, Berlin, Heidelberg, New York: Springer-Verlag p. Dbc 1-17
88. Guillain, M., Fairouz, K., Mar, S.R., Monique, F., Jacques, L. (2009). *Attrition-free pyrolysis to produce bio-oil and char*. *Bioresource Technology*, **100** (23): p. 6069-6075.

89. Guarrant, G.O. and Brown, D.E. (1965). *Thermal Stability, Thermal Decomposition of High-Analysis Fertilizers Based on Ammonium Phosphate*. Journal of Agricultural and Food Chemistry, **13** (6): p. 493-497.
90. Schaber, P.A., Colson, J., Higgins, S., Thielen, D., Anspach, B., Brauer, J. (2004). *Thermal decomposition (pyrolysis) of urea in an open reaction vessel*. Thermochemica Acta, **424** (1-2): p. 131-142.
91. Xue, J., Sands, R., Clinton, P.W. (2004). *Effect of biuret on growth and nutrition of Douglas-fir (Pseudotsuga menziesii (Mirb) Franco) seedlings*. Forest Ecology and Management, **192** (2-3): p. 335-348.
92. Aciego Pietri, J.C. and Brookes, P.C. (2008). *Relationships between soil pH and microbial properties in a UK arable soil*. Soil Biology and Biochemistry, **40** (7): p. 1856-1861.
93. Kemmitt, S.J., Lanyon, C.V., Waite, I.S., Wen, Q., Addiscott, T.M., Bird, N.R.A., O'Donnell, A.G., Brookes, P.C. (2008). *Mineralization of native soil organic matter is not regulated by the size, activity or composition of the soil microbial biomass - a new perspective*. Soil Biology and Biochemistry, **40** (1): p. 61-73.
94. Vance, E.D., Brookes, P.C., Jenkinson, D.S. (1987). *An extraction method for measuring soil microbial biomass C*. Soil Biology and Biochemistry, **19** (6): p. 703-707.
95. Durenkamp, M. and Brookes, P.C. (2010). *Impact of solidified bio-oil on soil microbial biomass (Poster)*, at Bioten Conference, Birmingham (UK)

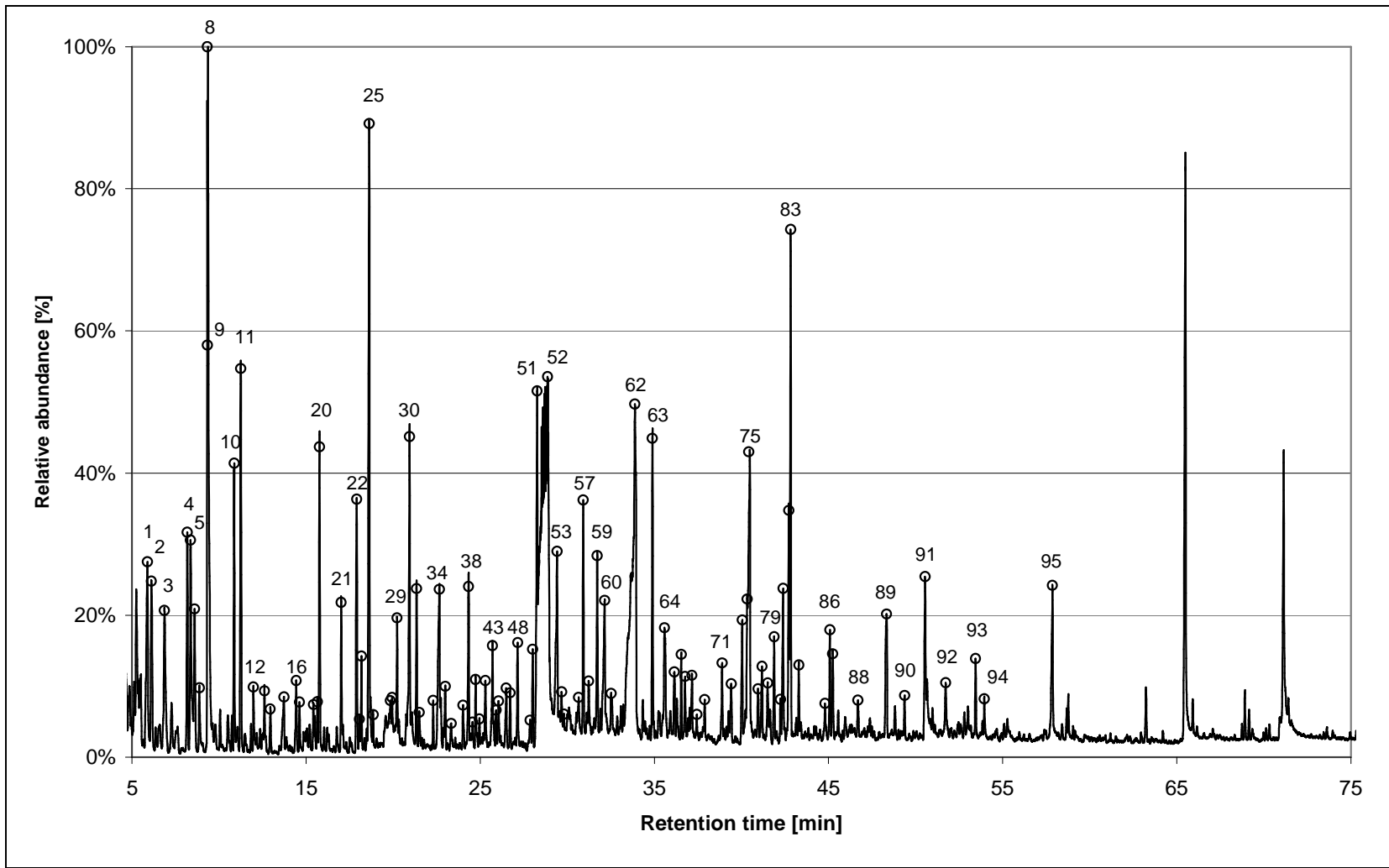
## Appendix

### ***Appendix A: Py-GC-MS analysis of high nitrogen feedstocks***

The pyrolysis vapour chromatograms of the high nitrogen feedstocks, DDGSs and rape meals, and suggested peak assignments are presented in appendix A as mentioned in section 4.2.5. The Py-GC-MS analysis was performed with CDS 2500 Pyrolyser® and PerkinElmer GC-MS. The following chromatograms and suggested peak assignment tables are included:

- barley DDGS pyrolysis vapour chromatogram
- barley DDGS suggested peak assignment table
- wheat DDGS pyrolysis vapour chromatogram
- wheat DDGS suggested peak assignment table
- maize DDGS pyrolysis vapour chromatogram
- maize DDGS suggested peak assignment table
- Green Dragon rape meal pyrolysis vapour chromatogram
- Green Dragon rape meal suggested peak assignment table
- ADM rape meal pyrolysis vapour chromatogram
- ADM rape meal suggested peak assignment table

The peaks with suggested peak assignments are marked with a circle, but not all peak assignment numbers are displayed for reasons of readability.

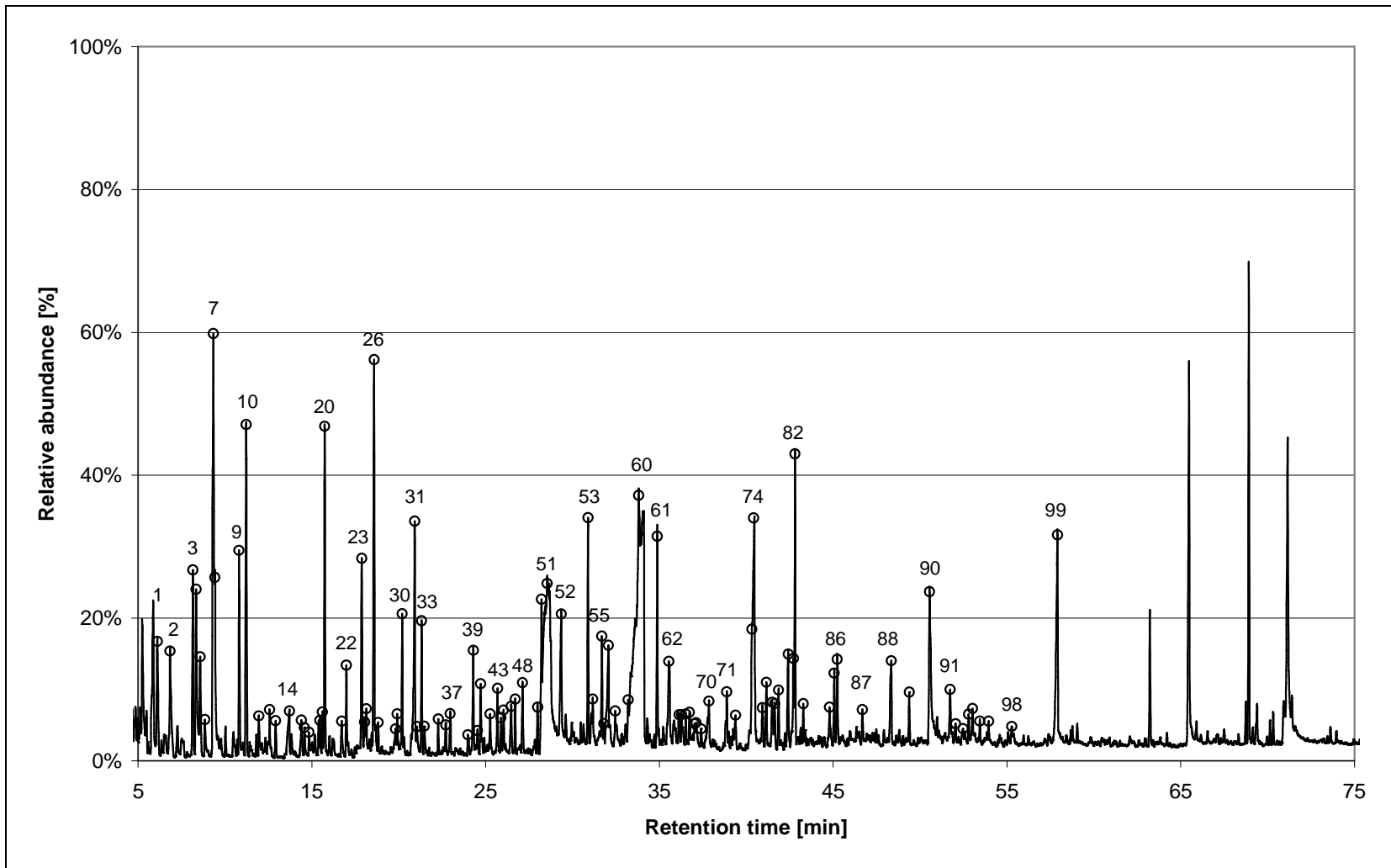


Pyrolysis vapour chromatogram of barley DDGS

## Suggested Peak assignments for barley DDGS

| Peak # | RT     | Base Peak | Component                              | MW  |
|--------|--------|-----------|--|-----|
| 1      | 5.882  | 41        | 2-Methyl-Propanal                      | 72  |
| 2      | 6.114  | 82        | Methylfuran                            | 82  |
| 3      | 6.861  | 43        | 2,3-Butanedione                        | 86  |
| 4      | 8.174  | 44        | 3-Methyl-Butanal                       | 86  |
| 5      | 8.361  | 29/41     | 2-Methyl-Butanal                       | 86  |
| 6      | 8.593  | 96        | 2,5-Dimethyl-Furan                     | 96  |
| 7      | 8.871  | 43        | 3-Methyl-Buten-2-one                   |     |
| 8      | 9.325  | 45        | Acetic Acid                            | 60  |
| 9      | 9.34   | 43        | Acetic Acid Anhydride with Formic Acid | 102 |
| 10     | 10.87  | 43        | Acetic Acid Methyl ester               | 74  |
| 11     | 11.243 | 91        | Toluene                                | 92  |
| 12     | 11.97  | 79        | Pyridine                               | 79  |
| 13     | 12.612 | 45        | 1,2-Propanediol                        | 76  |
| 14     | 12.94  | 43        | 3-Methyl-Butanenitril                  | 83  |
| 15     | 13.732 |           | unknown                                |     |
| 16     | 14.434 | 55        | 2-Propanoic acid methyl ester          | 86  |
| 17     | 14.621 | 72        | Propanoic acid                         | 72  |
| 18     | 15.424 | 57        | 1-Hydroxy-2-butanone                   | 88  |
| 19     | 15.651 | 91        | Ethylbenzene                           | 106 |
| 20     | 15.762 | 67        | Pyrrole                                | 67  |
| 21     | 17.014 | 84        | (2H)-Furan-3-one                       | 84  |
| 22     | 17.903 | 43        | Acetic anhydride                       | 102 |
| 23     | 18.054 | 60        | Butanoic acid                          | 88  |
| 24     | 18.18  | 45        | 2,3-Butandiol                          | 90  |
| 25     | 18.625 | 96        | Furfural                               | 96  |
| 26     | 18.852 | 55        | 4-Methyl-Pentane-nitrile               | 94  |
| 27     | 19.841 | 43        | unknown                                |     |
| 28     | 19.942 | 80        | 2-Methyl-1H-Pyrrole                    | 79  |
| 29     | 20.22  | 80        | 3-Methyl-1H-Pyrrole                    | 79  |
| 30     | 20.942 | 41        | 3-Furfuryl alcohol                     | 98  |
| 31     | 21.34  | 43        | 1-Acetyloxypropane-2-one               | 116 |
| 32     | 21.502 | 67        | 2-Methyl-2-Cyclopentene-1-one          | 95  |
| 33     | 22.3   | 95        | 2-Acetylfural                          | 110 |
| 34     | 22.653 | 57        | unknown                                |     |
| 35     | 22.991 | 42        | 4-Cyclopentene-1,3-dione               | 96  |
| 36     | 23.33  | 43        | unknown                                |     |
| 37     | 24.011 | 68        | unknown                                |     |
| 38     | 24.329 | 98        | 2-Hydroxy-2-Cyclopentene-1-one         | 99  |
| 39     | 24.552 | 94        | 2,5-Dimethyl-1H-Pyrrole                |     |
| 40     | 24.733 | 44        | unknown                                |     |
| 41     | 24.95  | 43        | 2,5-Hexanedione                        | 114 |
| 42     | 25.294 | 42        | unknown                                |     |
| 43     | 25.702 | 110       | 5-Methyl-2-Furaldehyde                 | 110 |
| 44     | 25.909 | 57        | unknown                                |     |
| 45     | 26.051 | 43        | unknown                                |     |
| 46     | 26.49  | 96        | 3-Methyl-2-Cyclopentene-1-one          |     |
| 47     | 26.712 | 42        | Butyrolactone                          | 86  |
| 48     | 27.151 | 55        | Lysidine                               | 84  |
| 49     | 27.863 | 55        | unknown                                |     |
| 50     | 28.01  | 110       | unknown                                |     |

| Peak # | RT     | Base Peak | Component                                       | MW  |
|--------|--------|-----------|---|-----|
| 51     | 28.272 | 114       | 4-Hydroxy-5,6-dihydro-2H-pyran-2-one            | 114 |
| 52     | 28.863 | 45        | unknown   |     |
| 53     | 29.413 | 112       | 2-Hydroxy-1-methyl-1-cyclopentene-3-one         | 112 |
| 54     | 29.671 | 45        | unknown   |     |
| 55     | 29.802 | 44        | unknown   |     |
| 56     | 30.65  | 91        | unknown   |     |
| 57     | 30.913 | 94        | Phenol  | 94  |
| 58     | 31.231 | 95        | 1H-Pyrrole-2-Carboxaldehyde                     | 95  |
| 59     | 31.72  | 109       | Guaiacol  | 124 |
| 60     | 32.144 | 43        | 2,5-Dimethyl-4-Hydroxy-3(2H)Furanone            | 128 |
| 61     | 32.518 | 94        | 1-(1H-Pyrrol-2yl)-Ethanone                      |     |
| 62     | 33.881 | 61        | Glycerin  | 92  |
| 63     | 34.89  | 107       | Methylphenol                                    | 108 |
| 64     | 35.582 | 85        | unknown   |     |
| 65     | 36.152 | 43        | 4H-Pyron-4-one-2,3-Dihydro-3,5Dihydroxy-6Methyl |     |
| 66     | 36.541 | 123       | 3-Methyl-Guaiacol                               | 138 |
| 67     | 36.764 | 44        | Anhydrosugar                                    | 132 |
| 68     | 37.157 | 142       | 4H-Pyran-4-one-3,5Dihydroxy-2Methyl             |     |
| 69     | 37.44  | 59        | Pentanamide                                     |     |
| 70     | 37.89  | 43        | 1,2,3-Propanetriol-Monoacetate                  |     |
| 71     | 38.894 | 107       | 4-Ethyl-Phenol                                  | 122 |
| 72     | 39.414 | 56        | unknown   |     |
| 73     | 40.05  | 45        | unknown   |     |
| 74     | 40.328 | 137       | 4-Ethyl-Guaiacol                                | 152 |
| 75     | 40.42  | 95        | Pyridinal                                       |     |
| 76     | 40.954 | 43        | Anhydro-D-Galetosan                             | 144 |
| 77     | 41.181 | 71        | Anhydro-D-Manosan                               | 144 |
| 78     | 41.509 | 109       | unknown   |     |
| 79     | 41.883 | 69        | Dianhydro-glucopyranose                         | 144 |
| 80     | 42.241 | 56        | unknown   |     |
| 81     | 42.393 | 57        | Anhydro-D-Xylofuranose                          | 132 |
| 82     | 42.721 | 120       | unknown   |     |
| 83     | 42.832 | 150       | 4-Vinyl-Guaiacol                                | 150 |
| 84     | 43.302 | 57        | unknown   |     |
| 85     | 44.801 | 110       | Catechol  | 110 |
| 86     | 45.084 | 85        | Syringol  | 154 |
| 87     | 45.24  | 117       | Indole  | 117 |
| 88     | 46.69  |           | unknown   |     |
| 89     | 48.34  | 57        | Anhydrosugar                                    |     |
| 90     | 49.375 | 110       | Hydroquinone                                    | 110 |
| 91     | 50.551 | 45        | unknown   |     |
| 92     | 51.733 | 45        | unknown   |     |
| 93     | 53.444 | 107       | 4-Hydroxy-Benzeneethanol                        | 138 |
| 94     | 53.954 | 180       | Dimethoxy-Phenyl-Ethanone                       |     |
| 95     | 57.862 | 60        | Levoglucosan                                    | 162 |

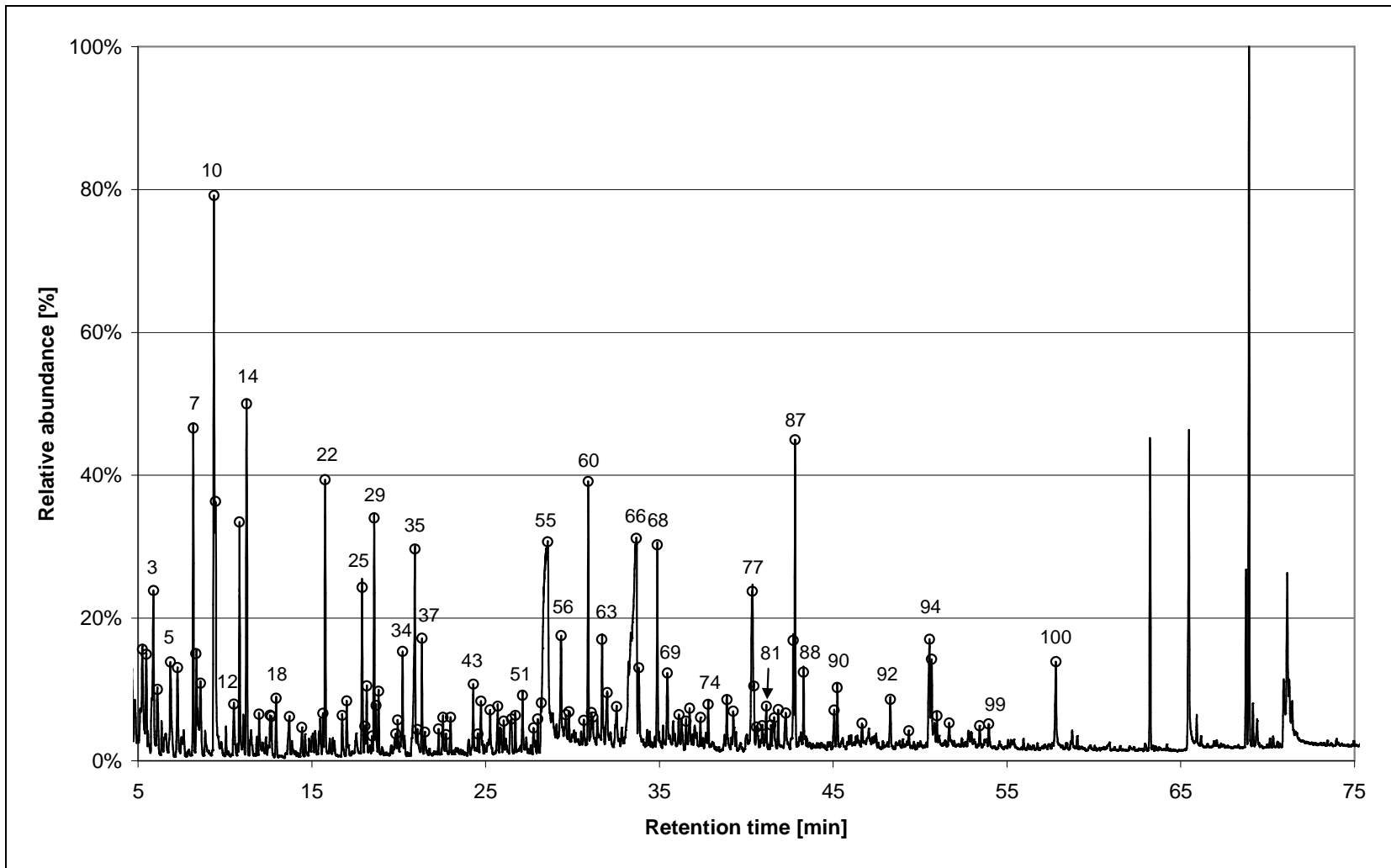


Pyrolysis vapour chromatogram of wheat DDGS

## Suggested Peak assignments for wheat DDGS

| Peak # | RT     | Base Peak | Component                              | MW  |
|--------|--------|-----------|--|-----|
| 1      | 6.103  | 82        | 2-Methylfuran                          | 82  |
| 2      | 6.84   | 43        | 2,3-Butanedione                        | 86  |
| 3      | 8.153  | 44        | 3-Methyl-Butanal                       | 86  |
| 4      | 8.344  | 41        | 2-Methyl-Butanal                       | 86  |
| 5      | 8.572  | 96        | 2,5-Dimethyl-Furan                     | 98  |
| 6      | 8.844  | 43        | 3-Methyl-3-Buten-2-one                 | 84  |
| 7      | 9.324  | 43        | Acetic Acid                            | 60  |
| 8      | 9.42   | 43        | unknown                                |     |
| 9      | 10.808 | 43        | Acetic Acid Methyl Ester               | 74  |
| 10     | 11.222 | 91        | Toluene                                | 92  |
| 11     | 11.944 | 79        | Pyridine                               | 79  |
| 12     | 12.57  | 45        | 1,2Propandiol                          | 76  |
| 13     | 12.914 | 43        | 3Methyl-Butanenitrile                  | 83  |
| 14     | 13.706 |           | unknown                                |     |
| 15     | 14.398 | 55        | unknown                                |     |
| 16     | 14.57  | 72        | unknown                                |     |
| 17     | 14.832 | 93        | 2Methyl-Pyridine                       | 93  |
| 18     | 15.463 | 94        | Methyl-Pyrazine                        | 96  |
| 19     | 15.61  | 91        | Ethylbenzene                           | 106 |
| 20     | 15.741 | 67        | Pyrrole                                | 67  |
| 21     | 16.72  | 45        | 4Methyl-Pentanol                       | 102 |
| 22     | 16.983 | 84        | (2H)Furan-2-one                        | 84  |
| 23     | 17.871 | 43        | Acetic Anhydride                       | 102 |
| 24     | 18.033 | 93        | 2Methyl-Pyridine                       | 93  |
| 25     | 18.134 | 45        | 2,3-Butanediol                         | 90  |
| 26     | 18.583 | 96        | Furfural                               | 96  |
| 27     | 18.82  | 55        | 4Methyl-Pentanenitrile                 | 97  |
| 28     | 19.81  | 43        | unknown                                |     |
| 29     | 19.911 | 80        | 3Methyl-1H-Pyrrole                     | 81  |
| 30     | 20.199 | 80        | 2Methyl-1H-Pyrrole                     | 81  |
| 31     | 20.92  | 41        | 3-Furfuryl Alcohol                     | 98  |
| 32     | 21.047 | 74        | 2Methyl-Butanoic Acid                  | 102 |
| 33     | 21.319 | 43        | 1-Acetyloxypropane-2-one               | 116 |
| 34     | 21.471 | 67        | 2-Methyl-2-Cyclopenten-1-one           | 96  |
| 35     | 22.273 | 95        | 2-Acetylfuran                          | 110 |
| 36     | 22.702 | 57        | unknown                                |     |
| 37     | 22.96  | 96        | 4-Cyclopenten-1,3-dione                | 96  |
| 38     | 23.98  |           | unknown                                |     |
| 39     | 24.293 | 98        | 2-Hydroxy-2-Cyclopenten-1-one          | 98  |
| 40     | 24.52  | 94        | 2,5-Dimethyl-1H-Pyrrole                | 95  |
| 41     | 24.712 | 80        | 3-Ethyl-1H-Pyrrole                     | 95  |
| 42     | 25.262 | 42        | 2,4Dimethyl-Cyclopentanone             |     |
| 43     | 25.681 | 110       | 5-Methyl-2-furaldehyde                 | 110 |
| 44     | 25.883 | 57        | unknown                                |     |
| 45     | 26.029 | 43        | unknown                                |     |
| 46     | 26.463 | 96        | 3-Methyl-2-Cyclopenten-1-one           | 96  |
| 47     | 26.701 | 42        | Butyrolactone                          | 86  |
| 48     | 27.12  | 55        | Lysidine                               | 84  |
| 49     | 27.993 |           | unknown                                |     |
| 50     | 28.22  | 114       | 4-Hydroxy-5,6-dihydro-(2H)-pyran-2-one | 114 |

| Peak # | RT     | Base Peak | Component                               | MW  |
|--------|--------|-----------|---|-----|
| 51     | 28.543 |           | unresolved                              |     |
| 52     | 29.351 | 112       | 2-Hydroxy-1-methyl-1-cyclopentene-3-one | 112 |
| 53     | 30.891 | 94        | Phenol                                  | 94  |
| 54     | 31.163 | 95        | 1H-Pyrrole-2-Carboxaldehyde             | 95  |
| 55     | 31.693 | 109       | Guaiacol                                | 124 |
| 56     | 31.804 | 59        | 3Methyl-Butanamide                      |     |
| 57     | 32.062 | 43        | 2,5-Dimethyl-4-Hydroxy-3(2H)Furanone    | 128 |
| 58     | 32.455 | 94        | 1-(1H-Pyrrol-2yl)-Ethanone              |     |
| 59     | 33.203 |           | unknown                                 |     |
| 60     | 33.808 | 61        | Glycerin                                | 92  |
| 61     | 34.873 | 107       | Methylphenol                            | 108 |
| 62     | 35.545 | 85        | unknown                                 |     |
| 63     | 36.141 | 47        | unknown                                 |     |
| 64     | 36.277 | 117       | Iso-Cyano-Methyl-Benzene                |     |
| 65     | 36.524 | 123       | 3-Methyl-Guaiacol                       | 123 |
| 66     | 36.731 | 44        | Anhydrosugar                            | 132 |
| 67     | 37.019 | 107       | 4-Ethyl-Phenol                          | 122 |
| 68     | 37.11  | 142       | 2Methyl-3,5Dihydroxy-4H-Pyran-4-one     |     |
| 69     | 37.403 | 59        | 4-Methyl-Pentaamide                     |     |
| 70     | 37.852 | 43        | 1,2,3-Propanetriol Monoacetate          |     |
| 71     | 38.882 | 107       | 4-Ethyl-Phenol                          | 122 |
| 72     | 39.381 | 80        | 4Methyl-2(1H)Pyridinone                 |     |
| 73     | 40.32  | 137       | 4-Ethyl-Guaiacol                        | 152 |
| 74     | 40.42  | 95        | Pyrimidinamide                          | 95  |
| 75     | 40.921 | 43        | Anhydro-D-Galetosan                     | 144 |
| 76     | 41.159 | 71        | Anhydro-D-Manosan                       | 144 |
| 77     | 41.492 | 109       | unknown                                 |     |
| 78     | 41.633 | 42        | unknown                                 |     |
| 79     | 41.855 | 69        | Dianhydro-glucopyranose                 | 144 |
| 80     | 42.411 | 57        | Anhydro-D-xylofuranose                  | 162 |
| 81     | 42.709 | 120       | unknown                                 |     |
| 82     | 42.8   | 150       | 4-Vinyl-Guaiacol                        | 150 |
| 83     | 43.284 | 57        | Dodecane                                | 170 |
| 84     | 44.789 | 110       | Catechol                                | 110 |
| 85     | 45.061 | 85        | Syringol                                | 154 |
| 86     | 45.233 | 117       | Indole                                  | 117 |
| 87     | 46.682 | 98        | unknown                                 |     |
| 88     | 48.343 | 57        | Anhydrosugar                            |     |
| 89     | 49.383 | 110       | Hydroquinone                            | 110 |
| 90     | 50.54  | 84        | unknown                                 |     |
| 91     | 51.731 |           | unknown                                 |     |
| 92     | 52.044 | 43        | unknown                                 |     |
| 93     | 52.473 | 60        | Anhydro-D-Mannopyranose                 | 162 |
| 94     | 52.792 | 84        | Acetoxymethyl-Alpha-Pyrrolidone         |     |
| 95     | 53.019 | 45        | unknown                                 |     |
| 96     | 53.443 | 107       | Hydroxy-Benzene-Ethanol                 | 138 |
| 97     | 53.938 | 180       | Dimethoxy-Phenyl-Ethanone               | 180 |
| 98     | 55.28  | 60        | D-Allose                                |     |
| 99     | 57.911 | 60        | Levoglucosan                            | 162 |

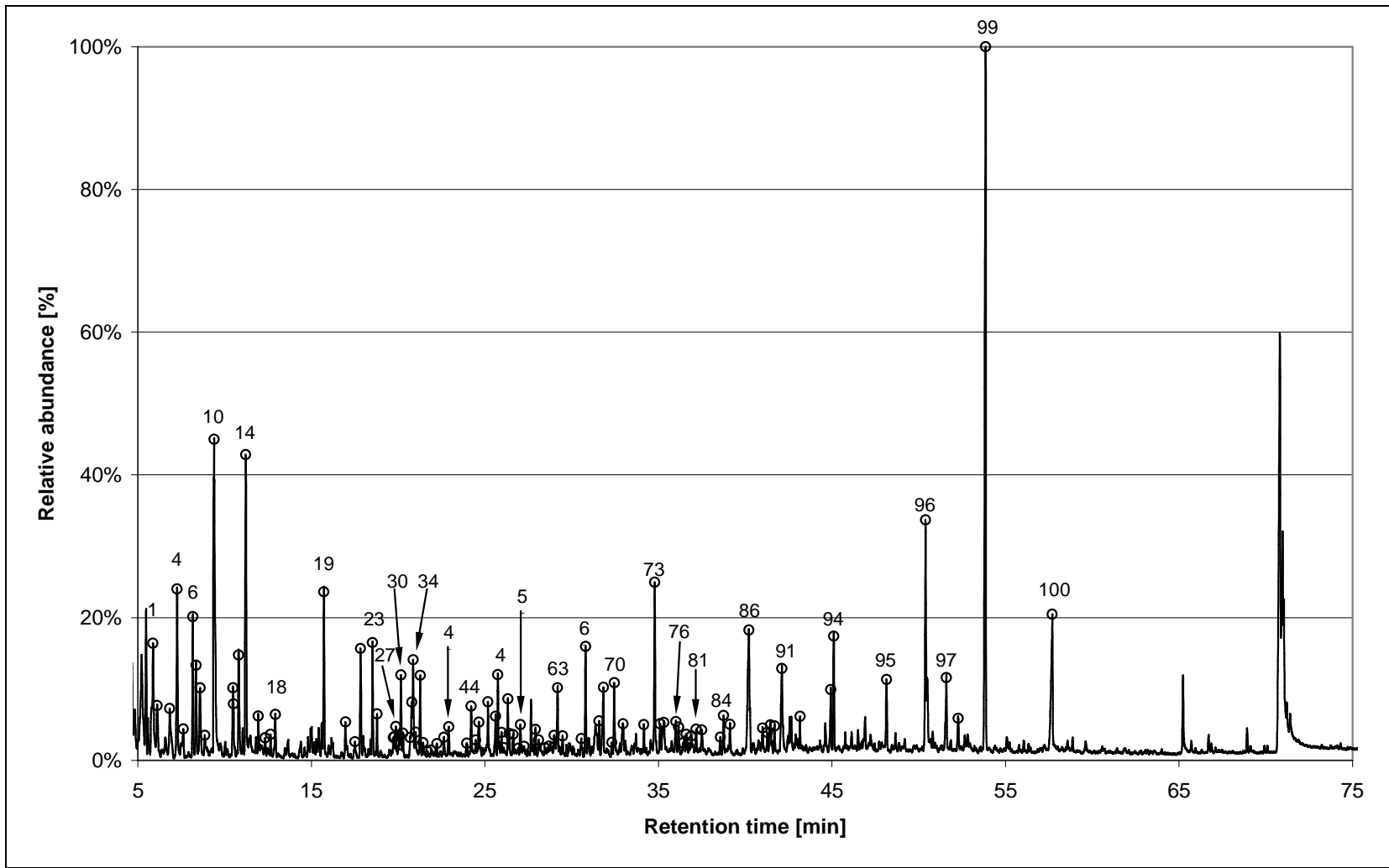


Pyrolysis vapour chromatogram for maize DDGS

## Suggested Peak assignments for maize DDGS

| Peak # | RT     | Base Peak | Component                               | MW  |
|--------|--------|-----------|---|-----|
| 1      | 5.251  | 43        | (1-Propen-2-ol, Acetate)                | 100 |
| 2      | 5.473  | 56        | (3,4-Dimethyl-1-Hexene)                 | 112 |
| 3      | 5.882  | 43        | 2-Methyl-Propanal                       | 72  |
| 4      | 6.114  | 82        | 2-Methyl-Furan                          | 82  |
| 5      | 6.861  | 43        | 2,3-Butanedione                         | 86  |
| 6      | 7.27   | 41        | (4-Methyl-1-Hexene)                     | 98  |
| 7      | 8.174  | 44        | 3-Methyl-Butanal                        | 86  |
| 8      | 8.3161 | 29/41     | 2-Methyl-Butanal                        | 86  |
| 9      | 8.593  | 96        | 2,5-Dimethyl-Furan                      | 96  |
| 10     | 9.37   | 45        | Acetic Acid                             | 45  |
| 11     | 9.456  | 43        | Acetic Acid, Anhydride with Formic Acid | 88  |
| 12     | 10.511 | 43        | unkown                                  |     |
| 13     | 10.834 | 43        | Acetic-Acid-Methylester                 | 74  |
| 14     | 11.243 | 91        | Toluene                                 | 92  |
| 15     | 11.96  | 79        | Pyridine                                | 79  |
| 16     | 12.601 | 45        | 1,2-Propandiol                          | 76  |
| 17     | 12.677 | 54        | unkown                                  |     |
| 18     | 12.94  | 43        | 3-Methyl-Butanenitril                   |     |
| 19     | 13.707 | 45/74     | Propanoic Acid                          | 74  |
| 20     | 14.424 | 55        | 2-Propanic-Acid-Mehyl-Ester             | 86  |
| 21     | 15.641 | 91        | (Ethyl-Benzene)                         | 106 |
| 22     | 15.762 | 67        | Pyrrole                                 | 67  |
| 23     | 16.741 | 45        | 4-Methyl-2-Pentanol                     | 102 |
| 24     | 17.009 | 84        | (2H)-Furan-3-one                        | 84  |
| 25     | 17.893 | 43        | Acetic anhydride                        | 102 |
| 26     | 18.044 | 60        | unkown                                  |     |
| 27     | 18.16  | 45        | unkown                                  |     |
| 28     | 18.473 |           | unkown                                  |     |
| 29     | 18.584 | 96        | Furfural                                | 96  |
| 30     | 18.69  | 45        | 2,3-Butanediol                          | 90  |
| 31     | 18.842 | 55        | 4-Methyl-Pentanenitrile                 | 97  |
| 32     | 19.831 | 43        | unkown                                  |     |
| 33     | 19.932 | 80        | 2-Methyl-1H-Pyrrole                     | 81  |
| 34     | 20.22  | 80        | 3-Methyl-1H-Pyrrole                     | 81  |
| 35     | 20.932 | 41        | 3-Furfuryl-Alcohol                      | 98  |
| 36     | 21.073 | 74        | 2-Methyl-Butanoic Acid                  | 102 |
| 37     | 21.331 | 43        | 1-Acetyloxypropane-2-one                | 116 |
| 38     | 21.502 | 67        | 2-Methyl-2-Cyclopenten-1-one            | 96  |
| 39     | 22.29  | 95        | 2-Acetylfuran                           | 110 |
| 40     | 22.542 | 57        | Methyl-butyrnaldehyde derivate          |     |
| 41     | 22.714 |           | unkown                                  |     |
| 42     | 22.982 | 42        | 4-Cyclopenten-1,3-dione                 | 96  |
| 43     | 24.289 | 98        | 1-Hydroxy-2-Cyclopente-1-one            | 98  |
| 44     | 24.552 | 94        | 2,5-Dimethyl-1H-Pyrrole                 | 95  |
| 45     | 24.734 | 80        | 3-Ethyl-1H-Pyrrole                      | 95  |
| 46     | 25.259 |           | unkown                                  |     |
| 47     | 25.698 | 110       | 5-Methyl-2-furaldehyde                  | 110 |
| 48     | 26.041 | 43        | unknown                                 |     |
| 49     | 26.49  | 96        | 2-Methyl-2-Cyclopenten-1-one            | 96  |
| 50     | 26.713 | 42        | Butyrolactone                           | 86  |

| Peak # | RT     | Base Peak | Component                               | MW  |
|--------|--------|-----------|---|-----|
| 51     | 27.121 | 55        | Lysidine                                | 84  |
| 52     | 27.752 | 54        | unknown                                 |     |
| 53     | 28.000 | 110       | unknown                                 |     |
| 54     | 28.202 | 114       | 4-Hydroxy-5,6-dihydro-(2H)-pyran-2-one  | 114 |
| 55     | 28.570 | 45        | Hydroxy-Propanoic Acid, Ethylester      | 118 |
| 56     | 29.343 | 112       | 2-Hydroxy-1-methyl-1-cyclopentene-3-one | 112 |
| 57     | 29.620 | 43        | unknown                                 |     |
| 58     | 29.792 | 45        | unknown                                 |     |
| 59     | 30.650 | 91        | unknown                                 |     |
| 60     | 30.903 | 94        | Phenol                                  | 94  |
| 61     | 31.084 |           | unknown                                 |     |
| 62     | 31.170 | 95        | 1H-Pyrrole-2-Carboxaldehyde             | 95  |
| 63     | 31.695 | 109       | Guaiacol                                | 124 |
| 64     | 31.993 | 43        | 2,5-Dimethyl-4-Hydroxy-3(2H)Furanone    | 128 |
| 65     | 32.533 |           | unkonwn                                 |     |
| 66     | 33.674 | 61        | Glycerin                                | 92  |
| 67     | 33.811 | 126       | Maltol                                  | 126 |
| 68     | 34.881 | 107       | Methylphenol                            | 108 |
| 69     | 35.462 | 85        | unknown                                 |     |
| 70     | 36.123 | 43        | unknown                                 |     |
| 71     | 36.527 | 123       | 3-Methyl-Guaiacol                       | 123 |
| 72     | 36.744 | 44        | Anhydrosugar                            | 132 |
| 73     | 37.370 | 59        | Pentaamide                              | 101 |
| 74     | 37.804 | 43        | 1,2,3-Propanetriol-Monoacetate          | 134 |
| 75     | 38.890 | 107       | 4-Ethyl-Phenol                          | 122 |
| 76     | 39.253 | 69        | unknown                                 |     |
| 77     | 40.349 | 95        | Pyrimidinamide                          | 95  |
| 78     | 40.430 | 99        | unknown                                 |     |
| 79     | 40.591 | 43        | 4-Methyl-Pentanoic acid                 | 114 |
| 80     | 40.919 | 43        | Anhydro-D-Galetosan                     | 144 |
| 81     | 41.152 | 71        | Anhydro-D-Manosan                       | 144 |
| 82     | 41.424 | 79        | Aminophenol                             | 109 |
| 83     | 41.606 | 42        | unknown                                 |     |
| 84     | 41.843 | 69        | Dianhydro-glucopyranose                 | 144 |
| 85     | 42.277 | 57        | Anhydro-D-xylofuranose                  | 162 |
| 86     | 42.701 | 120       | unkown                                  |     |
| 87     | 42.807 | 150       | 4-Vinyl-Guaiacol                        | 150 |
| 88     | 43.292 | 57        | Dodecane                                | 170 |
| 89     | 45.059 | 85        | Syringol                                | 154 |
| 90     | 45.231 | 117       | Indole                                  |     |
| 91     | 46.660 | 98        | 5-Methyl-1H,1,2,4-Triazol-3-Amine       | 98  |
| 92     | 48.291 | 130       | Methyl-Indole                           | 131 |
| 93     | 49.351 | 110       | Hydroquinone                            | 110 |
| 94     | 50.543 | 43        | Methyl-Undecene                         | 168 |
| 95     | 50.668 | 55        | unknown                                 |     |
| 96     | 50.972 |           | unknown                                 |     |
| 97     | 51.674 | 45        | unknown                                 |     |
| 98     | 53.431 | 107       | Hydroxy-Benzene-Ethanol                 | 138 |
| 99     | 53.946 | 180       | Dimethoxy-Phenyl-Ethanone               | 180 |
| 100    | 57.818 | 60        | Levoglucosan                            | 162 |

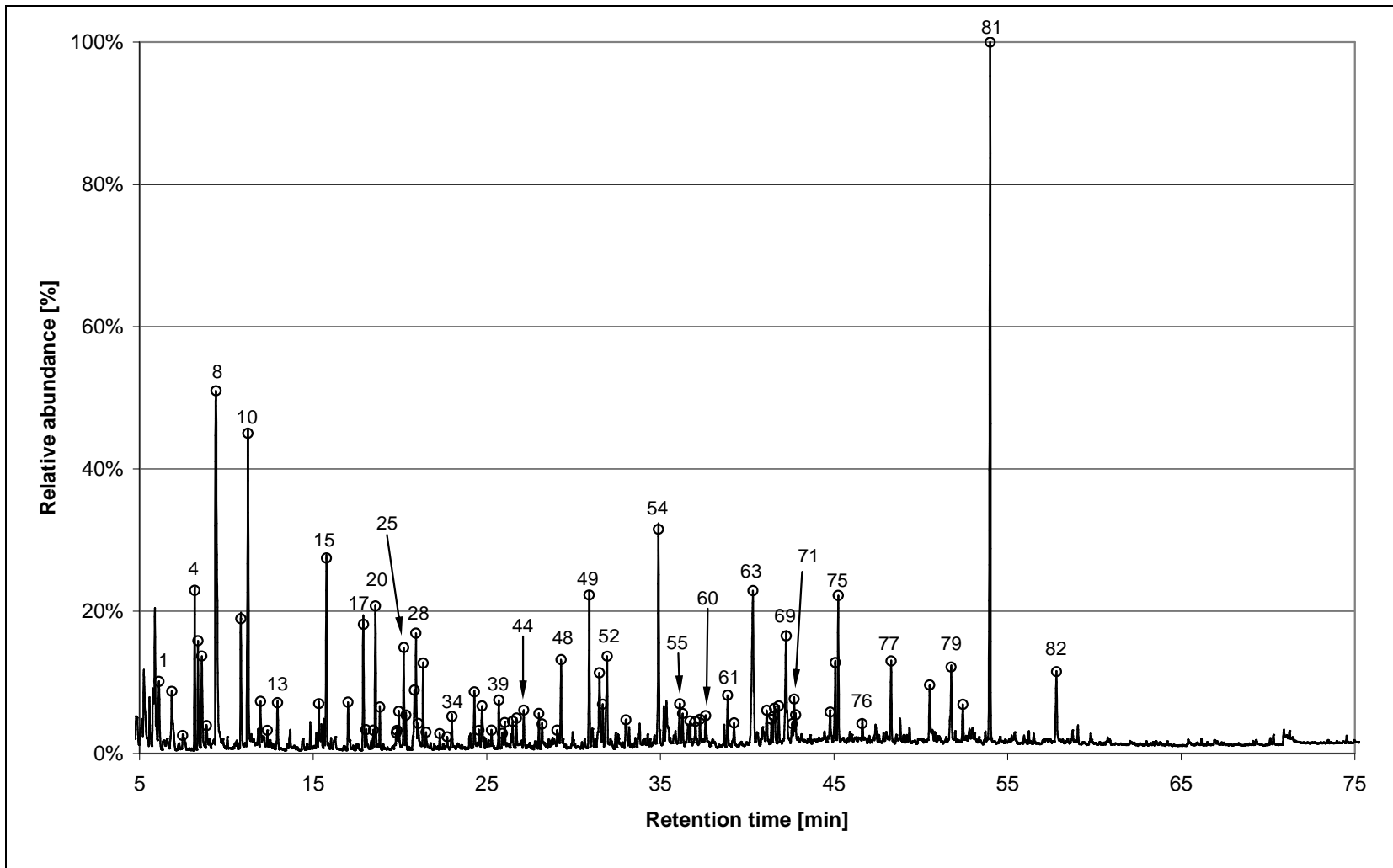


Pyrolysis vapour chromatogram of Green Dragon rape meal

## Suggested peak assignments for Green Dragon rape meal

| Peak # | RT     | Base Peak | Component                       | MW  |
|--------|--------|-----------|---------------------------------|-----|
| 1      | 5.87   | 43        | 2-Methyl-Propanal               |     |
| 2      | 6.109  | 82        | 3-Methylfuran                   | 82  |
| 3      | 6.834  | 43        | 2,3-Butanedione                 | 86  |
| 4      | 7.261  | 56        | 2,3-Dimethyl-Pentane            |     |
| 5      | 7.614  | 78        | unknown                         |     |
| 6      | 8.162  | 44        | 3-Methyl-Butanal                | 86  |
| 7      | 8.348  | 41        | 2-Methyl-Butanal                | 86  |
| 8      | 8.58   | 96        | 2,5-Dimethyl-Furan              | 98  |
| 9      | 8.852  |           | unknown                         |     |
| 10     | 9.39   | 43        | Acetic Acid                     | 60  |
| 11     | 10.477 | 43        | unknown                         |     |
| 12     | 10.804 | 43        | Acetic-Acid-Methylester         | 74  |
| 13     | 10.051 | 41        | unknown                         |     |
| 14     | 11.212 | 91        | Toluene                         | 92  |
| 15     | 11.931 | 79        | Pyridine                        | 79  |
| 16     | 12.329 | 55        | 2-Methyl-Butanenitril           | 83  |
| 17     | 12.646 | 54        | unknown                         |     |
| 18     | 12.923 | 43        | 3-Methyl-Butanenitril           | 83  |
| 19     | 15.72  | 67        | Pyrrole                         | 67  |
| 20     | 16.963 | 84        | (2H)Furan-2-one                 | 84  |
| 21     | 17.512 | 54        | unknown                         |     |
| 22     | 17.834 | 43        | Acetic Anhydride                | 102 |
| 23     | 18.523 | 96        | Furfural                        | 96  |
| 24     | 18.78  | 55        | 4-Methyl-Pentanenitrile         | 97  |
| 25     | 19.721 | 58        | unknown                         |     |
| 26     | 19.78  |           | unknown                         |     |
| 27     | 19.872 | 80        | 3Methyl-1H-Pyrrole              | 81  |
| 28     | 20.013 | 43        | unknown                         |     |
| 29     | 20.068 | 41        | unknown                         |     |
| 30     | 20.159 | 80        | 2Methyl-1H-Pyrrole              | 81  |
| 31     | 20.27  | 91        | unknown                         |     |
| 32     | 20.687 | 55        | 2,3-Dihydro-5-methylfuran-2-one | 98  |
| 33     | 20.788 | 60        | 3-Methyl-Butanoic Acid          | 102 |
| 34     | 20.863 | 41        | 3-Furfuryl alcohol              | 98  |
| 35     | 21.004 | 74        | 2-Methyl-Butanoic Acid          | 102 |
| 36     | 21.271 | 43        | 1-Acetyloxypropane-2-one        | 116 |
| 37     | 21.432 | 67        | 2-Methyl-2-Cyclopenten-1-one    | 96  |
| 38     | 21.699 | 107       | 2,6-Dimethyl-Pyridine           |     |
| 39     | 21.9   | 44        | unknown                         |     |
| 40     | 22.232 |           | unknown                         |     |
| 41     | 22.63  | 95        | 2-Acetylfuran                   | 110 |
| 42     | 22.916 | 96        | 4-Cyclopenten-1,3-dione         | 96  |
| 43     | 23.953 | 40        | unknown                         |     |
| 44     | 24.21  | 98        | Dihydro-methyl-furanone         | 98  |
| 45     | 24.471 | 94        | 2,5-Dimethyl-1H-Pyrrole         | 95  |
| 46     | 24.657 | 80        | 3-Ethyl-1H-Pyrrole              | 95  |
| 47     | 25.171 | 41        | unknown                         |     |
| 48     | 25.613 | 110       | 5-Methyl-2-furaldehyde          | 110 |
| 49     | 25.739 | 55        | unknown                         |     |
| 50     | 25.961 | 43        | unknown                         |     |

| Peak # | RT     | Base Peak | Component                                       | MW  |
|--------|--------|-----------|---|-----|
| 51     | 26.076 | 67        | unknown   |     |
| 52     | 26.318 | 41        | unknown   |     |
| 53     | 26.403 | 96        | 3-Methyl-2-Cyclopenten-1-one                    | 96  |
| 54     | 26.62  | 42        | Butyrolactone                                   | 86  |
| 55     | 26.927 | 94        | 4-Ethyl-2Methyl-Pyrrole                         |     |
| 56     | 27.043 | 55        | Lysidine  | 84  |
| 57     | 27.254 | 67        | unknown   |     |
| 58     | 27.913 | 42        | unknown   |     |
| 59     | 28.094 | 114       | 4-Hydroxy-5,6-dihydro-(2H)-pyran-2-one          | 114 |
| 60     | 28.472 | 108       | Trimethyl-Pyrrole                               |     |
| 61     | 28.703 | 94        | unknown   |     |
| 62     | 28.995 | 94        | 4,4-Dimethyl-2-Pentenenitrile                   | 109 |
| 63     | 29.186 | 112       | 2-Hydroxy-1-methyl-1-cyclopentene-3-one         | 112 |
| 64     | 29.473 | 68        | unknown   |     |
| 65     | 30.55  | 91        | unknown   |     |
| 66     | 30.802 | 94        | Phenol  | 94  |
| 67     | 31.582 | 109       | Guaiacol  | 124 |
| 68     | 31.828 | 43        | 2,5-Dimethyl-4-Hydroxy-3(2H)Furanone            | 128 |
| 69     | 32.316 | 95        | 1H-Pyrrole-2-Carboxaldehyde                     | 95  |
| 70     | 32.452 | 41        | unknown   |     |
| 71     | 32.956 | 61        | Glycerin  | 92  |
| 72     | 34.159 | 68        | unknown   |     |
| 73     | 34.783 | 107       | Methylphenol                                    | 108 |
| 74     | 35.1   | 68        | unknown   |     |
| 75     | 35.306 |           | unknown   |     |
| 76     | 36.005 | 43        | 4H-Pyron-4-one-2,3-Dihydro-3,5Dihydroxy-6Methyl |     |
| 77     | 36.161 | 117       | unknown   |     |
| 78     | 36.413 | 123       | 3-Methyl-Guaiacol                               | 123 |
| 79     | 36.594 | 44        | Anhydrosugar                                    | 132 |
| 80     | 36.901 | 107       | Dimethyl-Phenol                                 | 122 |
| 81     | 37.173 | 59        | 4-Methyl-Pentaamide                             |     |
| 82     | 37.495 | 55        | Pentanoic acid Ethyl Ester                      |     |
| 83     | 38.567 | 97        | unknown   |     |
| 84     | 38.748 | 107       | 4-Ethyl-Phenol                                  | 122 |
| 85     | 39.12  | 55        | unknown   |     |
| 86     | 40.212 | 95        | Pyrimidinamide                                  | 95  |
| 87     | 41.002 | 42        | Anhydro-D-Manosan                               | 144 |
| 88     | 41.274 | 109       | Amino-Phenol                                    |     |
| 89     | 41.45  | 42        | unknown   |     |
| 90     | 41.692 | 69        | Dianhydro-glucopyranose                         | 144 |
| 91     | 42.114 | 57        | Anhydro-D-xylofuranose                          | 162 |
| 92     | 43.161 | 57        | unkown  |     |
| 93     | 44.928 | 154       | Syringol  | 154 |
| 94     | 45.104 | 117       | Indole  | 117 |
| 95     | 48.143 | 130       | Methyl-Indolizine                               |     |
| 96     | 50.393 | 55        | unknown   |     |
| 97     | 51.59  | 167       | 4-Ethyl-Syringol                                | 182 |
| 98     | 52.28  | 60        | Anhydro-D-Mannopyranose                         | 162 |
| 99     | 53.85  | 165       | Dimethoxy-Phenyl-Ethanone                       | 180 |
| 100    | 57.69  | 60        | Levoglucosan                                    | 162 |



Pyrolysis vapour chromatogram of ADM rape meal

## Suggested peak assignments for ADM rape meal

| Peak # | RT     | Base Peak | Component                               | MW  |
|--------|--------|-----------|---|-----|
| 1      | 6.114  | 82        | 2-Methylfuran                           | 82  |
| 2      | 6.851  | 43        | 2,3-Butanedione                         | 86  |
| 3      | 7.487  | 54        | Unknown                                 |     |
| 4      | 8.169  | 44        | 3-Methyl-Butanal                        | 86  |
| 5      | 8.361  | 41        | 2-Methyl-Butanal                        | 86  |
| 6      | 8.583  | 96        | 2,5-Dimethyl-Furan                      | 98  |
| 7      | 8.86   | 43        | 3-Methyl-3-Buten-2-one                  | 84  |
| 8      | 9.4    | 43        | Acetic Acid                             | 60  |
| 9      | 10.829 | 43        | Acetic Acid Methylester                 | 74  |
| 10     | 11.238 | 91        | Toluene                                 | 92  |
| 11     | 11.96  | 79        | Pyridine                                | 79  |
| 12     | 12.359 | 55        | 2-Methyl-Butanenitril                   | 83  |
| 13     | 12.939 | 43        | 3-Methyl-Butanenitril                   | 83  |
| 14     | 15.322 | 41        | unknown                                 |     |
| 15     | 15.761 | 67        | Pyrrole                                 | 67  |
| 16     | 17.008 | 84        | (2H)Furan-2-one                         | 84  |
| 17     | 17.892 | 43        | Acetic Anhydride                        | 102 |
| 18     | 18.043 | 93        | 2Methyl-Pyridine                        | 93  |
| 19     | 18.462 | 57        | unknown                                 |     |
| 20     | 18.583 | 96        | Furfural                                | 96  |
| 21     | 18.841 | 55        | 4Methyl-Pentanenitrile                  | 97  |
| 22     | 19.78  | 58        | unknown                                 |     |
| 23     | 19.83  | 43        | unknown                                 |     |
| 24     | 19.931 | 80        | 3Methyl-1H-Pyrrole                      | 81  |
| 25     | 20.219 | 80        | 2Methyl-1H-Pyrrole                      | 81  |
| 26     | 20.34  | 55        | unknown                                 |     |
| 27     | 20.83  | 60        | 3-Methyl-Butanoic Acid                  | 102 |
| 28     | 20.921 | 41        | 3-Furfuryl alcohol                      | 98  |
| 29     | 21.047 | 74        | 2-Methyl-Butanoic Acid                  | 102 |
| 30     | 21.33  | 43        | 1-Acetyloxypropane-2-one                | 116 |
| 31     | 21.501 | 67        | 2-Methyl-2-Cyclopenten-1-one            | 96  |
| 32     | 22.294 | 95        | 2-Acetylfuran                           | 110 |
| 33     | 22.713 | 69        | unknown                                 |     |
| 34     | 22.991 | 96        | 4-Cyclopenten-1,3-dione                 | 96  |
| 35     | 24.283 | 98        | 2-Hydroxy-2-Cyclopenten-1-one           | 98  |
| 36     | 24.551 | 94        | 2,5-Dimethyl-1H-Pyrrole                 | 95  |
| 37     | 24.732 | 80        | 3-Ethyl-1H-Pyrrole                      | 95  |
| 38     | 25.273 | 41        | unknown                                 |     |
| 39     | 25.692 | 110       | 5-Methyl-2-furaldehyde                  | 110 |
| 40     | 25.904 | 57        | unknown                                 |     |
| 41     | 26.03  | 43        | unknown                                 |     |
| 42     | 26.484 | 96        | 3-Methyl-2-Cyclopenten-1-one            | 96  |
| 43     | 26.711 | 42        | Butyrolactone                           | 86  |
| 44     | 27.13  | 55        | Lysidine                                | 84  |
| 45     | 28.004 | 39        | unknown                                 |     |
| 46     | 28.191 | 114       | 4-Hydroxy-5,6-dihydro-(2H)-pyran-2-one  | 114 |
| 47     | 29.059 | 94        | 4,4-Dimethyl-2-Pentenenitrile           | 109 |
| 48     | 29.281 | 112       | 2-Hydroxy-1-methyl-1-cyclopentene-3-one | 112 |
| 49     | 30.902 | 94        | Phenol                                  | 94  |
| 50     | 31.488 | 57        | 1,5-Hexadien-3-ol                       |     |

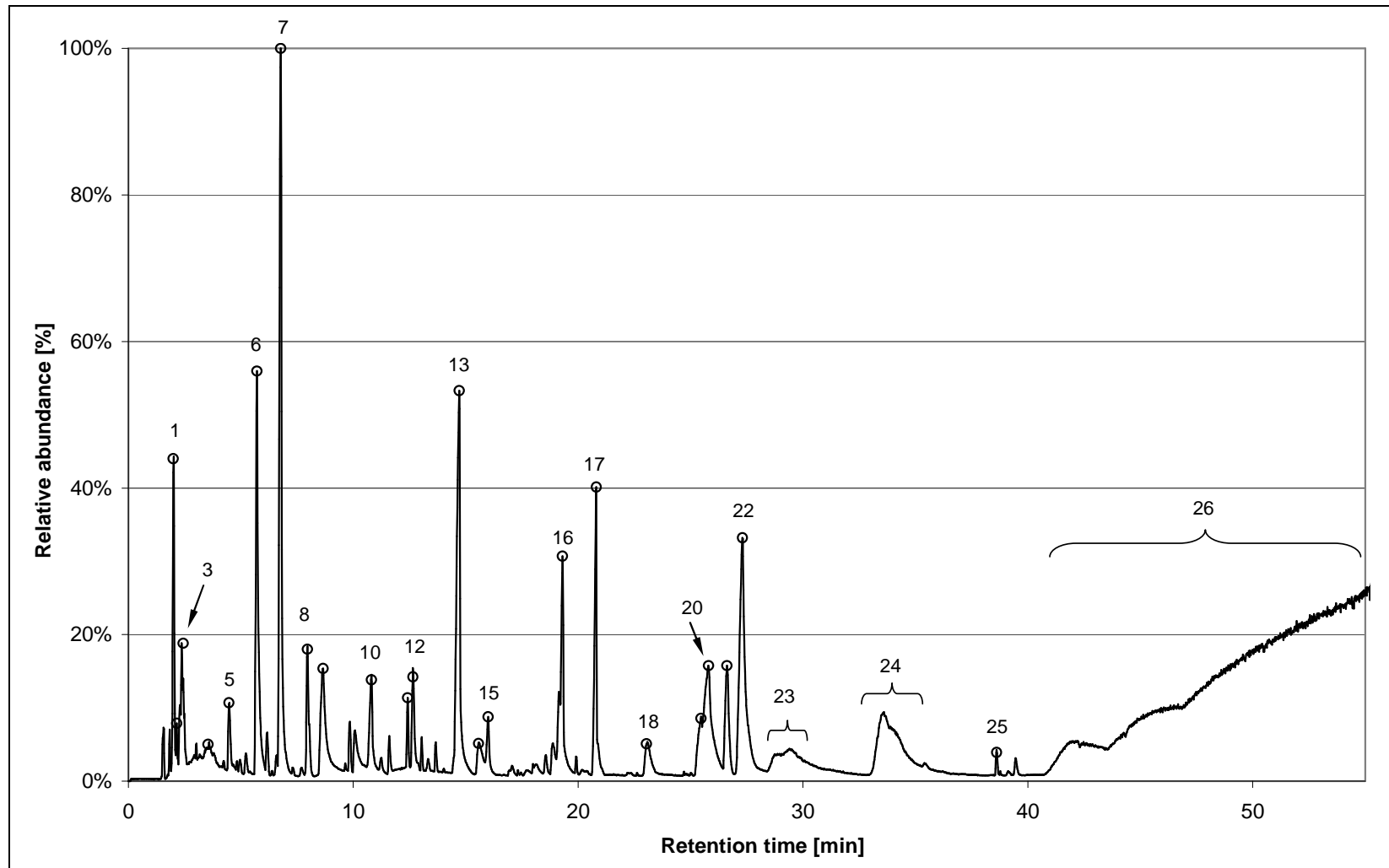
| Peak # | RT     | Base Peak | Component                            | MW  |
|--------|--------|-----------|--------------------------------------|-----|
| 51     | 31.68  | 109       | Guaiacol                             | 124 |
| 52     | 31.942 | 43        | 2,5-Dimethyl-4-Hydroxy-3(2H)Furanone | 128 |
| 53     | 33.017 | 61        | Glycerin                             | 92  |
| 54     | 34.89  | 107       | Methylphenol                         | 108 |
| 55     | 36.122 | 43        | unknown                              |     |
| 56     | 36.279 | 117       | Iso-Cyano-Methyl-Benzene             |     |
| 57     | 36.708 | 44        | Anhydrosugar                         | 132 |
| 58     | 37.021 | 107       | Dimethyl-Phenol                      | 122 |
| 59     | 37.283 | 59        | unknown                              |     |
| 60     | 37.611 | 55        | unknown                              |     |
| 61     | 38.874 | 107       | 4-Ethyl-Phenol                       | 122 |
| 62     | 39.252 | 80        | unknown                              |     |
| 63     | 40.338 | 95        | Pyrimidinamide                       | 95  |
| 64     | 41.13  | 42        | Anhydro-D-Manosan                    | 144 |
| 65     | 41.403 | 109       | Amino-Phenol                         |     |
| 66     | 41.529 | 91        | unknown                              |     |
| 67     | 41.58  | 42        | unknown                              |     |
| 68     | 41.822 | 69        | Dianhydro-glucopyranose              | 144 |
| 69     | 42.241 | 57        | Anhydro-D-xylofuranose               | 162 |
| 70     | 42.599 | 79        | unknown                              |     |
| 71     | 42.711 | 120       | unknown                              |     |
| 72     | 42.791 | 150       | 4-Vinyl-Guaiacol                     | 150 |
| 73     | 44.781 | 110       | Catechol                             | 110 |
| 74     | 45.078 | 154       | Syringol                             | 154 |
| 75     | 45.25  | 117       | Indole                               | 117 |
| 76     | 46.623 | 42        | unknown                              |     |
| 77     | 48.289 | 130       | Methyl-Indolizine                    |     |
| 78     | 50.521 | 84        | unknown                              |     |
| 79     | 51.748 | 167       | 4-Ethyl-Syringol                     | 182 |
| 80     | 52.424 | 60        | Anhydro-D-Mannopyranose              | 162 |
| 81     | 53.999 | 165       | Dimethoxy-Phenyl-Ethanone            | 180 |
| 82     | 57.821 | 60        | Levoglucofan                         | 162 |

## ***Appendix B: Analytical Py-GC-MS in inert and reactive gas***

For the comparative study via analytical Pyrolysis-Gas Chromatography-Mass Spectroscopy in inert and reactive gas atmosphere cellulose, xylan (for hemicellulose) and Organosolv lignin were analyzed to form a data base of possible decomposition products (see section 8.2). The equipment used was a CDS 5200 Pyroprobe® with trap coupled to a Varian GC-450 Gas Chromatograph and MS-220 Mass Spectrometer via a heated transfer line held at 310°C. The following chromatograms and suggested peak assignment tables are included:

- cellulose pyrolysis vapour chromatogram
- cellulose suggested peak assignment table
- xylan pyrolysis vapour chromatogram
- xylan suggested peak assignment table
- Organosolv lignin pyrolysis vapour chromatogram
- Organosolv lignin suggested peak assignment table

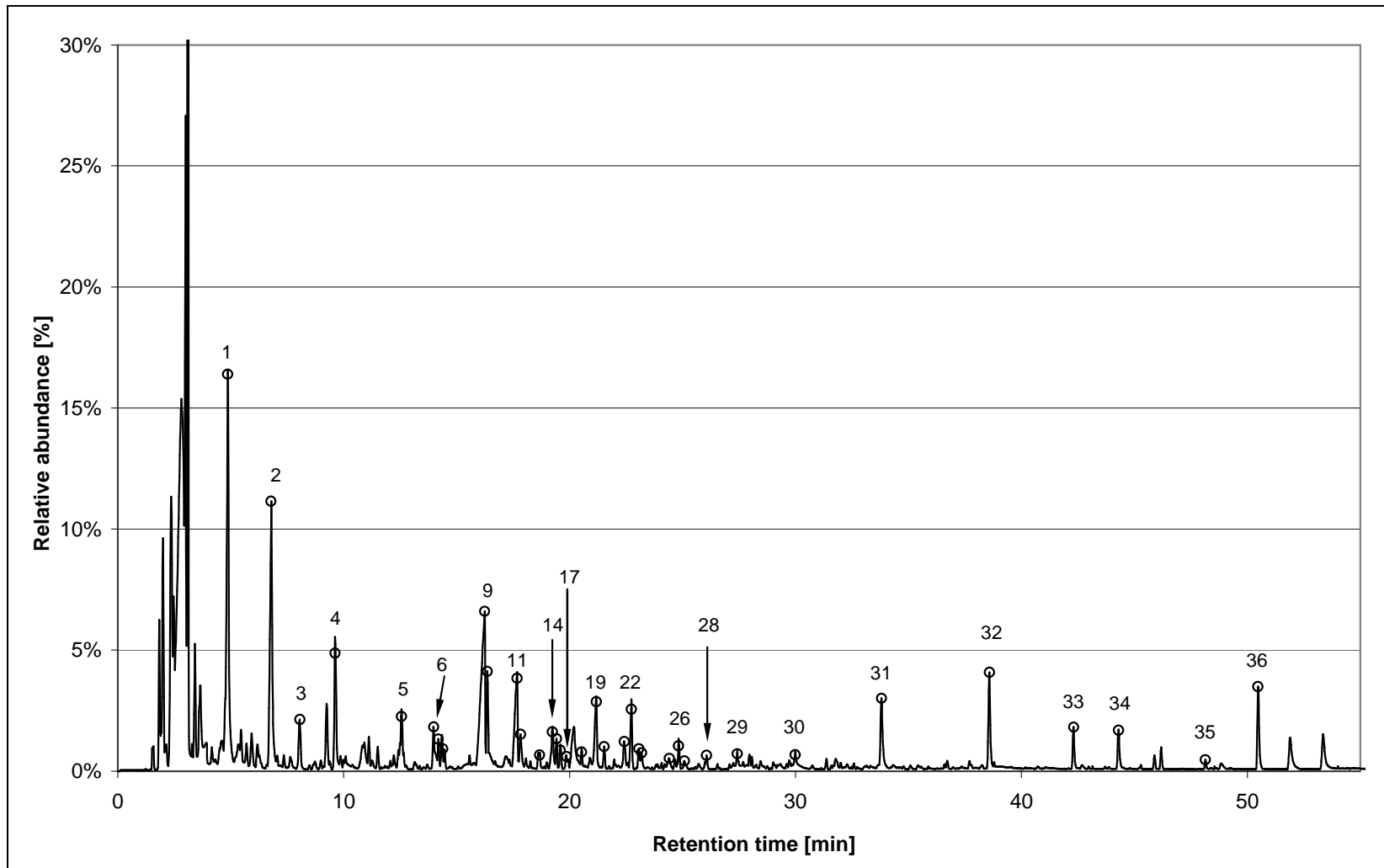
The peaks with suggested peak assignments are marked with a circle, but not all peak assignment numbers are displayed for reasons of readability.



Pyrolysis vapour chromatogram of cellulose

## Suggested peak assignments for cellulose

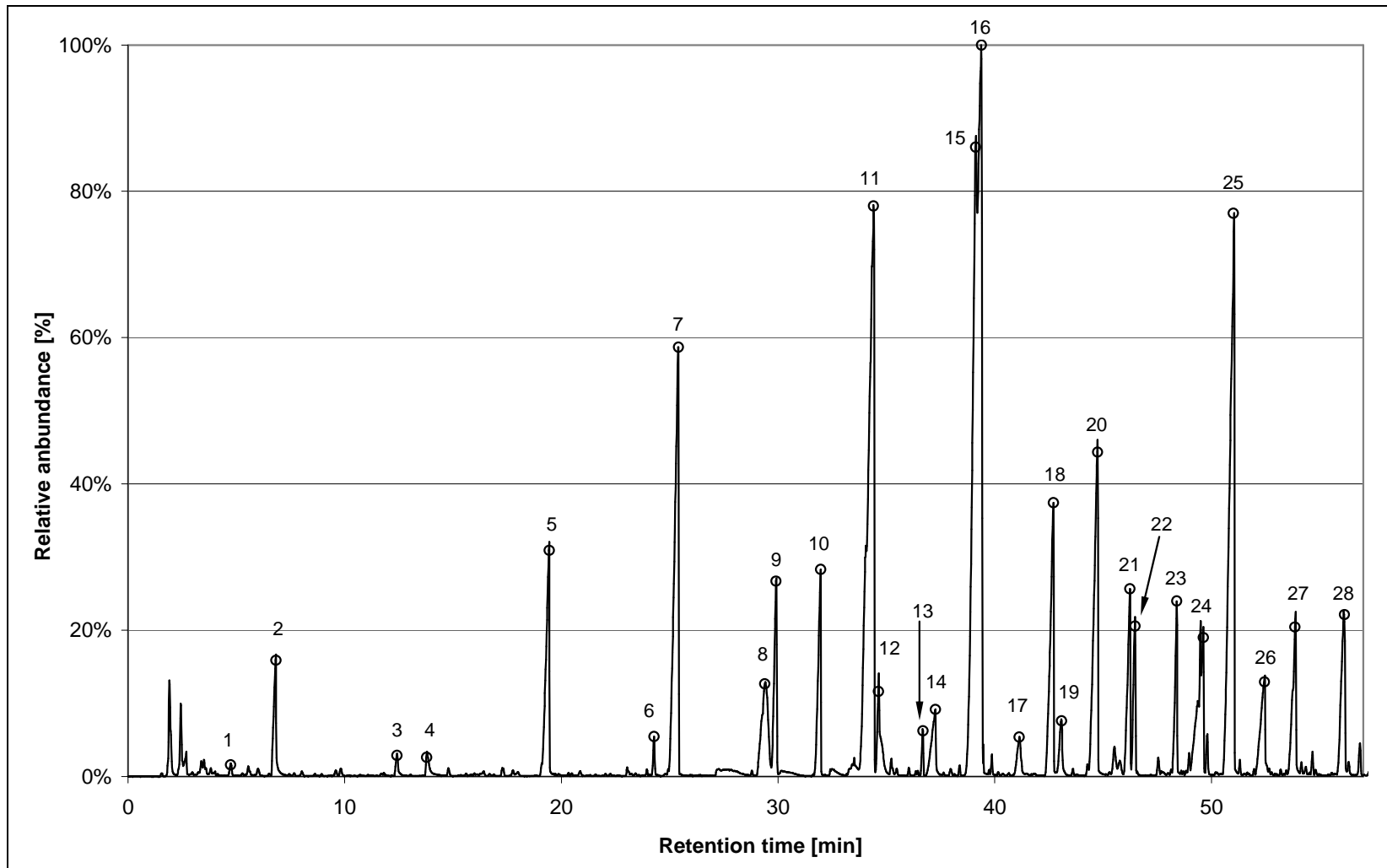
| Peak # | RT     | M     | Base Peak | Assigned compound                                 |
|--------|--------|-------|-----------|---|
|        | min    | g/mol | at m/z    |   |
| 1      | 2.002  | 68    | 68        | Furan   |
| 2      | 2.148  | 66    | 66        | 1,3-Cyclopentadiene                               |
| 3      | 2.442  | 82    | 82        | 3-Methylfuran                                     |
| 4      | 3.547  | 96    | 96        | 2,5-Dimethylfuran                                 |
| 5      | 4.470  |       |           | unknown   |
| 6      | 5.719  | 84    | 55        | 2(3H)Furanone                                     |
| 7      | 6.776  | 96    | 96        | Furfural  |
| 8      | 7.962  | 110   | 43        | 2-Propylfuran                                     |
| 9      | 8.662  |       |           | unknown   |
| 10     | 10.812 | 98    | 98        | 1,3-Cyclopentanedione                             |
| 11     | 12.416 | 110   | 110       | 5-Methyl-2-furaldehyde                            |
| 12     | 12.659 | 86    | 56        | Butyrolactone                                     |
| 13     | 14.715 | 114   | 114       | 4-Hydroxy-5,6-dihydro-(2H)-pyran-2-one            |
| 14     | 15.575 | 112   | 112       | 2-Hydroxy-1-methyl-1-cyclopentene-3-one           |
| 15     | 16.001 | 112   | 112       | 2-Hydroxy-3-methyl-2cyclopenten-1-one             |
| 16     | 19.304 | 128   | 128       | 2-Methoxy-2,3-dihydro-furan-3-carboxaldehyde      |
| 17     | 20.807 | 126   | 98        | Levoglucosenone                                   |
| 18     | 23.039 | 144   | 43        | 3,5-Dihydroxy-6-methyl-2,3-dihydro-4H-pyran-4-one |
| 19     | 25.467 | 142   | 57        | 4-Ethoxy-cyclohexanone                            |
| 20     | 25.806 | 142   | 142       | 3,5-Dihydroxy-2-methyl-4H-pyran-4-one             |
| 21     | 26.619 |       |           | unknown   |
| 22     | 27.305 | 144   | 69        | 1,4:3,6-Dianhydro-a-d-glucopyranose               |
| 23     | 28-30  |       |           | unresolved peak of sugars                         |
| 24     | 33-35  |       |           | unresolved peak of sugars                         |
| 25     | 38.610 | 168   | 168       | Vanillic acid                                     |
| 26     | 41-56  |       |           | unresolved peak of sugars                         |



Pyrolysis vapour chromatogram of xylan (for hemicellulose)

## Suggested peak assignments for xylan (for hemicellulose)

| Peak # | RT     | M     | Base Peak | Assigned compound                       |
|--------|--------|-------|-----------|---|
|        | min    | g/mol | at m/z    |   |
| 1      | 4.869  | 58    | 58        | Propanal                                |
| 2      | 6.781  | 96    | 96        | Furfural                                |
| 3      | 8.064  | 106   | 91        | Dimethylbenzene                         |
| 4      | 9.623  | 96    | 67        | 2-Methyl-2-cyclopenten-1-one            |
| 5      | 12.557 | 96    | 95        | Furaldehyde                             |
| 6      | 13.987 | 110   | 95        | 2-Acetylfuran                           |
| 7      | 14.186 | 110   | 110       | 5-Methyl-2-furaldehyde                  |
| 8      | 14.384 | 112   | 69        | 2,5-Dihydro-3,5-dimethyl-2-Furanone     |
| 9      | 16.243 | 112   | 112       | 2-Hydroxy-1-methyl-1-cyclopenten-3-one  |
| 10     | 16.358 | 110   | 67        | 2,3-Dimethyl-2-cyclopenten-1-one        |
| 11     | 17.678 | 126   | 126       | 2,4-Dimethyl-1,3-cyclopentanedione      |
| 12     | 17.826 | 108   | 108       | 2-Methyl-phenol (cresol)                |
| 13     | 18.671 | 126   | 126       | 3-Hydroxy-2-methyl-pyran-4-one (maltol) |
| 14     | 19.243 | 124   | 109       | Guaiacol (*)                            |
| 15     | 19.423 | 126   | 126       | 3-Ethyl-2-hydroxy-2-cyclopenten-1-one   |
| 16     | 19.585 | 126   | 41        | 4-Methyl-4-hepten-3-one                 |
| 17     | 19.865 | 124   | 124       | Catechol, 3-methyl- (*)                 |
| 18     | 20.533 | 122   | 122       | 2,6-Dimethyl-phenol                     |
| 19     | 21.184 | 126   | 126       | 3-Ethyl-2-hydroxy-2-cyclopenten-1-one   |
| 20     | 21.529 | 124   | 109       | 2,3,4-Trimethyl-2-Cyclopenten-1-one     |
| 21     | 22.427 | 140   | 140       | unknown                                 |
| 22     | 22.737 | 140   | 112       | 2-Ethyl-2-methyl-1,3-cyclopentanedione  |
| 23     | 23.064 | 122   | 107       | Dimethyl-phenol                         |
| 24     | 23.195 | 122   | 107       | Dimethyl-phenol                         |
| 25     | 24.417 | 122   | 107       | Dimethyl-phenol                         |
| 26     | 24.826 | 136   | 121       | Anisol, 2,4-dimethyl (*)                |
| 27     | 25.087 | 138   | 123       | Guaiacol, 3-methyl- (*)                 |
| 28     | 26.067 | 140   | 140       | Catechol, 3-methoxy- (*)                |
| 29     | 27.421 | 154   | 126       | unknown                                 |
| 30     | 29.988 | 150   | 132       | 2,6-Dimethyl-benzoic acid               |
| 31     | 33.806 | 154   | 154       | Syringol (*)                            |
| 32     | 38.59  | 168   | 168       | Syringol, 4-methyl- (*)                 |
| 33     | 42.31  | 182   | 137       | Syringol, 3-ethyl- (*)                  |
| 34     | 44.303 | 180   | 180       | Syringol, 4-vinyl- (*)                  |
| 35     | 48.142 | 194   | 194       | Syringol, 4-propenyl- (cis) (*)         |
| 36     | 50.475 | 194   | 194       | Syringol, 4-propenyl- (trans) (*)       |
|        |        |       |           | (*) contamination with lignin           |



Pyrolysis vapour chromatogram of Organosolv lignin

## Suggested peak assignments for Organosolv lignin

| Peak # | RT     | M     | Base Peak | Assigned compound             |
|--------|--------|-------|-----------|-------------------------------|
|        | min    | g/mol | at m/z    |                               |
| 1      | 4.736  | 92    | 91        | Toluene                       |
| 2      | 6.826  | 96    | 96        | Furfural                      |
| 3      | 12.413 | 110   | 110       | Benzenediol (Catechol)        |
| 4      | 13.78  | 94    | 94        | Phenol                        |
| 5      | 19.434 | 124   | 124       | Catechol, 4-methyl-           |
| 6      | 24.275 | 138   | 123       | Guaiacol, 3-methyl-           |
| 7      | 25.402 | 138   | 138       | Guaiacol, 4-methyl-           |
| 8      | 29.381 | 140   | 140       | Catechol, 3-methoxy-          |
| 9      | 29.904 | 152   | 137       | Guaiacol, 4-ethyl-            |
| 10     | 31.965 | 150   | 150       | Guaiacol, 4-vinyl-            |
| 11     | 34.407 | 154   | 154       | Biphenyl                      |
| 12     | 34.636 | 154   | 154       | Syringol                      |
| 13     | 36.687 | 164   | 164       | Eugenol                       |
| 14     | 37.262 | 152   | 151       | Vanillin                      |
| 15     | 39.115 | 168   | 168       | Syringol, 4-methyl-           |
| 16     | 39.39  | 168   | 168       | Vanillic acid                 |
| 17     | 41.13  | 166   | 151       | Acetoguaiacone                |
| 18     | 42.704 | 182   | 167       | Syringol, 4-ethyl-            |
| 19     | 43.083 | 180   | 137       | Coniferyl alcohol             |
| 20     | 44.745 | 180   | 180       | Syringol, 4-vinyl-            |
| 21     | 46.232 | 194   | 194       | Syringol, 4-allyl-            |
| 22     | 46.477 | 196   | 167       | Syringol, 4-propyl            |
| 23     | 48.395 | 194   | 194       | Syringol, 4-propenyl- (cis)   |
| 24     | 49.627 | 182   | 182       | Syringaldehyde                |
| 25     | 51.01  | 194   | 194       | Syringol, 4-propenyl- (trans) |
| 26     | 52.446 | 210   | 167       | Syringyl acetone              |
| 27     | 53.85  | 210   | 167       | Syringyl acetone              |
| 28     | 56.131 | 210   | 181       | Propiosyringone               |